



Dissecting mechanisms of host colonization by *C. albicans*

Untersuchungen zur Wirtskolonisierung durch *C. albicans*

Doctoral thesis for a doctoral degree
at the Graduate School of Life Sciences,
Julius-Maximilians-Universität Würzburg,
Section: Infection and Immunity

submitted by

Lena Böhm

from

Werneck

Würzburg, 2019

Submitted on:

Members of the Supervisory Committee:

Chairperson: **Prof. Dr. Thomas Rudel**

Primary Supervisor: **Dr. J. Christian Pérez**

Supervisor (Second): **Prof. Dr. Joachim Morschhäuser**

Supervisor (Third): **Dr. Kai Sohn**

Date of Public Defence:

Date of Receipt of Certificates:

Acknowledgments

First and foremost, I want to thank my primary supervisor Dr J Christian Pérez for giving me the opportunity to work on this interesting project. His continuous support and guidance, his unlimited enthusiasm and the many helpful discussions are the cornerstones of this thesis work. Finally, offering me the opportunity to continue my PhD after maternity leave and having a 1-year old baby at home is something I fail to express how grateful I am for. Christian, it has been a real pleasure to work with you.

I would also like to extend my gratitude to Prof Dr Joachim Morschhäuser and Dr Kai Sohn. Thank you for your advice and support as my thesis committee members. I enjoyed the very fruitful committee meetings a lot.

Many thanks also go to the GSLS for their support and their well-organized study program. With the help of your GSLS travel fellowships I was able to attend international conferences expanding my scientific knowledge and experience.

I would like to express my special thanks to all former and current members of the Pérez lab: Su, Pedrina, Valentina, Sanda, Marie, Juliane, Sergio and Philipp. Thank you for your unconditional support that has been essential all these years. Thanks go to Irene and Mona for teaching me essential techniques at the beginning of my PhD. And to all former and current members of the Morschhäuser lab for their scientific support in all Candida questions and for being a great company in the office.

Finally, I dedicate this thesis to my whole family who generously provided their moral support throughout all the periods of my PhD. I have an amazing family, perfect in many ways, but unique in many others as well. They shared every great moment with me and supported me whenever I needed them. Special thanks to my mom and dad for educating me in the believe that with hard work I can achieve whatever I want. Mom and dad, without you I wouldn't be the person I am today. Special thanks also to my siblings, Philipp, Thomas, Sophia and Lukas that were constantly receptive to listening to all my problems. Further, thanks to all of you for your invaluable help in raising my child.

Las but not least, my warmest thanks go to my husband Fabian and my lovely little son Freddi. Thank you, Fabian for encouraging me and supporting me to fulfill my dream of a PhD. Thank you for your endless patience and love. Without you and your help in raising our lovely son this work would have been impossible. And to the center of my life, my darling Freddi for being such a good little baby in the past two years, making it possible for me to complete what I started and being the strongest and sweetest motivation.

Summary

The human body is laden with trillions of microorganisms that belong to all three domains of life. Some species of this microbiota subsist as harmless commensals in healthy adults, but under certain circumstances, they can cause mucosal disease or even systemic, life-threatening infections. While the bacterial members of our microbiota are heavily studied today, much less attention is afforded to eukaryotic species that colonize different mucocutaneous surfaces of the human body. This dissertation focuses on identifying regulatory circuits that enable a prominent member of these eukaryotes, *C. albicans*, to, on the one hand, live on a specific mammalian mucosal surface as a harmless commensal and, on the other hand, proliferate as a pathogen. Since the ultimate source of many fatal *Candida* infections is the gastrointestinal (GI) tract of the infected individual, this organism is particularly suited to distinguishing traits essential for the gut colonization of commensal fungi and their ability to cause disease. Sequence-specific DNA-binding proteins that regulate transcription are important to most biological processes; I thus used these proteins as starting points to gain insights into 1) how a specific transcription regulator promotes virulence in *C. albicans*; 2) which traits *C. albicans* requires to inhabit the GI tract of a specific, well-defined mouse model as a harmless commensal; and 3) how three previously undescribed transcriptional regulators contribute to the commensal colonization of the digestive tract of this mouse model. Altogether, this work advances the knowledge concerning the biology of commensal fungi in the mammalian gut and genetic determinants of fungal commensalism, as well as pathogenicity.

Zusammenfassung

Der menschliche Körper wird von unzähligen Mikroorganismen aus allen drei Domänen des Lebens besiedelt. Einige Spezies dieser so genannten Mikrobiota leben mit gesunden Menschen als harmlose Kommensale, können jedoch unter bestimmten Umständen auch Erkrankungen der Schleimhäute oder sogar systemische, lebensbedrohliche Krankheiten verursachen. Der bakterielle Anteil unserer Mikrobiota wurde bereits ausgiebig untersucht. Sehr viel weniger Aufmerksamkeit haben bisher eukaryotische Organismen erlangt, die unterschiedliche Schleimhäute des menschlichen Körpers besiedeln. Ziel dieser Dissertation ist es regulatorische Kreisläufe zu identifizieren, die es einem prominenten eukaryotischen Mitglied unserer Mikrobiota, *Candida albicans*, ermöglichen auf der einen Seite eine spezielle mukokutane Oberfläche von Säugern zu besiedeln, und sich auf der anderen Seite als Pathogen zu verbreiten. Da man annimmt, dass viele bedrohliche *Candida* Infektionen ihren Ursprung im Gastrointestinaltrakt desselben Individuums haben, eignet sich dieser Organismus im speziellen um Eigenschaften zu identifizieren, die es kommensalen Pilzen ermöglicht den Darm zu besiedeln aber auch Krankheiten zu verursachen. Sequenz-spezifische DNA Bindeproteine, die die Transkription regulieren sind zentrale Akteure in den meisten biologischen Prozessen; aus diesem Grund verwende ich diese Proteine als Startpunkte um Einblicke in Folgendes zu erlangen: Zuerst, wie ein spezieller Transkriptionsregulator *C. albicans*' Virulenz beeinflusst. Dann welche Eigenschaften von *C. albicans* Voraussetzung für die Kolonisierung des Gastrointestinaltrakts eines klar definierten Mausmodells sind. Und zuletzt wie drei bisher nicht beschriebene Transkriptionsregulatoren zu der kommensale Kolonisierung des Verdauungstrakts dieses Mausmodells beitragen. Zusammenfassend trägt diese Arbeit dazu bei, das Wissen über die Biologie kommensaler Pilze im Säugertrakt und über genetische Determinanten zu erweitern, die zum Kommensalismus aber auch zur Pathogenität von Pilzen beitragen.

Abbreviation index

Δ	delta; Deletion
°C	Degree Celcius
μg	micro-gram
μM	micro-Molar
μmol	micro-Mol
AG	Arbeitsgruppe
ATP	Adenosintriphosphate
BAM	Binary Alignment Map
Bind	Binding
BSA	Bovine Serum Albumin
BWA	Burrows-Wheeler Aligner
<i>C. albicans</i>	<i>Candida albicans</i>
<i>Ca</i>	<i>Candida albicans</i>
cAMP	cyclic Adenosine Monophosphate
cDNA	complementary DNA
CFU	Colony-forming Units
CFW	Calcofluor White
CGD	Candida Genome Database
ChIP	Chromatin Immunoprecipitation
Cl ₂ Zn	Zinc Chloride
cm	Centimeter
CO ₂	Carbon dioxide
ConA	Concanavalin A
CR	Congo Red
CY5	Cyanine 5
d	day
DAPI	4',6-Diamidino-2-Phenylindole
DBD	DNA binding Domain
DC-SIGN	Dendritic Cell-Specific Intercellular Adhesion molecule-3-Grabbing Non-integrin
dH ₂ O	distilled Water
DNA	Deoxyribonucleic Acid
dom	Domain
DTT	Dithiothreitol
<i>E. coli</i>	<i>Escherichia coli</i>
e.g.	exempli gratia
EDTA	Ethylenediaminetetraacetic Acid
EMSA	Electromobility Shift Assay
EtOH	Ethanol
F/for	forward
FACS	Fluorescence-activated Cell Sorting
FISH	Fluorescence <i>in situ</i> Hybridization

FPKM	Fragment per kilobase per million mapped reads
g	gram
G-CSF	Granulocyte-colony stimulating Factor
GEF	Guanosine exchange Factor
GFP	Green Fluorescent Protein
GI	gastrointestinal
GO	Gene Ontology
GPI	Glycosylphosphatidylinositol
GTP	Guanosine-5'-triphosphate
GUT	Gastrointestinally induced Transition
h	hour
HCl	Hydrogen Chloride
HCO ₃	Bicarbonate
HDC	Haematogenously disseminated Candidiasis
HIV	Human Immunodeficiency Virus
Hog	High-osmolarity Glycerol
HPLC	High Performance Liquid Chromatography
HSG	Hyphal specific Genes
IL	Illinois
IPTG	Isopropyl β -D-1-Thiogalactopyranoside
ITS	internal transcribed Spacer
K ₂ HPO ₄	Dipotassium Phosphate
kb	kilo-Base
KH ₂ PO ₄	Monopotassium Phosphate
M	molar
MA	Massachusetts
mA	milli-Ampere
MAPK	Mitogen-activated Protein Kinase
MAPKK	Mitogen-activated Protein Kinase Kinase
MAPKKK	Mitogen-activated Protein Kinase Kinase Kinase
mg	milli-gram
MgCl ₂	Magnesium Chloride
min	Minute(s)
ml	milli-Liter
mM	milli-Molar
MO	Missouri
mRNA	messenger RNA
mRNP	messenger Ribonucleoprotein Particles
mut	mutated
Na ₂ HPO ₄	Disodium Phosphate
NaCl	Sodium Chloride

NaH ₂ PO ₄	Monosodium Phosphate
NaOH	Sodium Hydroxide
ng	nano-Gram
Ni-NTA	Nickel-Nitrilotriacetic Acid
nM	nano-Molar
nm	nano-Meter
NS	not significant
OE	Over-Expression
Oligo	Oligonucleotide
ORF	Open Reading Frame
P _{adj}	adjusted P-value
PAGE	Polyacrylamide Gel Electrophoresis
PAK	p21-activated Kinase
PAS	Periodic Acid Schiff
PBS	Phosphate Buffered Saline
PBST	Phosphate Buffered Saline with Tween-20
PCR	Polymerase Chain Reaction
PKA	Protein Kinase A
Pkc1	Protein Kinase C
PMSF	Phenylmethylsulfonylfluorid
PRR	Pattern Recognition Receptors
PVDF	Polyvinylidene Fluoride
qPCR	quantitative PCR
R/rev	reverse
RNA	Ribonucleic Acid
RNA-Seq	RNA-Sequencing
ROS	Reactive Oxygen Species
rpm	Revolutions per Minute
rRNA	ribosomal RNA
RT	Room Temperature
<i>S. cerevisiae</i>	<i>Saccharomyces cerevisiae</i>
SAP	Secreted Aspartyl Proteinases
SC	Synthetic Complete
SD	Standard Deviation
SDS	Sodium Dodecyl Sulfate
SSC	Saline-Sodium Citrate
TBS	Tris-buffered Saline
TBST	Tris-buffered Saline with Tween-20
TEM	Transmission Electron Microscopy
TGE	Tris-Glycine-EDTA
TLR	Toll-like Receptor
Tris-Cl	Tris-Chloride
UK	United Kingdom

USA	United States of America
V	Volt
VRC	Ribonucleoside Vanadyl Complexes
W	Watt
WGA	Wheat Germ Agglutinin
WIG	wiggle
WT/wt	Wild-type
YM	Yeast Mold
YNB	Yeast Nitrogen Base
YPD	Yeast Extract–Peptone–Dextrose
ZnSO ₄	Zinc Sulfate

List of Figures

Figure 1: <i>Candida albicans</i> transition from commensal to pathogen.	21
Figure 2: Composition of the <i>C. albicans</i> cell wall.....	23
Figure 3: The putative DNA binding domains of <i>ZCF21</i> and <i>ORF19.2623</i> show higher amino acid identity than <i>ZCF21</i> and <i>UPC2</i> (Bohm et al., 2016).....	34
Figure 4: The putative transcriptional regulator <i>ZCF21</i> originated at the base of the CTG clade (Bohm et al., 2016).....	35
Figure 5: <i>ZCF21</i> influences the sensitivity to a <i>Tor1</i> inhibitor (Bohm et al., 2016).....	36
Figure 6: Zcf21p governs expression of cell wall related proteins and enzymes (Bohm et al., 2016).	38
Figure 7: DNA sequence motif significantly overrepresented in the intergenic regions upstream of the direct targets of Zcf21p (Bohm et al., 2016).....	39
Figure 8: The purified DNA-binding domain of Zcf21p gel-shifts a DNA fragment harboring a wild-type instance of the putative motif (Bohm et al., 2016).	40
Figure 9: Two instances of the Zcf21p binding motif occur in the intergenic regions upstream of its direct targets (Bohm et al., 2016).	41
Figure 10: Two instances of the putative binding domain mediate binding of two Zcf21p copies (Bohm et al., 2016).	42
Figure 11: Expression of <i>ZCF21</i> influences susceptibility to cell wall intercalating agents (Bohm et al., 2016).	45
Figure 12: Zcf21p influences the activity of a cell wall integrity pathway (Bohm et al., 2016).....	46
Figure 13: Fibril-like structures on the cell surface are altered in the absence of <i>ZCF21</i> (Bohm et al., 2016).	47
Figure 14: Zcf21p influences the composition of the cell wall (Bohm et al., 2016).....	48
Figure 15: Deletion of <i>ZCF21</i> does not affect the phosphomannan content in the cell wall (Bohm et al., 2016).	49
Figure 16: Zcf21p influences the structure of the cell wall (Bohm et al., 2016).....	50

Figure 17: Model depicting how cell surface components, virulence determinants included, are controlled through <i>ZCF21</i> in <i>C. albicans</i> (Bohm et al., 2016).....	55
Figure 18: <i>Candida albicans</i> colonizes different locals of the human body (Underhill et al., 2014).....	57
Figure 19: Sterile containers used to raise and maintain germ-free mice.....	59
Figure 20: <i>Candida albicans</i> is a polymorphic yeast.....	60
Figure 21: <i>Candida albicans</i> is able to colonize gnotobiotic animals (Bohm et al., 2017).	70
Figure 22: <i>Candida albicans</i> colonizes the intestinal tract of gnotobiotic animals in its round-shaped yeast form (Bohm et al., 2017).....	71
Figure 23: Identification of <i>C. albicans</i> transcription regulators that govern gut colonization in gnotobiotic mice (Bohm et al., 2017).	75
Figure 24: The observed gut fitness defect phenotype of three newly identified genes could be restored by adding back a wild-type copy to the deletion mutant (Bohm et al., 2017).	77
Figure 25: The deletion mutants <i>zfu2</i> , <i>zcf8</i> , and <i>try4</i> display wrinkling - a proxy for filamentation - under non-inducing conditions (Bohm et al., 2017).	78
Figure 26: The regulators <i>ZCF8</i> , <i>ZFU2</i> , and <i>TRY4</i> promote adherence to mucin coated surfaces (Bohm et al., 2017).	79
Figure 27: Model depicting gut colonization of germ-free animals.	83
Figure 28: <i>ZCF8</i> , <i>ZFU2</i> , and <i>TRY4</i> belong to well known classes of transcription factors.	86
Figure 29: Different ways of mRNA localization.....	88
Figure 30: <i>SHE3</i> -dependent mRNA transport in <i>S. cerevisiae</i>	89
Figure 31: Kinases involved in <i>Candida albicans</i> morphogenesis.....	91
Figure 32: Confirmation of 13xMYC tag of <i>SHE3</i> using Western blot analysis.	98
Figure 33: Transcriptional regulatory network based on whole transcriptome analysis of <i>ZCF8</i> , <i>ZFU2</i> , and <i>TRY4</i> (Bohm et al., 2017).	107
Figure 34: <i>FGR17</i> , a common target of <i>ZCF8</i> , <i>ZFU2</i> , and <i>TRY4</i> , negatively regulates filamentation and invasive growth in <i>C. albicans</i>	109

Figure 35: The triple deletion strain *zcf8 zfu2 try4* exhibits hyperfilamentation phenotypes.111

Figure 36: The triple deletion mutant *try4 zcf8 zfu2* displays faster response to filamentation cues.....113

Figure 37: *ITS2* localizes in *C. albicans* to a specific area of the nucleus.115

Figure 38: Deletion of the three regulators disturbs localization of *SHE3*-associated transcripts.....116

Figure 39: The level and localization of She3p is affected by the three regulators.....117

Figure 40: Deletion of the regulators induces cell wall rearrangements.....119

Figure 41: Mutant of all three regulators induces increased killing by immune cells...119

Figure 42: The transcriptional regulators *ZCF8*, *ZFU2*, and *TRY4* control various biological aspects in *C. albicans*.125

Figure S 1: Genes encoding ‘cell surface’ and ‘cell wall’ components are overrepresented in an enlarged set of *ZCF21*-target genes (Bohm et al., 2016).137

Figure S 2: Putative Zcf21p motif occurs preferentially in regions bound and controlled by the regulator (Bohm et al., 2016).....137

List of Tables

Table 1: <i>Candida albicans</i> strains used in chapter 1.....	25
Table 2: Oligos used in chapter 1.....	25
Table 3: Plasmids used in chapter 1.....	26
Table 4: <i>Candida albicans</i> strains used in chapter 2.....	64
Table 5: Plasmids used in chapter 2.....	64
Table 6: Oligos used in chapter 2.....	65
Table 7: <i>Candida albicans</i> strains used in chapter 3.....	94
Table 8: Oligos used in chapter 3.....	94
Table 9: Plasmids used in chapter 3.....	95
Table 10: FISH probes used in chapter 3.....	95
Table 11: Top common targets of regulation.....	108
Table S 1: RNA Seq results.....	138
Table S 2: RNA Seq $p_{adj} < 0.1$	139
Table S 3: RNA seq $p_{adj} < 0.05$	152
Table S 4: RNA seq $p_{adj} < 0.01$	163

Table of Contents

Acknowledgments	I
Summary	II
Zusammenfassung	III
Abbreviation index	IV
List of Figures	VIII
List of Tables	XI
Table of Contents	XII
1) Introduction	16
2) ZCF21 - a regulator of disseminated infection	20
2.1) Summary	20
2.2) Introduction	21
2.2.1) How <i>C. albicans</i> causes disseminated infections	21
2.2.2) The composition of the <i>Candida albicans</i> cell wall	22
2.2.3) Transcription regulators of disseminated infections	23
2.3) Material & Methods:	25
2.3.1) <i>Candida albicans</i> strains used in this chapter	25
2.3.2) Oligos used in this chapter	25
2.3.3) Plasmids used in this chapter	26
2.3.4) Transcriptome analysis	26
2.3.5) Motif and promoter search	27
2.3.6) Protein purification	27
2.3.7) Electrophoretic Mobility Shift Assay (EMSA)	28
2.3.8) Phylogeny	29
2.3.9) Western Blot	30

2.3.10) Cell wall stainings	31
2.3.12) Spotassays.....	31
2.3.13) Electron microscopy	32
2.4) Results:.....	33
2.4.1) The <i>ZCF21</i> gene is exclusively found in the CTG clade and encodes a zinc cluster transcription factor.....	33
2.4.2) Zcf21p exerts its functions as transcriptional repressor.....	35
2.4.3) Zcf21p governs expression of cell wall related proteins and enzymes.	43
2.4.4) Zcf21p influences the structure of the cell wall.....	44
2.5) Discussion	51
3) <i>C. albicans</i> morphology is a key determinant of gut colonization in gnotobiotic mice	56
3.1) Summary.....	56
3.2) Introduction	57
3.2.1) Gut colonization by <i>Candida albicans</i>	57
3.2.2) Mouse models to study <i>Candida albicans</i> gut colonization.	58
3.2.3) <i>Candida albicans</i> morphologies.....	60
3.2.4) Gnotobiotic mouse models.....	62
3.3) Material & Methods:	64
3.3.1) <i>Candida albicans</i> strains used in this chapter	64
3.3.2) Plasmids used in this chapter	64
3.3.3) Oligos used in this chapter	65
3.3.4) Addback strains	65
3.3.5) Gastrointestinal tract colonization	66
3.3.6) Tissue collection	66
3.3.7) Histology.....	67
3.3.8) Immunohistochemistry.....	67
3.3.9) Colony morphology assay.....	68
3.3.10) Adherence assay.....	68
3.3.11) Statistical analyses.....	69
3.4) Results:.....	70
3.4.1) <i>Candida</i> colonizes the gut of gnotobiotic mice.....	70
3.4.2) Transcriptional regulators that contribute to the fitness of <i>C. albicans</i> in the gut of gnotobiotic animals.....	73

3.4.3)	The round-shaped yeast form of <i>Candida albicans</i> promotes persistence in the gut of gnotobiotic mice.	77
3.4.4)	<i>ZCF8</i> , <i>ZFU2</i> , and <i>TRY4</i> promote <i>C. albicans</i> adherence.	78
3.5)	Discussion	80
4)	Dissecting the molecular function of three <i>C. albicans</i> regulators of gut colonization.	85
4.1)	Summary	85
4.2)	Introduction	86
4.2.1)	<i>ZCF8</i> , <i>ZFU2</i> , <i>TRY4</i> – three transcriptional regulators in <i>C. albicans</i>	86
4.2.2)	Subcellular mRNA localization	87
4.2.3)	Kinases in <i>C. albicans</i> filamentation	90
4.3)	Material & Methods:	94
4.3.1)	<i>Candida albicans</i> strains used in this chapter	94
4.3.2)	Oligos used in this chapter	94
4.3.3)	Plasmids used in this chapter	95
4.3.4)	Probes used in this chapter.....	95
4.3.5)	Deletion mutants.....	96
4.3.6)	Overexpression strain.....	96
4.3.7)	MYC-tagging	97
4.3.8)	Filamentation assays	98
4.3.9)	Fluorescence <i>in situ</i> hybridization (FISH)	99
4.3.10)	Immunohistochemistry.....	102
4.3.11)	Neutrophil killing assay.....	102
4.3.12)	Western Blot	103
4.3.13)	Transcriptome analysis.....	105
4.4)	Results:	106
4.4.1)	The transcription regulators <i>ZCF8</i> , <i>TRY4</i> , and <i>ZFU2</i> share a large set of target genes	106
4.4.2)	The triple mutant strain <i>try4 zcf8 zfu2</i> displays a stronger filamentation phenotype than the single mutant strains	110
4.4.3)	Localization of <i>SHE3</i> -associated transcripts depends on <i>ZCF8</i> , <i>TRY4</i> , and <i>ZFU2</i> .	114
4.4.4)	<i>ZCF8</i> , <i>ZFU2</i> , and <i>TRY4</i> influence recognition by immune cells.....	118
4.5)	Discussion	121
5)	Conclusion and Outlook	127

6)	Supporting Information	136
6.1)	Supplementary Figures	136
6.2)	Supplementary Tables.....	138
7)	References.....	171
8)	List of Publications.....	189
9)	CV.....	190
10)	Affidavit.....	192

1) Introduction

With an estimated 2.8 to 3.3 million species, fungi represent one of the largest eukaryotic kingdoms, accounting for approximately 10% of all eukaryotic organisms found on Earth (Hawksworth et al., 2017). With its great diversity—including rusts, smuts, mildews, molds, mushrooms, and yeast—this group is ubiquitous in our environment and impacts various ecosystems. In fact, fungi play an indispensable role in decomposing dead organic material, forming the basis for not only nutrient recycling and exchange but therefore also the growth of new organisms. Numerous plants could not grow without their symbiotic fungi in the form of mycorrhizae that inhabit their roots and provide them essential nutrients. In the gut of grazing mammals, fungi enable the uptake of plant-derived molecules through the decomposition of plant material. Countless of our household and industrial processes rely on fungi or fungi-derived biomolecules: the process of fermentation to produce wine, beer, or soy sauce and using fungi as leavening in baking, for instance. In 1928, Alexander Fleming discovered the medical relevance of fungi after identifying a fungal substance that inhibits bacterial growth—now known as penicillin (Fleming, 2001). This discovery was the starting point of the production of the first series of antibiotics, most of them derived from fungi. Finally, studying fungi contributed to the present understanding of fundamental biological processes. With their simple *in vitro* growth conditions and the relatively easy ways of genetic manipulation, they are useful in studying many aspects of cell and molecular biology, genetic engineering, and other biological disciplines. Fungi can have serious negative effects on several processes as well. Food production and local economies can be impacted through the complete loss of crops due to fungal diseases, such as the rice blast disease, for example. Moreover, fungi grow on damaged or rotten fruits and vegetables, humid bread, and humid walls and ceilings, causing a number of problems for humans.

The fungal kingdom accommodates seven phyla: *Chytridiomycota*, *Blastocladiomycota*, *Neocallimastigomycota*, *Microsporidia*, *Glomeromycota*, *Ascomycota*, and *Basidiomycota* (Hibbett et al., 2007). *Chytridiomycota* belong to the early diverging fungal groups and reproduce with zoospores, which is rather unusual among fungi. They are essential to the decomposition of organic material but can also act as parasites in amphibians, algae, and other eukaryotic and prokaryotic microbes (Barr, 2001; Sparrow, 1960). *Blastocladiomycota*, another early diverging phylum, was the first to exhibit alternation of

generations (Sparrow, 1960). Similar to *Chytridiomycota*, some groups of *Blastocladiomycota* contribute to the decomposition of organic material, while others live as parasites of midges, nematodes, crustaceans, and other members of the *Blastocladiomycota* (Alexopoulos et al., 1996). The phylum *Neocallimastigomycota* contains mainly anaerobic fungi that live symbiotically in the gut of ruminants, helping them to digest plant material (Wang et al., 2017). *Microsporidia* consists of spore-forming unicellular parasites that infect insects, crustaceans, and fish; some species can even infect humans (Selman et al., 2011). *Glomeromycota* comprises symbiotic fungi that form mycorrhizas with the roots of terrestrial plants that supply mostly carbon and energy to the fungi (Oehl et al., 2011). Finally, *Ascomycota* and *Basidiomycota* form the subkingdom *Dikarya*, which is home to about 98% of all identified fungi (Wallen et al., 2018). The hallmark of this subkingdom is the formation of the dikaryon during cell division, which begets the term *Dikarya*. The newly formed daughter cell holds two nuclei with a common cytoplasm, one of each compatible mating type, and later forms the diploid cell with the 2n condition (Wallen et al., 2018). *Basidiomycota* includes mushrooms, smuts, rusts, mycorrhizae, and yeast-like human pathogens, among other substances (Coelho et al., 2017), whereas *Ascomycota*, the largest phylum of the kingdom Fungi (Schoch et al., 2009), features species of commercial and medical importance and prominent model organisms used in laboratory research.

In our daily routines, we are continuously in contact with a large assortment of fungal species, most of them present in the environment and harmless or commensally associated with our bodies. However, a small fraction—about 150 species—are considered opportunistic pathogens, able to infect warm-blooded animals and humans, resulting in a wide range of diseases (Underhill et al., 2015). Contact with some of these fungal species induces harmless but unpleasant infections in healthy individuals, as is the case for many dermatophytes and *Malassezia* species. Conversely, fungal species such as *Aspergillus fumigatus*, *Cryptococcus neoformans*, and *Candida albicans* can induce life-threatening infections with high mortality rates in humans. A prerequisite for almost all of these harmful infections is the immunosuppression of the affected individual; after organ transplantations or chemotherapy, and in HIV-infected persons, these fungi can enter the bloodstream, disseminate, and grow in virtually every organ in the human body. This thesis focuses on one of the most prominent species belonging to the *Ascomycota*, *Candida albicans*. Around 200 different *Candida* species have been identified. The main

characteristic of all these species was long considered to be the complete absence of any sexual form (Odds, 1988). Today, we know that *C. albicans* has the ability to mate *in vitro*, as well as *in vivo* (Hull et al., 2000). Since more than half of all *Candida* species cannot grow at 37°C, they are not associated with warm-blooded animals but subsist as environmental saprophytes (Calderone, 2002). Only 20 have been linked to diseases in humans (Akpan et al., 2002; Williams et al., 2013), and *Candida albicans* accounts for approximately 60% of infections caused by *Candida* species. The apparent absence of *C. albicans* in environmental reservoirs suggests that this species evolved extensively with its warm-blooded hosts (Odds, 1988). Its genome is completely sequenced and consists of more than 6,000 genes located on eight chromosomes (Braun et al., 2005). To date, over 70% of the listed open reading frames remain uncharacterized, based on data obtained from the *Candida* Genome Database (CGD). In healthy humans, *C. albicans* is a harmless colonizer of mucosal surfaces such as the mouth, the GI tract, and the female urogenital tract. This fungus can adapt to various external conditions, which may explain its ability to colonize diverse human body sites. It can grow, for instance, at a wide range of different temperatures (from 5°C to 45°C) and pH levels (from 2.5 to 10) (Hubbard et al., 1986; Odds, 1988), in the absence of oxygen (Eklund et al., 1983), and under high levels of CO₂ (Webster et al., 1987). Under certain circumstances, *C. albicans* can cause mucosal or even life-threatening infections in humans. Poor hygiene, burned skin, and surgeries predispose mucosal surfaces for an overgrowth of *C. albicans*. These infections are generally not life-threatening and can be treated with existing medications. In some cases, however, when the immune system is compromised through organ transplantation or chemotherapy, or after HIV infection, *C. albicans* can invade underlying epithelial cells and disseminate via the bloodstream. It thus reaches nearly every organ in the human body, and solid overgrowth in these organs often causes life-threatening infections with high mortality rates ranging from 30% to 50%, even with aggressive antifungal therapy (Edmond et al., 1999). Attributes critical to this process include the ability of the fungus to shift between differing morphological forms (yeast, hyphal, and pseudohyphal cells) and the dynamic structure of its cell surface. Distinct *C. albicans* morphologies seem to be associated with different processes during infection: the hyphal form may be essential to invading epithelial cells, whereas the yeast form may be required for efficient dissemination through the bloodstream (Calderone, 1993). Shaping the composition of its

cell surface affects the recognition of *C. albicans* by immune cells, since this is its first point of contact with these cells.

Even though infections caused by *C. albicans* were first described centuries ago, a significant increase in infections has been occurring over the last few decades, presumably owing to medical advances in cancer therapy and organ transplantation (Perfect et al., 2006). *C. albicans* is therefore considered one of the most prevalent human fungal pathogens, and the development of new antifungal treatments is urgently needed.

In this dissertation, I report the identification and characterization of several *C. albicans* transcription regulatory genes that enable the fungus to, on the one hand, live in the mammalian gut as a harmless commensal and, on the other hand, proliferate as a pathogen. First, I demonstrate how a previously identified transcriptional regulator contributes to the pathogenicity of *C. albicans*. Using commonly used chemicals to identify cell wall mutants, fluorescence stainings, and transmission electron microscopy (TEM), I establish that the deletion or overexpression of this regulator impacts the composition and overall structure of the cell wall of the fungus, potentially contributing to an altered recognition by immune cells. I then focus on *C. albicans*' commensal colonization of the mammalian digestive tract. While a great deal of effort has been dedicated to cataloging the vast microbial community in this niche, little is known about the traits and underlying mechanisms employed by the microbes, and particularly non-bacterial species, to colonize and proliferate in this locale. Utilizing gnotobiotic mice monocolonized with the fungus, I prove that the morphology of *C. albicans* plays a critical role in gut colonization. A genetic screen conducted in the same animal model of intestinal colonization identified novel regulators that allow the fungus to live in this niche. In the last part of this thesis, I dissect some of the cellular functions governed by the newly identified transcriptional regulators. Full transcriptome analysis indicated that the three regulators may significantly control overlapping biological processes, including the She-dependent subcellular localization of transcripts. These findings uncovered new regulatory circuits that are instrumental in pathogenicity and the commensal colonization of the fungus *Candida albicans*.

2) ZCF21 – a regulator of disseminated infection

2.1) Summary

The *Candida albicans* cell surface has a dynamic architecture and represents the fungi's first point of contact with host immune cells. While it is clear that the host environment can impact the composition and/or structure of the cell surface, the molecular mechanisms that effect these changes remain unclear. Here I report that a previously undescribed *C. albicans* transcription regulator has a major role in determining the composition of the surface of the fungus and thus influences the outcome of the interactions between *Candida* and host immune cells. The deletion or overexpression of this regulator altered the susceptibility or resistance to chemicals that intercalate into the fungal cell wall. Staining with fluorescently labeled sugar-specific dyes revealed that this regulator affects the total amount of mannan and the exposure of chitin. Similarly, a TEM analysis of the overall ultrastructure of the cell wall established that the regulator controls the structure of the outermost layer. Consistent with a role in cell surface remodeling that is relevant in the host, the deletion or overexpression of the regulator influenced the recognition of *Candida* by macrophages. My results confirm that this regulator functions mostly by repressing gene transcription; a balanced expression of cell wall components therefore seems to be the key to producing a surface suited for proliferation within the host.

2.2) Introduction

2.2.1) How *C. albicans* causes disseminated infections.

Candida albicans is the most prominent fungal species that resides in humans. It colonizes mucocutaneous surfaces of the GI tract (Hoffmann et al., 2013), the mouth (Ghannoum et al., 2010), the skin (Findley et al., 2013; Oyeka et al., 2002), and the female reproductive tract (Drell et al., 2013; Merenstein et al., 2013) of most healthy adults as a harmless commensal (Odds, 1988). However, under certain circumstances, this member of the normal microbiota can become a harmful pathogen, where the fungus can cause life-threatening infections with high mortality rates (Edwards, 2014; Perlroth et al., 2007; Pfaller et al., 2007). Many of these harmful infections are believed to originate in the GI tract of the infected individual. What induces *C. albicans*' transition from being a benign member of the microbiota to causing localized or even systemic infections remains unclear; nevertheless, a balance between fungal proliferation and host immune recognition seems to be necessary for it to maintain its commensal state (Hall et al., 2013b), since almost all systemic infections caused by *C. albicans* are found in immunocompromised individuals.

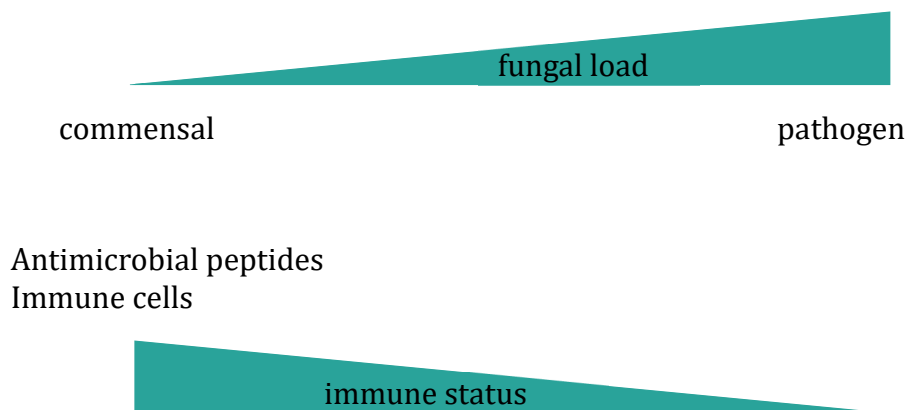


Figure 1: *Candida albicans* transition from commensal to pathogen.

In a healthy individual with an intact immune status the fungal load is kept low via antimicrobial peptides and immune cells. In an immunocompromised individual, *C. albicans* is able to evade the immune system, the fungal load increases, and it turns into a pathogen.

When the immune system is compromised due to organ transplantation, chemotherapy, or HIV infection, for example, *C. albicans* can proliferate and disseminate into the

bloodstream and then to virtually every organ (Clancy et al., 2012) (Figure 1). The first point of contact for fungal and host immune cells is the fungal cell wall, a dynamic structure composed of numerous proteins and carbohydrates. The regulation of its composition may thus represent an effective strategy of the fungus to dampen host immune recognition and cause disease.

2.2.2) The composition of the *Candida albicans* cell wall.

In fungal cells, the cell wall must provide characteristics for various aspects: it needs to enable the maintenance of the cell shape, resist environmental stresses, and regulate immunogenicity (Hall et al., 2013b). In some cases, this requires the precise coordination of slightly opposing traits. The permeability of the cell wall, for instance, needs to facilitate the import of nutrients and secretion of proteins while preventing the entrance of environmental hydrolases. Furthermore, the stability of the cell wall must ensure not only the cell's shape but also cell expansion, cell division, and morphogenesis (Hall et al., 2013b). The fungal cell wall is unique in its structure and differs significantly from plant cell walls (Bowman et al., 2006). It is composed primarily of three polysaccharides: chitin, glucan, and mannan. In *C. albicans*, the cell wall is organized in two layers, an inner layer of chitins and β 1,3-glucans and an outer layer of β 1,6-glucans and highly glycosylated mannoproteins (Figure 2). These proteins are attached to the skeletal chitin layer via a truncated glycosylphosphatidylinositol (GPI) anchor (Heilmann et al., 2012) and heavily decorated with *O*- and *N*-linked mannosides (Hall et al., 2013b). Among the GPI-anchored proteins, cell wall remodeling enzymes are involved in cell wall biogenesis (Douglas et al., 1997; Dunkler et al., 2005), the modification of polysaccharides and proteins that are needed for adhesion (Buurman et al., 1998; Hoyer, 2001), and biofilm formation (Nobile et al., 2006b; Zhao et al., 2006), processes known to contribute to *C. albicans* pathogenicity.

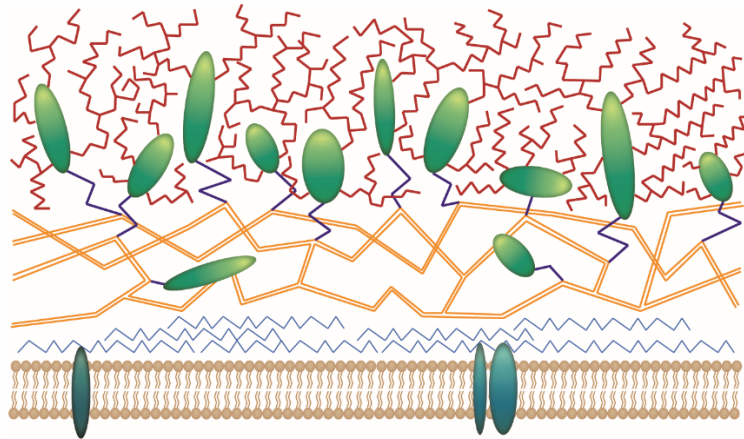


Figure 2: Composition of the *C. albicans* cell wall.

Scheme depicting the major components of *C. albicans* cell wall and their special distribution. Chitin (blue) is located close to the cell membrane providing stability to the cells. A layer mainly composed of β -(1,3)-glucan (orange) is located on top of the chitin layer further stabilizing the cells shape. A variety of cell wall proteins (green), most of them heavily decorated with mannans (red) are anchored mainly via GPI (glycosylphosphatidylinositol)-anchors in this β -(1,3)-glucan layer (Gow *et al.*, 2011, modified).

Mammalian immune cell receptors detect different sugars contained in the fungal cell wall. For instance, O-mannan is recognized through TLR4 (Netea *et al.*, 2006); N-mannan via the Mannose receptor, Dectin-2, DC-SIGN, Mincle, and Galectin-3 (Fradin *et al.*, 2000; McGreal *et al.*, 2006; Rouabhia *et al.*, 2005; Tada *et al.*, 2002; Taylor *et al.*, 2004); and β -glucans by the phagocytic receptor Dectin-1 and complement receptor 3 (Brown *et al.*, 2001; Thornton *et al.*, 1996). Pathogenicity and immune recognition therefore largely depend on the composition of the cell wall in *C. albicans*.

2.2.3) Transcription regulators of disseminated infections.

Dissemination into the bloodstream and colonization of deep tissues such as lungs, kidney, and liver may demand other traits in *C. albicans* than living as a commensal in the GI tract. The fungus needs to be able to adhere to and invade into tissue to get into the bloodstream and internal organs. Moreover, it needs to escape from host immune cells to avoid clearance and adapt to different environments (pH, nutrients) to colonize these diverse sites. Several transcriptional regulators were proved to control the expression of genes required for these pathogenicity-related processes; Efg1p, for example, is necessary

for full virulence in *C. albicans* (Lo et al., 1997; Lorenz et al., 2004). It is a major regulator of genes involved in hyphal development (Doedt et al., 2004; Stoldt et al., 1997). The ability to shift between morphological forms is crucial for the fungus to invade tissue and cause infections, since mutants—unable to form hyphae—were verified to be avirulent (Leberer et al., 1997; Lo et al., 1997; Romani et al., 1991). Another regulator connected to *C. albicans* pathogenicity is Tec1p, which affects *C. albicans* virulence on the following levels: it controls the expression of three types of secreted aspartyl proteinases (SAPs) (Schweizer et al., 2000), secreted hydrolytic enzymes, involved in tissue adherence and invasion (Ollert et al., 1993; Ruchel et al., 1991; Sanglard et al., 1997) and regulates the expression of genes necessary for the hyphal outgrowth of host immune cells (Schweizer et al., 2000). The latter is an effective way to evade the immune system and clearance of the host.

Here, I explore the role of Zcf21p, another transcriptional regulator, attested to be essential for full virulence in *C. albicans* (Perez et al., 2013b). I demonstrate that this regulator controls the expression of cell wall-related genes and enzymes predicted to be involved in cell wall-related processes by direct binding to a specific motif located upstream of its target genes. Two observations confirmed a connection between Zcf21p and the cell wall: strains lacking *ZCF21* and ectopically expressing *ZCF21* first illustrate an altered susceptibility to chemicals intercalating into the cell wall and second present rearrangements of the sugars contained therein. Finally, Zcf21p influences the recognition of *C. albicans* by host immune cells (Muralidhara, 2015), which could clarify its previous virulence defect in a mouse model of disseminated candidiasis (Perez et al., 2013b).

2.3) Material & Methods:

2.3.1) *Candida albicans* strains used in this chapter

Table 1: *Candida albicans* strains used in chapter 1.

Strain	Genotype	Source
SN152	$\frac{ura3\Delta::\lambda imm434::URA3-IRO1}{ura3\Delta::\lambda imm434}$ $\frac{arg4::hisG}{arg4::hisG}$ $\frac{his1::hisG}{his1::hisG}$ $\frac{leu2::hisG}{leu2::hisG}$	Noble and Johnson, 2005
SN250	$\frac{ura3\Delta::\lambda imm434::URA3-IRO1}{ura3\Delta::\lambda imm434}$ $\frac{arg4::hisG}{arg4::hisG}$ $\frac{his1::hisG}{his1::hisG}$ $\frac{leu2::hisG::CdHIS1}{leu2::hisG::CmLEU2}$	Homann <i>et al.</i> , 2009
TF24	$\frac{ura3\Delta::\lambda imm434::URA3-IRO1}{ura3\Delta::\lambda imm434}$ $\frac{arg4::hisG}{arg4::hisG}$ $\frac{his1::hisG}{his1::hisG}$ $\frac{leu2::hisG}{leu2::hisG}$ $\frac{zcf21\Delta::CdHIS1}{zcf21\Delta::CmLEU2}$	Homann <i>et al.</i> , 2009
JCP178	$\frac{ura3\Delta::\lambda imm434::URA3-IRO1}{ura3\Delta::\lambda imm434}$ $\frac{arg4::hisG}{arg4::hisG}$ $\frac{his1::hisG}{his1::hisG}$ $\frac{leu2::hisG}{leu2::hisG}$ $\frac{ZCF21::AgTEF1p-NAT1-AgTEF1UTR-TDH3p-GFP-ZCF21}{zcf21\Delta::CdHIS1}$	This work
JCP193	$\frac{ura3\Delta::\lambda imm434::URA3-IRO1}{ura3\Delta::\lambda imm434}$ $\frac{arg4::hisG}{arg4::hisG}$ $\frac{his1::hisG}{his1::hisG}$ $\frac{leu2::hisG}{leu2::hisG}$ $\frac{zcf21\Delta::CdHIS1}{zcf21\Delta::CmLEU2}$ $\frac{rps10\Delta::ZCF21--SAT1}{RPS10}$	This work
JCP642	$\frac{ura3\Delta::\lambda imm434::URA3-IRO1}{ura3\Delta::\lambda imm434}$ $\frac{arg4::hisG}{arg4::hisG}$ $\frac{his1::hisG}{his1::hisG}$ $\frac{leu2::hisG}{leu2::hisG}$ $\frac{cek1\Delta::CdHIS1}{cek1\Delta::CmLEU2}$	AG Morschhäuser
JCP646	$\frac{ura3\Delta::\lambda imm434::URA3-IRO1}{ura3\Delta::\lambda imm434}$ $\frac{arg4::hisG}{arg4::hisG}$ $\frac{his1::hisG}{his1::hisG}$ $\frac{leu2::hisG}{leu2::hisG}$ $\frac{mkc1\Delta::CdHIS1}{mkc1\Delta::CmLEU2}$	AG Morschhäuser

2.3.2) Oligos used in this chapter

Table 2: Oligos used in chapter 1.

Name	Description	Sequence (5'to3')
JCP586	add-back ZCF21 F	GAACACTCGAGTTTTCCCCCAATTAACTTTCAAAT
JCP587	add-back ZCF21 R	CCGCTCGAGTCAAGTGATCAATTTGGAAATGG
JCP1354	ZCF21 DNA-bind dom F	AGCAGCCCCGGGACCAATACCAATGCGCATACTCAG
JCP1356	ZCF21 DNA-bind dom R	GTGGTGCTCGAGTTATGAACTATTGGCATCCAATTTTTTC
JCP1357	Test insertion F	GCACCATCATCATCACCATC
JCP1358	Test insertion R	CTTTCGGGCTTTGTTAGCAG
JCP1369	WT motif F	CAAGAAGTACATGTACGAAACTAACAAA
JCP1370	WT motif R	TTTGTTAGTTTCGTACATGTACTTCTTG
JCP1371	mut motif F	CAAGAAGTACATGAATTAACACTAACAAA
JCP1372	mut motif R	TTTGTTAGTTTAATTCATGTACTTCTTG
JCP1669	mut1 motif F	CAAGATTGTTATGTACGAAACTAACAAA
JCP1670	mut1 motif R	TTTGTTAGTTTCGTACATAACAATCTTG
JCP1671	mut2 motif F	CAAGAAGTACATGTACGAAATCTTGAAA
JCP1672	mut2 motif R	TTTCAAGATTTTCGTACATGTACTTCTTG
JCP1373	2xmotif R	GGAAACAATTTCCAACCTCAATC
JCP1374	2xmotif F	CAAAGTATAGTGTCTGAAGAGG

2.3.3) Plasmids used in this chapter

Table 3: Plasmids used in chapter 1.

Name	Description	Source
pLIC-H3	6His-tag for protein-tagging	Cain <i>et al.</i> , 2012

2.3.4) Transcriptome analysis

Whole transcriptome analysis was performed on *Candida albicans* wild-type reference strain (SC5314) cells and *zcf21* deletion mutant cells grown under four different conditions: cells grown to late exponential phase in YPD broth at 30°C and cells grown on Todd-Hewitt agar at 37°C for 24 h, each in the presence or absence of 15 or 5 mM caffeine (Carl Roth, Karlsruhe, Germany). Cells from liquid culture were collected via centrifugation and cells grown on solid medium were scraped off the plates. Both type of cells were washed twice in dH₂O and counted in a hemocytometer (Neubauer). 1×10^8 cells were used to extract total RNA using the RiboPure™ RNA purification kit for yeast (Ambion, Thermo Fisher Scientific, Waltham, MA, USA) according to the manufacturer's instructions. RNA samples were sent to GATC Biotech (Konstanz, Germany), where library preparation (poly(A)+ RNA selection, mRNA fragmentation, random primer cDNA synthesis, adapter ligation) and Illumina (HiSeq 2500) sequencing (single read mode, 1×50 base pair read length) were performed following standard operating procedures. BWA version 0.5.9-r16 (Li *et al.*, 2009) with default parameters was used to map the generated reads to the reference genome (*Candida albicans* SC5314 Assembly 21) and BAM files were created. I converted these files into WIG files to visualize and analyze them in MochiView (Homann *et al.*, 2010). For each sample, I observed 30 - 55 million high-quality, unique mapped reads; between 75-85% of the generated reads could be mapped to annotated regions (open reading frames; ORFs) of the *C. albicans* genome (Build 21). Mapping to ORFs assigns reads to transcripts and FPKM (fragment per kilobase per million mapped reads) values were determined for each transcript. To further define transcript starts and endpoints I used previously published RNA-seq based annotations (Grumaz *et al.*, 2013; Tuch *et al.*, 2010). The FPKM cutoff for transcripts to be involved in my analysis was set to 1 in all samples. Differential gene expression was analyzed using two approaches: Cuffdiff 2 and 'raw counts' (Trapnell *et al.*, 2013). Cuffdiff 2 integrates additionally a statistical significance scoring system in its algorithm. Both ways of analysis generated lists of transcripts that showed a significant overlap. Since I observed a more consistent set of differentially expressed genes using the 'raw counts' approach, I based

my analysis included in Figure 6 and Figure S 1 on gene expression changes obtained by this method. Bruno et al. used a similar ‘raw counts’ approach to analyze gene expression in *C. albicans* RNA-seq datasets (Bruno *et al.*, 2010).

2.3.5) Motif and promoter search

To find a putative Zcf21p DNA binding domain, first its direct targets were identified combining the results of whole transcriptome analysis (Figure 6B, Figure S 1, Table S 1) and the results of an *in vivo* binding study (Perez *et al.*, 2013b). From these direct targets, sequences were extracted 500 nt upstream and downstream of the highest point of the observed ChIP peak. These sequences were loaded to and analyzed by MochiView (Homann *et al.*, 2010) to derive the putative Zcf21p DNA-binding motif. In Figure 9 transcription start sites were approximated based on our own and published RNA-seq data (Grumaz *et al.*, 2013; Nobile *et al.*, 2012; Tuch *et al.*, 2010).

2.3.6) Protein purification

Buffers:

Lysisbuffer:	Washbuffer:	Elutionbuffer:	Storagebuffer:
50 mM NaH ₂ PO ₄	50 mM NaH ₂ PO ₄	50 mM NaH ₂ PO ₄	40 mM Tris
600 mM NaCl	600 mM NaCl	400 mM NaCl	400 mM NaCl
10 mM Imidiazole	30 mM Imidiazole	250 mM Imidiazole	5 mM DTT
pH8	pH8	pH8	pH 7

An N-terminal 6His-tag was fused to the putative DNA-binding domain of the *C. albicans* Zcf21 protein (amino acids 96–187) and expressed in *Escherichia coli* as described (Fitzgerald *et al.*, 2006). Briefly, the putative DNA binding domain of the *C. albicans* Zcf21 protein was amplified using Primer JCP_1354 and JCP_1356 (Table 2). The purified PCR product was inserted downstream of the 6His-tag in the plasmid pLIC-H3 (Table 3). To identify correct insertions, the produced plasmid was transformed in *E. coli* DH5 α . Correct amino acid sequence of the DNA binding domain was verified by sequencing using primers JCP_1357 and JCP_1358 (Table 2). To produce the protein, correct plasmids were transformed in *E. coli* BL21. Protein expression was induced in an *E. coli* BL21 exponential phase culture (OD₆₀₀ 0.5-0.9) by adding 0.5 M Isopropyl- β -D-thiogalactopyranosid (IPTG) (Sigma-Aldrich, St. Louis, MO, USA) and 100 μ M Cl₂Zn (Sigma-Aldrich, St. Louis, MO, USA) for 3 h at 25-30°C shaking. Cells were collected and washed once in water. Cells were lysed in 15 ml Lysisbuffer containing protease inhibitor without EDTA, Lysozym, β -

Mercaptoethanol and Phenylmethylsulfonylfluorid (PMSF) (40 ml Lysis buffer + 2 tablets protease inhibitor without EDTA (Roche, Basel, Switzerland), 0.5 mg/ml Lysozym (Sigma-Aldrich, St. Louis, MO, USA), 5 mM β -Mercaptoethanol (gibco, Thermo Fisher Scientific, Waltham, MA, USA) and 1 mM Phenylmethylsulfonylfluorid (PMSF) (Sigma-Aldrich, St. Louis, MO, USA) for 20 min on ice and sonicated subsequently (M572/0) 60 cycles, 4 min each. Cell debris was removed by centrifugation (5000 rpm, 4°C, 15 min). The recombinant protein was affinity purified using Ni-NTA agarose beads (Qiagen, Hilden, Germany). Therefore, Ni-NTA agarose beads were washed three times in ice cold lysis buffer and the supernatant of the sonicated cells was added to the beads. After 45 min slightly shaking at 4°C, beads covered with protein were collected by centrifugation (3 min, 1000 rpm, 4°C) and washed four times in 10 ml Washbuffer containing 1 mM PMSF (5 min incubation 4°C + centrifugation 1 min, 1000 rpm, 4°C). Subsequently, beads were resuspended in ice cold Elutionbuffer containing 1 mM PMSF and 1 tablet protease inhibitor without EDTA/10 ml Elutionbuffer. Beads were incubated 20-30 min at 4°C shaking, centrifuged 1 min, 1000 rpm at room temperature and the supernatant was collected. Elution procedure was repeated 3-4x with reduced incubation (10 min) and supernatant was collected. Eluted proteins were concentrated using Ambicon Ultra-15 centrifugal filters (30K and 10K, Merc Millipore, Burlington, MA, USA) as far as possible without precipitation at 3200g in 5 min intervals. The purified protein was stored at -20°C in Storagebuffer and 50% glycerol. Its purity was estimated to be > 99%. Concentrations were estimated in Rothi®-blue (Carl Roth, Karlsruhe, Germany) quick-stained gels (6% DNA Retardation Gels, Invitrogen, Thermo Fisher Scientific, Waltham, MA, USA) using known concentrations of bovine serum albumin as standards.

2.3.7) Electrophoretic Mobility Shift Assay (EMSA)

EMSAs were carried out as described previously (Cain *et al.*, 2012).

Annealing/Labeling Oligos

JCP_1369 and 70 (wild-type) and JCP_1371 and 72 (inserted point mutation) were combined to a final concentration of 50 μ M and annealed as follows: 95°C – 5 min, 90°C – 5min, 85°C – 5 min, (...), 35°C – 5 min, 25°C – 30 min. For labeling oligos radioactively needed for one reaction following reagents were combined in this order: 2,5 μ l 10xPNK buffer, 2 μ l DNA (1 μ M), 17,5 μ l H₂O, 2 μ l γ -32-ATP, 1 μ l T4PNK Kinase. The reaction was incubated 20 min at 37°C, 15 min at 65°C and 5 min at 95°C and spun down. After 10 min

incubation at room temperature the radiolabeled mix was put slowly in a G25 column (BioRad, Hercules, CA, USA) and centrifuged 4 min at 1000g.

Gel shift assay

The purified protein was diluted in 1x minimal buffer (5xminimal buffer: 100 mM Tris pH 8.0, 250 mM NaCl, 25% glycerol) starting at 100 nM in 1:4 dilutions. A mastermix was prepared for one reaction as follows:

DTT 0.1M	0,12µl
5x minimal buffer	1,8µl
MgCl ₂	0,6µl
NP40	0,12µl
BSA (1mg/ml)	3µl
ZnSO ₄	0,12µl
H ₂ O	2,24µl

3 µl purified, diluted protein and 1 µl labeled DNA (500 fmol) were added to 10 µl Mastermix, loaded on a 6% polyacrylamid gel and run 90 min 120 V, 1000 W and 100 mA in EMSA buffer (0.5X Tris-Glycine-EDTA and 2.5% glycerol). The gel was dried, transferred to a phospho-screen (GE Healthcare, Chicago, IL, USA) and exposed for 3 hours. The screen was scanned using a TYPHOON imager (FLA 7000).

2.3.8) Phylogeny

I used only the DNA binding domain for phylogenetic analysis since the full-length Zcf21 protein produced no extensive alignment beyond the DNA binding domain. MUSCLE (Edgar, 2004) was used to align the DNA-binding domain sequences. To determine the best-fitting phylogenetic model according to the Akaike Information Criteria (Akaike, 1973), I checked multiple phylogenetic models via RAxML (Stamatakis, 2006). Thereby, I identified PROTGAMMAJTT as the best fitting model. MEGA 6.06 (Tamura *et al.*, 2013) was used to develop the maximum likelihood phylogeny. Synteny was assessed using the *Candida* Gene Order Browser (Maguire *et al.*, 2013).

2.3.9) Western Blot

Buffers:

10x TBS:	SDS Samplebuffer:	Transferbuffer:
0.2 M Tris	0.06 M Tris-Cl	14 g Glycin
1.5 M NaCl	5% Glycerol	3 g Tris
	2% SDS	100 ml Methanol
	4% β -Mercaptoethanol	400 ml H ₂ O
	0.0025% Bromophenol Blue	

Wild-type reference, *zcf21* deletion mutant, *ZCF21* ectopic expression mutant, *cek1* deletion mutant and *mkc1* deletion mutant cells were grown in liquid YPD to late exponential phase and exposed to Congo red (CR) (Carl Roth, Karlsruhe, Germany) (0.04 mg/ml) 1 h before harvesting. 3×10^7 cells were spun down and washed once in dH₂O, 5000 rpm, 1 min. Cells were resuspended in 100 μ l H₂O. 100 μ l NaOH (0.2M) were added and the cells were incubated 10 min at room temperature. Subsequently, cells were collected via centrifugation and resuspended in 50 μ l SDS sample buffer. Cells were incubated 5 min at 100°C. Cell debris was spun down and the supernatant containing whole cell extracts was combined with NuPAGE™ LDS Sample Buffer (Invitrogen, Thermo Fisher Scientific, Waltham, MA, USA) and resolved by PAGE (NuPAGE™ 4-12% Bis-Tris Gels, Invitrogen, Thermo Fisher Scientific, Waltham, MA, USA) (150 V, 100 mA, 1.5 h) in MES SDS Running Buffer (novex, Invitrogen, Thermo Fisher Scientific, Waltham, MA, USA). The proteins were transferred to a PVDF membrane (pore size 0,45 μ m, Carl Roth, Karlsruhe, Germany) in Transferbuffer (30 V, 500 mA, 2 h). The membrane was washed in 1x TBS and blocked in 1x TBS containing 5% milk, 1 hour at room temperature. After sequential washes in 1xTBS the proteins were probed with a mouse monoclonal anti-Phospho-p44/42 MAPK (Erk1/2) (Thr202/Tyr204) antibody (Cell Signaling, Danvers, MA, USA, 9106) or a rabbit polyclonal anti-Actin antibody (Sigma-Aldrich, St. Louis, MO, USA, A5060) (Loading control) 1:4800 diluted in 1x TBS containing 5% milk for 2 hours at room temperature. Unbound antibody was removed with 1x TBST (1xTBS + 0.05% Tween20) and the proteins were incubated with 1:12000 diluted secondary antibodies conjugated to horseradish peroxidase for 1 h at room temperature in 1x TBS containing 5% milk. Unbound secondary antibody was removed with 1x TBST and the proteins were imaged using SuperSignal™ West Femto Maximum Sensitivity Substrate (Thermo Fisher Scientific, Waltham, MA, USA, 34095).

2.3.10) Cell wall stainings

Wheat germ agglutinin and Concanavalin A staining

Cell wall stainings were performed as described earlier (Hall *et al.*, 2013a). Briefly, wild-type reference, *zcf21* deletion mutant and *ZCF21* ectopic expression mutant cells were grown to mid-exponential phase in YPD broth. Cells were washed in dH₂O and fixed for 30 min in paraformaldehyde at room temperature. Remaining paraformaldehyde was removed with three washes in dH₂O and stained in 50 µg/mL Wheat Germ Agglutinin (WGA) - Alexa Fluor® 488 (Life technologies, Thermo Fisher Scientific, Waltham, MA, USA, W11261) or Concanavalin A (ConA) - Texas Red (Life technologies, Thermo Fisher Scientific, Waltham, MA, USA, C825) for 30 min. Unbound dye was removed with sequential washes. Cell wall staining was evaluated either in a FACS machine (Accuri, BD, Franklin Lakes, NJ, USA) or in a fluorescence microscope (Leica, Wetzlar, Germany).

Alcian Blue assay

The phosphomannan content was determined as described earlier (Hall *et al.*, 2013a) with minor modifications. Briefly, reference strain and *zcf21* deletion mutant (5×10^6 cells/mL) cells were grown in YPD broth at 37°C for 4 hours. 1×10^7 cells were collected, washed and stained with 30 µg/mL Alcian blue (Sigma-Aldrich, St. Louis, MO, USA) for 10 min at room temperature. Cells were spun down and the amount of Alcian blue in the supernatant was determined using a TECAN 96-well plate reader (Tecan, Männedorf, Switzerland). Using these values, the amount of Alcian blue bound per cell could be estimated.

2.3.12) Spotassays

Wild type reference, *zcf21* deletion mutant, *ZCF21* ectopic expression mutant and add-back strain cells were grown over night to stationary phase in YPD broth at 30°C shaking. Spot assays were performed as described earlier (Ram *et al.*, 2006). Briefly, cells were harvested, washed in dH₂O and counted in a haematocytometer. Starting with 5×10^4 cells, tenfold dilutions were spotted on YPD/SC agar plates containing Calcofluor white (Sigma-Aldrich, St. Louis, MO, USA), Congo red (Carl Roth, Karlsruhe, Germany) and Caffeine (Carl Roth, Karlsruhe, Germany) in indicated concentrations. Plates were incubated at 37°C for 24-48 hours prior to evaluation.

2.3.13) Electron microscopy

Buffers:

Fixationbuffer:

2% paraformaldehyde

2.5% glutaraldehyde

0.1 M sodium cacodylate

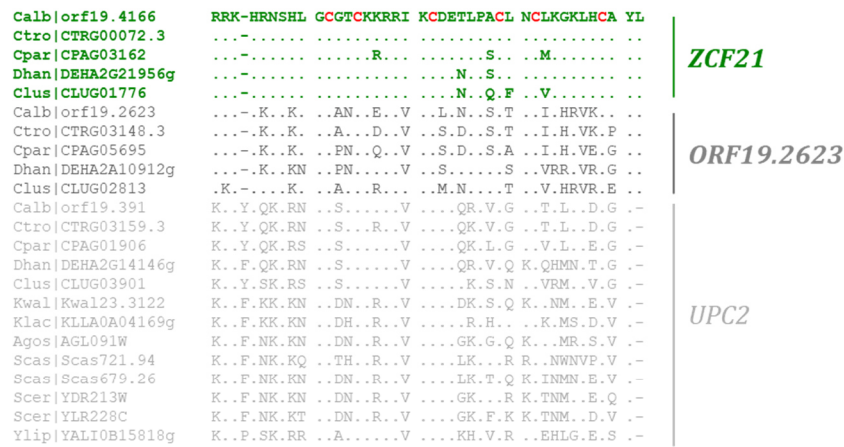
C. albicans wild-type, *zcf21* deletion mutant and *ZCF21* overexpression mutant cells were grown over night to stationary phase in liquid YPD medium. About 7.5×10^7 cells were harvested and fixed with 1 mL Fixationbuffer for 1-2 hours at 4°C. 900 µl of the Fixationbuffer was removed and samples were washed five times for 3 min in 50 mM cacodylate buffer. For contrasting, uranyl acetate was added and incubated overnight. For dehydration samples were incubated in increasing concentrations of ethanol. After infiltration, the samples were embedded in epon. For polymerization, the samples were incubated for 48 hours at 60°C. Ultra-thin sections of about 80nm were prepared using a microtome and stained with 2.5% uranyl acetate and Reynolds lead citrate for 1 hour at room temperature. The samples were examined using a JEOL JEM-2100 (200 kV) transmission electron microscope. Digital images were prepared using a TVIPS F416 digital camera.

2.4) Results:

2.4.1) The *ZCF21* gene is exclusively found in the CTG clade and encodes a zinc cluster transcription factor.

The starting point for this project was the identification of the putative transcriptional regulator Zcf21p in a previous study (Perez *et al.*, 2013b). The authors showed that a *zcf21* deletion mutant strain displayed decreased virulence in a standard mouse model of disseminated candidiasis (Perez *et al.*, 2013b). Besides this effect on virulence, there was nothing known about this regulator. A first look at its nucleotide sequence revealed that it contains a distinctive zinc cluster DNA binding domain. Therefore, it belongs to a well-known class of fungal proteins (MacPherson *et al.*, 2006). Phylogenetic reconstructions revealed no orthologs of Zcf21p beyond species belonging to the *Candida* lineage (CTG-clade) in the Hemiascomycota (Figure 4). Previous large-scale reconstructions of fungal gene families (Wapinski *et al.*, 2007) and synteny analyses (Candida Gene Order Browser (Maguire *et al.*, 2013)) also suggest that *ZCF21* is present exclusively in the *Candida* lineage. The *ZCF21*'s two closest homologs are *ORF19.2623* and *UPC2*.

A



B

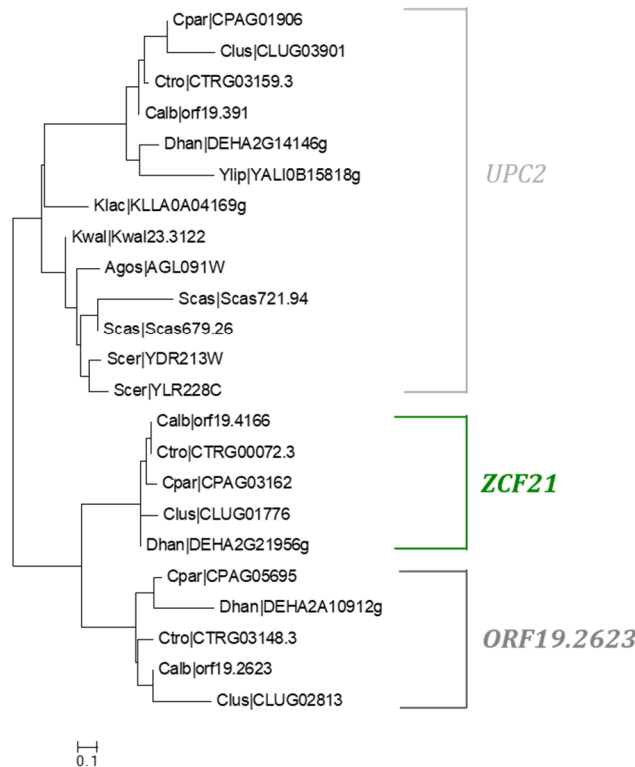


Figure 3: The putative DNA binding domains of ZCF21 and ORF19.2623 show higher amino acid identity than ZCF21 and UPC2 (Bohm et al., 2016).

(A) The putative DNA binding domains of ZCF21 (green), ORF19.2623 (dark grey) and UPC2 (light grey) were aligned. Dots represent identical amino acids. Gaps are indicated with dashes. In red are the six conserved cysteines, the hallmark of zinc-cluster DNA binding proteins. The putative DNA binding domains of ZCF21 and orf19.2623 are 62% identical in their amino acid sequence, whereas ZCF21 and UPC2 show only 52-60% identity.

(B) Maximum likelihood phylogenetic tree constructed based on the alignment shown in (A).

An alignment of the amino acid sequences corresponding to their DNA binding domain revealed that *ZCF21* and *ORF19.2623* exhibit the highest amino acid identity (62%) and *ZCF21* and *UPC2* (*ORF19.391* in *C. albicans*; *YDR213W* in *S. cerevisiae*) the second highest (52-60%) (Figure 3A). A phylogenetic tree built based on the alignment (Figure 3B) suggests that *ZCF21* and *ORF19.2623* originated by duplication at the base of the CTG clade (Figure 4).

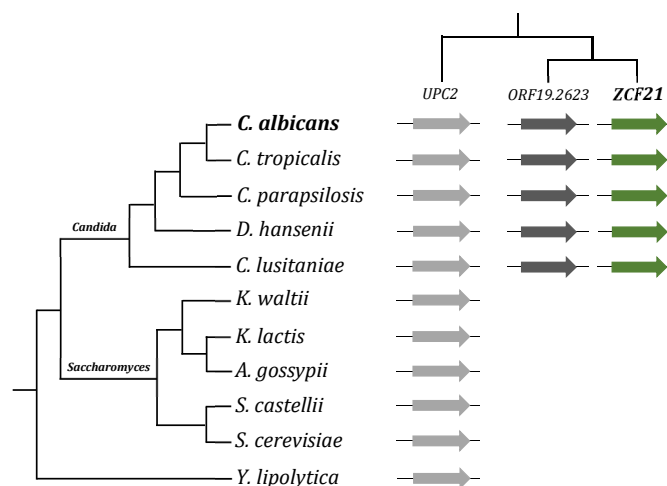


Figure 4: The putative transcriptional regulator *ZCF21* originated at the base of the CTG clade (Bohm *et al.*, 2016).

(A) Cladogram depicting the phylogenetic relationships among extant species of the *Candida* and *Saccharomyces* clades (Hemiascomycetes). The arrows on the right of the tree represent the distribution of the *ZCF21* gene (green) and its closest homologs *ORF19.2623* (dark grey) and *UPC2* (light grey). The relationships among the three genes, inferred from the reconstructed phylogeny, are shown on top of the arrows.

2.4.2) Zcf21p exerts its functions as transcriptional repressor.

To discover functions and processes that are controlled by the transcriptional regulator Zcf21p I identified transcripts whose expression depends on Zcf21p by transcriptome analysis (RNA Sequencing). RNA sequencing was carried out under four conditions: cells grown logarithmically under standard laboratory growth conditions (liquid YPD, at 30°C), but also cells grown on a semisolid surface at 37°C using Todd Hewitt medium. Perez *et al.* showed that the latter conditions induce expression of several regulators with roles in the host (Perez *et al.*, 2013b), possibly due to the fact that the temperature (37°C) and attachment to a surface are closer to the conditions present in the host. In one of the first

experiments I found that the *zcf21* deletion mutant was more resistant to Caffeine (Figure 5), a drug that targets the yeast kinase *TOR* (Kuranda *et al.*, 2006; Reinke *et al.*, 2006; Wanke *et al.*, 2008).

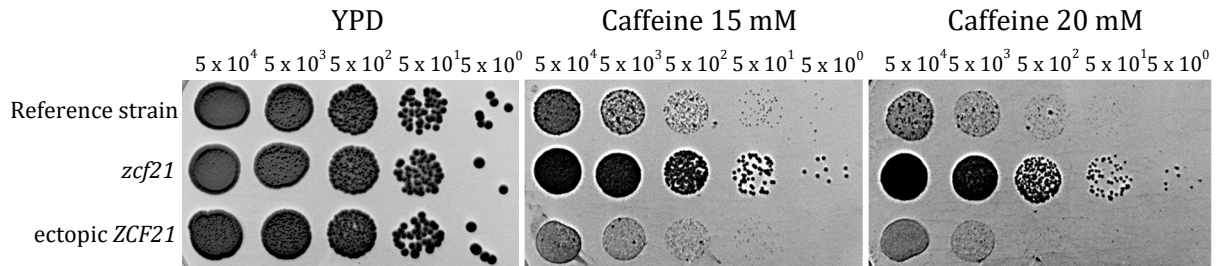


Figure 5: ZCF21 influences the sensitivity to a *Tor1* inhibitor (Bohm *et al.*, 2016).

The susceptibility of a *zcf21* deletion mutant and a strain ectopically expressing *ZCF21* to caffeine, a *TOR* inhibitor was compared to the reference strain. Starting with 5×10^4 cells, tenfold dilutions were spotted on YPD agar plates with and without 15 mM or 20 mM caffeine. Plates were incubated at 37° for 48 h. The *zcf21* deletion mutant showed an increased resistance against caffeine compared to the reference strain.

This observation and the fact that *TOR* inhibition in *C. albicans* promotes the expression of cell surface proteins through the activation of multiple transcriptional activators (Bastidas *et al.*, 2009), raised the idea to include additionally transcriptome analysis of cells grown in the presence or absence of Caffeine. Thus, in total, RNA sequencing of the reference strain and the *zcf21* deletion mutant was performed under four conditions: liquid YPD, 30°C and semisolid Todd-Hewitt medium, 37°C in the presence and absence of caffeine each. Expression levels of protein-coding transcripts in the deletion mutant were compared to the ones in the reference strain.

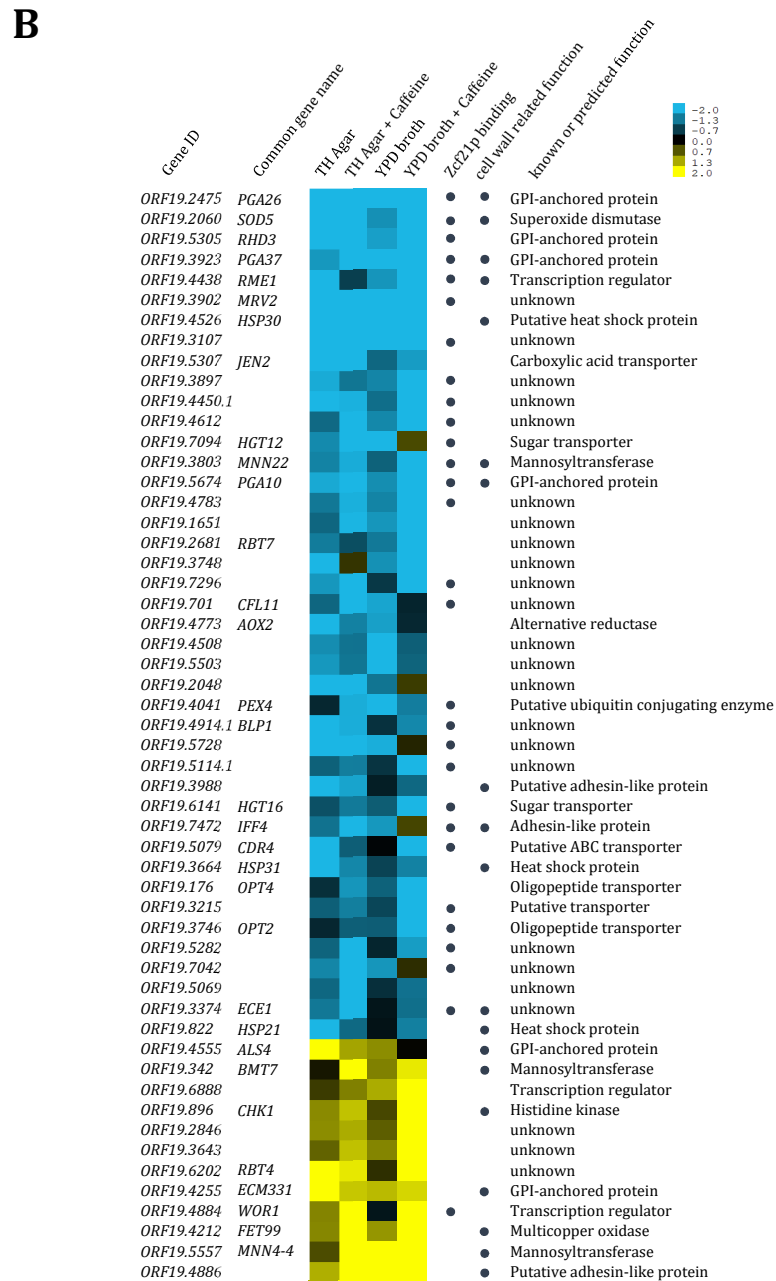
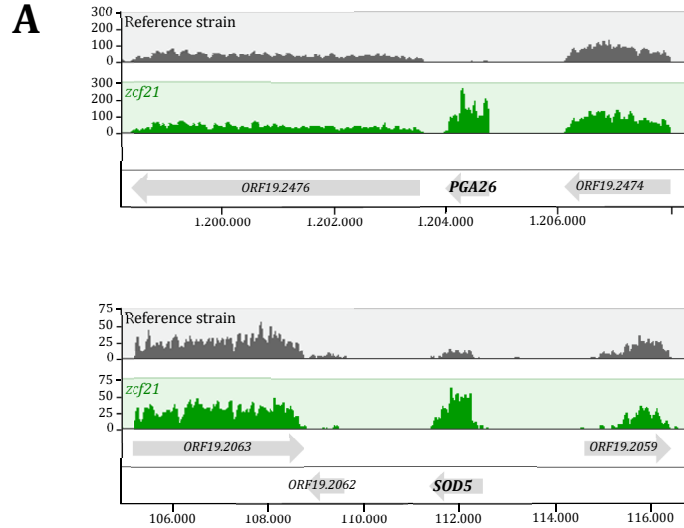


Figure 6: Zcf21p governs expression of cell wall related proteins and enzymes (Bohm *et al.*, 2016).

(A) Two representative RNA-seq tracks of the reference strain (grey) and the *zcf21* deletion mutant (green) are displayed. On top, a 10 kb segment of chromosome 1 and at the bottom a 12 kb segment of chromosome 2 is shown. In both examples, the surrounding ORFs show similar expression levels in the mutant and the reference, whereas *PGA26* in the middle of the first example and *SOD5* in the second showed an increased expression in the mutant compared to the reference.

(B) Heatmap including the 54 *C. albicans* transcripts where I found differences in expression levels based on the RNA-seq data. I performed whole genome RNA sequencing under four different conditions: in liquid YPD, 30°C or in Todd-Hewitt agar, 37°C either in the presence or absence of caffeine. Here in this heatmap the transcripts are shown that displayed a >2-fold difference in expression in the *zcf21* deletion mutant compared to the reference strain in at least three of the four conditions I tested. Using the FPKM values, representing the expression level, I calculated the $\log_2(\text{wt}/\text{mut})$ for each transcript. Blue color indicates that the transcript was upregulated in the deletion mutant compared to the reference (negative \log_2), whereas yellow indicates decreased expression in the mutant compared to the reference strain (positive \log_2). In the first column on the right of the heatmap I included the results of an *in vivo* binding study of the regulator Zcf21p (Perez *et al.*, 2013b). A dot in this column indicates that upstream of the respective gene binding of Zcf21p was detected. In the second column I marked the genes, that based on literature connect to cell wall related functions. A gene ontology analysis uncovered 'cell surface' and 'cell wall' as highly overrepresented terms in this dataset ($P = 2.06 \times 10^{-5}$).

As illustrated in Figure 6A, the RNA-Seq experiment revealed *PGA26* and *SOD5* as two of the top transcripts under control of *ZCF21*. Taken together, 54 transcripts showed a > 2-fold expression change in the *zcf21* deletion mutant compared to the reference strain in at least three of four conditions tested (Figure 6B). For 20 transcripts there was a consistent > 2-fold expression change in all four conditions. Thirty-seven additional transcripts showed a >2-fold expression change in only two of the four conditions evaluated (Figure S 1).

To distinguish now between direct and indirect effects of Zcf21p on the expression levels of the identified targets I compared our dataset to *in vivo* binding data obtained by chromatin-immunoprecipitation (Perez *et al.*, 2013b). This analysis uncovered binding of Zcf21p upstream of > 55% of the genes where we observed expression changes, identifying them as direct targets of Zcf21p. We extracted the sequences upstream of these direct targets and found a short DNA sequence motif (Figure 7) being significantly overrepresented (Figure S 2A).



Figure 7: DNA sequence motif significantly overrepresented in the intergenic regions upstream of the direct targets of Zcf21p (Bohm *et al.*, 2016).

Putative Zcf21p DNA motif derived from its identified direct targets. A comparison of the transcripts identified via RNA sequencing and *in vivo* binding data (Perez *et al.*, 2013b) revealed the direct targets of Zcf21p. The sequences upstream of these direct targets were extracted and this putative binding motif was overrepresented.

To test if the identified sequence is able to mediate binding of Zcf21p, I purified its DNA binding domain and performed gel-shift assays using a sequence containing the putative wild-type binding motif and sequences containing point mutations either directly in the motif or in the surrounding nucleotides. The purified DNA binding domain of Zcf21p was able to gel-shift a sequence containing the putative wild-type motif, whereas a sequence containing point mutations in the putative binding motif was not shifted (Figure 8A). These results indicate that the short motif that we found upstream of Zcf21p's direct targets of regulation is able to mediate binding of Zcf21p. Introducing point mutations in the sequence surrounding the binding motif did not affect the shifting in contrast to the mutations inside the motif, further confirming that binding of Zcf21p is mediated by the small identified motif (Figure 8B).

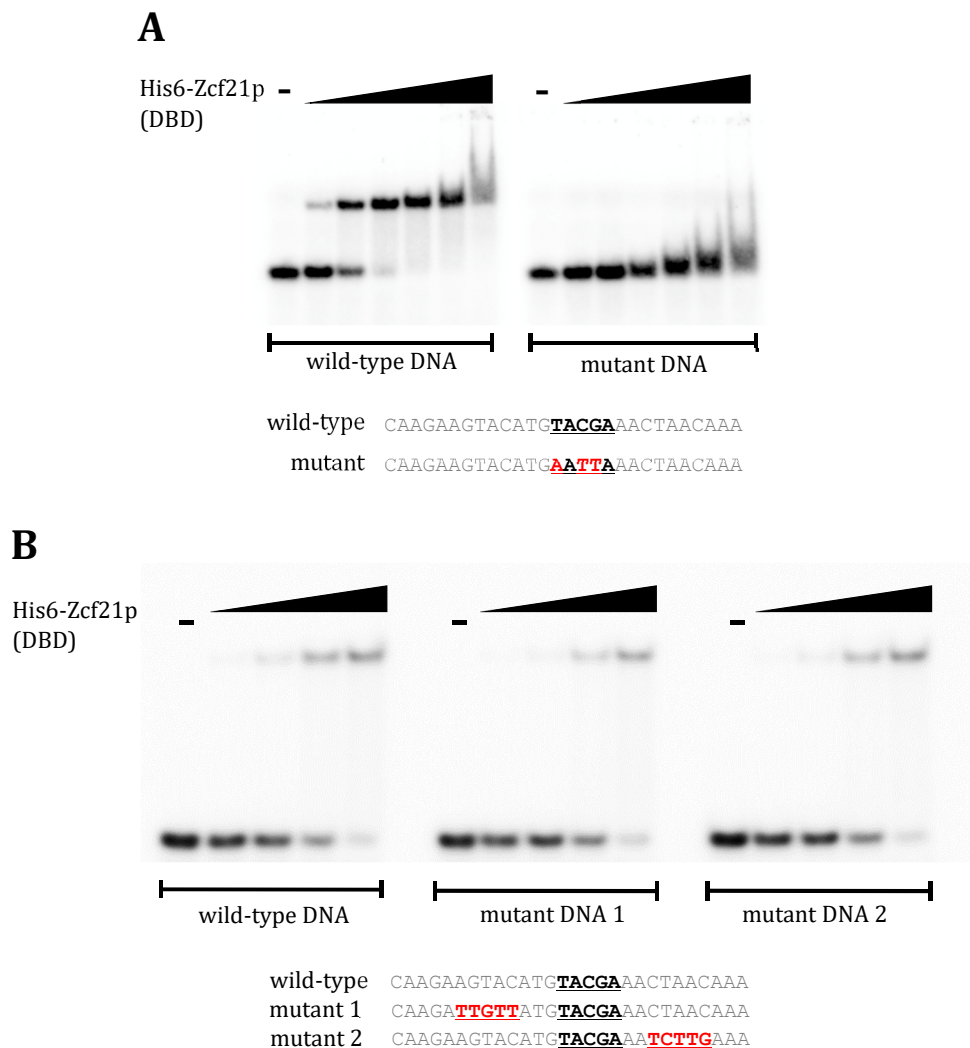


Figure 8: The purified DNA-binding domain of Zcf21p gel-shifts a DNA fragment harboring a wild-type instance of the putative motif (Bohm *et al.*, 2016).

(A) Gel shift assays illustrating binding of the purified DNA binding domain of Zcf21p to the identified motif. Two DNA fragments, one containing a wild-type copy of the predicted motif (upstream of *ORF19.2060*) and one with introduced point mutations inside the predicted motif (indicated in red) were radioactively labeled and incubated with increasing concentrations (0, 0.18, 0.72, 2.8, 11.2, 44.7 and 179 nM) of the purified DNA binding domain (amino acids 96–187) of the Zcf21 protein for 30 min at room temperature in EMSA buffer (chapter 2.3.7). The reactions were run in 6% polyacrylamide gels in 0.5× TGE. The purified DNA binding domain of Zcf21p was not able to shift the fragment containing point mutations in the predicted binding motif.

(B) Point mutations introduced in the surrounding area of the predicted Zcf21p DNA binding motif do not affect binding of the regulator. The DNA fragment containing a wild-type copy of the predicted binding motif (used in Figure 8A) and two additional fragments containing point mutations in the surrounding area of the motif (indicated in red) were radioactively labeled. The three fragments (~0.4 nM) were incubated with increasing concentrations (0, 2.8, 11.2, 44.7 and 179 nM) of the purified DNA binding domain (amino acids 96 to 187) of the Zcf21 protein for 30 min at room temperature in EMSA buffer (chapter 2.3.7). The reactions were run in 6% polyacrylamide gels run in 0.5× TGE. Mutations in the area outside of the predicted binding motif do not affect binding of Zcf21p to its target sequence., in contrast to the mutations within the predicted binding site (Figure 8A).

A similar DNA binding sequence (TCGTATAA) has been reported for Upc2p (MacPherson *et al.*, 2005). The authors of this study tested the DNA binding motif of Upc2p in a gel shift assay and found that it preferentially bound the sequence mentioned above. This observation supports the idea that *ZCF21* and *UPC2* share a recent common ancestor (Figure 4). Taken together, this data shows that Zcf21p exerts its functions by direct binding to a specific DNA regulatory sequence located upstream of its direct targets.

A detailed analysis of the regions upstream of Zcf21p's direct targets of regulation (Figure 6B) revealed that the identified binding sequence occurs in pairs in close proximity to each other but with variable spacers (Figure 9). Furthermore, the binding sites typically occurred >300 nucleotides upstream of the predicted transcription start sites (approximated from our own and published RNA-seq data (Grumaz *et al.*, 2013; Nobile *et al.*, 2012; Tuch *et al.*, 2010).

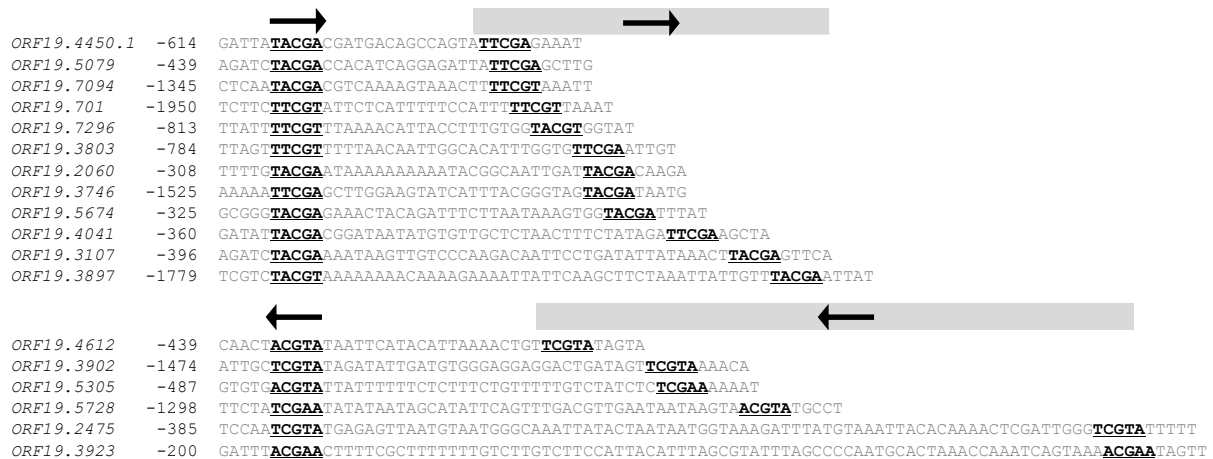


Figure 9: Two instances of the Zcf21p binding motif occur in the intergenic regions upstream of its direct targets (Bohm *et al.*, 2016).

Appearance of the Zcf21p binding motif in the putative promoter regions extracted from its direct targets of regulation. The DNA binding motif of Zcf21p occurs in pairs and >300 bp upstream of the predicted transcription start site.

The fact that the DNA binding sites of Zcf21p appear in pairs in the upstream regions of its direct targets (Figure 9) suggests that this regulator exerts its function by binding as dimer, a hallmark of zinc-cluster DNA-binding proteins (MacPherson *et al.*, 2006). Binding as a dimer to short DNA sequences separated by variable spacers has also been shown for other members of the zinc cluster family of transcription regulators (Perez *et al.*, 2014). To evaluate if two copies of the motif mediate binding of two copies of the regulator, I

performed another gel-shift assay using a DNA fragment containing two instances of the binding motif (Figure 10). I observed two shifts of the radioactive labeled DNA fragment (Figure 10), indicating that the protein occupies both binding sites in the fragment. This observation supports the idea that Zcf21p, as other zinc cluster transcription regulators, carries out its functions by binding to its targets as dimer.



Figure 10: Two instances of the putative binding domain mediate binding of two Zcf21p copies (Bohm *et al.*, 2016).

The DNA binding domain of Zcf21p binds to a DNA fragment containing two wild-type copies of the protein's predicted binding motif. A DNA fragment (located in the intergenic region between *ORF19.1330* and *ORF19.1331*) that contains two wild-type copies of the binding motif was radioactively labeled. The fragment (~0.4 nM) was incubated with increasing concentrations (0, 0.175, 0.7, 2.8, 5.6, 11.2, 22.35 and 44.7 nM) of the purified DNA binding domain (amino acids 96 to 187) of Zcf21p for 30 min at room temperature in EMSA buffer (chapter 2.3.7). The reactions were run in 6% polyacrylamide gels in 0.5× TGE. The DNA binding domain of Zcf21p gel-shifts a DNA fragment containing two instances of the binding motif two times, indicating binding of two copies of the regulator.

The occurrence of the binding sites >300 nucleotides upstream of the predicted transcription start sites suggests that Zcf21p acts as transcriptional repressor, since regulatory yeast proteins that act as transcriptional repressors typically bind at similar positions far away from transcription start sites (Covitz *et al.*, 1993). A detailed analysis of our transcriptome data revealed that more than 75% of Zcf21p's targets are upregulated in the mutant compared to the reference suggesting that Zcf21p represses their expression. Combining the available ChIP data (Perez *et al.*, 2013b) and the transcriptome analysis of this study indicates that Zcf21p binding events take place

almost exclusively in front of Zcf21p-repressed genes (Figure 6B). There was only one exception (*WOR1*). Altogether, these findings strongly support the idea that Zcf21p exerts its functions primarily as transcriptional repressor.

2.4.3) Zcf21p governs expression of cell wall related proteins and enzymes.

The next question to be addressed was which biological functions are controlled by Zcf21p. RNA sequencing revealed a variety of different functions and processes. To find out if there are processes or functions overrepresented among the targets of regulation, I performed a Gene Ontology analysis. This analysis revealed the terms ‘cell surface’ and ‘cell wall’ as significantly overrepresented (p-value = 2.06×10^{-5} including the 54 transcripts that displayed expression changes in at least three of four conditions tested; p-value = 9.18×10^{-9} including 91 transcripts with expression changes in at least two of four conditions). One large group of genes included in the targets of Zcf21p encode for cell surface proteins that play roles in the interaction of *C. albicans* and its mammalian host (Figure 6B): The GPI-anchored protein Rhd3p, for instance, was shown to induce less damage to *in vitro* cell lines and to be less virulent in a mouse model of haematogenously disseminated candidiasis (HDC) (de Boer *et al.*, 2010). Pga26p, another GPI-anchored protein, has been shown to influence filamentation, biofilm formation and virulence in a mouse model of disseminated candidiasis (de Boer *et al.*, 2010; Laforet *et al.*, 2011); Sod5p, a cell surface superoxide dismutase, allows *C. albicans* to survive in the presence of reactive oxygen species (ROS) produced in the oxidative burst reaction by mammalian innate immune cells. Therefore, Sod5p enables evasion from the host immune surveillance *in vivo* (Frohner *et al.*, 2009); two other GPI-anchored proteins, Pga10p and Pga37p, were shown to be involved in processes needed for biofilm formation (Cabral *et al.*, 2014; Perez *et al.*, 2006). Another group of proteins regulated by Zcf21p are cell wall related enzymes: Mnn22p, Mnn4-4p and Bmt7p. These three proteins encode for known or putative mannosyltransferases. Mannosyltransferases are enzymes required for mannan biosynthesis. Mannan is a polysaccharide found in the outer cell wall and can make up to 40% of the cell wall dry weight (Bates *et al.*, 2006; Hall *et al.*, 2013a; Mora-Montes *et al.*, 2010). Taking together, the transcriptome analysis suggested that a major function of Zcf21p in *C. albicans* is to regulate the expression of multiple cell wall determinants including virulence determinants. In addition to cell wall related proteins and enzymes I also found transporters predicted to uptake sugars (Hgt12p and Hgt16p), oligopeptides (Opt2p and Opt4p) and short chain carboxylic acids (Jen2p) among the

targets of Zcf21p. Expression of *HGT12* was shown to be induced by phagocytosis (Lorenz *et al.*, 2004) and in its absence germ tube development inside macrophages is affected (Luongo *et al.*, 2005), indicating a role in *C. albicans* survival inside the host (Luo *et al.*, 2007). Piekarska *et al.* showed that phagocytosis by neutrophils and macrophages induces the expression of *JEN2* (Piekarska *et al.*, 2006), a dicarboxylate plasma membrane transporter. Jen2p is known to transport malic and succinic acids, two non-fermentable carbon sources that may be crucial for *C. albicans* growth inside its host (Vieira *et al.*, 2010). Finally, there were also other transcriptional regulators under control of Zcf21p: Rme1p, a regulator of meiosis in *S. cerevisiae*; Wor1p, a master regulator of white-opaque switching in *C. albicans*; and *ORF19.6888* with unknown functions.

2.4.4) Zcf21p influences the structure of the cell wall.

The transcriptome analysis revealed that multiple cell wall proteins and enzymes predicted to be involved in cell wall related functions are controlled by Zcf21p. This finding suggested that the *zcf21* deletion strain may have an altered cell wall structure. To test this hypothesis, I used compounds that target the cell wall. First, I measured the susceptibility of wild-type, *zcf21* deletion mutant and ectopic *ZCF21* expression strain to Calcofluor white, an anionic dye that interferes with the construction of the cell wall and is commonly used to identify yeast cell wall mutants (Ram *et al.*, 2006). The *zcf21* deletion mutant showed an increased susceptibility to Calcofluor white, whereas the ectopic expression of *ZCF21* resulted in increased resistance compared to the wild-type reference strain (Figure 11A). By using a second anionic dye, Congo red, a chemical that targets β -glucan contained in the cell wall (Figure 11B) I observed similar results: the *zcf21* deletion mutant showed an increased susceptibility to Congo red whereas an ectopic expression mutant was more resistant to Congo red. These results further support the connection between Zcf21p and the cell wall. Adding-back a wild-type copy of the gene to the deletion mutant, restored the wild-type phenotype, confirming that the observed changes in susceptibility are due to the absence of Zcf21p (Figure 11C+D).

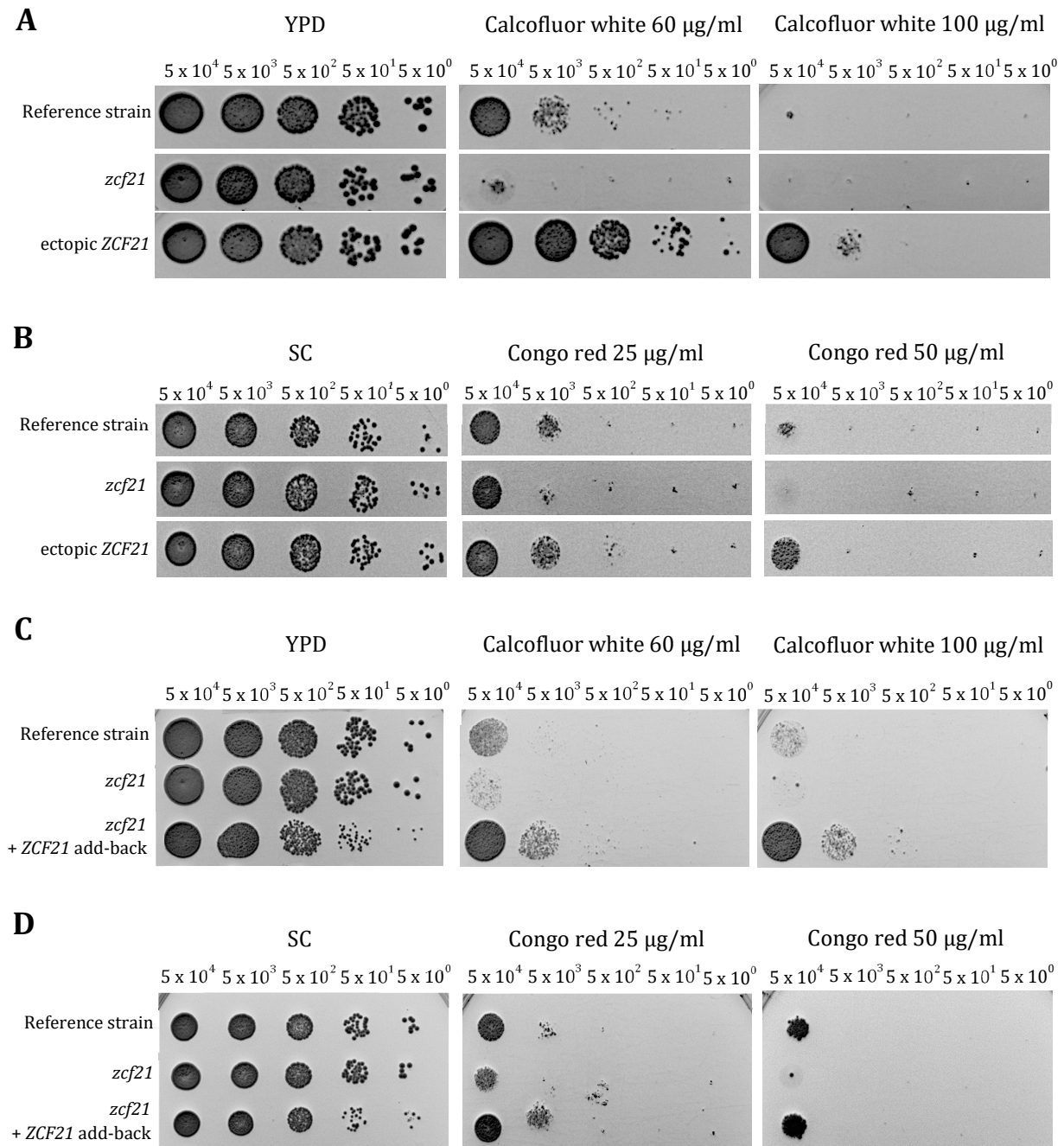


Figure 11: Expression of *ZCF21* influences susceptibility to cell wall intercalating agents (Bohm *et al.*, 2016).

Growth of wild-type reference, *zcf21* mutant and a strain ectopically expressing *ZCF21* on Calcofluor white, a chemical that targets chitin in the fungal cell wall. Cells were grown over night to stationary phase in YPD broth at 30°C. Cells were diluted to 5×10^4 cells/ μl and 10 μl of 10fold dilutions (indicated on top of each picture) were spotted on YPD plates containing either 60 or 100 $\mu\text{g/ml}$ Calcofluor white (A+C) and SC plates containing 25 or 50 $\mu\text{g/ml}$ Congo red (B+D). Growth differences were recorded following incubation of the plates for 24-48 h at 37°C. *zcf21* deletion mutant cells showed increased susceptibility to Calcofluor white (A) and Congo red (B), whereas cells ectopically expressing *ZCF21* showed an increased resistance to both agents compared to wild-type reference cells (A+B). Adding back a wild type copy of the gene restored wild type reference susceptibility to both agents (C+D).

The altered susceptibility of cells either lacking or overproducing *ZCF21* to cell wall intercalating agents are indicative of a role of Zcf21p in cell wall structuring. To further evaluate the link between the regulator and the cell wall, I tested the activity of the *C. albicans* cell wall integrity pathway. To do so, I measured the phosphorylation level of the two major kinases of the cell wall integrity pathway Cek1 and Mkc1. The phosphorylation level of these two kinases and therefore the activity of the cell wall integrity pathway was altered when *ZCF21* was deleted or ectopically expressed (Figure 12), further supporting the idea that this regulator influences the structure of *C. albicans*' cell wall.

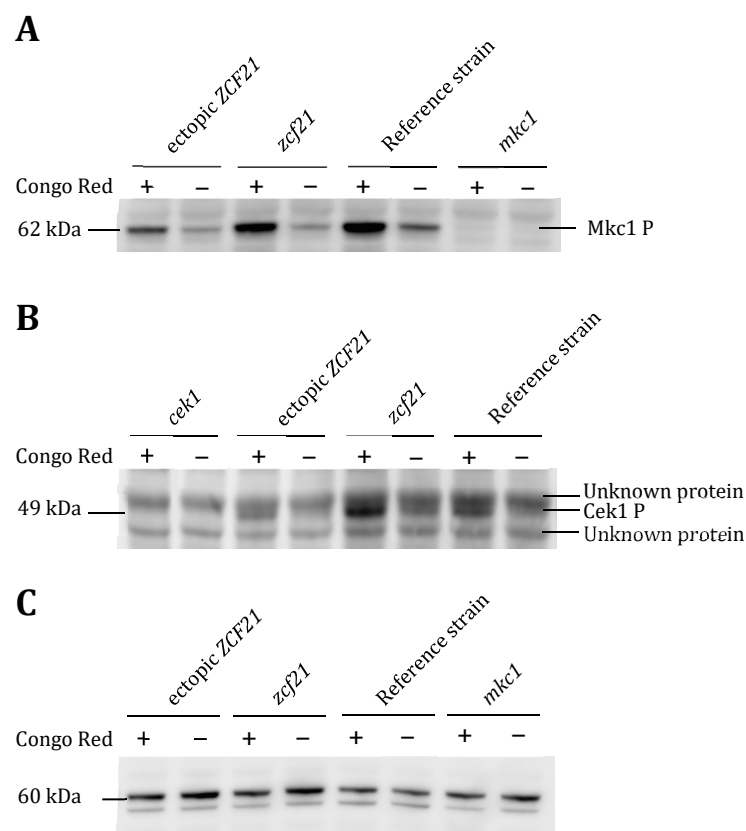


Figure 12: Zcf21p influences the activity of a cell wall integrity pathway (Bohm *et al.*, 2016). Phosphorylation level of Mkc1p and Cek1p was tested in the wild-type reference strain, the *zcf21* deletion mutant, the ectopically expressing *ZCF21* strain and as control an *mkc1* deletion mutant and *cek1* deletion mutant by Western blot analysis. Cells were grown in YPD at 30°C to late exponential phase and exposed to 0.04 mg/ml Congo red 1 h before collecting. Whole cell extracts were prepared and resolved by PAGE. Proteins were transferred to a PVDF membrane and phosphorylated Mkc1p (Mkc1-P) (A) and Cek1p (Cek1-P) (B) were stained using a mouse monoclonal anti-Phospho-p44/42 MAPK (Erk1/2) (Thr202/Tyr204) antibody. As loading control actin was stained using a rabbit polyclonal anti-Actin antibody (C). In (B) two unknown proteins were stained non-specifically. In the strain ectopically expressing *ZCF21* Mkc1p and Cek1p are lower phosphorylated compared to the wild-type reference strain. In the *zcf21* deletion mutant levels of phosphorylated Cek1p are higher compared to the wild-type reference strain.

The next question was if the effects that Zcf21p has on the cell wall of *C. albicans* could be visualized. To this end, I performed transmission electron microscopy (TEM) of wild type reference cells, *zcf21* deletion mutant cells and cells ectopically expressing *ZCF21* to illustrate the overall ultrastructure of the cell wall. I measured the thickness of the inner cell wall of all three strains and found no significant difference (deletion mutant: 146.2 ± 42.3 nm, ectopic expression mutant: 141.2 ± 28.1 nm, reference strain: 160.3 ± 19.1 nm). However, I detected prolonged fibrils in the outermost layer of the cell wall in the *zcf21* deletion mutant (Figure 13) compared to the wild-type and ectopic expression mutant. These results indicate that Zcf21p may have an effect on the constitution and/or distribution of various carbohydrates in the outer cell wall.

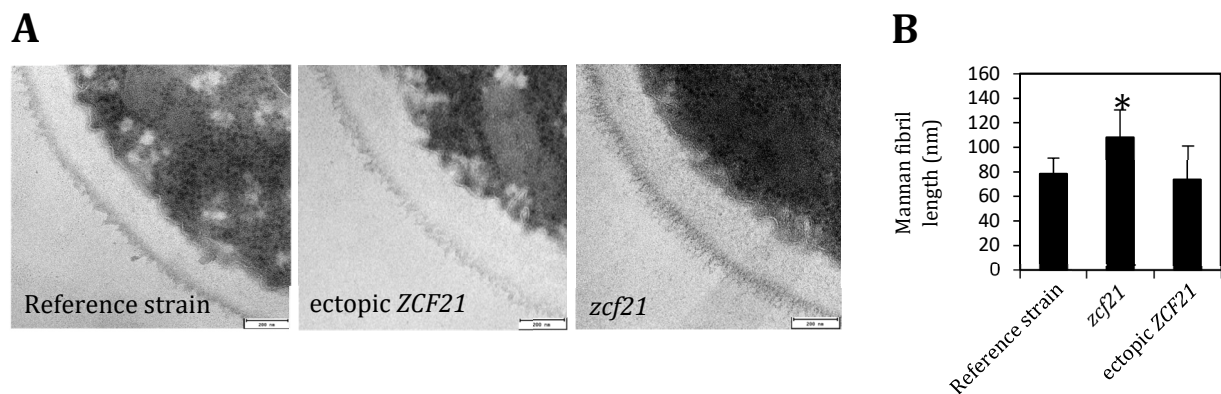


Figure 13: Fibril-like structures on the cell surface are altered in the absence of ZCF21 (Bohm *et al.*, 2016).

(A) TEM images of the cell wall of wild-type reference, *zcf21* deletion mutant and cells ectopically expressing *ZCF21*. Fibrils in the outermost layer of the cell wall are prolonged in the deletion mutant compared to the other two strains.

(B) Bar graph depicting mean and SD of the estimated mannan fibril length of each strain. Measured were 50 randomly selected cells. Each cell was measured in 4 different locations. The mannan fibril length was significantly increased in the mutant compared to wild-type reference and ectopic expression mutant.

To test the hypothesis that Zcf21p affects carbohydrates in the outer cell wall of *C. albicans*, I analyzed the carbohydrates in the cell wall using fluorescently labeled sugar-specific dyes. One dye I used was concanavalin A (ConA)-Texas Red, a dye that specifically stains mannans in the cell wall. Using fluorescence microscopy I detected a stronger signal in the cell wall of the *zcf21* mutant strain compared to either wild-type reference or *ZCF21* ectopic expression strains (Figure 14A), suggesting that the overall amount of mannan in the cell wall is increased when *ZCF21* is absent. FACS analysis confirmed an increase in fluorescence in the *zcf21* deletion mutant cells stained with Concanavalin A – Texas Red

compared to wild-type reference and ectopic expression mutant cells (Figure 14B). These findings are consistent with the prolonged fibril-like structures in the outer cell wall of this mutant strain (Figure 13) since these fibrils are mainly composed of proteins heavily decorated with mannan (Hall *et al.*, 2013a; Hall *et al.*, 2013b).

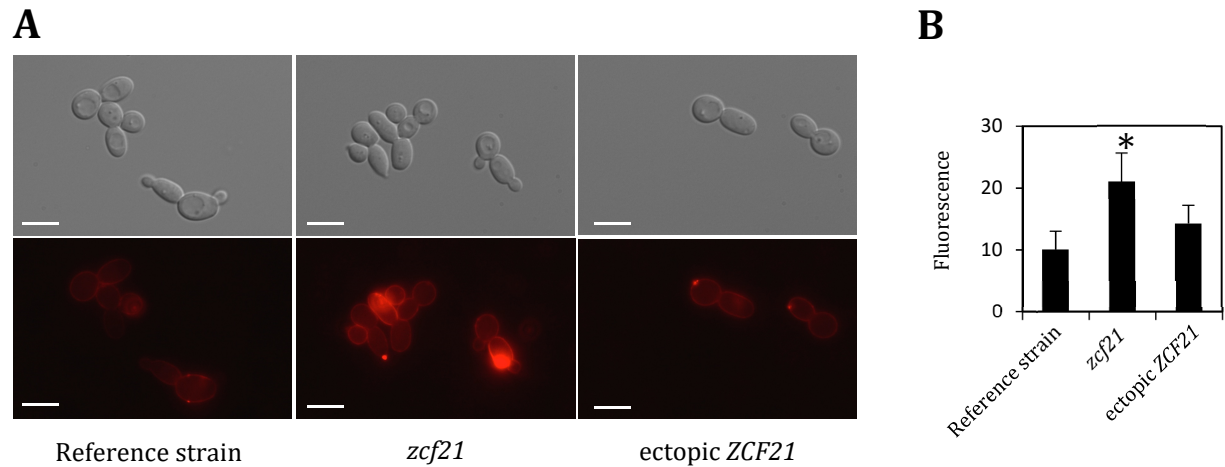


Figure 14: Zcf21p influences the composition of the cell wall (Bohm *et al.*, 2016).

(A) Light- and Fluorescence microscopy pictures of wild-type reference, *zcf21* deletion mutant and *ZCF21* ectopic expression mutant cells stained with Concanavalin A, a chemical that specifically stains mannan in the cell wall. Cells of all strains were grown to mid exponential phase, fixed and stained with Concanavalin A - Texas Red. Scale bars in the left lower corner of the pictures represent 7.5 μm . In all fluorescence pictures the exposure is standardized. *zcf21* deletion mutant cells display a higher intensity of the mannan staining compared to wild-type reference and ectopic expression mutant, suggesting a higher amount of cell surface mannan when *ZCF21* is absent.

(B) Bar graph depicting the mean and SD of the fluorescence associated with each strain. Fluorescence was determined by FACS analysis of mid exponential phase cells, fixed and stained with Concanavalin A-Texas Red. The *zcf21* deletion mutant cells showed an increased fluorescent signal when stained with Concanavalin A - Texas Red compared to wild-type reference and ectopic expression mutant.

To determine if the content of phosphomannan, a specific subtype of the cell surface mannan, is affected when *ZCF21* is absent, cells were stained with Alcian blue. Alcian blue is a cationic dye that binds to the negatively charged phosphomannan at the cell surface and is commonly used to quantify its content (Hall *et al.*, 2013a; Mora-Montes *et al.*, 2010). The *zcf21* mutant displayed similar amounts of phosphomannan at the cell surface as the wild-type reference strain (Figure 15). Therefore, the increase in cell surface mannan in the *zcf21* deletion mutant is not due to changes in the phosphomannan content.

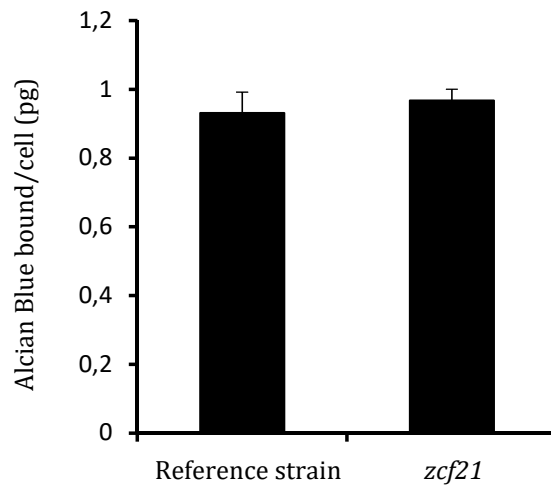


Figure 15: Deletion of *ZCF21* does not affect the phosphomannan content in the cell wall (Bohm *et al.*, 2016).

Bar graph representing the amount of Alcian Blue bound per *C. albicans* cell. Alcian Blue specifically binds to phosphomannan in the cell wall. Cells were grown in YPD medium, 1×10^7 wild-type or *zcf21* mutant cells were incubated with 30 $\mu\text{g}/\text{ml}$ Alcian Blue and the ability to bind Alcian Blue was measured. Data represent the mean amount of dye bound per cell + SD from three independent experiments performed in triplicates.

The other dye I used to analyze Zcf21p's effects on carbohydrates of the cell wall, was wheat germ agglutinin (WGA)-Alexa Fluor® 488. This dye stains specifically chitin, a sugar typically located adjacent to the cell membrane and only accessible for WGA-Alexa Fluor® 488 in budding areas where it gets exposed (Hall *et al.*, 2013a). I performed FACS analysis of wild-type reference, *zcf21* deletion mutant and *ZCF21* ectopic expression mutant cells grown to mid exponential phase in YPD at 30°C and stained with WGA-Alexa Fluor® 488. With this analysis I found an increase in fluorescence in the *zcf21* deletion mutant strain (50%) and in the strain ectopically expressing *ZCF21* (2-fold) compared to the wild-type reference strain (Figure 16B). To further analyze the chitin in the cell wall depending in Zcf21p, I performed fluorescence microscopy of cells treated in the same way as for FACS analysis. Thereby, I found that in wild-type reference and *zcf21* mutant cells only the chitin exposed in budding areas was stained, albeit in the mutant with higher intensity. In contrast, cells ectopically expressing *ZCF21* fluorescence microscopy revealed that WGA-Alexa Fluor® 488 stained the cell wall of about 35% of the cells (Figure 16A). This finding suggests that ectopic expression of *ZCF21* induces cell wall rearrangements leaving chitin no longer restricted to the inner cell wall layer. Altogether

these findings suggest that the transcriptional regulator Zcf21p affects on the one hand the overall amount of mannan exposed to the cell surface and on the other hand the accessibility of chitin in the cell wall.

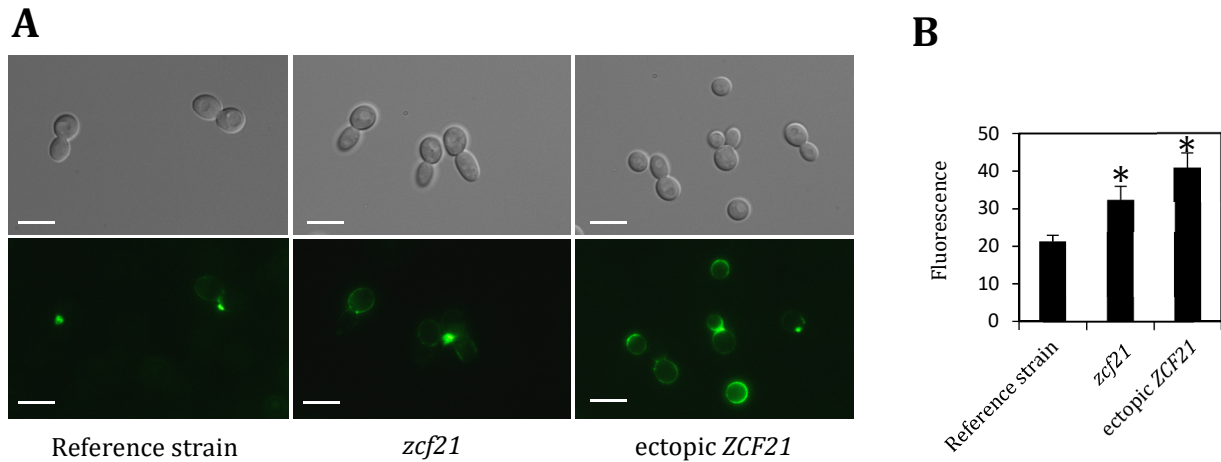


Figure 16: Zcf21p influences the structure of the cell wall (Bohm *et al.*, 2016).

(A) Light- and Fluorescence microscopy pictures of wild-type reference, *zcf21* deletion mutant and ZCF21 ectopic expression mutant cells stained with Wheat germ agglutinin, a chemical that specifically binds chitin in the cell wall. Cells of all strains were grown to mid exponential phase, fixed and stained with WGA - Alexa Fluor® 488. Scale bars in the left lower corner of the pictures represent 7.5 μm . In all fluorescence pictures the exposure is standardized. Wild-type reference and *zcf21* deletion mutant cells display staining of budding areas. *zcf21* deletion mutant cells with higher intensity. In the ectopic expression mutant WGA stained whole cell walls of about 35% of the cells.

(B) Bar graph depicting the mean and SD of the fluorescence associated with each strain. Fluorescence was determined by FACS analysis of mid exponential phase cells, fixed and stained with WGA-Alexa Fluor® 488. The *zcf21* deletion mutant and the ectopic expression mutant cells showed an increased fluorescent signal (50% and 2-fold, respectively) when stained with WGA-Alexa Fluor® 488 compared to wild-type reference cells.

2.5) Discussion

In this part of the thesis, I have indicated that the transcriptional regulator Zcf21p, previously identified as a virulence factor in *C. albicans*, plays a vital role in defining the composition and structure of the cell wall. Transcriptome analysis revealed that genes encoding for cell wall proteins and enzymes that are predicted to be involved in cell wall-related processes are overrepresented in the targets of Zcf21p (Figure 6B, Figure S 1). Supporting the idea that Zcf21p is important to the structuring of the cell wall, I found increased susceptibility in a strain ectopically expressing *ZCF21* and increased resistance in a *zcf21* deletion mutant strain to chemicals that are commonly used to identify cell wall mutants in *C. albicans* (Figure 11). TEM further confirmed alterations in the outer layer of the cell wall in the *zcf21* deletion mutant compared to the reference strain (Figure 13). Sugar-specific stainings uncovered qualitative and quantitative differences in the total amount of mannan and the chitin exposed to the surface in the *zcf21* deletion and the *ZCF21* ectopic expression mutants (Figure 14, Figure 16). Mammalian macrophages phagocytose and kill the *zcf21* deletion mutant strain more efficiently than the wild type (Muralidhara, 2015), whereas the ectopic expression of *ZCF21* results in decreased phagocytosis and increased survival (Muralidhara, 2015). This phenomenon implies that *ZCF21* impacts the recognition and killing of *C. albicans* cells by murine macrophages. Together, these findings prove that *ZCF21* controls the composition and structure of the *C. albicans* cell surface, possibly leading to an altered interaction between fungal and host immune cells.

The complex structure of the cell wall in *C. albicans* seems to require an interplay of various global transcriptional regulators known to control the expression of cell wall-related genes: *EFG1* (Sohn et al., 2003), *BCR1* (Nobile et al., 2005), *RIM101* (Nobile et al., 2008), *TUP1*, and *NRG1* (Bastidas et al., 2009; Braun et al., 2001; Murad et al., 2001a; Murad et al., 2001b), for instance. All these regulators were demonstrated to be highly pleiotropic in a large-scale phenotypic screening (Homann et al., 2009). Conversely, the deletion of *ZCF21* results in neither significant growth defect nor gross colony morphology phenotypes under any of a large set of *in vitro* conditions (Homann et al., 2009), suggesting that this regulator controls more-defined processes.

The combination of *in vitro* (Figure 8) and *in vivo* (Figure 6B) experiments described in this section indicates that Zcf21p directly binds to the putative promoter regions of a number of its target genes, implying that it controls its functions via direct transcriptional

control (Figure 17A). Based on the transcriptome data, this regulator seems to function mainly by repressing the transcription of its targets (Figure 6B, Figure 9). The regulation of the expression of cell surface determinants differs in other transcriptional regulators: *BCR1* and *RIM101* promote (Nobile et al., 2005; Nobile et al., 2008) while *TUP1* and *NRG1* repress the expression of cell surface genes (Bastidas et al., 2009; Braun et al., 2001; Murad et al., 2001a; Murad et al., 2001b). *EFG1* can have positive and negative effects (Sohn et al., 2003). Since many regulators in *C. albicans* control the expression of overlapping (but not identical) sets of cell wall components, they may exert their effects at disparate times or in response to different stimuli (Perez et al., 2013b). Another explanation for overlapping target genes is that these regulators are all needed simultaneously to generate the complex pattern of gene expression required for an appropriate cell surface. Fusion to a GFP reporter disclosed that *ZCF21* is transcribed at relatively high levels irrespective of media and growth conditions (data not shown), indicating that *ZCF21* is constitutively expressed in the cell. *ZCF21*'s role in the complex composition and structure of the cell wall in *C. albicans* might thus be to keep the expression of cell wall components down and thereby set a default state for their expression. Whenever these components are necessitated, transcriptional activators such as the ones described above can then induce their expression (Figure 17A).

In addition to regulating cell wall components, *ZCF21* seems to control the expression of genes involved in other cellular functions, some of which may influence growth in the host. Two such functions controlled by *ZCF21* are nutrient acquisition and copper-dependent processes. *ZCF21* controls the expression of several transporters required for nutrient acquisition in the host: the oligopeptides transporters *OPT4* and *OPT2*, as well as transporters predicted to uptake sugars (*HGT12* and *HGT16*) and short-chain carboxylic acids (*JEN2*). The ability of *C. albicans* to assimilate a large assortment of nutrients in the mammalian host, non-fermentable carbon sources included, seems to be essential for virulence (Vieira et al., 2010). *JEN2*, for example, a malate and succinate transporter, is highly expressed when *C. albicans* is phagocytosed by macrophages (Piekarska et al., 2006); malate and succinate are two non-fermentable carbon sources that may be crucial for *C. albicans*' growth in the host (Vieira et al., 2010). However, I found various surface and cytoplasmic enzymes in the targets of *ZCF21* that bind to extracellular or intracellular copper (*SOD5* and *FET99* [Figure 6B]; *CUP1*, *FRE7*, *FRE30*, and *FET33* [Figure S 1B]), which signifies that regulating the copper level is another function *ZCF21* is involved in. Copper

is an essential metal in most cells, but when it accumulates to levels beyond cellular needs, it can be toxic to invading microorganisms (Festa et al., 2012). As a result, pathogenic bacteria and fungi developed mechanisms to survive in the presence of high copper levels (Festa et al., 2012). *ZCF21*'s role in regulating the expression of copper-related genes may therefore be conducive to the overall fitness of *C. albicans* during systemic infection.

The last group of genes whose expression depends on *ZCF21*, based on our dataset, are other transcriptional regulators. We found *WOR1*, a master regulator of white-opaque switching, in *C. albicans* (Lohse et al., 2008; Soll, 2004). It was revealed to be a factor in mouse gut colonization (Pande et al., 2013), but contrary to the reduced fitness of the *zcf21* mutant (Perez et al., 2013b), the *wor1* mutant exhibits wild-type fitness in the standard murine model of disseminated candidiasis (J.C. Pérez and A.D. Johnson, unpubl. results). It thus remains unclear whether an upregulation of *WOR1* affects *Candida*'s infections and whether the activity of *ZCF21* plays a role. The other transcriptional regulators in the targets of *ZCF21* include *RME1*, which controls meiosis in *S. cerevisiae* but has no known function in *C. albicans*, and *ORF19.6888*, which has no known functions. *Candida albicans* requires the coordination of multiple cellular functions, such as cell surface remodeling (Gow et al., 2011; Hall, 2015), yeast-to-filament transition (Lo et al., 1997; Xu et al., 2015), and metabolic flexibility (Brown et al., 2014; Lorenz, 2013), to mount a systemic, disseminated infection. In a simplistic model, each of these processes is controlled by a specific non-overlapping set of transcriptional regulators; nevertheless, a more interconnected scenario seems more likely (Perez et al., 2013a). It has been proven, for example, that regulators known to control these functions govern more than a singular cellular function. In the case of the transcriptional regulators *RTG1*, *RTG3*, and *HMS1*, acknowledged to be crucial for systemic infections (Perez et al., 2013b), they control the expression of genes involved in metabolism and yeast-to-filament transition. Similarly, *ZCF21* is involved in the regulation of cell surface remodeling (Figure 6) but also controls the expression of nutrient acquisition genes (Figure 6), which implies that it may contribute to metabolic flexibility.

Among the targets of regulation of *ZCF21*, at least three genes have reported virulence defects in the standard mouse model of disseminated candidiasis: *PGA26* (Laforet et al., 2011), *RHD3* (de Boer et al., 2010), and *ALS1* (Fu et al., 2002). The expression of all three genes was higher in the *zcf21* deletion mutant compared to the wild-type reference strain when grown *in vitro* (Figure 6B), indicating that not only the absence of these genes but

also their overexpression may impact *Candida's* fitness in the host. The *zcf21* mutant strain presents extensive cellular aggregation in response to TOR inhibition (Muralidhara, 2015). The formation of these aggregates could be connected to the adhesin *ALS1*, since the double deletion mutant *zcf21 als1* no longer exhibited this phenotype (Muralidhara, 2015). The single *als1* deletion mutant demonstrated no effect on virulence in a mouse model of disseminated candidiasis (data not shown); we therefore postulate that the *zcf21* virulence phenotype results from the combined effect of several of its targets of regulation, including GPI-anchored proteins, changes in the mannan content (Figure 16A, Figure 17B), and rearrangements in the cell wall that expose chitin to the surface (Figure 16B, Figure 17B). Consistent with this notion, alterations in mannoprotein content and structure (Hall et al., 2013a; Mora-Montes et al., 2010), as well as chitin (Wagener et al., 2014), are recognized as key determinants of the immune response to *C. albicans*.

The fact that the regulators known to control the abovementioned processes are connected with one another through transcriptional feedback and feed-forward loops supports the idea of a more interconnected regulation of *C. albicans* traits (Perez et al., 2013b). Having a complex network controlling the functions that *Candida* needs to proliferate may allow the fungus to adequately coordinate the expression of gene products required for the adaptation to different environments in the host. Alternatively, the high levels of interconnectedness observed in these transcriptional circuits may simply be the consequence of natural drift and not reflect a particular adaptive value (Sorrells et al., 2015).

Perez et al. identified a large gene network in *C. albicans* that regulates the proliferation of the fungus in two host niches. In this network, two nodes, *ZCF21* and *LYS14*, exposed a phenotype in a mouse model of disseminated candidiasis but not in a murine model of commensalism. Both regulators control cell wall-related genes, suggesting that regulating the composition of the cell surface is particularly relevant in the pathogenic phase of *C. albicans*. A comparison to genes known to be upregulated in *C. albicans* cells that reside in the murine intestine (Rosenbach et al., 2010) revealed no overlap with the targets of *ZCF21* or *LYS14* but with the targets of the regulators *RTG1/3*, which displayed a phenotype in the murine model of commensalism. These observations establish that even though *Candida's* growth in the host is controlled by a complex and interconnected network, it is possible to identify biological functions and sets of genes tailored to particular needs of one or another niche.

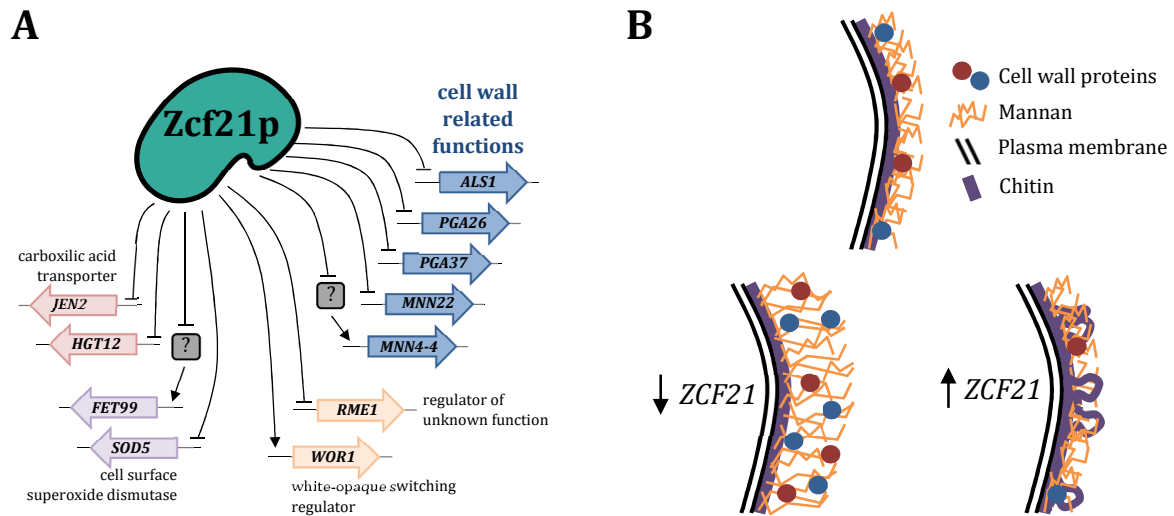


Figure 17: Model depicting how cell surface components, virulence determinants included, are controlled through ZCF21 in *C. albicans* (Bohm *et al.*, 2016).

A. The zinc cluster transcription factor Zcf21p regulates the expression of various cell surface components including GPI-anchored proteins such as *PGA26* and *PGA37*, cell wall remodeling enzymes like *MNN22* and adhesins like *ALS1*. Moreover, it has an effect on the expression of other cell wall determinants, the mannosyltransferase *MNN4-4*, for example, presumably indirectly. The circuitry that promotes transcription of cell surface genes was shown to include other regulators like Efg1p and Bcr1p. Additionally to cell surface components, Beside the regulation of cell surface determinants Zcf21p regulates the expression of two other group of genes: other transcriptional regulators like *WOR1* (governing white-opaque switching) and *RME1* (with unknown functions in *C. albicans*) and genes involved in nutrient acquisition and copper related enzymes.

B. The cell surface of *C. albicans* changes remarkably depending on ZCF21. When the regulator is absent, the fibril like structures of the outermost layer of the cell wall are prolonged and the mannan content is increased. These findings correlate with higher rates of phagocytosis and elimination by macrophages. Ectopic ZCF21 expression induces rearrangements of the cell wall leaving chitin no longer restricted to the plasma membrane, presumably correlating with less phagocytosis and reduced killing by macrophages.

3) *C. albicans* morphology is a key determinant of gut colonization in gnotobiotic mice.

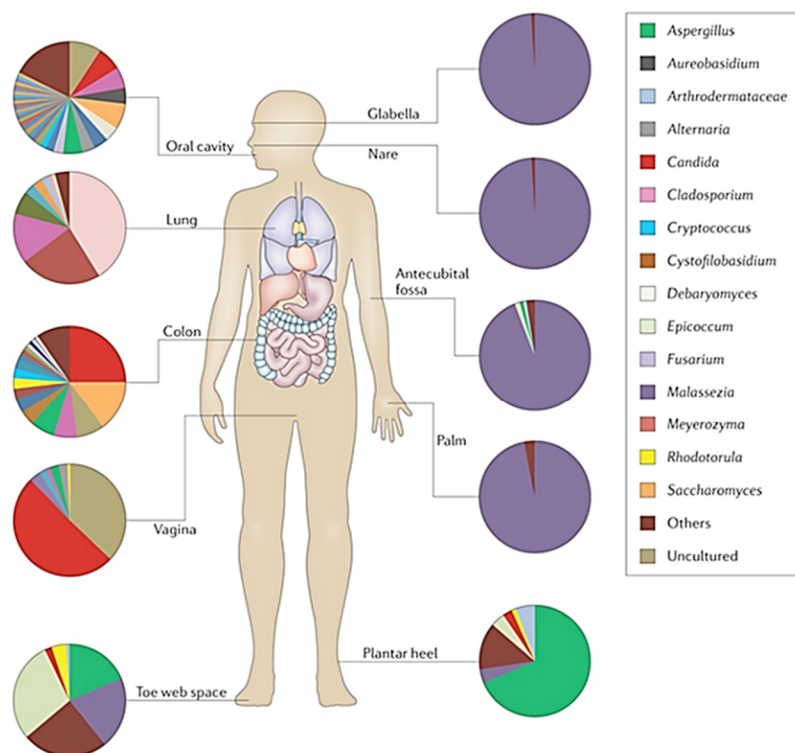
3.1) Summary

Our lab established gnotobiotic mice monocolonized with *C. albicans* as a well-defined experimental system that can be used to explore the biology of the fungus in the mammalian intestine. Mice monocolonized with *C. albicans* present no overt signs of illness, indicating that the fungus maintains its commensal state in this experimental setup. I used classical histology and immunohistochemistry to visualize *C. albicans* at the interface between the fungus and the intestinal mucosa. These analyses illustrated that *C. albicans* largely adopts the oval yeast form in this niche. This contrasted the mixed morphologies observed in antibiotic-treated conventionally raised rodents. I moreover conducted a genetic screen to identify *C. albicans* regulators of gut colonization. This screening found four previously undescribed factors that are fundamental in gut colonization. Phenotypic analysis of the factors unraveled a connection between three of them and the morphology of the fungus, supporting the notion that morphology plays an important role in gut colonization of this animal model. Furthermore, I discovered a defect in the adherence of these three regulators to mucus containing-surfaces. Overall, my results indicate that morphology and adherence are critical to the fitness of *C. albicans* in the intestine of germ-free animals.

3.2) Introduction

3.2.1) Gut colonization by *Candida albicans*.

C. albicans is the most prominent fungal species that resides in humans. It colonizes several different sites of the human body, such as the skin, tongue, and GI tract, without causing any obvious harm (Figure 18). It is thus believed to live there mostly as a commensal.



Nature Reviews | Immunology

Figure 18: *Candida albicans* colonizes different locals of the human body (Underhill *et al.*, 2014).

Besides the well-studied microbiota, describing bacterial species associated with the human body, there is also a so called mycobiota associated with healthy humans that describes fungal species. It has been shown, that the skin and all mucosal surfaces of the human body are colonized by different fungal species. In the scheme depicted here different niches if the human body colonized by fungal species are shown. For each local a pie chart represents the composition of the fungi that were found to colonize this niche. *C. albicans* depicted in red is known to be associated with the oral cavity, the plantar heel the toe web space the vagina and the colon, without causing disease (Underhill *et al.*, 2014).

However, the very same organism can cause severe infections, either localized infections where the fungus overgrows in one specific organ—for example, the female genitourinary tract—or systemic, life-threatening infections where the fungus colonizes nearly every organ in the human body. Many of these harmful infections are thought to originate in the GI tract of the infected individual (Odds, 1987). To understand how the very same organism that lives in the GI tract of most healthy adults without causing any harm can become a life-threatening pathogen, we first must understand the biology of this fungus colonizing this niche.

3.2.2) **Mouse models to study *Candida albicans* gut colonization.**

Fungal gastrointestinal colonization and dissemination are typically studied in laboratory mice. It should be noted that mice are no natural hosts of *Candida albicans* (Huppert et al., 1955; Naglik et al., 2008). When *C. albicans* is orally gavaged to adult mice carrying their normal indigenous microbiota, the fungus is rapidly outcompeted by the indigenous flora.

Antibiotic-treated mouse model. One way to use conventional animals to study gut colonization by *C. albicans* is to reduce the indigenous flora before colonization. This is generally achieved using an antibiotic cocktail in the drinking water. When *C. albicans* is orally gavaged to these pretreated animals, it can persist in the GI tract, and these animals can then be used as *in vivo* models to study gut colonization by the fungus. One caveat of this mouse model is the undefined remaining flora. It is well known that the indigenous flora of conventional mice varies widely depending on age, nutrition, and the vendor. This observation and the additional unselective reduction using an antibiotic cocktail leads to an undefined remaining flora that may confound studies on the colonization by *C. albicans*.

Dietary mouse model. Another way to use conventional mice to study gut colonization by *C. albicans* is to administer a specific purified diet (Yamaguchi et al., 2005) to the mice before colonization or the oral application of regular dosages of *C. albicans* mixed with food powder (Samonis et al., 1990). It has been reported that both models yield considerable amounts of the fungus in stool samples but are not widely used mostly due to the complicated experimental setup.

Germ-free mouse model. Pioneering studies in the 1960s and '70s demonstrated that the GI tract of germ-free raised mice can be colonized stably by *C. albicans* (Clark, 1971; Phillips et al., 1966). These animals are raised in a completely microbe-free environment in sterile containers (Figure 19) and therefore do not harbor any microbes in their GI tracts.



Figure 19: Sterile containers used to raise and maintain germ-free mice.

A germ-free colony of mice requires breeding in sterile containers. Nowadays, flexible film isolators are used to maintain a germ-free environment, not that heavy, expensive, and way more flexible than stainless steel containers used in the past. Before food, water, and other supplies are transferred to the mice, everything needs to be sterilized. Pictures were taken in the germ-free mouse facility in Stockholm, Sweden where the animal experiments described in this thesis were conducted.

Oral gavage of *C. albicans* to these animals produces a persistent gut colonization by the fungus without the need of antibiotics (Clark, 1971; Phillips et al., 1966). Monocolonized (gnotobiotic) animals are healthy and exhibit no overt signs of disease. Because of its low complexity, this animal model could be used as a starting point to dissect the mechanisms of host colonization by *C. albicans*.

Neonatal mouse model. The composition of the gut microbiota in the neonatal mammalian host differs remarkably from that in human adults (Wang et al., 2009). Since the expression of gut immune effectors such as antimicrobial peptides and cytokines are stimulated by the indigenous flora (Cash et al., 2006), the composition of these molecules differs as well. The gut of neonatal mammalian hosts is thus more predisposed to *Candida* colonization and dissemination. Infant mice (five-to-seven days old) can be colonized by *C. albicans* (Domer, 1988; Pope et al., 1979), and no antibiotics are needed. Gut colonization persists up to 20 days post oral gavage. Afterward, when the mice grow up and start to establish a more adult indigenous flora, *Candida* is outcompeted.

3.2.3) *Candida albicans* morphologies.

Candida albicans is a polymorphic yeast that can adopt multiple distinct morphologies depending on environmental conditions (Figure 20): amongst others a unicellular yeast form, one of two filamentous forms (pseudohyphae or hyphae), and a chlamyospore form (Sudbery et al., 2004). In addition to differences in its morphology, its multiple cell types have been revealed to be associated with differences in the mode of division, occurrence, and virulence potential (Noble et al., 2017).

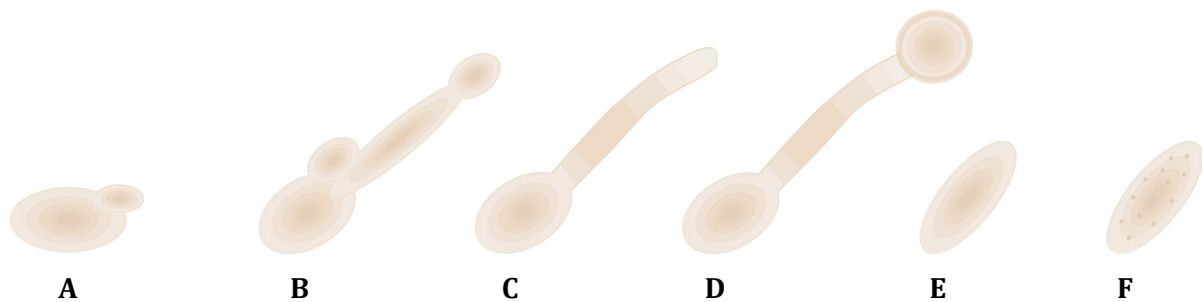


Figure 20: *Candida albicans* is a polymorphic yeast.

The opportunistic pathogen *Candida albicans* adopts several different morphologies. The ability to switch between these different morphologies enables the fungus to colonize different niches of its host. (A) Oval-shaped yeast form. Traditionally considered to be associated with *C. albicans* commensal state but possesses also features of invading important for virulence. (B) Pseudohyphal form and (C) hyphal form. Filamentous forms of *C. albicans* are traditionally associated with pathogenicity exhibiting mechanisms to invade tissue and evade the immune system. (D) Chlamyospore. Thick-walled cell, formed at hyphal tips. This form is induced under harsh *in vitro* conditions. (E) GUT cell. Cell form believed to be specialized for living commensally in the gastrointestinal tract. (F) Opaque cell. Mating associated morphological form with superior fitness in skin colonization.

The round-shaped yeast cells replicate by budding. Nuclear division occurs at the junction between mother and daughter cell (Sudbery et al., 2004; Whiteway et al., 2007). The yeast morphology is traditionally considered to be associated with *C. albicans*' commensal state (Noble et al., 2017); however, diverse processes known to be important for virulence, including colonization and rapid dissemination to host tissues, adhesion to host cell surfaces, and biofilm formation, are features of this morphological form as well (Gow et al., 2002; Odds, 1988). *C. albicans* forms two filamentous forms, hyphae and pseudohyphae. Hyphae are prolonged filamentous cells that remain attached after cytokinesis. After nuclear division, which occurs inside

daughter cells, one nucleus returns to the mother cell. After cytokinesis, cells remain firmly attached. Following cell divisions thus generate multicellular, filamentous structures called mycelia (Whiteway et al., 2007). Pseudohyphal cells exhibit characteristics of both cell types, yeast and filamentous cells. Nuclear division occurs at mother–daughter junctions as it does in yeast cells. After cytokinesis, cells remain attached and form mycelia, the same as in hyphal cells, but the junctions remain visible through indentations (Noble et al., 2017). Hyphal cells are traditionally associated with pathogenicity in *C. albicans*; they can invade epithelial cell layers (Kumamoto et al., 2005), damage endothelial cells (Kumamoto et al., 2005; Zink et al., 1996), and when phagocytosed, they can induce the lysis of macrophages and neutrophils (Korting et al., 2003; Lo et al., 1997). Finally, chlamydospores are large round cells with thick cell walls (Fabry et al., 2003). This cell form develops at the ends of hyphal filaments under certain harsh *in vitro* conditions, such as starvation and hypoxia (Martin et al., 2005). After nuclear division in a suspensor cell, one nucleus migrates to the chlamydospore, while the newly formed chlamydospore remains attached to its mother cell (Martin et al., 2005).

Its ability to switch between different morphological forms enables *C. albicans* to adapt to diverse conditions present in the different niches of its host. In the GI tract, for instance, cells must be able to adhere to the mucosal surface to prevent being flushed out (Kennedy, 1988; Kennedy et al., 1985). Moreover, to cause disease, cells must be able to invade host tissues. The yeast–hyphal transition is particularly important for the virulence of the fungus, since mutants that are trapped in one morphological form were proved to have altered virulence capacities: cells genetically manipulated to form only yeast cells display a severe virulence defect in mouse models of systemic candidiasis (Lo et al., 1997). When this strain is induced to perform a yeast–hyphal transition, virulence can be restored (Saville et al., 2003). Conversely, cells that can form only hyphae were verified to be more virulent in a mouse model of systemic candidiasis (Carlisle et al., 2009).

Apart from adopting the three major morphologies, *C. albicans* can assume other less prominent and/or less defined morphologies, including opaque and gray cells, two forms that the fungus adopts depending on mating. Opaque cells have been reported to have superior fitness during skin colonization (Kvaal et al., 1999; Xie et al., 2013), and grey cells may be the fastest proliferating cell type in an *ex vivo* tongue infection model (Tao et al., 2014). Another morphology is the gastrointestinally induced transition (GUT) cell

type, which has been proposed to exhibit higher fitness in the mammalian GI tract (Pande et al., 2013).

3.2.4) Gnotobiotic mouse models

The term “gnotobiotic mouse” refers to the fact that the exact composition of the flora of the animal is known (Carter et al., 2006). In practice, this typically means that a germ-free animal is inoculated with one or more microbial species. Contact with microorganisms present in the mother’s vagina and skin must be precluded to generate germ-free organisms. This can be achieved by Caesarean section or hysterectomy (Martin et al., 2016). Another possibility is to transfer cleansed embryos to germ-free recipient mothers under well-controlled conditions. The advantage of this technique is that the mother delivers normally and can care for her offspring, thus enhancing the survival rate of her offspring. Germ-free animals are maintained in a sterile environment in sterile isolators (Figure 19) throughout their lives. When a stable colony of germ-free animals has been established, they can be used to enlarge the colony by crossing germ-free individuals (Martin et al., 2016).

The rationale for using gnotobiotic organisms in research is that they combine some features of conventional animals with the controlled nature of *in vitro* experiments. *In vitro* experiments cannot represent the *in vivo* complexity of an animal colonized by its indigenous microflora. Conventional animals, however, represent the complex *in vivo* conditions but have features that cannot be controlled or remain unknown. Instead, gnotobiology enables the controlled *in vivo* examination of the effect of one specific member of the microbiota on its host. Furthermore, microbe–microbe interactions can be assessed directly in a more complex environment (Martin et al., 2016).

The first experiments using gnotobiotic organisms were performed at the end of the 19th century to test Pasteur’s assertion that animals are in such a close relationship with their indigenous microbiota that they cannot survive when raised in a sterile environment (Bibiloni, 2012; Gordon et al., 1971; Luckey, 1963; Luckey, 1965). In the 1940s and ’50s, it was established that animals can actually live without contact with microbes (Gustafsson, 1948). In the 20th century, several laboratories with germ-free facilities were built in Europe, the United States, and Japan, and scientists started to use gnotobiotic animals to study different aspects of host–microbe interactions (Kubelkova et al., 2016). These studies have mainly addressed the immune system (Cebra, 1999; Hooper et al., 2012), structural functions and metabolism (Backhed et al., 2010; Karlsson et al., 2013;

Tilg et al., 2011), the development of vertebrate functional systems (Butler et al., 2009; Grover et al., 2014; Thompson et al., 1971; Umesaki, 2014), carcinogenesis (Brawner et al., 2014; Bultman, 2014; Francescone et al., 2014; Schwabe et al., 2013; Tlaskalova-Hogenova et al., 2014), and host–pathogen interactions and reveal that organisms must contact microbes for their well-being and optimal health (Kubelkova et al., 2016). These studies have confirmed links between altered microbiota and differences in epithelial cell renewal, architecture, and differentiation (Cherbuy et al., 2010); intestinal motility (Falk et al., 1998); and host glycosylation patterns and gene expression (Hooper et al., 2001). Moreover, microbes with key roles in the development of the intestinal immune system have been identified (Umesaki, 2014; Umesaki et al., 2000). Studies on host–pathogen interactions using gnotobiotic animals have the advantage that their nearly naïve immune systems provide a base for studying interactions during very early colonization and infection. Basic microbiological and immunological questions, vaccine development, and general questions on commensal–pathogen transition were therefore perfectly suited to being studied using this animal model.

Here, I employ gnotobiotic mice mono-colonized with *Candida albicans* to study basic aspects of the biology of this fungus in the mammalian intestine. Using classical histological stainings and immunohistochemistry, I found that the fungus colonizes this niche in close proximity to the mucus layer, and it does so mostly in its round-shaped yeast form. A genetic screening of a transcription factor mutant library identified four previously undescribed factors that contribute to the colonization of the GI tract. Mutations in the identified genes resulted in increased filamentation under *in vitro* conditions. Together with the results of the histology and immunohistochemistry, this outcome implies that the morphology of *C. albicans* plays a critical role in gut colonization. Finally, using an *in vitro* adherence assay, I demonstrated that the three identified factors also contribute to the adherence of the fungus to mucus-containing surfaces.

3.3) Material & Methods:

3.3.1) *Candida albicans* strains used in this chapter

Table 4: *Candida albicans* strains used in chapter 2.

Strain	Genotype	Source
SN152	$\frac{ura3\Delta::\lambda imm434::URA3-IRO1}{ura3\Delta::\lambda imm434} \frac{arg4::hisG}{arg4::hisG} \frac{his1::hisG}{his1::hisG} \frac{leu2::hisG}{leu2::hisG}$	Noble and Johnson, 2005
SN250	$\frac{ura3\Delta::\lambda imm434::URA3-IRO1}{ura3\Delta::\lambda imm434} \frac{arg4::hisG}{arg4::hisG} \frac{his1::hisG}{his1::hisG} \frac{leu2::hisG::CdHIS1}{leu2::hisG::CmLEU2}$	Homann <i>et al.</i> , 2009
TF55	$\frac{ura3\Delta::\lambda imm434::URA3-IRO1}{ura3\Delta::\lambda imm434} \frac{arg4::hisG}{arg4::hisG} \frac{his1::hisG}{his1::hisG} \frac{leu2::hisG}{leu2::hisG} \frac{try4\Delta::CdHIS1}{try4\Delta::CmLEU2}$	Homann <i>et al.</i> , 2009
TF116	$\frac{ura3\Delta::\lambda imm434::URA3-IRO1}{ura3\Delta::\lambda imm434} \frac{arg4::hisG}{arg4::hisG} \frac{his1::hisG}{his1::hisG} \frac{leu2::hisG}{leu2::hisG} \frac{orf19.5910\Delta::CdHIS1}{orf19.5910\Delta::CmLEU2}$	Homann <i>et al.</i> , 2009
TF120	$\frac{ura3\Delta::\lambda imm434::URA3-IRO1}{ura3\Delta::\lambda imm434} \frac{arg4::hisG}{arg4::hisG} \frac{his1::hisG}{his1::hisG} \frac{leu2::hisG}{leu2::hisG} \frac{zfu2\Delta::CdHIS1}{zfu2\Delta::CmLEU2}$	Homann <i>et al.</i> , 2009
TF141	$\frac{ura3\Delta::\lambda imm434::URA3-IRO1}{ura3\Delta::\lambda imm434} \frac{arg4::hisG}{arg4::hisG} \frac{his1::hisG}{his1::hisG} \frac{leu2::hisG}{leu2::hisG} \frac{zcf8\Delta::CdHIS1}{zcf8\Delta::CmLEU2}$	Homann <i>et al.</i> , 2009
JCP686	$\frac{ura3\Delta::\lambda imm434::URA3-IRO1}{ura3\Delta::\lambda imm434} \frac{arg4::hisG}{arg4::hisG} \frac{his1::hisG}{his1::hisG} \frac{leu2::hisG}{leu2::hisG} \frac{try4\Delta::CdHIS1}{try4\Delta::CmLEU2} \frac{rps10\Delta::TRY4-SAT1}{RPS10}$	This work
JCP721	$\frac{ura3\Delta::\lambda imm434::URA3-IRO1}{ura3\Delta::\lambda imm434} \frac{arg4::hisG}{arg4::hisG} \frac{his1::hisG}{his1::hisG} \frac{leu2::hisG}{leu2::hisG} \frac{zfu2\Delta::CdHIS1}{zfu2\Delta::CmLEU2} \frac{rps10\Delta::ZFU2-SAT1}{RPS10}$	This work
JCP758	$\frac{ura3\Delta::\lambda imm434::URA3-IRO1}{ura3\Delta::\lambda imm434} \frac{arg4::hisG}{arg4::hisG} \frac{his1::hisG}{his1::hisG} \frac{leu2::hisG}{leu2::hisG} \frac{zcf8\Delta::CdHIS1}{zcf8\Delta::CmLEU2} \frac{rps10\Delta::ZCF8-SAT1}{RPS10}$	This work
JCP759	$\frac{ura3\Delta::\lambda imm434::URA3-IRO1}{ura3\Delta::\lambda imm434} \frac{arg4::hisG}{arg4::hisG} \frac{his1::hisG}{his1::hisG} \frac{leu2::hisG}{leu2::hisG} \frac{orf19.5910\Delta::CdHIS1}{orf19.5910\Delta::CmLEU2} \frac{rps10\Delta::ORF19.5910-SAT1}{RPS10}$	This work

3.3.2) Plasmids used in this chapter

Table 5: Plasmids used in chapter 2.

Plasmid	Description	Source
pCJN542	pTDH3 for overexpression	Nobile <i>et al.</i> , 2008
pSFS2a derivative	Add-back construction	Reuss <i>et al.</i> , 2014

3.3.3) Oligos used in this chapter

Table 6: Oligos used in chapter 2.

Name	Description	Sequence (3'-5')
JCP1910	orf19.6781_addback_for	CATGCTCGAGATGTCTAAAAGAAGAACGGTGAAACGATCAA GAAATGGTTGTTTAAAGTTGTAAAAAATTACGAATAAAATGT GATGAATCTAAACCAACA
JCP1589	orf19.6781_addback_rev	CATGCTCGAGTTAATTAACATCTAGTTCAGGAAATTC
JCP1584	orf19.1718_addback_for	CATGCTCGAGATGGAAAAGTAATCTATCTAATACTG
JCP1585	orf19.1718_addback_rev	CATGCTCGAGTTATTCAAAGATATTTGGTTCAACAC
JCP1592	orf19.5975_addback_for	CATGCTCGAGATGTCTTTACCAATGTCACCTG
JCP1593	orf19.5975_addback_rev	CATGCTCGAGTTAACTGACCAACATATTAAGT
JCP1578	orf19.5910_addback_for1	CATGCATATGCTCGAGATGAATCTGGTACTGGCAAACCTG
JCP1579	orf19.5910_addback_rev1	TGTGAATTCTTTCCCGAAATAGAATTTAAAGAAATAACAGC
JCP1580	orf19.5910_addback_for2	GAAAGAATTACAATATGGGTACCAATCGATAGATCAGCTC GAACAGGATGTCGAAAATTTGCG
JCP1581	orf19.5910_addback_rev2	CATGAAGCTTCTCGAGCTAGTCTTGCAAAAATTTCTCTAACT C
JCP1679	test_addback_orf19.6781_for	TCATCAACAACGAGCACTGG
JCP1680	test_addback_orf19.6781_rev	CAAGGGCAAATATACTGTTTCGA
JCP1675	test_addback_orf19.5975_for	TACCTCAAGCACCACCACAA
JCP1676	test_addback_orf19.5975_rev	TCGGAACCACTTTTACTGTCA
JCP1673	test_addback_orf19.1718_for	GCCTCAACCTCCTTCACAAC
JCP1674	test_addback_orf19.1718_rev	TGGGGTGACATTGAGTTGGA
JCP1677	test_addback_orf19.5910_for	AGACGAGTCCCACAGTTGAG
JCP1678	test_addback_orf19.5910_rev	CCCCACATTCGTCGTAATGG

3.3.4) Addback strains

Addback strains were constructed following the strategy described in (Perez *et al.*, 2013b): Briefly, the full-length wild type *ORF19.1718*, *ORF19.6781*, *ORF19.5975*, and *ORF19.5910* were amplified by PCR (oligos are listed in Table 6) and cloned into the XhoI restriction site of a derivative of plasmid pSFS2a (Reuss *et al.*, 2004). Since inside the gene body of *ORF19.5910* there is a natural XhoI restriction site, I first mutated this site while keeping the amino acid sequence intact using the plasmid pUC19. The full-length sequence of *ORF19.5910* containing the mutated XhoI restriction site was excised from pUC19 and inserted in the XhoI restriction site of the pSFS2a derivative as it was done for the other addbacks; the linearized plasmids were used to introduce a full-length copy of *ORF19.1718*, *ORF19.6781*, *ORF19.5975*, and *ORF19.5910* into the *RPS10* locus of the respective deletion strain. Positive clones were identified by colony PCR amplifying a part of each gene body (oligos are listed in Table 6). Positive clones were tested for proper nucleotide sequence by sequencing.

3.3.5) Gastrointestinal tract colonization

For gastrointestinal tract colonization *C. albicans* WT and mutant cells were grown to stationary phase in liquid YPD at 30°C overnight. Cells were washed twice in sterile 1x PBS and counted in a hemocytometer (Neubauer). 1×10^7 *C. albicans* cells in 100 or 200 μ l were gavaged to female germ free NMRI mice. To keep the monocolonized status of the rodents, they were kept in sterile isolators throughout the whole experiment. Successful colonization of the mice was controlled via collection of fresh fecal pellets at distinct timepoints after gavage. Fecal pellets were plated on YM agar, incubated at 30°C for 24 h and colony forming units were counted. After the experiment was finished, cecum content was collected and plated as well. The genetic screening was performed as described earlier (Noble *et al.*, 2010; Perez *et al.*, 2013b). Briefly, a signature-tagged *C. albicans* deletion mutant library of 77 known or predicted transcriptional regulators (Perez *et al.*, 2013b) were orally gavaged to germ free mice in pools of 15-20 mutants per mice (to reduce the number of required animals). Freshly produced fecal pellets were collected at distinct timepoints to evaluate the ability of the mutants to colonize the gut of germ-free mice. The inoculum and the fecal pellets were plated on YM agar and incubated at 30°C for at least 24 h. To determine the relative abundance of each mutant, CFUs were collected, washed twice in water and DNA was extracted. This DNA was used to perform real time PCR using primers detecting the signature tag unique for each mutant, as described earlier (Noble *et al.*, 2010). Conversion of the threshold cycle values (C_T), derived from the real time PCR, to linear scale was conducted using the equation: linear value = 2^{-C_T} . Since mutants were gavaged in pools, for each experiment 15-20 values for the inoculum (I) and 15-20 for the recovered pool (R_{raw}) were derived. These R_{raw} values were therefore normalized by multiplication with median (I) / median (R_{raw}). Finally, the amount of recovered CFUs over inoculated CFUs were calculated for each mutant strain and converted to \log_2 values (shown in Figure 23B). To keep a reasonable balance between statistical power and high costs of germ-free animals (Fan *et al.*, 2015), we set the number of animals per group (n) to four to five. All experiments with germ free animals were conducted in the Core Facility for Germ-Free Research of the Karolinska Institute (Stockholm, Sweden).

3.3.6) Tissue collection

21 days after oral gavage (at the end of the experiment) complete colons were excised from the animals and cut in ~ 1 cm pieces, each containing one feces pellet. All tissue

samples were immediately fixed in a specific way as described earlier (Johansson *et al.*, 2012) with minor modifications to protect the sensitive mucus layer. Briefly, immediately after excision, colon pieces were covered with Methacarn solution (60% methanol, 30% chloroform, 10% acetic acid) for 5 days. Methacarn solution was changed every day. After 5 days tissue samples were washed successively in methanol for 35 min and ethanol for 30 min until no sign of acid was detectable in the samples. Subsequently, colon pieces were embedded in paraffin using a paraffin embedding machine (Leica EG 1160, Wetzlar, Germany) and a standard program consisting of washing steps in increasing ethanol concentrations, several xylol baths and 3 hours in melted paraffin at 62°C. For sectioning, each sample was enclosed in a paraffin block and stored at room temperature.

3.3.7) Histology

For histological analysis, paraffin blocks were cut in 2–4 µm sections and attached to microscope slides. The slides containing the sections were incubated overnight at 30°C to soften the paraffin. Next day, the slides were incubated twice for 10 min in xylol to remove the paraffin. Samples were rehydrated via three times dipping in decreasing ethanol concentrations (96%, 96%, 70%, 50%) and chilled 5 min in water. After rehydration, samples were stained using a standard PAS (Periodic Acid Schiff) staining. Briefly, sections were incubated 10 min in freshly prepared 0.5% Periodic acid (Sigma-Aldrich, St. Louis, MO, USA) and washed subsequently with running tap water to flush out residual periodic acid. 15 min incubation in Schiff's reagent (Sigma-Aldrich, St. Louis, MO, USA) and 3x 2 min in sulfite water (18,25 ml 1 M HCl, 50 g Potassium pyrosulfite, filled up to 500 ml with dH₂O) followed. Residual Schiff's reagent and sulfite water were removed with running tap water. Nuclei in the samples were stained using Hematoxylin (Sigma-Aldrich, St. Louis, MO, USA) for 8 min and residual color was removed with running tap water. To differentiate the hematoxylin dye, sections were dipped three times in HCl EtOH. Residual HCl EtOH was removed with dH₂O. Warm tap water was used subsequently for blueing. Sections were finally dehydrated via 3x dipping in increasing Ethanol concentrations (70% and 96%), Isopropanol and Xylol. Samples were embedded in Entellan.

3.3.8) Immunohistochemistry

For immunohistochemistry, 2-4 µm sections were processed as described (Earle *et al.*, 2015). Briefly, sections were attached to microscope slides and incubated at 56°C for

30 min to soften the paraffin. Paraffin was removed using two subsequent incubations in xylol for 10 min. After rehydration via three times dipping in decreasing ethanol concentrations (96%, 96%, 70%, 50%) sections were washed 5 min in dH₂O and chilled in PBST (1xPBS + 0.5% Tween-20). Sections were boiled subsequently in citrate buffer, pH6 for 20 min for antigen retrieval followed by washing in 0.5% Triton X 100 for 30 min at room temperature. 1% BSA was added for 30 min at room temperature for blocking. *C. albicans* cells were stained using a rabbit anti-*C. albicans* antibody (Abcam, Cambridge, UK, ab53891) diluted 1:500 in blocking buffer at 4°C for 12–16 h in a humid chamber. Afterwards, sections were washed 3x in PBST for 10 min. The secondary antibody (Alexa Fluor 488 goat anti-rabbit IgG, Life Technologies, Thermo Fisher Scientific, Waltham, MA, USA) was applied at a 1:500 dilution in blocking buffer with 10 µg/ml DAPI (Sigma-Aldrich, St. Louis, MO, USA) and incubated for 2 hours at RT in a humid chamber. Slides were washed again with PBST (3x, 10min each) and mounted in Mowiol (Sigma-Aldrich, St. Louis, MO, USA).

3.3.9) Colony morphology assay

To evaluate the colony morphology of *C. albicans*, wild type and mutant cells were grown to stationary phase in liquid YPD at 30°C shaking overnight. Cells were washed two times in dH₂O and counted in a hemocytometer (Neubauer). 5x10⁴ cells were spotted on YPD agar and plates were incubated at 30°C for 48 h.

3.3.10) Adherence assay

The wells of conventional cell culture six-well plates were covered with a thin layer of 1% agar containing 50% mucin (Mucin from porcine stomach Type III, Sigma-Aldrich, St. Louis, MO, USA) or 1x PBS as control. The plates were incubated at 4°C overnight to let the agar solidify. *C. albicans* wild-type and mutant cells were grown to stationary phase overnight at 30°C in YPD shaking. Cells were washed 2 times in 1x PBS and counted in a hemocytometer (Neubauer). ~1x10³ *C. albicans* cells were added to each well and plates were incubated 8 hours at 37°C under anaerobic conditions to enable attachment of the fungal cells. Subsequently, each well was washed two times using 1x PBS to remove non-adherent cells. After non-adherent cells were removed, all wells were overlaid with YPD soft agar and the plates were incubated at 30°C until colonies could be visualized and quantified.

3.3.11) Statistical analyses

The t-test (two-tailed) for unpaired samples assuming unequal variance was used to compare the adherence of multiple strains to the mucin-covered agar (Figure 26B).

3.3.12) Ethics statement

The animal studies and protocols (permission numbers 55.2-2531.01-50/14 and N181/14) were approved by the local government of Lower Franconia (Regierung von Unterfranken), Germany, and by the Stockholm's Animal Ethics Committee (Stockholms Norra djurförsöksetiska nämnd), Sweden, respectively. All animal studies were performed in strict accordance with the guidelines for animal care and experimentation of the German Animal Protection Law and EU directive 2010/63/EU.

3.4) Results:

3.4.1) *Candida* colonizes the gut of gnotobiotic mice.

Gut colonization by the fungus *Candida albicans* is typically studied in mice. Conventionally raised mice harbor trillions of microorganisms in their gut. Since *Candida albicans* is no natural member of this mouse indigenous microbiota, the fungus gets rapidly outcompeted when gavaged in these animals. The indigenous mouse flora needs to be reduced using an antibiotic cocktail before *Candida* is able to colonize this niche. These conventionally raised, antibiotic treated animals (hereafter termed ‘conventional’) have been employed to investigate multiple aspects of intestinal colonization by the fungus (Koh *et al.*, 2008; Pande *et al.*, 2013; Perez *et al.*, 2013b; White *et al.*, 2007). However, the remaining undefined microbiota may confound some results. Therefore, we established an alternative experimental system to study fungal traits required for colonization of the digestive tract: gnotobiotic animals mono-colonized with *C. albicans*.

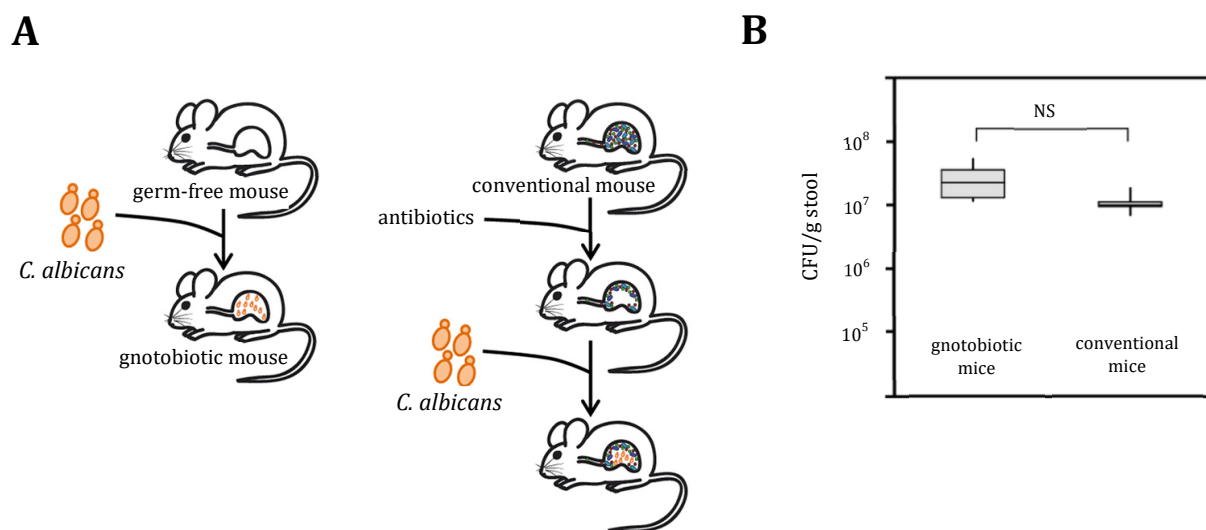


Figure 21: *Candida albicans* is able to colonize gnotobiotic animals (Bohm *et al.*, 2017).

(A) Diagram illustrating two models to study gut colonization by *C. albicans*: conventional antibiotic treated and germ-free mice. After oral gavage, the fungus can persist in the gastrointestinal tract of both models.

(B) Graph depicting the fungal load in colony-forming units (CFU) per gram of stool in gnotobiotic and conventional animals 21 days after oral gavage. For both models, we evaluated six animals. Shown is the median (horizontal line in the middle of the grey box) with interquartile range (grey box) and the distance to the minimum and maximum values (whisker). We could not detect a statistically significant difference between both models.

Germ free mice are raised in a microbe-free environment. Therefore, the gastrointestinal tract of these animals is devoid of any microbes, providing a clearly defined study system. *Candida albicans* cells are orally gavaged to these animals (Figure 21A). Oral gavage of 10^7 *C. albicans* cells results in similar fungal loads (in colony forming units per gram of stool) in gnotobiotic animals compared to antibiotic-treated conventional animals (Figure 21B). This observation is in agreement with other reports (Fan *et al.*, 2015; White *et al.*, 2007).

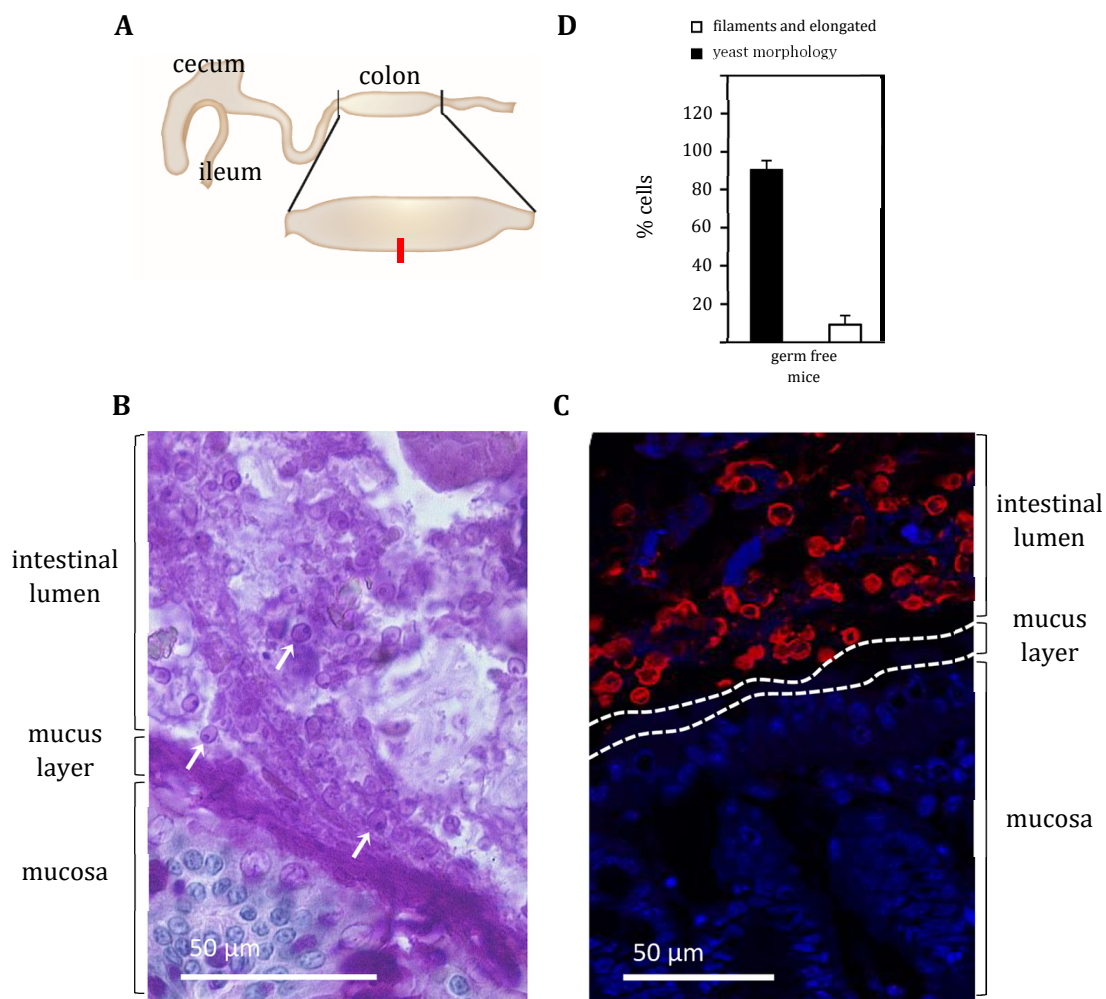


Figure 22: *Candida albicans* colonizes the intestinal tract of gnotobiotic animals in its round-shaped yeast form (Bohm *et al.*, 2017).

(A) Cartoon depicting the area of the intestine of germ-free mice monocolonized with *C. albicans* that were taken for histological and immunohistochemistry analyses.

(B) Representative tissue section from the area of the intestine indicated in (A) after Periodic acid-Schiff (PAS) staining. PAS stains polysaccharides, including those on the surface of *C. albicans*, in purple-magenta color. The mucosa is located at the bottom with the mucus layer attached and the intestinal lumen on top where indicated with the arrows abundant oval shapes were found that correspond to *C. albicans* cells. Evaluated were sections of the intestine of at least three mice.

(C) Representative tissue section from the area of the intestine indicated in (A) after staining with DAPI (blue) and an anti-*Candida* antibody (red). The mucosa is located at the bottom with the mucus layer attached (indicated with the dotted lines) and the intestinal lumen on top where in red abundant oval shapes were found that correspond to *C. albicans* cells. Evaluated were sections of the intestine of at least three mice.

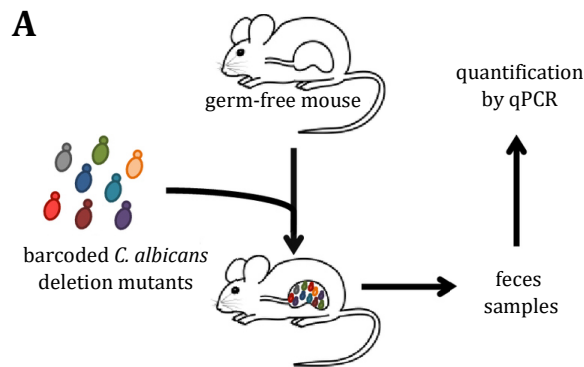
(D) Quantification of *C. albicans* cell morphologies found in gnotobiotic mice. 100–500 cells were scored in 3–5 animals. The predominant morphology in mice monocolonized with *C. albicans* were yeast cells.

To visualize the fungus in the gut of mono-colonized animals, we removed the colon of these animals. Colon samples (Figure 22A) were fixed and processed using a method that preserves the mucus layer structure and is compatible with histology and immunofluorescence (Earle *et al.*, 2015; Johansson *et al.*, 2012). For histological analysis, Periodic acid-Schiff (PAS) staining was used, since this procedure stains polysaccharides on the surface of *C. albicans*. Additionally, PAS distinguishes the intestinal mucus layer and mucus containing cells. I found a large number of round-shaped cells—reminiscent of the typical yeast morphology of *C. albicans*—located in close proximity to the mucus layer of the intestine of gnotobiotic mice (Figure 22B+C). I quantified the different cell morphologies and found that round shaped yeast cells are the predominant form in gnotobiotic mice (Figure 22D).

This observation was in contrast to what is expected for niches of the mammalian host since the body temperature of mammals is around 37°C. This temperature is known as a strong inducer of filamentation in *Candida albicans*. In other places of the murine body *Candida* consistently shows its filamentous form (also termed hyphae). In the murine oral or vaginal mucosae or the kidneys, for instance, hyphae are the predominant morphology. To confirm that the yeast-like structures observed in gnotobiotic mice (Figure 22B) indeed correspond to *C. albicans*, I used immunofluorescence. Colon sections similar to those used for histological analysis were stained with an anti-*Candida* specific antibody and DAPI (to stain nuclei in the epithelium). A strong fluorescent signal originating from the anti-*Candida* antibody was detected in the intestinal lumen in close proximity to the mucus layer (Figure 22C). These results indicate that in mice monocolonized with *C. albicans*, the fungus is located in the colon in the vicinity of the mucus layer and that the yeast form of the fungus is the most prevalent morphology in this niche. Therefore, using germ-free mice monocolonized with *Candida albicans* provides a tractable system to study the interplay between the yeast form of *C. albicans* and the mammalian host *in vivo*.

3.4.2) Transcriptional regulators that contribute to the fitness of *C. albicans* in the gut of gnotobiotic animals.

In the next step, I wanted to identify *C. albicans* traits that are needed by the fungus to colonize the gastrointestinal tract of gnotobiotic mice. Therefore, I screened a transcription factor deletion mutant library for their ability to persist in the gut of monocolonized mice (Figure 23A). The same set of ~60 deletion mutants that have previously been probed in other mouse models (Perez *et al.*, 2013b) were used for the screening. The mutant strains included in this set displayed no growth defect or any other major phenotype under >50 laboratory conditions tested (Homann *et al.*, 2009). Transcription factors are key players in the regulation of many biological processes; hence, they are good candidates for playing crucial roles in gastrointestinal colonization. Since no mutant displayed significant *in vitro* phenotypes I expected members of this library to be part of regulatory circuits that might be relevant *in vivo*. To minimize the number of mice needed for the screen, the mutants were tested in pools of 15–18 strains each. Feces were collected at distinct time points and the abundance of each signature tagged strain quantified by qPCR as described (Perez *et al.*, 2013b)(Figure 23A).



B

	day 1				day 21			
<i>orf19.4941</i>	-1,2	-1,8	-2,3	0,4	-8,0	-10,0	-10,0	-10,0
<i>orf19.2315</i>	-0,3	-1,1	-0,6	-0,6	-10,0	-10,0	-10,0	-10,0
<i>orf19.5910</i>	0,8	0,8	1,2	1,2	-10,0	-10,0	-6,0	-10,0
<i>try4 orf19.5975</i>	-1,1	-1,6	-1,2	-1,2	-6,1	-7,5	-4,4	-9,4
<i>orf19.921</i>	0,2	-0,7	0,6	-0,2	-7,9	-4,0	-10,0	-10,0
<i>zfu2 orf19.6781</i>	-0,3	-0,3	-0,3	-0,3	-6,6	-5,2	-9,1	-10,0
<i>orf19.4722</i>	-1,4	-1,5	-3,4	-1,7	-5,6	-3,4	-9,3	-10,0
<i>zcf8 orf19.1718</i>	-0,4	-0,3	-0,2	-0,9	-3,6	-6,9	-10,0	-10,0
<i>orf19.3876</i>	0,2	0,4	0,1	0,9	-1,6	-3,9	-5,3	-8,2
<i>orf19.5097</i>	0,1	-1,5	-1,1	-1,4	-2,1	-3,7	-10,0	
<i>orf19.2612</i>	0,7	0,3	0,1	-0,2	-3,4	-4,1	-6,8	
<i>orf19.4778</i>	0,5	0,6	1,7	0,0	0,7	3,3	-0,9	2,2
<i>orf19.1035</i>	0,3	0,6	2,2	-0,1	2,0	2,2	0,7	2,4
<i>orf19.5249</i>	0,3	0,2	2,3	0,1	1,7	3,5	0,6	2,6
<i>orf19.3308</i>	-0,1	0,5	-0,7	0,2	0,6	2,6	-0,5	3,9
<i>orf19.4972</i>	1,1	1,2	1,4	1,3	1,4	4,2	3,5	4,7
<i>orf19.4145</i>	-0,9	-0,6	-0,5	-0,4	-0,1	3,1	4,0	2,9
<i>orf19.217</i>	1,3	1,1	1,3	1,3	4,7	0,4	1,2	1,8
<i>orf19.5940</i>	1,0	0,7	1,4	1,2	3,2	1,0	0,8	1,4
<i>orf19.6817</i>	-0,1	0,3	0,5	0,3	4,2	0,0	1,8	0,8
<i>orf19.4225</i>	-0,1	0,1	0,2	-0,1	3,1	0,4	0,1	1,1
<i>orf19.431</i>	0,8	0,3	1,6	0,0	1,6	-3,3	0,3	-0,9
<i>orf19.7371</i>	-0,5	0,1	0,0	-0,4	3,5	-1,6	-0,5	
<i>orf19.5380</i>	0,3	0,3	1,7	0,3	0,3	3,3	2,1	-0,3
<i>orf19.5498</i>	0,5	0,4	-0,3	-0,2	0,2	2,7	0,4	-0,8
<i>orf19.5026</i>	0,6	0,5	1,9	0,3	1,1	2,1	-0,1	0,8
<i>orf19.5855</i>	1,3	0,8	1,3	1,2	-0,1	2,4	0,2	0,9
<i>orf19.4647</i>	0,1	0,5	-0,1	-2,2	-2,5	2,8	1,0	0,3
<i>orf19.2743</i>	0,3	0,5	1,7	0,0	-1,8	1,3	1,4	1,2
<i>orf19.6514</i>	0,3	0,7	1,1	0,1	-3,5	0,8	1,6	
<i>orf19.2647</i>	0,3	1,0	0,6	1,0	-2,4	3,2	0,8	1,8
<i>orf19.4524</i>	0,1	0,0	-0,5	-0,8	0,4	0,1	-0,7	0,3
<i>orf19.7518</i>	-0,2	-0,4	-1,3	-0,3	-0,8	-0,7	0,2	-0,3
<i>orf19.3865</i>	-1,2	-0,7	-0,8	-0,5	-0,1	-1,5	1,2	
<i>orf19.3928</i>	-1,9	-1,3	-1,5	-1,2	-1,3	1,1	-0,8	0,7
<i>orf19.4288</i>	-0,5	-0,8	-0,6	-0,8	-0,9	0,6	-0,4	2,7
<i>orf19.6680</i>	-0,3	-0,5	-0,1	-0,2	-3,4	-0,5	-0,2	-0,2
<i>orf19.4438</i>	-0,5	-0,7	-0,6	-0,7	-1,9	1,1	1,0	0,0
<i>orf19.6888</i>	1,4	-0,4	0,2	-0,6	-2,4	-1,1	-0,6	1,3
<i>orf19.5729</i>	0,7	0,4	0,6	0,8	-0,4	-0,3	-1,8	2,3
<i>orf19.5651</i>	0,6	0,3	-1,0	-0,1	-2,1	-1,7	1,2	1,9
<i>orf19.4573</i>	0,0	0,2	0,0	-0,1	-2,1	-2,3	2,1	0,6
<i>orf19.837.1</i>	0,0	0,5	0,2	0,3	-0,3	-0,5	2,6	1,1
<i>orf19.6038</i>	-0,2	0,2	-0,1	0,2	0,0	-0,1	2,2	0,2
<i>orf19.1757</i>	0,4	-0,5	-0,8	-0,8	-1,2	-0,6	3,1	
<i>orf19.4166</i>	2,0	1,8	1,7	0,3	0,2	-1,2	1,7	0,8
<i>orf19.3190</i>	1,5	2,0	1,9	1,1	-3,8	0,4	1,3	-0,5
<i>orf19.5548</i>	-0,6	-0,7	-3,3	-2,4	0,3	-0,5	-3,3	-0,9
<i>orf19.4767</i>	-0,3	-0,3	-6,8	-0,1	0,0	2,0	-2,9	-3,2
<i>orf19.7319</i>	-0,9	-0,5	-3,7	-1,3	-1,8	-1,6	0,1	-1,8
<i>orf19.7372</i>	0,7	0,6	-2,4	-3,0	-0,1	-0,5	1,4	-2,2
<i>orf19.4450</i>	0,6	-2,6	-2,3	-1,4	-1,6	2,2	1,0	-0,1
<i>orf19.3625</i>	-0,5	-0,7	0,6	-1,5	-2,2	1,4	-1,8	-3,3
<i>orf19.3305</i>	0,5	-0,6	0,1	0,5	0,7	3,1	-1,5	-2,1
<i>orf19.1274</i>	-4,0	-0,6	-1,0	-0,2	1,5	2,0	-1,6	-0,1
<i>orf19.3434</i>	1,3	1,0	1,5	1,3	2,2	-3,9	3,2	-5,2
<i>orf19.4251</i>	-0,9	-1,3	-1,2	-1,3	-1,3	1,8	2,8	-6,9
<i>orf19.1150</i>	0,9	0,3	0,8	0,8	0,0	2,2	1,5	-4,6
<i>orf19.4649</i>	0,0	0,2	0,1	0,4	5,4	-3,1	-4,5	1,1
<i>orf19.2730</i>	0,5	-1,3	-1,3	-0,7	2,4	-3,4	-10,0	

Figure 23: Identification of *C. albicans* transcription regulators that govern gut colonization in gnotobiotic mice (Bohm *et al.*, 2017).

(A) Scheme depicting the screening approach that was used to identify transcriptional regulators contributing to the *in vivo* fitness of *C. albicans*. The transcription factor mutant library (~60 mutants) was divided in four pools each one consisting of 15–18 signature-tagged strains. Each one of these pools was orally gavaged to four germ-free mice. Fresh feces pellets were collected at distinct timepoints and via unique signature-tags the abundance of each mutant strain was determined by qPCR.

(B) Table containing the results of the genetic screen. Shown are the log₂ (recovered/inoculum) values for each of the ~60 transcription factor deletion mutants 1, and 21 days post gavage (each column represents one mouse). Blue indicates reduction of the mutant compared to the inoculum whereas red indicates accumulation. Intensity of the colors corresponds to the level of reduction/accumulation. The mutants were ordered according to hierarchical clustering. The eight mutants that cluster at the top displayed a reduction compared to the inoculum in all mice at day 21. Four of them (*orf19.4941*, *orf19.2315*, *orf19.921*, and *orf19.4722*) had previously been identified in a screening conducted in the antibiotic-treated conventional mouse model. The deletion mutants *try4* [*orf19.5975*], *zfu2* [*orf19.6781*], *zcf8* [*orf19.1718*], and *orf19.5910* cluster together with the previous group but had not been identified before in any other mouse setting.

With this genetic screening, I identified eight *C. albicans* deletion mutants with reduced fitness in gnotobiotic mice (Figure 23B). Four of the identified hits (*tye7* [*orf19.4941*], *rtg3* [*orf19.2315*], *hms1* [*orf19.921*], and *rtg1* [*orf19.4722*]) had previously been shown to display phenotypes in murine models of disseminated infection and/or antibiotic-promoted gut colonization (Perez *et al.*, 2013b). The fact that they also appear in our study serves as validation of our experimental model and the screening approach. *Zcf8* [*orf19.1718*], *zfu2* [*orf19.6781*], *try4* [*orf19.5975*], and *orf19.5910*, the other four hits, did not have any effect on virulence or colonization in any other mouse model. I decided to focus on studying the functions of *ZCF8*, *ZFU2*, and *TRY4* and excluded *ORF19.5910* from further analysis. *ORF19.5910* is predicted to be part of a histone remodeling complex and therefore its effects on gene expression are most likely pleiotropic. To validate the results of the screen, where pools of mutants were evaluated, we tested the gut colonization phenotype of the *zcf8*, *zfu2*, and *try4* deletion mutant strains independently at different time points after oral gavage (Figure 24A). To confirm that the gut colonization phenotype corresponds to the identified loci a wild type copy of each gene was added back to the corresponding deletion mutant and their ability to colonize the gut of germ-free animals was monitored. Adding back a wild type of each gene to the deletion mutants restored, to a large extent, *in vivo* fitness (Figure 24B).

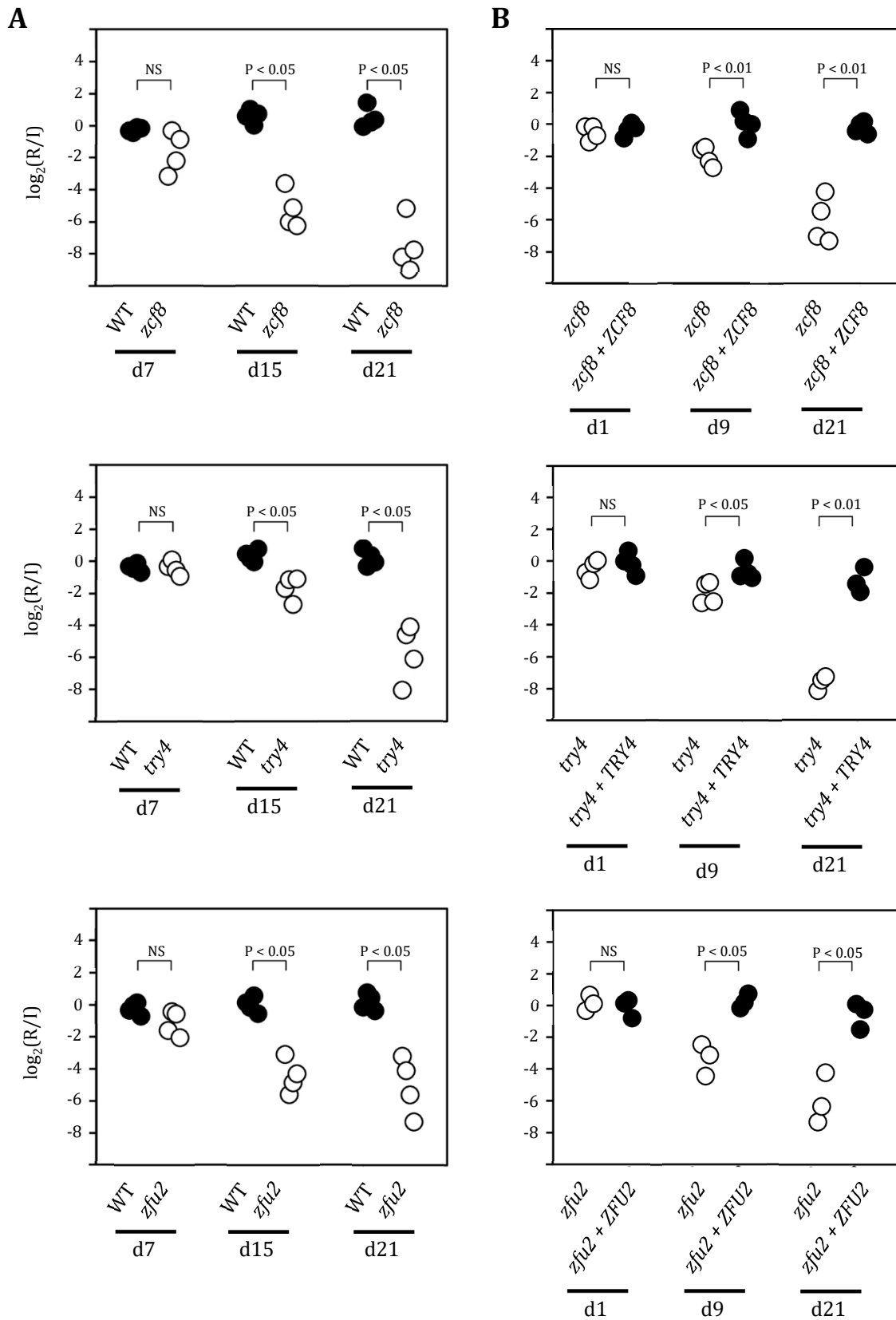


Figure 24: The observed gut fitness defect phenotype of three newly identified genes could be restored by adding back a wild-type copy to the deletion mutant. (Bohm *et al.*, 2017).

(A) Wild-type reference strain and *zcf8*, *zfu2*, or *try4* were mixed 1:1 and orally gavaged to germ-free animals. Inoculum (I) and fecal pellets (R) from day 7, 15 and 21 were plated on YM plates. Colonies were collected after 24 h, DNA was extracted, and the abundance of each strain was determined via qPCR (strains were barcoded). Each circle in these graphs represents the measurement from one mouse. The results for the wild-type reference strain are depicted with the filled circles and for the mutant with the opened circles. Throughout the whole experiment the wild-type reference strain colonizes the GI-tract of germ-free animals consistently. The deletion mutant strains were progressively depleted from the fecal pellets (P values are indicated on top of each comparison). Statistical analysis by the Mann-Whitney test. NS, not significant.

(B) 1:1 mixtures of each deletion mutant and the corresponding gene add-back strain were orally gavaged to three or four germ free mice. Inoculum (I) and fecal pellets (R) from day 1, 9 and 21 were plated on YM plates. Colonies were collected after 24 h, DNA was extracted, and the abundance of each strain was determined via qPCR (amplification of a region of the respective genebody, primers listed in Table 6). Each circle in these graphs represents the measurement from one mouse. The results for the add-back strains are depicted with the filled circles and for the deletion mutant strains with the opened circles. The deletion mutant strains were depleted over time from the fecal pellets, whereas the add-back strains colonized the animals consistently similar to the wild-type strain (shown in (A)) (P values are indicated on top of each comparison). Statistical analysis was determined by two-tailed unpaired t-test assuming unequal variance. NS, not significant.

3.4.3) The round-shaped yeast form of *Candida albicans* promotes persistence in the gut of gnotobiotic mice.

ZCF8, *ZFU2*, and *TRY4* lack clear orthologs in the model yeast *Saccharomyces cerevisiae* (Maguire *et al.*, 2013). To start dissecting the roles of *ZCF8*, *ZFU2*, and *TRY4* in gut colonization, the fitness of the deletion mutants was tested in spot assays under a variety of *in vitro* conditions that had not been analyzed before. As mentioned above, Homann *et al.* (Homann *et al.*, 2009) analyzed the fitness of these mutants under standard laboratory conditions but found no overt phenotype. With ethanol as carbon source in minimal synthetic medium the mutants showed slight growth impairment (YNB without amino acids) (data not shown). On rich medium (YPD) we observed wrinkling colonies (Figure 25) for all three mutants under conditions in which the wild-type forms smooth colonies. Colony wrinkling in *C. albicans* is a well-established proxy for filamentation. Microscopy confirmed that the wrinkling colonies were composed of a mixture of yeast and filamentous cells. The smooth colonies formed by the wild-type strain, on the other hand, consisted almost completely of yeast cells. To confirm that the colony wrinkling was due to mutations in the specified loci we added back a wild-type copy of each gene to the deletion mutant and evaluated their colony morphology. For all three genes adding back a wild type copy of the gene to the deletion mutant restored, to a large extent, the smooth colony phenotype (Figure 25). Together with the observation from the histology, where

we saw *C. albicans* cells residing in the colon of gnotobiotic rodents mainly in its round shaped yeast form (Figure 22B+C), these findings suggest that an increased filamentation may account, at least in part, for the gut colonization defect of the *zcf8*, *zfu2*, and *try4* mutants. This implies that filamentation itself might be a detrimental factor for intestinal colonization.

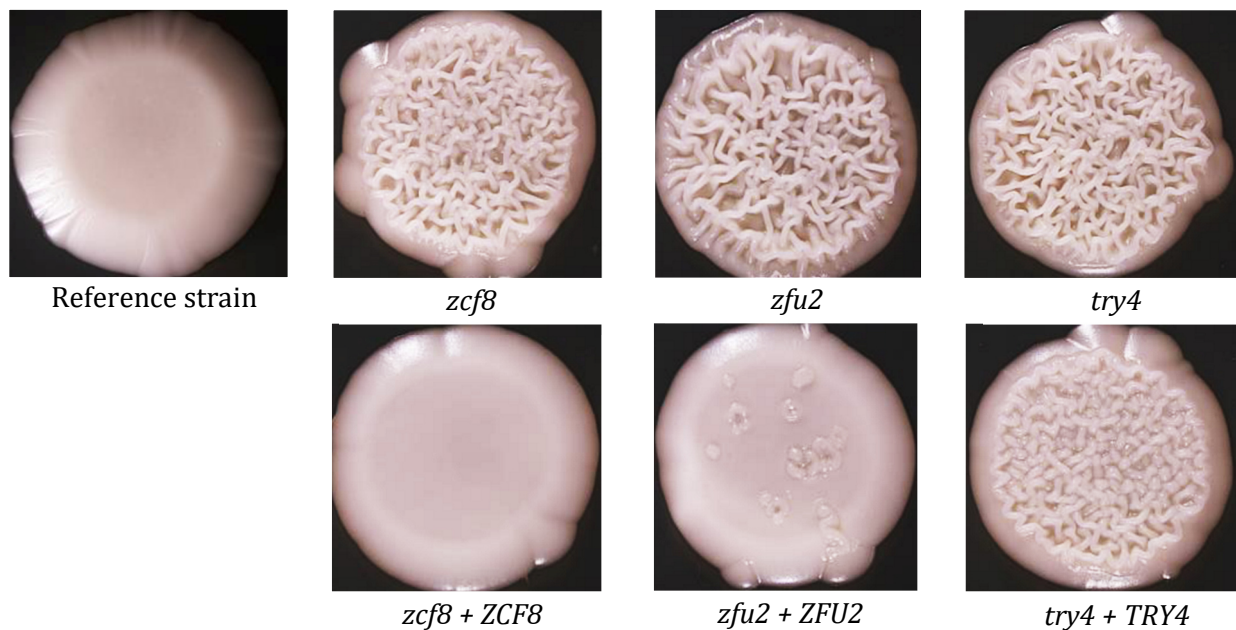


Figure 25: The deletion mutants *zfu2*, *zcf8*, and *try4* display wrinkling - a proxy for filamentation - under non-inducing conditions (Bohm *et al.*, 2017).

The wild-type reference strain and the three deletion mutants were spotted on YPD agar and incubated at 30°C for 48 h. The wild-type strain formed smooth colonies whereas the deletion mutants displayed wrinkling colonies, indicating filamentation under non-inducing conditions. Adding-back a wild-type copy of *ZCF8*, *ZFU2*, and *TRY4* to the deletion mutant strains restored, at least in part, smooth colony phenotype.

3.4.4) *ZCF8*, *ZFU2*, and *TRY4* promote *C. albicans* adherence.

An alternative or possibly additional explanation for the observed gut colonization defect in the mono-colonized animals might be the reduced ability of the *zcf8*, *zfu2*, and *try4* mutants to adhere to surfaces. In a previous study all three strains had been shown to have a defect in an *in vitro* adherence assay using silicone poly-dimethyl siloxane as substrate (Finkel *et al.*, 2012). This raised the possibility that, *ZCF8*, *ZFU2*, and *TRY4* not only contribute to the adherence to silicone but also play a role in the attachment to surfaces relevant in the context of the gastrointestinal tract. I tested this idea with an *in vitro* adherence assay using mucin as substrate, the main component of the intestinal

mucus. In this assay, that I developed based on the protocol described by Van den Abbeele (Van den Abbeele *et al.*, 2009), the *C. albicans* reference strain and the deletion mutants were added on top of an agar layer containing mucin or PBS as control (Figure 26A). The addition of mucin enhanced the capacity of the reference strain to adhere to the agar layer compared to the PBS control (Figure 26B). In contrast, the three deletion mutant strains showed no difference in adherence irrespective of the presence or absence of mucin (Figure 26B). Thus, *ZCF8*, *ZFU2*, and *TRY4* function as positive regulators of adherence to surfaces coated with silicone (Finkel *et al.*, 2012) or mucin. The absence of these regulators might therefore affect the capacity of the fungus to adhere to surfaces in the GI-tract which may lead to a colonization defect.

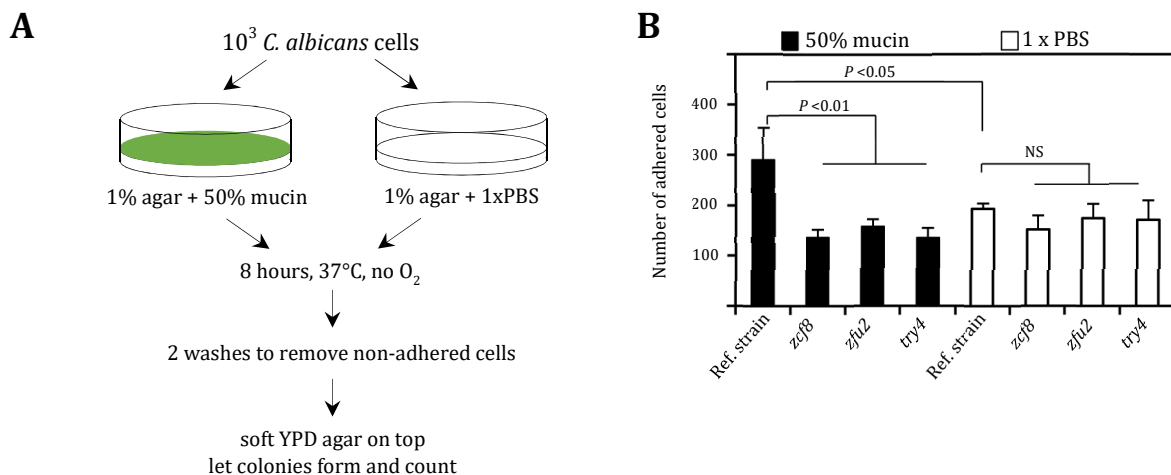


Figure 26: The regulators *ZCF8*, *ZFU2*, and *TRY4* promote adherence to mucin coated surfaces (Bohm *et al.*, 2017).

(A) Overview of the developed *in vitro* assay to test the ability of *C. albicans* cells to adhere to a semisolid surface containing intestinal mucin.

(B) Bar chart depicting the number of *C. albicans* cells (wild-type reference strain or deletion mutants) that adhered to agar (semisolid surface) containing either mucin (filled bars) or PBS as control (opened bars). The bars represent the mean \pm SD of at least three independent experiments; statistical analysis by t-test as described in Materials and methods. The wild-type reference strain showed an increased adherence to mucin-containing agar compared to the PBS containing control. The three deletion mutants did not show a difference in adherence to agar containing mucin compared to the PBS control.

3.5) Discussion

In this part of the thesis, I have employed gnotobiotic mice mono-colonized with *C. albicans* as an experimental system to study gut colonization by the fungus. In this niche, the fungus almost exclusively adopts its oval-shaped yeast form and can be found in close proximity to the mucus layer. Furthermore, using this model, I identified three previously undescribed transcriptional regulators (*ZCF8*, *ZFU2*, and *TRY4*) that are conducive to the fitness of the fungus in this niche. These three regulators negatively control filamentation and promote the adherence of the fungus to a mucin-containing surface. These results indicate that in addition to adherence, the morphology of *C. albicans* plays an instrumental role in the murine intestine. It is becoming increasingly clear that fungi are significant components of the human microbiota (Findley et al., 2013; Underhill et al., 2014); however, little is known about the interplay between commensal fungi and the mammalian host. The use of gnotobiotic animals provides a well-defined experimental system that may serve as a starting point to study and dissect the mechanisms of intestinal colonization by fungi and other eukaryotic microbes.

The fungus *Candida albicans* can colonize numerous niches in the human body and other warm-blooded animals. While it is a common dweller of the GI tract and other mucosal surfaces, it can also cross protective barriers and colonize virtually every organ in the human body. Some cues in the mammalian host can induce specific morphologies of *C. albicans*: The mammalian body temperature (37°C) and the presence of serum, for example, are well-known inducers of the filamentous form of the fungus. *C. albicans* is therefore found almost always in its filamentous form in the histology sections of infected mammalian tissues (oral and vaginal mucosae or internal organs such as kidneys). Nevertheless, the main reservoir of *C. albicans* and the probable source of many induced infections is the mammalian gut. In this niche, the fungus lives mostly as a harmless commensal without causing disease. *C. albicans* adopted almost solely its oval-shaped yeast form in the colon of gnotobiotic mice (Figure 22). The conditions present in the gut environment or some unknown host-derived factors must thus be able to overcome the strong filamentation inducers (37°C and serum), although a particular *C. albicans* morphology has been postulated to be specialized for living in the GI tract (Noble et al., 2017; Pande et al., 2013). My observations of the colon of gnotobiotic rodents reveal that the fungus colonizes this niche in its yeast form (Figure 22); I therefore see no need to invoke additional morphologies to explain the commensal state of the fungus in the GI

tract. One potential explanation for the preference of its yeast form in the gut of gnotobiotic mice is that the filamentous form induces the release of gut-immune effectors (e.g., antimicrobial peptides) or that this morphology has a higher susceptibility to these factors. Consistent with this notion, a strain ectopically expressing a well-established positive regulator of filamentation elicits the production of the neutrophil-stimulating chemokine G-CSF (granulocyte colony-stimulating factor) (Bohm et al., 2017), supporting the idea that the filamentous form induces an immune response and might thus be cleared of the host. By adopting its yeast form, *C. albicans* probably avoids the expression of filament-associated virulence factors that would damage host cells and induce an immune response. An alternative or additional explanation could be based on the different abundancies of metabolites in the GI tract of germ-free and conventional animals. The presence of other microbes could be associated with differences in the availability of various metabolites in the gut environment. The predominance of yeast cells in this niche could thus be due to this morphological form having better fitness under these conditions. Finally, in conventional animals, the fungus must face other competing and/or antagonistic microbes. To be able to persist in such a complex ecosystem, the fungus may have to employ heterogeneous morphologies.

In addition to the morphology, the distribution of *C. albicans* cells in the colon of gnotobiotic animals differed from antibiotic-treated conventional animals. Fungal cells were in close proximity to the mucus layer (Figure 22, Figure 27), whereas in conventional animals, only very few *C. albicans* cells located to the equivalent region (Bohm et al., 2017). One potential explanation is the fact that the intestinal mucus layer of gnotobiotic rodents can be penetrated more easily than that of conventional animals (Johansson et al., 2015). Moreover, the underdeveloped immune system of germ-free animals could affect the distribution of *C. albicans* cells in the intestine. In conventional animals, secreted antimicrobial peptides may generate a spatial segregation between their intestinal mucus layer and microbes (Vaishnava et al., 2011). The nearly naïve immune system of germ-free animals could lead to a reduction of this segregation and therefore be the source of the fungal cells' close proximity to the mucus layer.

The genetic screening performed in gnotobiotic mice mono-colonized with *C. albicans* revealed three transcriptional regulators (*ZCF8*, *ZFU2*, and *TRY4*) that are needed by the fungus to colonize the gut but did not reveal any phenotype in similar screenings conducted in the standard mouse model of disseminated candidiasis (Noble et al., 2010;

Perez et al., 2013b). These three regulators may contribute to fitness in the GI tract through two potential mechanisms: on the one hand, they are negative regulators of filamentation under certain conditions (Figure 25), and on the other hand, they promote adherence to mucin-containing surfaces (Figure 26).

Several intestinal bacteria (*Lactobacillus rhamnosus*, *Streptococcus gallolyticus*) harbor genes encoding proteins that enable binding to mucus (Kankainen et al., 2009; Martins et al., 2015) and play crucial roles in the colonization of the mouse colon (Martins et al., 2015). For fungi, no equivalent has been described so far. The results described in this study suggest that the three transcriptional regulators in *C. albicans* may control a similar function. Mutations in these genes not only caused reduced ability to bind to a surface containing mucin (Figure 26) and to mucus-producing cells (Bohm et al., 2017) but also resulted in a gut colonization defect. Furthermore, in histology sections, the fungal cells located in clusters and in close proximity to the intestinal mucus layer (Figure 22), further supporting the idea that *C. albicans* exhibits mechanisms to adhere to intestinal mucus.

It has been proven that the regulators *ZCF8*, *ZFU2*, and *TRY4* have roles in mediating the adherence of *C. albicans* cells to medical devices such as catheters and prostheses (Finkel et al., 2012). The attachment to these devices and the following biofilm formation is a major cause and risk factor of recurrent and drug-resistant *C. albicans* infections (Desai et al., 2014; Douglas, 2003). The yeast form of *C. albicans* is fundamental in biofilm formation because the layer directly in contact with the device consists mainly of cells in the yeast form (Nobile et al., 2012). This observation highlights a connection between the three identified regulators and the adherence of the yeast cell morphology, contrary to the adherence of the filamentous form controlled by other factors (Phan et al., 2007). *C. albicans* might therefore use the regulation of adherence by *ZCF8*, *ZFU2*, and *TRY4* in different contexts (intestine and medical devices). It is thus plausible that at least to some extent the same genes that enable *C. albicans* to colonize the mammalian gut as a commensal also direct adherence to other surfaces, potentially resulting in serious bloodstream infections.

In the genetic screening conducted on gnotobiotic mice monocolonized with *C. albicans*, eight transcriptional regulators were identified (*TYE7*, *RTG1*, *RTG3*, *HMS1*, *ZFU2*, *ZCF8*, *TRY4*, and *ORF19.5910*), indicating a gut colonization defect. Four of them (*TYE7*, *RTG1*, *RTG3*, and *HMS1*) displayed a similar phenotype in a gut colonization model in antibiotic-treated conventionally raised animals (Perez et al., 2013b), implying that they are

primarily involved in controlling functions that the fungus requires to cope with host-derived demands (compared to functions that it requires to cope with demands originating from competing microbes). *TYE7*, *RTG1*, and *RTG3* were shown to be associated with the regulation of nutrient acquisition and metabolism (Askew et al., 2009; Dalal et al., 2016; Kastora et al., 2017), which probably explains their contribution to gut colonization independently of the presence of other microbes. Conversely, *ZCF8*, *ZFU2*, *TRY4*, and *ORF19.5910* presented a fitness defect only in gnotobiotic mice monocolonized with *C. albicans*. The fact that mutants of these regulators display a gut colonization defect only in the absence of other microbes and not in conventional antibiotic-treated mice exhibiting a residual microbiota suggests an effect of the residual microbes themselves or, alternatively, of differences in the murine response to the presence of other microbes. Further studies are required to understand these effects, although it should be stressed that mice are not natural hosts of *C. albicans*, and their indigenous flora might therefore not be relevant for gut colonization of the fungus.

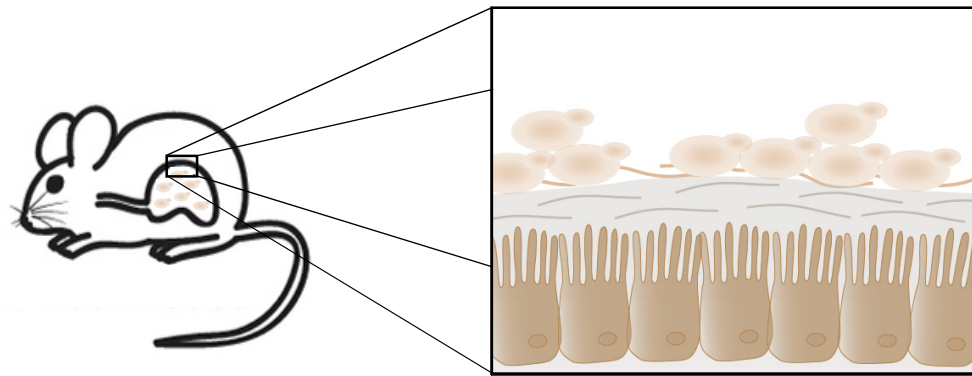


Figure 27: Model depicting gut colonization of germ-free animals.

Based on the results I showed in this chapter, I conclude that after oral gavage *Candida albicans* colonizes the gastrointestinal tract of germ-free animals predominantly in its oval-shaped yeast form negotiating the presence of two strong filamentation inducers 37°C (body temperature) and serum. Furthermore, it colonizes this niche in close proximity to the intestinal mucosa.

In conclusion, the use of germ-free animals provides a complementary system that can be used to uncover new aspects of gut colonization by *C. albicans*. This experimental system is particularly suited to studying the biology of *C. albicans* as a commensal in the mammalian gut. Since other microbes appear to significantly impact the morphology and

distribution of the fungus in the GI tract, the use of gnotobiotic rodents should become a valuable tool to explore the interplay between the fungus and other members of the microbiota. Finally, gnotobiotic animals may allow further identification of fungal traits that the fungus needs to colonize the GI tract, as well as factors that promote invasive proliferation and cause disease.

4) Dissecting the molecular function of three *C. albicans* regulators of gut colonization.

4.1) Summary

In the previous chapter, the genes *ZCF8*, *ZFU2*, and *TRY4* were identified in the genetic screen conducted in mice monocolonized with *C. albicans*. RNA-Seq experiments indicated that these three regulators share a substantial set of targets of regulation, implying that they significantly control overlapping cellular functions. Indeed, while each one of the three deletion strains exhibits a slight increase in filamentation under certain conditions, the triple deletion strain (*try4 zcf8 zfu2*) presented a more robust overfilamentation phenotype. Dissecting the basis of this phenotype revealed three mechanisms whereby the regulators may contribute to morphological control: first, through the transcriptional control of *FGR17*, a known regulator of hyphal formation; second, through modulations of the phosphorylation state of two major kinases (Mkc1 and Cek1) in signaling pathways that affect filamentation; and third, through the control of the She-dependent mRNA transport system. One of the major transcripts that is mislocalized in the triple deletion strain is *CHT2*, a gene that affects the exposure of chitin in the cell surface. The three identified alterations are likely to be factors in the triple deletion strain's increased susceptibility to killing by freshly isolated human neutrophils.

4.2) Introduction

4.2.1) *ZCF8*, *ZFU2*, *TRY4* – three transcriptional regulators in *C. albicans*.

The three putative transcriptional regulators *ZCF8*, *ZFU2*, and *TRY4* were identified in a genetic screening conducted in the GI tract of germ-free animals (Figure 23). Mutants of the three regulators were unable to persist in the GI tract of monocolonized animals (Figure 24). The three regulators lack clear orthologs in *S. cerevisiae*. Each of them contains a canonical DNA-binding domain. Based on the structure of these binding domains, they are assigned to the largest transcription factor families in yeasts: *TRY4* contains two zinc finger motifs (C_2H_2) and therefore belongs to the zinc finger transcription factor family, most common among all eukaryotes. *ZCF8* and *ZFU2* instead contain a binuclear zinc cluster (Zn_2Cys_6) and thus belong to the zinc cluster transcription factor family, largely specific to fungi. While large-scale phenotypic characterizations have highlighted the importance of transcription factors (Homann et al., 2009; Vandeputte et al., 2011), the specific functions of most of them remain unknown.

C. albicans - *TRY4*



C. albicans - *ZFU2*



C. albicans - *ZCF8*

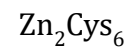


Figure 28: *ZCF8*, *ZFU2*, and *TRY4* belong to well known classes of transcription factors.

TRY4 belongs to the class of zinc finger transcription factors. It contains two C_2H_2 repeats. *ZFU2* and *ZCF8* contain a binuclear zinc cluster (Zn_2Cys_6). Therefore, they belong to the zinc cluster transcription factor family. Key amino acids of the DNA binding domains are displayed in red.

A phenotypic screening revealed that the deletion of any of the three genes results in colony wrinkling (Figure 25), a proxy for filamentation in *C. albicans*. They therefore negatively regulate filamentation in the fungus. Because *C. albicans* is colonizing the GI tract of monocolonized animals almost exclusively in its round-shaped yeast form (Figure

22B+C), the induction of filamentation due to the absence of the three regulators may cause a fitness defect in this particular host environment. Another study found a connection between *ZCF8*, *ZFU2*, and *TRY4* and adherence to a silicone (polydimethylsiloxane) substrate (Finkel et al., 2012). Strains harboring deletions in any of the three regulators exhibited a defect in adherence to a mucin-containing surface (Figure 26B) and mucus-producing cell-line (Bohm et al., 2017). This reduced adherence phenotype may hence provide another or an additional explanation for the previously identified gut colonization defect, since *C. albicans* cells were proved to colonize the GI tract of gnotobiotic animals in close proximity to the mucus layer (Figure 22B+C).

4.2.2) Subcellular mRNA localization

Cell polarity is required for differentiation, development, and cell motility in various organisms, including yeasts, insects, and mammals (Bashirullah et al., 1998; Kloc et al., 2002). One way to establish cell polarity is to place varying gradients of proteins in distinct sites of the cells. Such an asymmetry of proteins inside cells is most often achieved by placing their mRNAs in distinct sites, since this indirect localization has several advantages; for example, their expression is thus prevented in sites where they are not needed or are even disadvantageous for the cells. In some cases, translated proteins cannot be transported throughout the cells, as they are coupled to other factors immediately after translation. Finally, the transport of mRNAs transfers the control of protein expression to individual compartments of the cells, enabling independent and rapid response to local requirements. The distinct distribution of mRNAs can be accomplished through local synthesis, diffusion (Meignin et al., 2010), prevention from degradation (Holt et al., 2009; Meignin et al., 2010), or active transport (Martin et al., 2009) (Figure 29).

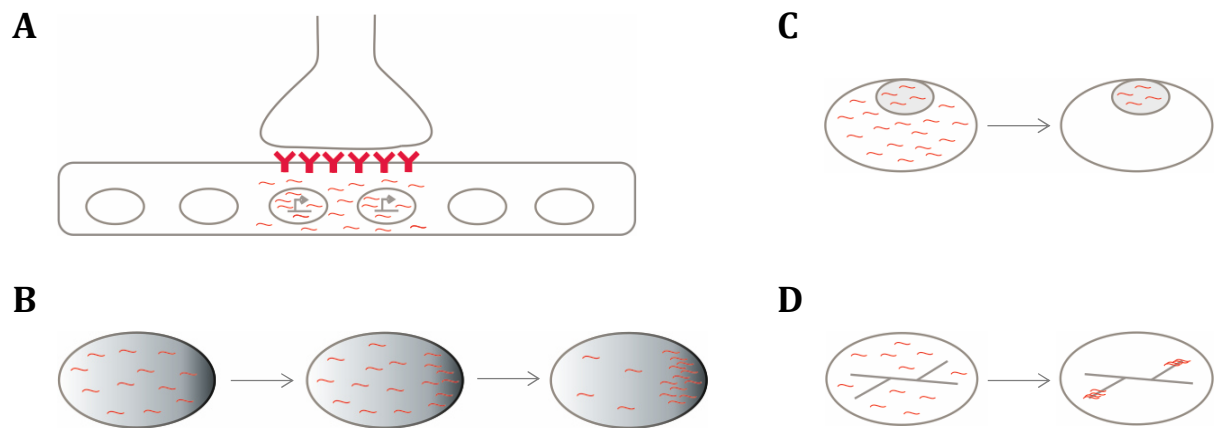


Figure 29: Different ways of mRNA localization.

Asymmetric localization of mRNAs is essential for differentiation and development in various cell types of different organisms. These specific patterns are achieved through different mechanisms. (A) Local synthesis. In multinucleated cells (e.g. muscle cells) mRNAs are only expressed in nuclei close to the desired location. In the case of muscles, only nuclei close to neuromuscular junctions express RNAs encoding the acetylcholine receptor, ensuring that translation is localised there as well. This phenomenon ensures the availability of important factors in pre- and postsynaptic areas and allows neurons to rapidly respond to extrinsic cues (Redondo *et al.*, 2011).

(B) Diffusion and entrapment. mRNAs diffuse freely throughout the cytoplasm and are captured in a distinct area through a previously deposited anchor protein. In *Drosophila* in this way the *nanos* mRNA is captured at the posterior pole of the oocyte (Forrest *et al.*, 2003).

(C) Degradation. Localization of mRNAs at distinct sites of a cell can be achieved through degradation of the mRNAs anywhere else in the cell. A well studied example is the *hsp83* mRNA again in *Drosophila* embryos (Ding *et al.*, 1993). It is restricted to the posterior pole through degradation everywhere else in the embryo. Binding of the Smaug protein, present everywhere except of the posterior pole, to cis-acting elements contained in the *hsp83* mRNA destabilizes and degrades this mRNA outside of the posterior pole (Bashirullah *et al.*, 1999; Semotok *et al.*, 2008).

(D) Active transport. For active transport along microtubules or actin filaments to distinct areas of cells, mRNAs need to contain cis-acting sequences, called Zip codes or localization signals. These sequences are recognized by trans-acting RNA-binding proteins generating in combination with motor proteins so called motor-protein containing particles (mRNPs). mRNPs are transported by Dynein or Kinesin along microtubules or by Myosin along actin filaments to their designated area in the cell (Bullock, 2007). Prominent examples for this mechanism are the *stardust* mRNA in *Drosophila* follicle cells, that is apically transported by Dynein (Horne-Badovinac *et al.*, 2008), the *Vg1* mRNA in *Xenopus* oocytes, that is actively transported to the vegetal pole during mid-oogenesis (King *et al.*, 2005) and the *ash1* mRNA in *Saccharomyces cerevisiae*, that is transported during budding to daughter cells via actin (McBride, 2017).

The active transport of mRNAs to different areas of the cell most often requires the binding to RNA-binding proteins. Together with these proteins, mRNAs are incorporated into motor-protein containing particles (Martin *et al.*, 2009), also called messenger ribonucleoprotein particles (mRNPs). In this composition, mRNAs are transported via

microtubules or actin filaments to their designated sites, where after reorganization, local protein synthesis can be activated (Besse et al., 2008; Meignin et al., 2010) and cell polarity is established. The combination of mRNA localization and localized translation occurs in almost all eukaryotic cells (St Johnston, 2005); for instance, the early embryogenesis of *Drosophila melanogaster* is essentially based on the translation of asymmetrically distributed mRNAs. However, polarity established via the predisposition of mRNAs plays important roles in unicellular organisms as well. One of the most prominent and best studied examples in single-celled eukaryotes so far is the asymmetric distribution and translation of the *ASH1* mRNA in the ascomycete yeast *Saccharomyces cerevisiae*.

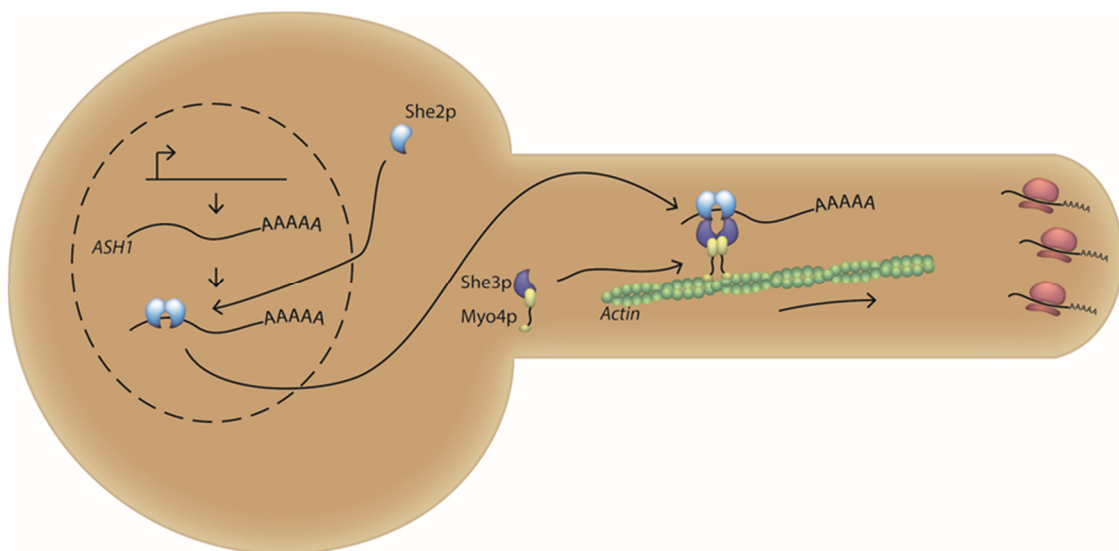


Figure 30: *SHE3*-dependent mRNA transport in *S. cerevisiae*.

Scheme depicting the transport of the *ASH1* mRNA via She2p/She3p/Myo4p to hyphal tips. *ASH1* mRNA is synthesized inside the nucleus of the mother cell. Already inside the nucleus it is bound by the mRNA binding protein She2. The *ASH1* mRNA, bound by She2p is transported outside of the nucleus and connected to She3p in the cytoplasm. She3p is typically bound by the motor protein Myo4p. The complex composed of the *ASH1* mRNA, She2p, She3p and Myo4p is subsequently transported along actin cables to the hyphal tips, where the mRNA is translated (McBride, 2017, modified).

The *ASH1* mRNA encodes a transcription factor that restrains cells from mating-type switching. Its mRNA is synthesized inside the nucleus and immediately bound by the

transport protein She2 (Figure 30). When transported outside the nucleus, the *ASH1* mRNA, together with She2p, is bound by another RNA-binding protein, She3, that is typically connected to the motor protein Myo4. This complex is subsequently transported along actin cables to the bud tip (Gonsalvez et al., 2005) (Figure 30). The distinct localization of the *ASH1* mRNA enables expression of the *ASH1* transcription factor solely in daughter cells, preventing them from mating-type switching (Jansen et al., 1996; Sil et al., 1996). In the hemiascomycete *Candida albicans*, an ortholog to the *S. cerevisiae* Ash1p, also called Ash1p, was identified (Inglis et al., 2002). During budding, it localizes similar to its ortholog, asymmetrically to daughter cells. Moreover, in hyphae, it localizes to apical nuclei (Elson et al., 2009; Inglis et al., 2002). The deletion of CaAsh1 causes defects in hyphal formation and lower virulence (Inglis et al., 2002), which indicates that *ASH1* has a role in *C. albicans*' hyphal formation. Identically to its ortholog, CaAsh1 is transported via She3p, since in the absence of the mRNA-binding protein, *ASH1* mRNA localization to bud and hyphal tips is disturbed (Elson et al., 2009). In *C. albicans* cells, 40 mRNAs whose localization depends on She3p were identified (Elson et al., 2009). In the presence of serum, *she3* deletion mutant cells display abnormal hyphal morphology, and embedded growth uncovered defects in extended hyphal growth (Elson et al., 2009). While *she3* cells caused less damage to epithelial cells *in vitro*, they do not affect virulence in a murine model of disseminated infection (Elson et al., 2009), further confirming that the asymmetric localization of specific proteins dependent on She3p impact hyphal differentiation in *Candida albicans*.

4.2.3) Kinases in *C. albicans* filamentation

C. albicans faces various environmental cues during host colonization, some of them inducing the transition from its yeast form to its filamentous form, including 37°C, serum, CO₂, increased pH, oxidative stress, and nutrient limitation (Brown, 2002; Brown et al., 1999; Mitchell, 1998). The sensors for most of these environmental signals remain unclear; however, the elements of different signaling cascades involved in transmitting the environmental cues and finally inducing the yeast-to-hyphal transition are heavily studied.

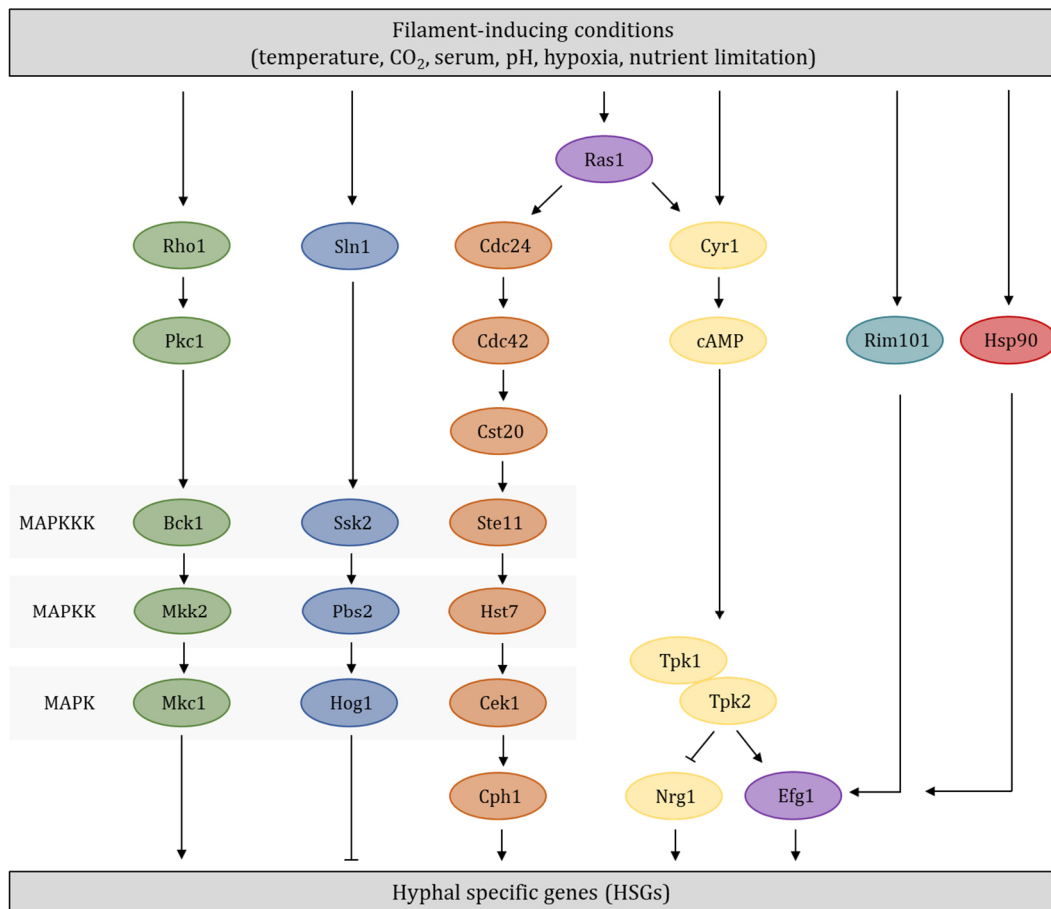


Figure 31: Kinases involved in *Candida albicans* morphogenesis.

Kinases play central roles in the yeast to hyphal transition in *C. albicans*. Displayed are the known components of three MAPK pathways: the Pkc1 MAPK pathway (green), the Hog1 MAPK pathway (blue) and the Cek1 MAPK pathway (orange). Further involved in filament induction through different environmental conditions are the cAMP PKA pathway (yellow) and the activation of Efg1 through the transcription factor Rim101 (turquoise) and the heatshock protein 90 (red). Components that play roles in different pathways are displayed in purple. MAPKKKs, MAPKKs and MAPKs are highlighted in bright grey. Different hyphal inducing conditions (temperature, CO₂, serum, pH, hypoxia or nutrient limitation) induce activation of different sensors located in the plasma membrane of the fungus, most of them unknown so far. These sensors activate downstream effectors that induce/repress the expression of hyphal specific genes (HSGs). For detailed description see text below.

The yeast-to-hyphal transition in *C. albicans* is generally governed by a complex network of signaling cascades whose activity is influenced by the presence or absence of filament-inducing cues. Two major kinase pathways are central to the morphological transition of the fungus: the cAMP-dependent protein kinase A (cAMP-PKA) and mitogen-activated protein kinase (MAPK) pathways (Biswas et al., 2007). In both types of pathways, the small GTPase Ras1 has vital roles. They result in the activation of hyphal-specific genes

(HSGs), inducing hyphal transition in *C. albicans* (Xie et al., 2016) (Figure 31). Serum induces hyphal transition through the activation of Cyr1, the only adenylyl cyclase expressed in *C. albicans* in two separate ways (Shapiro et al., 2009). On the one hand, one component of serum (bacterial peptidoglycan-like molecules) was revealed to activate Cyr1p directly via binding to a leucine-rich repeat region (Xu et al., 2008); on the other hand, serum is known to activate Ras1p, which in turn binds and activates Cyr1p (Fang et al., 2006). CO₂ is another filament-inducing cue that upon conversion into HCO₃ activates Cyr1p directly through interaction with its catalytic domain (Klengel et al., 2005). Cyr1p generates cAMP, which then activates the protein kinase complex A (PKA). Via Tpk1p and Tpk2p, this complex activates the terminal transcription factor Efg1, inducing the transcription of HSGs (Sudbery, 2011). Alkaline pH induces hyphal transition through the transcription factor Rim101, which after C-terminal cleavage activates Efg1p as well (Davis, 2009) (Figure 31). Elevated temperature sensed by heat shock protein 90 (Hsp90) (Kadosh, 2017; Shapiro et al., 2009) seems to be a prerequisite of all hyphal-inducing conditions (Sudbery, 2011). The fact that hyphal induction through raising the temperature requires an intact cAMP-PKA pathway suggests that this cue induces hyphal transition via the cAMP-PKA pathway and Efg1p (Figure 31). The activated PKA can also induce hyphal transition via repressing negative regulators of filamentation: it represses the transcription factor Nrg1, a negative regulator of HSGs, further inducing hyphal transition (Lu et al., 2014) (Figure 31). Ras1p is an important signal transducer in the Cek1 MAPK pathway; in response to nitrogen limitation and/or on certain carbon sources (Leberer et al., 1996; Liu et al., 1994), Ras1p activates the p21-activated kinase (PAK) Cst20 through Cdc42p and its guanosine exchange factor (GEF) Cdc24 (Gonzalez-Rubio et al., 2019). Cst20p phosphorylates and activates the serine/threonine (Ser/Thr) kinase MAPKKK (MAP kinase kinase kinase) Ste11, which in turn phosphorylates and activates its downstream effector, the MAPKK Hst7. Hst7p then phosphorylates the tyrosine and threonine residues at the activation loop (Thr-X-Tyr) of the MAPK Cek1. These phosphorylations stimulate conformational changes in Cek1p that fully activate the protein (Gonzalez-Rubio et al., 2019). Cek1p in its active form phosphorylates and activates the transcription factor Cph1, inducing the expression of HSGs, resulting in hyphal transition (Figure 31). Another MAPK pathway that controls hyphal formation in *C. albicans* is the high-osmolarity glycerol (Hog) pathway, which plays a repressive role in the filamentation of the fungus. Under filament-inducing conditions, the two-component

histidine kinase Sln1 located in the plasma membrane (Roman et al., 2019) induces the phosphorylation and activation of Ssk2p (MAPKKK). Active Ssk2p transfers the phosphoryl group to Pbs2p (MAPKK), which in turn phosphorylates and activates the MAPK Hog1 (Roman et al., 2007). In its active form, Hog1p translocates to the nucleus, where it represses HSGs, suppressing morphogenetic switching in the fungus (Roman et al., 2019) (Figure 31). One last MAPK pathway is involved in *C. albicans* morphogenesis: the Pkc1 pathway (Roman et al., 2007). Hyphal-inducing conditions induce the phosphorylation and activation of the protein kinase C (Pkc1) through the small GTPase Rho1 (Levin, 2005). The activated form of Pkc1p then phosphorylates and activates Bck1p (MAPKKK), Bck1p-P Mkk2 (MAPKK), and Mkk2-P, the MAPK Mkc1 (Kamada et al., 1996; Levin, 2005). The activated MAPK Mkc1 induces the expression of HSGs, resulting in morphogenetic switching (Figure 31).

In this chapter, I have further elucidated the role of the previously identified transcriptional regulators *ZCF8*, *ZFU2*, and *TRY4*. In the previous chapter, I demonstrated that the deletion of each one of the regulators impairs gut colonization of gnotobiotic animals by *Candida albicans* (Figure 23). Phenotypic screening revealed an increased filamentation under non-inducing conditions in mutants of each of the three regulators, indicating a role in the yeast-to-hyphal transition. Whole transcriptome analysis uncovered that these regulators controlled the expression of an overlapping set of genes. One of their common targets of regulation was *FGR17*, a known regulator of filamentation in *C. albicans*. A strain deleted for all three regulators was constructed to further explore their roles in the biology of *C. albicans*. *SHE3*, a key element of a recently described mechanism of mRNA localization involved in the yeast-to-hyphal transition, was another top common target of the three identified regulators. The triple deletion mutant was thus used to analyze whether the regulators affect morphogenesis through the impairment of *SHE3*-dependent mRNA localization. Finally, alterations in the composition of the cell wall possibly due to defects in the *SHE3*-dependent mRNA localization were connected to increased recognition by host immune cells observed in the mutants of all three regulators.

4.3) Material & Methods:

4.3.1) *Candida albicans* strains used in this chapter

Table 7: *Candida albicans* strains used in chapter 3.

Strain	Genotype	Source
SN152	$\frac{ura3\Delta::\lambda imm434::URA3-IRO1}{ura3\Delta::\lambda imm434} \frac{arg4::hisG}{arg4::hisG} \frac{his1::hisG}{his1::hisG} \frac{leu2::hisG}{leu2::hisG}$	Noble and Johnson, 2005
SN250	$\frac{ura3\Delta::\lambda imm434::URA3-IRO1}{ura3\Delta::\lambda imm434} \frac{arg4::hisG}{arg4::hisG} \frac{his1::hisG}{his1::hisG} \frac{leu2::hisG::CdHIS1}{leu2::hisG::CmLEU2}$	Homann <i>et al.</i> , 2009
TF55	$\frac{ura3\Delta::\lambda imm434::URA3-IRO1}{ura3\Delta::\lambda imm434} \frac{arg4::hisG}{arg4::hisG} \frac{his1::hisG}{his1::hisG} \frac{leu2::hisG}{leu2::hisG} \frac{try4\Delta::CdHIS1}{try4\Delta::CmLEU2}$	Homann <i>et al.</i> , 2009
TF114	$\frac{ura3\Delta::\lambda imm434::URA3-IRO1}{ura3\Delta::\lambda imm434} \frac{arg4::hisG}{arg4::hisG} \frac{his1::hisG}{his1::hisG} \frac{leu2::hisG}{leu2::hisG} \frac{fgr17\Delta::CdHIS1}{fgr17\Delta::CmLEU2}$	Homann <i>et al.</i> , 2009
TF120	$\frac{ura3\Delta::\lambda imm434::URA3-IRO1}{ura3\Delta::\lambda imm434} \frac{arg4::hisG}{arg4::hisG} \frac{his1::hisG}{his1::hisG} \frac{leu2::hisG}{leu2::hisG} \frac{zfu2\Delta::CdHIS1}{zfu2\Delta::CmLEU2}$	Homann <i>et al.</i> , 2009
TF141	$\frac{ura3\Delta::\lambda imm434::URA3-IRO1}{ura3\Delta::\lambda imm434} \frac{arg4::hisG}{arg4::hisG} \frac{his1::hisG}{his1::hisG} \frac{leu2::hisG}{leu2::hisG} \frac{zcf8\Delta::CdHIS1}{zcf8\Delta::CmLEU2}$	Homann <i>et al.</i> , 2009
JCP766	$\frac{ura3\Delta::\lambda imm434::URA3-IRO1}{ura3\Delta::\lambda imm434} \frac{arg4::hisG}{arg4::hisG} \frac{his1::hisG}{his1::hisG} \frac{leu2::hisG}{leu2::hisG} \frac{try4\Delta::CdHIS1}{try4\Delta::CmLEU2} \frac{zfu2\Delta}{zfu2\Delta}$	This work
JCP837	$\frac{ura3\Delta::\lambda imm434::URA3-IRO1}{ura3\Delta::\lambda imm434} \frac{arg4::hisG}{arg4::hisG} \frac{his1::hisG}{his1::hisG} \frac{leu2::hisG}{leu2::hisG} \frac{FGR17::AgTEF1p-NAT1-AgTEF1UTR-TDH3p-GFP-FGR17}{zcf21\Delta::CdHIS1}$	This work
JCP958	$\frac{ura3\Delta::\lambda imm434::URA3-IRO1}{ura3\Delta::\lambda imm434} \frac{arg4::hisG}{arg4::hisG} \frac{his1::hisG}{his1::hisG} \frac{leu2::hisG}{leu2::hisG} \frac{try4\Delta::CdHIS1}{try4\Delta::CmLEU2} \frac{zfu2\Delta}{zfu2\Delta} \frac{zcf8\Delta}{zcf8\Delta}$	This work
JCP1018	$\frac{ura3\Delta::\lambda imm434::URA3-IRO1}{ura3\Delta::\lambda imm434} \frac{arg4::hisG}{arg4::hisG} \frac{his1::hisG}{his1::hisG} \frac{leu2::hisG::CdHIS1}{leu2::hisG::CmLEU2} \frac{SHE3-13XMYC}{SHE3}$	This work
JCP1019	$\frac{ura3\Delta::\lambda imm434::URA3-IRO1}{ura3\Delta::\lambda imm434} \frac{arg4::hisG}{arg4::hisG} \frac{his1::hisG}{his1::hisG} \frac{leu2::hisG}{leu2::hisG} \frac{try4\Delta::CdHIS1}{try4\Delta::CmLEU2} \frac{zfu2\Delta}{zfu2\Delta} \frac{zcf8\Delta}{zcf8\Delta} \frac{SHE3-13XMYC}{SHE3}$	This work

4.3.2) Oligos used in this chapter

Table 8: Oligos used in chapter 3.

Name	Description	Sequence (3'-5')
JCP1887	upstream_region_zfu2_for	TAAAGGTACCTCCCCTTGGTAATTGTAAAAC
JCP1888	upstream_region_zfu2_rev	CAGTCTCGAGTGCAGAAAATGAAAATGATAAT
JCP1889	downstream_region_zfu2_for	CATTCGCGGATAGGTGTATACCTATATGTA
JCP1890	downstream_region_zfu2_rev	TATAGAGCTCTTAAGCCCCCTTCATTCATTTT
JCP1893	Test_deletion_zfu2_for	AAATTTGGCCTTGGAGCTTT
JCP1894	Test_deletion_zfu2_rev	TATCATCACCACCACCACCA
JCP2162	upstream_region_zcf8_for	AGACTTGGTACCCGTGGCTGTATTGATGGATTGT

JCP2163	upstream_region_zcf8_rev	AGATTACTCGAGAGAAGTTTGTGGCTGTTGGA
JCP2164	downstream_region_zcf8_for	AGACGCGGCCGCTGCAAGATCAAACCCTTAGTCT
JCP2165	downstream_region_zcf8_rev	AGCTAGCCGCGGACGAGTGTGTGTTGAAAGGT
JCP2166	Test_deletion_zcf8_for	ACAACCACAACAACAACCAGT
JCP2167	Test_deletion_zcf8_rev	ACGAGTGTGTGTTGAAAGGT
JCP2494	MYC_Tag_SHE3_for	TAACAACAACAACAACAATAGCAAAAAGAAATTCGCA ACTTTTCGATAATAACTTTGTATTAATGTACGGATC CCCGGGTTAATTAACGG
JCP2495	MYC_Tag_SHE3_rev	TAGTTATCCATTTTTTTAATAAAAACTAACGTGTA ATATGCTCTAAAAATATAAACCTCTATAGGCGGCCGC TCTAGAAGTAGTGGATC
JCP2496	Test_insertion_MYC_for	CGTCAACCAAGTCAGCAAAA
JCP1437	Test_insertion_MYC_rev	ACAACCTCAGAGCACGCTAGA
JCP_2040	<i>FGR17</i> _OE_for	GTCAAATTTATTAGAGAAAATTATGCTTATGAAAGA TACCCTCGATCTTAACAATAGTATTGAACGCCCTATC AAGCTTGCCTCGTCCCC
JCP_2041	<i>FGR17</i> _OE_rev	TACATTTTCTTCTACGTTTACGACAATTATCACAAGC AATTGAAACGTAAGATCTAGATTTTGACAGCATATT TGAATTC AATTGTGATG
JCP_2069	<i>FGR17</i> _test_OE_for	CCCTATGGATGAGTTGGTGTC
JCP_2070	<i>FGR17</i> _test_OE_rev	TCATGAATTCTGTGTCTGCCA

4.3.3) Plasmids used in this chapter

Table 9: Plasmids used in chapter 3.

Name	Description	Source
pADH34	coding sequence for a 13×myc repeat	Hernday <i>et al.</i> , 2010
pSFS2a	SAT1-flipper	Reuss <i>et al.</i> , 2004
pCJN542	coding sequence for the <i>C. albicans</i> TDH3 promoter	Nobile <i>et al.</i> , 2008

4.3.4) Probes used in this chapter

Table 10: FISH probes used in chapter 3.

Name	Description	Sequence	Source
ITS-2	FISH-Probe homolog to <i>ITS-2</i> of <i>S. cerevisiae</i>	[CY5] ATAGGCCAGCAATTTCAAGT [CY5] TAACTCCAAAGAGTATCACTC [CY5]	Zenklusen <i>et al.</i> , 2010
CHT_1	FISH-Probe homolog to a middle region of <i>CHT2</i>	[CY5] GCATCGTCAGCTTTGGCCAG [CY5] TGCCTCCAATCAAGTTGCTC [CY5]	This work
CHT_2	FISH-Probe homolog to the 3'end of <i>CHT2</i>	[CY5] CTGTTCCAGTATTCACTTTT [CY5] GAAGGTG GTGCTGCAGTTGC [CY5]	This work
CHT_3	FISH-Probe homolog to the 3'end of <i>CHT2</i>	[CY5] CTGCTGCTCCACAATGTCCA [CY5] TACCCTGATGCATCTCTTGG [CY5]	This work
ASH_1	FISH-Probe homolog to the 5'end of <i>ASH1</i>	[CY5] AGCAAGAAGTGCACCACCAT [CY5] CTCCTCCATATGAAACTG [CY5]	This work
ASH_2	FISH-Probe homolog to a middle region of <i>ASH1</i>	[CY5] TATTACAATTGAAAGAGCGC [CY5] CAACTCCCCCACCTCCA [CY5]	This work
ASH_3	FISH-Probe homolog to the 3'end of <i>ASH1</i>	[CY5] GGTGAATGGACCCTCATGCA [CY5] AAGCAAAGGAAAAGAGAC [CY5]	This work

4.3.5) Deletion mutants

The SAT1 flipping method (Reuss *et al.*, 2004) was used to construct the double deletion mutant *try4 zfu2* and the triple deletion mutant *try4 zfu2 zcf8*. Briefly, the upstream region of *ZFU2*, amplified with primers JCP1887 and JCP1888 (Table 8) was inserted in the KpnI/XhoI restriction sites upstream of the SAT1/flipper cassette in pSFS2a (Table 9) and transformed in *E.coli* DH5alpha. Clones, that inserted a complete plasmid were identified by antibiotic resistance. Subsequently, the downstream region of *ZFU2*, amplified with primers JCP1889 and JCP1890 (Table 8) was inserted in the SacII/SacI restriction sites downstream of the SAT1/flipper cassette in pSFS2a containing the upstream region of *ZFU2* and transformed in *E.coli* DH5alpha. Clones, that inserted a complete plasmid were identified by antibiotic resistance. Plasmids containing the correct up-, and downstream region of *ZFU2* were extracted and digested with KpnI/SacI to cut out the SAT1/flipper cassette flanked by the up-, and downstream regions of *ZFU2*. The linearized DNA fragment was transformed in strain TF55 (Table 7) using the heatshock method. Through sequence homology of the up- and downstream regions, the coding sequence of *ZFU2* was replaced by the SAT1/flipper cassette. Clones, that replaced the coding sequence of *ZFU2* successfully were identified by antibiotic resistance. After the removal of the SAT1/flipper cassette through growth on Maltose (Reuss *et al.*, 2004) the transformation was repeated to replace the second copy of *ZFU2*. The deletion of both copies of *ZFU2* was verified by PCR using primers JCP1893 and JCP1894 (Table 8). The same experimental procedure was used to construct the triple deletion mutant *try4 zfu2 zcf8*. Primers to amplify the upstream region of *ZCF8*, JCP2162 (KpnI) and JCP2163 (XhoI), and to amplify the downstream region of *ZCF8*, JCP2164 (NotI) and JCP2165 (SacII), are listed in Table 8. Plasmids containing the correct up-, and downstream region of *ZCF8* were extracted and digested with KpnI/SacII to cut out the SAT1/flipper cassette flanked by the up-, and downstream regions of *ZCF8*. The linearized DNA fragment was transformed in strain JCP766 (Table 7) using the heatshock method. The deletion of both copies of *ZCF8* was verified by PCR using primers JCP2166 and JCP2167 (Table 8).

4.3.6) Overexpression strain

FGR17 overexpression was achieved by placing a copy of the *TDH3* promoter upstream of its coding sequence as described previously (Nobile *et al.*, 2008). Briefly, the *TDH3* promoter sequence was amplified from plasmid pCJN542 (Table 9) using a forward and reverse primer (JCP_2040/2041, Table 8) that are composed of a a nucleotide sequence

complementary to an upstream sequence of the *FGR17* coding sequence and a nucleotide sequence complementary to *pTDH3*. In this way a fragment was constructed composed in the following order: homology to a sequence upstream of *FGR17* – *pTDH3* – homology to a sequence upstream of *FGR17*. This fragment was transformed in *C. albicans* SN250 cells (Table 7) using the heatshock method. Through sequence homology of the upstream region of *FGR17*, the coding sequence of *pTDH3* was placed upstream of the *FGR17* coding sequence. Clones, that incorporated the *TDH3* promoter successfully upstream of *FGR17* were identified by antibiotic resistance. Correct insertion and nucleotide sequence were tested by PCR and sequencing using primers JCP_2069/2070 (Table 8).

4.3.7) MYC-tagging

The procedure for gene tagging with MYC (13xMYC) has been described earlier (Hernday *et al.*, 2010). Briefly, *SHE3* was MYC-tagged via amplification of 13xMYC followed by the SAT1/flipper cassette from plasmid pADH34 (Table 9) with oligos JCP2494 and JCP2495 (Table 8). The first 67 nucleotides of the forward primer are homolog to the 3' end of *SHE3*, except of the STOP codon. The remaining 23 nucleotides are homolog to the 5' end of the 13xMYC tag contained in plasmid pADH34. The first 61 nucleotides of the reverse primer are homolog to the downstream region of *SHE3*. The remaining 29 nucleotides are homolog to the 3' end of the SAT1/flipper cassette contained in plasmid pADH34. Amplification of the 13xMYC followed by the SAT1/flipper cassette using primers JCP2494 and JCP2495 (Table 8) therefore constructs a DNA fragment with the following order: 3'end homology to *SHE3* (STOP codon excluded) – 13xMYC – SAT1/flipper cassette – homology to downstream region of *SHE3*. This DNA fragment was transformed in *C. albicans* strains SN250 and JCP958 (Table 7) using heat shock and via homologous recombination the 13xMYC tag was inserted downstream of *SHE3*. Successful tagging of one copy of *SHE3* was verified by PCR using primers JCP2496 and JCP1437 (Table 8). The SAT1/flipper cassette was removed as described (Reuss *et al.*, 2004). Correct insertion and nucleotide sequence of the 13xMYC tag was verified by sequencing and Western blot analysis described in chapter 4.3.12 (Figure 32).

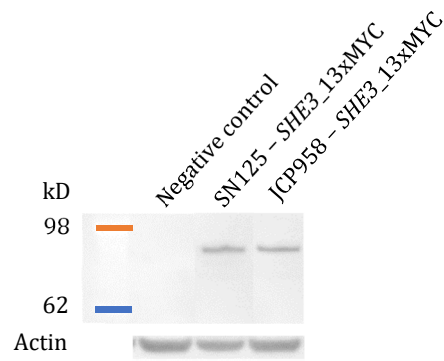


Figure 32: Confirmation of 13xMYC tag of *SHE3* using Western blot analysis.

The C-terminal tag of *SHE3* with 13 repeats of MYC in the *C. albicans* strains SN250 and JCP958 (Table 7) was confirmed using Western blot analysis. Untagged control, positive control and the two *SHE3*-MYC tagged strains were grown to stationary phase in YPD at 30°C shaking. Whole cell extracts were prepared and resolved by PAGE as described in chapter 2.3.9 and 4.3.12. Proteins were transferred to a PVDF membrane and the MYC tag was stained using a c-Myc Monoclonal Antibody. As loading control actin was stained using a rabbit polyclonal anti-Actin antibody (lower panel).

4.3.8) Filamentation assays

Embedded colonies. *C. albicans* wild-type and mutant strains were grown to stationary phase overnight in YPD liquid medium at 30°C shaking. Cells were washed once in 1x PBS and counted in a haematocytometer. 100 µl cell suspension containing approximately 100 cfus were placed on top of a thin layer of soft (1%) YPD agar. Before the soft agar solidified, another layer of soft agar was overlaid on top. After the agar solidified completely, plates were incubated at 37°C for 48 h prior to evaluation.

Spot assays. *C. albicans* wild-type and mutant strains were grown to stationary phase overnight in YPD liquid medium at 30°C shaking. Spot assays were performed as described earlier (Ram *et al.*, 2006). Briefly, cells were harvested, washed in dH₂O and counted in a haematocytometer. 5x10⁴ cells were spotted on SpiderAgar plates. Plates were incubated at 30° for 24 hours prior to evaluation.

Stab culture. Growth as stab culture was performed essentially as described (Elson *et al.*, 2009). Briefly, solidified SpiderAgar was cut in 1 mm thick pieces and placed on microscope slides. *C. albicans* wild-type and mutant cells were grown to stationary phase overnight in YPD liquid at 30° shaking. Cells were harvested and washed twice in 1x PBS. Cells were counted in a haematocytometer, 10 µl containing approximately 10 cfus were placed on the agar pieces and overlaid with coverslips. Stab cultures were incubated at 30°C in a humid chamber for 24-48 hours prior to evaluation.

Colonies under Coverslips. Colony morphology was assessed via growth of *C. albicans* strains under a coverslip as described (Elson *et al.*, 2009). Briefly, *C. albicans* wild-type and mutant cells were grown to stationary phase overnight in YPD liquid at 30°C. Cells were harvested and washed twice in 1xPBS. Cells were counted in a haemocytometer and 100 µl containing approximately 100 cfus were spread on a SpiderAgar plate. A microscope slide was placed atop the agar. Plates were incubated at 30°C for 5 days in an anaerobic chamber prior to evaluation.

Filamentation induction with serum. *C. albicans* wild-type and mutant cells were grown to stationary phase overnight in YPD liquid at 30°C. Cells were diluted 1:10 in YPD containing 10% serum and incubated shaking at 30°C for 30, 60, 180 min or over night.

4.3.9) Fluorescence *in situ* hybridization (FISH)

Buffers:

Potassium phosphate buffer 100 mM, pH7.5

83.4 ml 1M K₂HPO₄
16.6 ml 1M KH₂PO₄
adjust pH to 7.5
adjust to 1 Liter with dH₂O
store at RT

Potassium phosphate buffer 140 mM, pH7.5

116.76 ml 1M K₂HPO₄
23.24 ml 1M KH₂PO₄
adjust pH to 7.5
adjust to 1 Liter with dH₂O
store at RT

Sodium phosphate buffer 100 mM, pH7.5

80.95 ml 1M Na₂HPO₄
19.05 ml 1M NaH₂PO₄
adjust pH to 7.5
adjust to 1 Liter with dH₂O
store at RT

1xbuffer B

1.2 M Sorbitol
dissolved in 100 mM potassium phosphate buffer pH7.5
store at 4°C

1.4xbuffer B

1.7 M Sorbitol
dissolved in 140 mM potassium phosphate buffer pH7.5
store at 4°C

Competitor DNA

50 µl 10 mg/ml sheared salmon sperm DNA
50 µl 10 mg/ml *E. coli* tRNA
store at -20°C

20xSSC

800 ml dH₂O
175.3 g NaCl (3 M)
88.2g trisodium citrate (300 mM)
adjust pH to 7 with HCl
adjust volume to 1 Liter with dH₂O
store at RT

Spheroblasting buffer

1.8 ml 1.4x buffer B
5 µl β-mercaptoethanol (gibco, Thermo Fisher Scientific, Waltham, MA, USA)
250 µl 200 mM VRC (Sigma-Aldrich, St. Louis, MO, USA)
390 µl dH₂O

Hybridization buffer

50 ml deionized formamide
10 ml 20x SSC
40 ml H₂O

4% Paraformaldehyde

0.4 g paraformaldehyde
Heat up to 60°C, stirr until dissolved
Adjust pH to 6.9
Adjust volume to 10 ml with 1x PBS

Solution F (1 coverslip)

16 µl deionized formamide
2 µl 100 mM sodium phosphate buffer pH7.5
2 µl dH₂O

Solution H (4 coverslips)

15 µl dH₂O
10 µl 20x SCC
10 µl 20 mg/ml BSA
5 µl VRC (Sigma)
10 µl deionized formamide

Fluorescence *in situ* hybridization (FISH) was performed as described earlier (Zenklusen *et al.*, 2010), with several modifications.

Growth conditions

C. albicans wild-type and mutant cells were grown to stationary phase in YPD liquid at 30°C shaking overnight. Cells were diluted 1:10 in YPD containing 10% serum to induce

filamentation (For approximately 10 coverslips with cells; 2 ml stationary phase culture + 18 ml YPD/10% Serum). Cells were incubated 30 min at 30°C shaking.

Cell Fixation

Cells were harvested, resuspended in 10 ml freshly prepared 4% paraformaldehyde and incubated 45 min at RT on a nutator. Cells were washed 3x with 10 ml ice cold 1xbuffer B and centrifuged at 2400g, 5 min at 4°C.

Spheroblasting

Cells were resuspended in 1 ml spheroblasting buffer and 800 units Lyticase from *Arthrobacter luteus* (Sigma-Aldrich, St. Louis, MO, USA) were added to digest the cell wall. Spheroblasting was conducted at 30°C for 10-20 min. Digestion of the cell wall was checked first after 10 min, then every 5 min. After spheroblasting was completed, cells were collected 4 min at 1300g at 4°C, washed once in 1 ml ice cold 1xbuffer B and resuspended in 1 ml ice cold 1xbuffer B. 150 µl cell suspension was dropped on a poly-L-lysine coated coverslip. Coverslips were incubated at 4°C for at least 30 min to let the cells adhere to the coverslips. Subsequently, coverslips were washed once in 5 ml ice cold 1xbuffer B and stored in cell culture well plates in 5 ml 70%EtOH sealed with parafilm at -20°C up to 6 months.

Probe design

To achieve a perfect coverage, for each RNA that was chosen for FISH three probes were designed, each of them 38 - 40 nucleotides long and are listed in Table 10. One of them homolog to the 5' end of the respective gene, one to the middle and one to the 3' end of the gene. Probes were tested for secondary and tertiary structures that would decrease binding to the respective RNA. They were ordered with Cy5 tags at their 5' end, in their middle and their 3' end, HPLC purified and liquid in concentration of 0.01 µmol. A probe homolog to the *ITS-2* of *S. cerevisiae* (Table 10) (Zenklusen *et al.*, 2010) was used to establish this technique in *C. albicans*.

Hybridization

Coverslips were rehydrated by two sequential incubations in 2x SSC for 5 min at RT. Afterwards, coverslips were incubated in hybridization solution for 15 min at RT. The three probes designed to detect one specific RNA were combined and 1 ng was combined with 4 µl 10 mg/ml competitor DNA. 12 µl solution F and 12 µl solution H were added and 20 µl were dropped into a petridish. One coverslip was put face down onto the probe drop. A 50 ml Falcon tube cap was filled with hybridization solution and added to the petridish

to humidify the hybridization chamber. The chamber was sealed with parafilm and covered with aluminium foil, since the probes are light sensitive. Hybridization was performed 1 hour at a temperature depending on the probes (here for *CHT2*: 65°C, for *AHS1*: 55°C). Subsequently, the coverslips were washed twice in hybridization solution for 15 min at the same temperature as hybridization was performed. One washing step in 0.1% Triton X-100/2x SSC at RT and two washing steps in 1x SSC for 15 min on an orbital shaker followed. Nuclei were stained with DAPI and remaining cell wall with Calcofluor white for 2 min at RT. Coverslips were washed again using 1x PBS for 5 min and air dried. Coverslips were mounted using ProLong™ Diamond Antifade Mountant (Invitrogen, Thermo Fisher Scientific, Waltham, MA, USA), imaged or stored at -20°C.

4.3.10) Immunohistochemistry

C. albicans wild-type and *SHE3*-MYC-tagged strains (SN250, JCP1018 and JCP1019 (Table 7) were grown, spheroplasted and fixed on coverslips as it is described in section 4.3.9) Fluorescence *in situ* hybridization. After rehydration coverslips were washed in 1x TBS and blocked in 1x TBS containing 5% milk, 1 hour at room temperature. After sequential washes in 1x TBS the 13x MYC-tag of *SHE3* was probed with a mouse c-Myc Monoclonal Antibody (Invitrogen, Thermo Fisher Scientific, Waltham, MA, USA, 9E10.3) 1:500 diluted in 1x TBS containing 5% milk for 2 hours at room temperature. Unbound antibody was removed with 1x TBST (1xTBS + 0.05% Tween20). To be able to localize *SHE3* inside the cells, coverslips were incubated with Alexa Fluor™ 488 goat anti-mouse IgG, IgM (H+L) (Life Technologies, Thermo Fisher Scientific, Waltham, MA, USA, A10680) 1:500 diluted and DAPI (Sigma-Aldrich, St. Louis, MO, USA) to stain the nuclei for 1 hour at room temperature in 1x TBS containing 5% milk. Unbound secondary antibody was removed with 1x TBST. Coverslips were mounted in ProLong™ Diamond Antifade Mountant (Invitrogen, Thermo Fisher Scientific, Waltham, MA, USA) and imaged via fluorescence microscopy.

4.3.11) Neutrophil killing assay

The EasySep™ Human Neutrophil Enrichment Kit (Stemcell Technologies, Vancouver, Canada) was used to isolate neutrophils from leucocyte-containing cones, which had been prepared from whole blood of healthy donors (kindly provided by the Department of Transfusion Medicine, University Hospital Würzburg). The neutrophil killing assay was performed essentially as described (Urban, Reichard, Brinkmann, & Zychlinsky, 2006).

Briefly, neutrophils were seeded in RPMI 1640 medium supplemented with 2% human serum (Sigma-Aldrich, St. Louis, MO, USA) in 24-well plates and allowed to attach to the surface. Neutrophils were activated using 25 nM phorbol myristate acetate (Sigma-Aldrich, St. Louis, MO, USA). After 30 min incubation at 37 °C, the medium was carefully replaced with fresh RPMI, containing 2% human serum and incubated for another 20 min before infection with *C. albicans* at MOI 0.01. Samples were centrifuged at 700 g for 10 min and incubated at 37 °C and 5% CO₂ for 2 hours. *C. albicans* cells incubated under the same conditions but without neutrophils were used to calculate the percentage of *C. albicans* killing. Each assay was performed in triplicates.

4.3.12) Western Blot

Buffers:

<u>10xTBS:</u>	<u>SDS Samplebuffer:</u>	<u>Transferbuffer:</u>
0.2 M Tris	0.06 M Tris-Cl	14 g Glycin
1.5 M NaCl	5% Glycerol	3 g Tris
	2% SDS	100 ml Methanol
	4% β-Mercaptoethanol	400 ml H ₂ O
	0.0025% Bromophenol Blue	

MYC-tagged SHE3

Untagged control and MYC-tagged wild-type or triple deletion mutant cells were grown in liquid YPD to stationary phase at 30°C overnight shaking. Cells were diluted 1:10 in YPD/10% serum to induce filamentation and shaken at 30°C for 30 min before harvesting. 3x10⁷ cells were spun down and washed once in dH₂O, 5000 rpm, 1 min. Cells were resuspended in 100 µl H₂O. 100 µl NaOH (0.2M) were added and the cells were incubated 10 min at room temperature. Subsequently, cells were collected via centrifugation and resuspended in 50 µl SDS sample buffer. Cells were incubated 5 min at 100°C. Cell debris was spun down and the supernatant containing whole cell extracts was combined with NuPAGE™ LDS Sample Buffer (Invitrogen by Thermo Fisher Scientific, Waltham, MA, USA) and resolved by PAGE (NuPAGE™ 4-12% Bis-Tris Gels, Invitrogen by Thermo Fisher Scientific, Waltham, MA, USA) (150 V, 100 mA, 1.5 hours) in MES SDS Running Buffer (Novex by Thermo Fisher Scientific, Carlsbad, CA, USA). The proteins were transferred to a PVDF membrane (pore size 0,45 µm, Carl Roth, Karlsruhe, Germany) in Transferbuffer (30 V, 500 mA, 2 hours). The membrane was washed in 1x TBS and blocked in 1x TBS containing 5% milk, 1 hour at room temperature. After sequential washes in 1x TBS the

MYC-tagged proteins were probed with a c-Myc Monoclonal Antibody (Invitrogen by Thermo Fisher Scientific, Waltham, MA, USA, 9E10.3) and a rabbit polyclonal anti-Actin antibody (Sigma-Aldrich, St. Louis, MO, USA, A5060) (Loading control) 1:4800 diluted in 1x TBS containing 5% milk for 2 hours at room temperature. Unbound antibody was removed with 1x TBST (1x TBS + 0.05% Tween20) and the proteins were incubated with 1:120000 diluted secondary antibodies conjugated to horseradish peroxidase for 1 hour at room temperature in 1x TBS containing 5% milk. Unbound secondary antibody was removed with 1x TBST and the proteins were imaged using SuperSignal™ West Femto Maximum Sensitivity Substrate (Thermo Fisher Scientific, Waltham, MA, USA, 34095).

Phosphorylation level of Mkc1p/Cek1p

Wild-type and triple deletion mutant cells were grown in liquid YPD to stationary phase at 30°C overnight. Cells were diluted 1:10 in YPD/10% serum to induce filamentation and shaken at 30°C for 30, 60 and 180 min or over night before harvesting. 3×10^7 cells were spun down and washed once in dH₂O, 5000 rpm, 1 min. Cells were resuspended in 100 µl H₂O. 100 µl NaOH (0.2M) were added and the cells were incubated 10 min at room temperature. Subsequently, cells were collected via centrifugation and resuspended in 50µl SDS sample buffer. Cells were incubated 5 min at 100°C. Cell debris was spun down and the supernatant containing whole cell extracts was combined with NuPAGE™ LDS Sample Buffer (Invitrogen by Thermo Fisher Scientific, Waltham, MA, USA) and resolved by PAGE (NuPAGE™ 4-12% Bis-Tris Gels, Invitrogen by Thermo Fisher Scientific, Waltham, MA, USA) (150V, 100mA, 1.5 hours) in MES SDS Running Buffer (Novex by Thermo Fisher Scientific, Waltham, MA, USA). The proteins were transferred to a PVDF membrane (pore size 0,45 µm, Carl Roth, Karlsruhe, Germany) in Transferbuffer (30 V, 500 mA, 2 hours). The membrane was washed in 1x TBS and blocked in 1x TBS containing 5% milk, 1 hour at room temperature. After sequential washes in 1x TBS the phosphorylated fraction of Mkc1p and Cek1p were probed with a mouse monoclonal anti-Phospho-p44/42 MAPK (Erk1/2) (Thr202/Tyr204) antibody (Cell Signaling, Danvers, MA, USA, 9106) and a rabbit polyclonal anti-Actin antibody (Sigma-Aldrich, St. Louis, Missouri, USA, A5060) (Loading control) 1:4800 diluted in 1xTBS containing 5% milk for 2 hours at room temperature. Unbound antibody was removed with 1x TBST (1x TBS + 0.05% Tween20) and the proteins were incubated with 1:12000 diluted secondary antibodies conjugated to horseradish peroxidase for 1 hour at room temperature in 1xTBS containing 5% milk. Unbound secondary antibody was removed with 1x TBST and

the proteins were imaged using SuperSignal™ West Femto Maximum Sensitivity Substrate (Thermo Fisher Scientific, Waltham, MA, USA, 34095).

4.3.13) Transcriptome analysis

The *C. albicans* reference strain and deletion mutants were grown on Todd-Hewitt agar at 37°C for 24 h. Cell collection, RNA purification, library preparation and sequencing were carried out as I described in chapter 2.3.4. Two biological replicates of each strain were analyzed. We obtained between 27–42 million reads per sample. Low quality reads were eliminated, and adapter sequences trimmed using Trimmomatic (Bolger *et al.*, 2014) (v0.36) with default settings for single end reads. Over 95% of reads in every sample passed the quality control and were aligned to the *C. albicans* reference genome Build 21 using STAR (Dobin *et al.*, 2013) (v2.5.2b) with default parameters. From the resulting BAM files, raw read counts were extracted with HTSeq (Anders *et al.*, 2015) (v0.6.1) using the respective annotation. Read counts were loaded into R (v3.3.2) and analyzed with the DESeq2 (Love *et al.*, 2014) package (v1.14.1). With our depth of sequencing, we detected a significant number of reads in >6100 annotated ORFs (99%). Differential gene expression analysis was performed using the default DESeq2 workflow. Adjusted P-values of 0.1, 0.05 and 0.01, which were obtained through the Benjamini-Hochberg-method (Benjamini *et al.*, 2001), were taken as cut-offs for significance. To verify the validity of the analysis, we determined the P-value distribution across the samples. For the *ZCF8* dataset, an overestimation of the null model variance was detected and corrected using *fdrtool* (Strimmer, 2008). As an additional measure to reduce the rate of false positives in the corrected dataset, we applied a minimum fold-change threshold (\log_2 values of $|\log_2|$). This ad hoc measure does not change the overall structure of the inferred network. Cytoscape (Shannon *et al.*, 2003) (v3.4) was employed to visualize the network and generate the displayed graphs. Method description with minor modifications was taken from Böhm *et al.*, 2017.

4.4) Results:

4.4.1) The transcription regulators *ZCF8*, *TRY4*, and *ZFU2* share a large set of target genes.

The transcriptional regulators *ZCF8*, *ZFU2*, and *TRY4* were identified in a genetic screening described in chapter 3 (Figure 23). Deletion of each one of the three regulators showed a defect in gut colonization of gnotobiotic mice (Figure 24A) (Bohm *et al.*, 2017), suggesting that they control cellular functions that contribute to proliferation in the mammalian intestine. These regulators influence adherence to mucin containing surfaces (Figure 26) and negatively regulate filamentation under certain conditions (Figure 25). Work from the Pérez lab as well as other groups clearly indicate that filamentation in *C. albicans* is correlated with defects in gut colonization (Bohm *et al.*, 2017; Tso *et al.*, 2018; Witchley *et al.*, 2019). A connection between the identified regulators and filamentation could therefore explain their gut colonization defect in gnotobiotic mice. To uncover how *ZCF8*, *ZFU2*, and *TRY4* control filamentation and establish whether other cellular functions may also account for their gut colonization defect, I performed transcriptome analyses (RNA sequencing) comparing the wild-type reference strain to each one of the three deletion mutants. RNA was prepared from *C. albicans* cells growing under conditions that mimic some of the conditions present in the mammalian host: body temperature (37°C), growing on a semi-solid surface (Todd-Hewitt agar). In this experimental setup, microscopy analysis revealed that >99% of the *C. albicans* cells remain in the yeast form.

In total, the transcriptome analysis revealed 395 protein-coding transcripts whose expression was dependent on one or more of the three regulators evaluated ($P_{\text{adj}} < 0.01$; Figure 33A, Table S 4; 560 targets at $P_{\text{adj}} < 0.05$, (Table S 3); 670 targets at $P_{\text{adj}} < 0.1$, (Table S 2). Each of the three regulators controls the expression of its own set of target genes (*ZCF8*: 262, *ZFU2*: 192, *TRY4*: 211), but interestingly they share a large amount of target genes (89 transcripts in common for all the three proteins, $P = 6.09 \times 10^{-216}$; 38 additional transcripts shared only by *ZCF8* and *ZFU2*, $P < 8.09 \times 10^{-17}$; 37 shared only by *ZCF8* and *TRY4*, $P < 1.33 \times 10^{-14}$; and 15 in common only between *ZFU2* and *TRY4*, $P < 8.77 \times 10^{-4}$) suggesting that there is a significant degree of overlap in the functions governed by the three proteins (Figure 33B). A closer look at the shared targets revealed moreover that their expression is regulated (activated or repressed) by *ZCF8*, *ZFU2*, and *TRY4* in the same direction in all but 2 of the 179 shared targets (Figure 33B). A transcript whose expression

is dependent on *ZCF8*, *ZFU2*, and *TRY4* is therefore either activated by all three proteins or repressed by all three of them. The same is true for genes under the control of two of the regulators. All these features of the network are robust to threshold changes (see 4.3.13) and Table S 2, Table S 3, Table S 4). These findings indicate that *ZCF8*, *ZFU2*, and *TRY4* govern, to a significant extent, overlapping cellular functions.

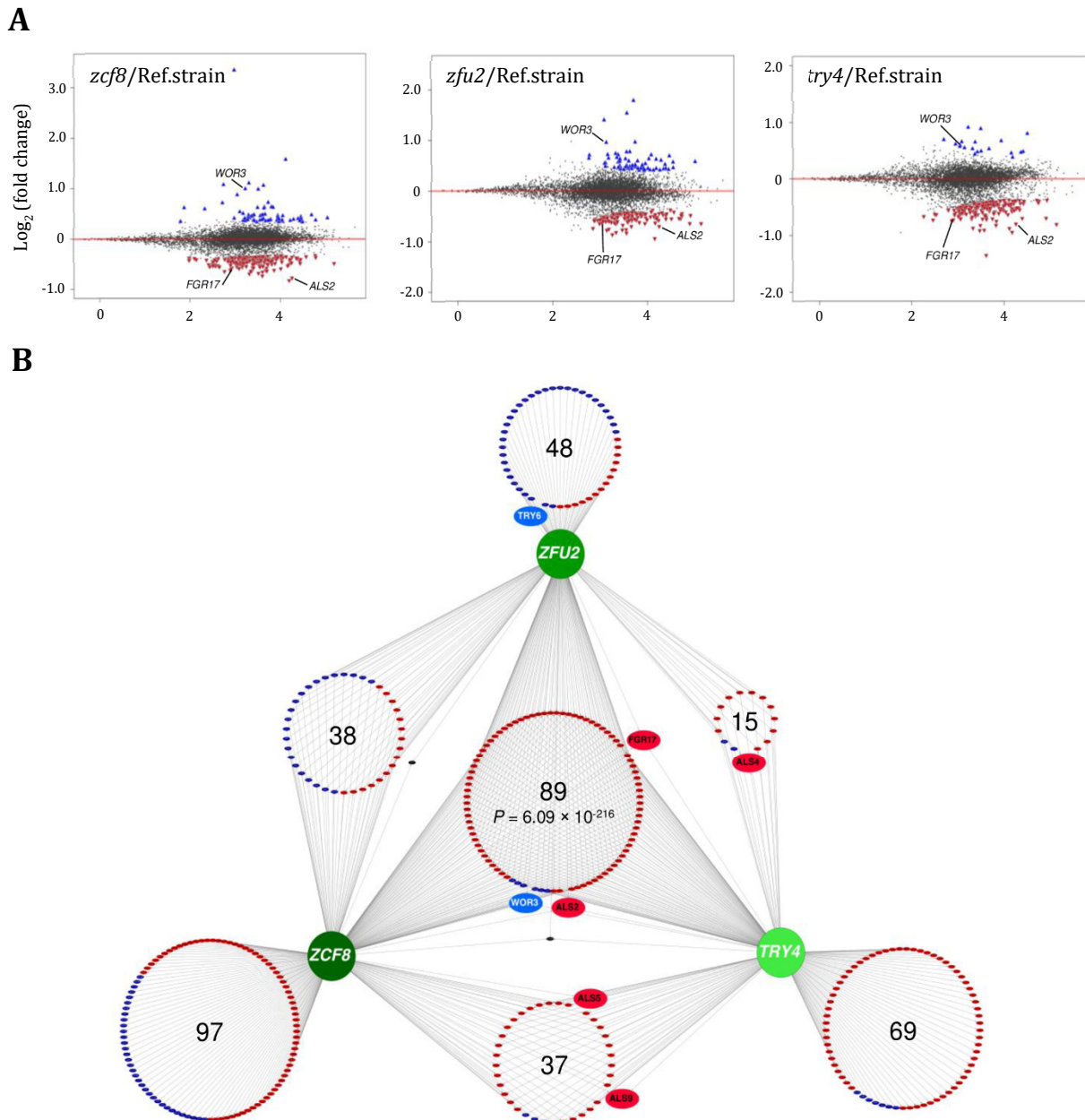


Figure 33: Transcriptional regulatory network based on whole transcriptome analysis of *ZCF8*, *ZFU2*, and *TRY4* (Bohm et al., 2017).

(A) Plots depicting the expression changes of all analyzed transcripts (~6100 genes; each dot represents one transcript) observed by comparing the expression levels in the indicated deletion

mutant to the expression levels in the wild-type reference strain. For each transcript the log₂ fold change in expression is shown on the Y-axis as a function of the mean of the normalized read counts (X-axis). Red triangles represent transcripts whose expression is activated (i.e. positive regulation), blue triangles represent repressed transcripts (i.e. negative regulation) by each regulator at P_{adj} < 0.01.

(B) Network depicting all genes whose expression is controlled by *ZCF8*, *ZFU2*, and *TRY4*. The green nodes of the network correspond to the transcription regulators identified in our genetic screen (Figure 23). The large circles with the numbers in the middle are composed of small colored ellipses. Each of these ellipses represents one target gene. Red ellipses represent positive regulation (i.e. activation), blue represents negative (i.e. repression). The two black ellipses represent the two genes that show discordant regulation (positive regulation by one regulator and negative by another). The shown network is completely based on RNA-seq data generated in this study.

The next question was, if the RNA-Seq data can uncover a link between the three regulators and filamentation. A closer look at the top common targets of regulation of *ZCF8*, *ZFU2*, and *TRY4* (based on the magnitude of expression differences between reference strain and deletion mutants) revealed the putative regulator *FGR17* (Table 11). This gene was previously shown to have an effect on filamentation in *C. albicans* even though the results are contradictory (Homann *et al.*, 2009; Uhl *et al.*, 2003).

Table 11: Top common targets of regulation.

Standard name	Common name	Log ₂ (mutant/WT)			Known or predicted function
		<i>try4</i>	<i>zcf8</i>	<i>zfu2</i>	
<i>ORF 19.5622</i>	<i>GLC3</i>	-0,944	-0,824	-0,94	Glucan branching enzyme
<i>ORF 19.2344</i>	<i>ASR1</i>	-1,352	-0,62	-0,589	Heat shock protein
<i>ORF 19.5614</i>		-0,905	-0,731	-0,831	Ribonuclease H1
<i>ORF 19.6202</i>	<i>RBT4</i>	-0,914	-0,681	-0,77	Secreted PRY family protein
<i>ORF 19.1097</i>	<i>ALS2</i>	-0,797	-0,772	-0,701	Adhesin
<i>ORF 19.1716</i>	<i>URA3</i>	-0,708	-0,692	-0,863	Orotidine-5'-phosphate decarboxylase
<i>ORF 19.5620</i>		-0,822	-0,531	-0,675	unknown
<i>ORF 19.99</i>	<i>HAL21</i>	-0,633	-0,575	-0,82	Phosphosulfate phosphatase
<i>ORF 19.3649</i>		-0,636	-0,544	-0,764	unknown
<i>ORF 19.3651</i>	<i>PGK1</i>	-0,805	-0,486	-0,622	Phosphoglycerate kinase
<i>ORF 19.3456</i>		-0,708	-0,586	-0,634	Kinase
<i>ORF 19.5525</i>		-0,821	-0,484	-0,622	unknown
<i>ORF 19.7284</i>	<i>ASR2</i>	-0,875	-0,531	-0,503	unknown
<i>ORF 19.5729</i>	<i>FGR17</i>	-0,724	-0,573	-0,575	Transcription regulator
<i>ORF 19.90</i>		-0,661	-0,577	-0,608	unknown
<i>ORF 19.4477</i>	<i>CSH1</i>	-0,749	-0,62	-0,461	Aldo-keto reductase
<i>ORF 19.85</i>	<i>GPX2</i>	-0,653	-0,654	-0,519	Glutathione peroxidase
<i>ORF 19.5612</i>	<i>BMT4</i>	-0,446	-0,632	-0,701	β-mannosyltransferase
<i>ORF 19.3417</i>	<i>ACF2</i>	-0,55	-0,552	-0,647	Endo-1,3-β-glucanase
<i>ORF 19.1085</i>		-0,651	-0,471	-0,614	unknown
<i>ORF 19.5526</i>	<i>SEC20</i>	-0,663	-0,492	-0,556	unknown
<i>ORF 19.5595</i>	<i>SHE3</i>	-0,56	-0,568	-0,589	mRNA binding protein
<i>ORF 19.6003</i>		0,547	0,505	0,719	unknown
<i>ORF 19.4599</i>	<i>PHO89</i>	0,798	0,401	0,693	Phosphate permease
<i>ORF 19.467</i>	<i>WOR3</i>	0,59	0,996	0,96	Transcription regulator
<i>ORF 19.3664</i>	<i>HSP31</i>	0,612	0,876	1,403	Heat shock protein

I tested the ability for filamentation of a *fgr17* deletion mutant under the *in vitro* conditions that we used to grow the cells for the RNA-Seq experiment and that mimic some conditions present in the gut (37°C and growing on a semisolid surface). Under these conditions, colonies of the *fgr17* deletion mutant displayed increased colony wrinkling (Figure 34) phenocopying the *zcf8*, *zfu2*, and *try4* deletion mutants (Figure 25). Microscopy analysis revealed that the wrinkling areas contained a mixture of yeast and filamentous cells. This result supports the idea that *FGR17* is a negative regulator of filamentation. Under different conditions, i.e. when grown embedded in soft agar, colonies of the *fgr17* deletion mutant formed longer and denser projections than wild-type colonies (Figure 34). Thus, the regulator *FGR17* is a common target of regulation of *ZCF8*, *ZFU2*, and *TRY4* and negatively regulates filamentation in *C. albicans*.

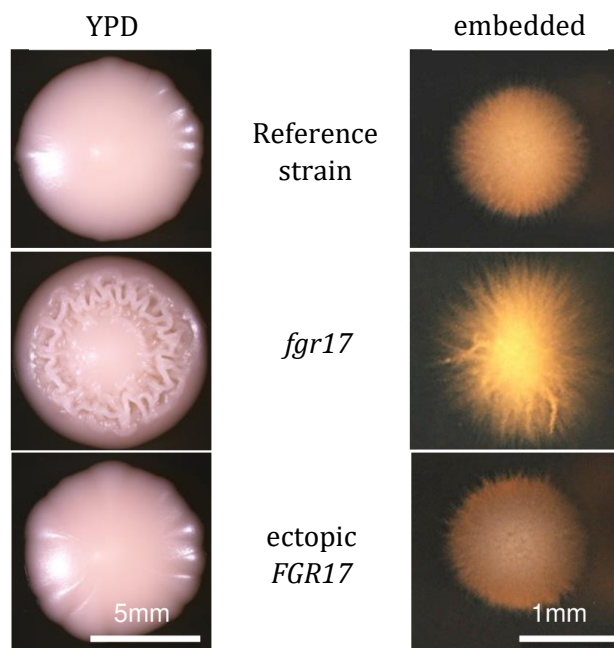


Figure 34: *FGR17*, a common target of *ZCF8*, *ZFU2*, and *TRY4*, negatively regulates filamentation and invasive growth in *C. albicans*.

Shown are photographs of colonies of the indicated strains. Wild-type, *fgr17* deletion mutant and a strain ectopically expressing *FGR17* were grown either on a semisolid surface and at 37°C (left) or embedded in soft agar (right). Colonies of the *fgr17* deletion mutant displayed colony wrinkling when grown on YPD agar in contrast to the other strains (left). When grown embedded in soft agar the deletion mutant forms longer and denser protrusions compared to the two other strains (right).

4.4.2) The triple mutant strain *try4 zcf8 zfu2* displays a stronger filamentation phenotype than the single mutant strains.

The results described above indicate that the *C. albicans* genes *ZCF8*, *ZFU2*, and *TRY4* regulate at least in part the same biological processes. Since the observed *in vitro* phenotypes for each single mutant were somewhat weak, double and triple mutants for all regulators were constructed. Colony morphology was assessed after incubation at 30°C for 24 hours and revealed that a double deletion mutant of *try4* and *zfu2* displayed increased filamentation compared to each single mutant and the wild-type reference strain (Figure 35A). Deletion of all three regulators increased filamentation even more (Figure 35A), further supporting the notion that these proteins work in parallel in *C. albicans*. The increased filamentation in the triple mutant *try4 zcf8 zfu2* was also observed in two other assays: In stab culture and in colonies grown under coverslips. In both assays (Elson *et al.*, 2009), the triple deletion mutant displayed increased filamentation compared to the wild-type reference strain (Figure 35B, C).

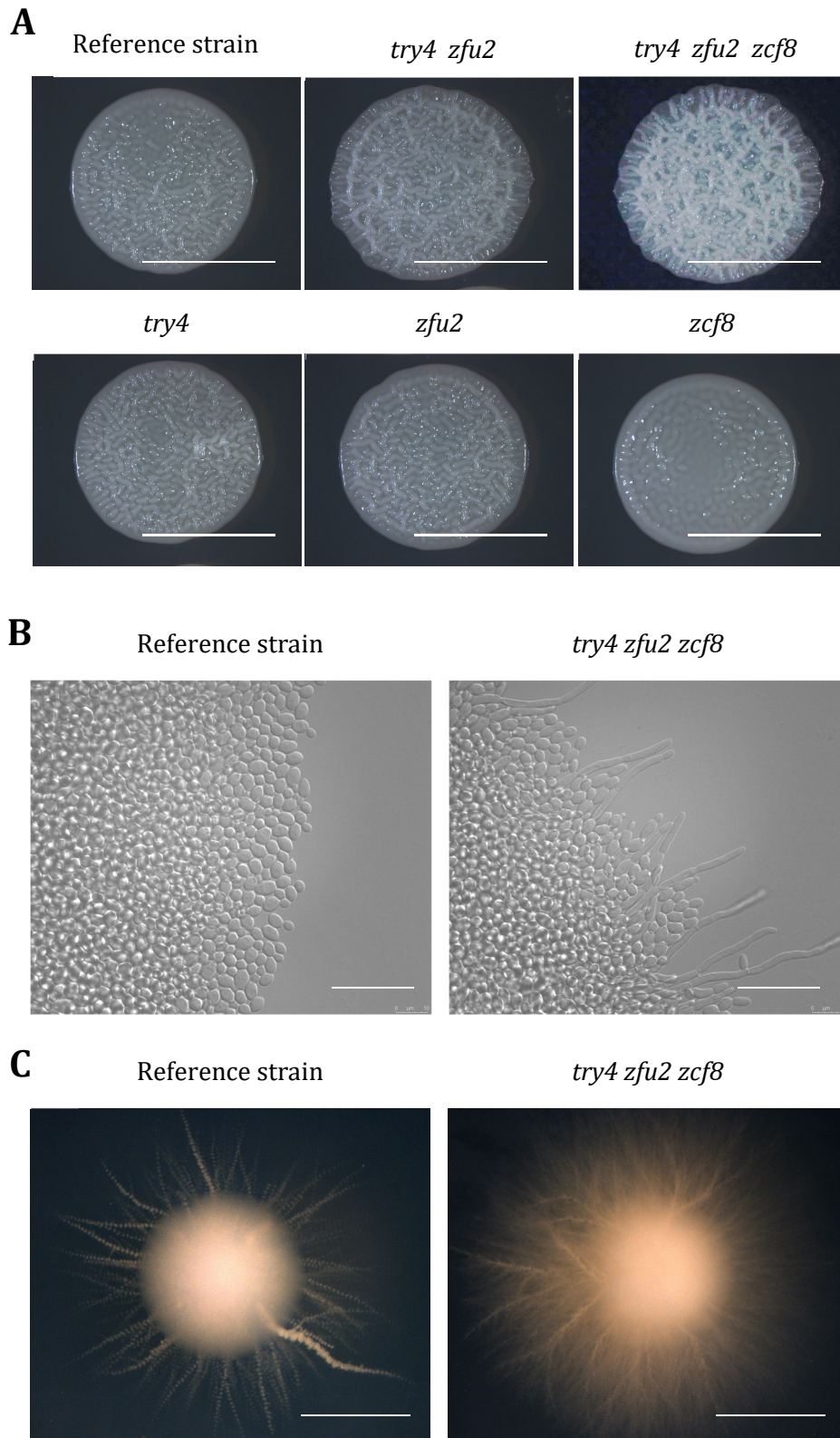


Figure 35: The triple deletion strain *zcf8 zfu2 try4* exhibits hyperfilamentation phenotypes. Shown are photographs of colonies of the wild-type reference strain, the single mutants *try4*, *zfu2*, and *zcf8*, the double deletion mutant *try4 zfu2* and the triple deletion mutant *zcf8 zfu2 try4* grown under different conditions.

(A) SpiderAgar plates incubated 24 h at 30° C. Scale bars in the right lower corner of the pictures represent 5 mm.

(B) 10 µl containing approximately 10 cfus were pipetted on top of a SpiderAgar piece placed on a microscope slide. Colonies were covered with a coverslip and grown 24 h at 30°C prior to evaluation. Scale bars in the right lower corner of the pictures represent 50 µm.

(C) 100 µl containing approximately 100 cfus were spread on a SpiderAgar played and a microscope slide was placed atop the cells. Colonies were grown 5 d at 30°C in an anaerobic chamber prior to evaluation. Scale bars in the right lower corner of the pictures represent 1 mm

Filamentation is an extensively regulated process in *C. albicans*. To further elucidate the role that the three newly identified regulators have in this process, I carried out a time course filamentation assay. To do so, transition from yeast to filamentous growth was induced with serum, a well-established inducer of this morphological transition (Brown, 2002; Brown *et al.*, 1999; Mitchell, 1998). Hyphal induction using 10% serum revealed that the triple deletion mutant *try4 zfu2 zcf8* started to filament earlier than the wild-type reference strain (Figure 36A). Already after 30 min there were first signs of hyphal induction in the triple deletion mutant whereas the wild-type reference strain showed these signs only after 1 hour (Figure 36A), implying that the three regulators may control the timing of the response to filamenting cues.

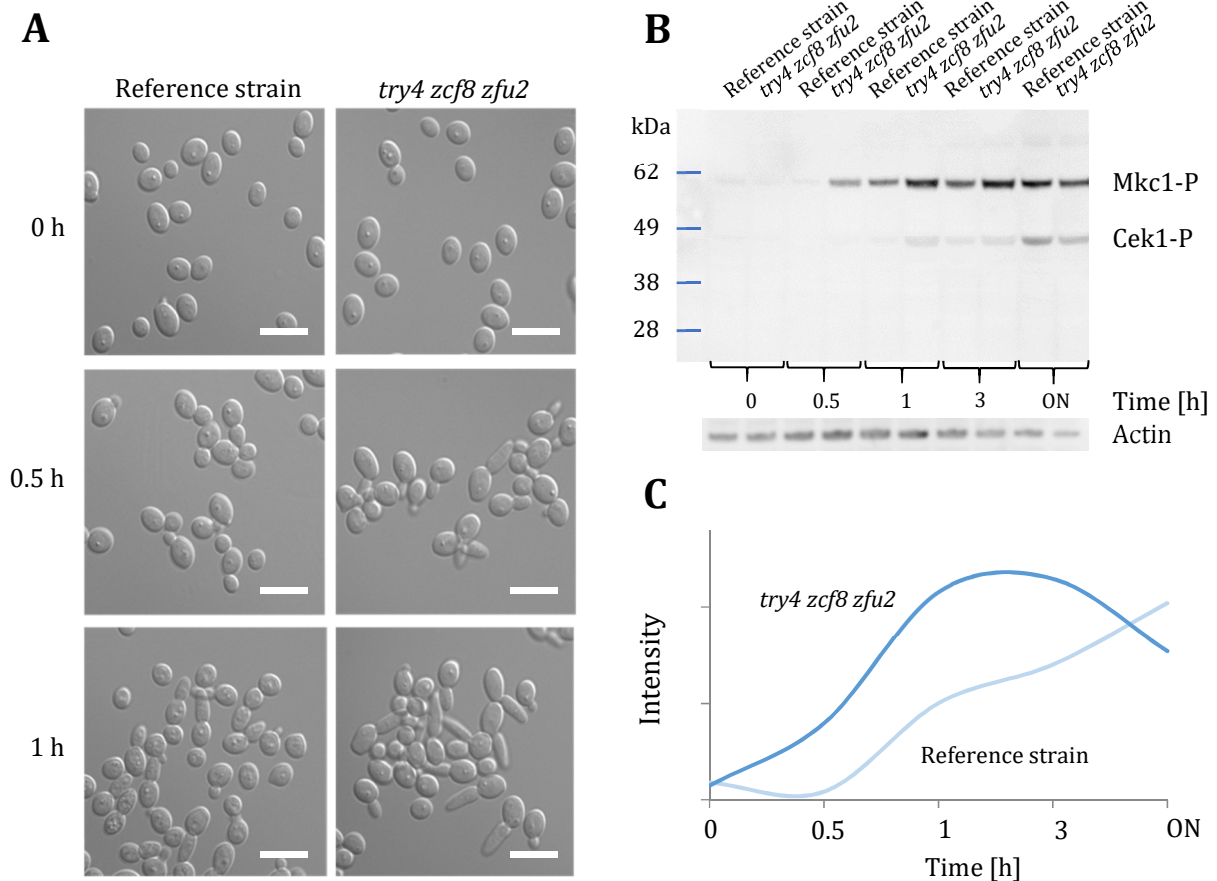


Figure 36: The triple deletion mutant *try4 zcf8 zfu2* displays faster response to filamentation cues.

(A) Shown are microscopy pictures taken from *C. albicans* wild-type reference and *try4 zfu2 zcf8* cells grown in response to 10% serum. Cells from stationary phase cultures were diluted 1:10 in YPD containing 10% serum and incubated at 30°C shaking. Pictures were taken as indicated on the left at timepoint 0, after 30 and after 60 min of hyphal induction with serum. The triple deletion mutant *try4 zfu2 zcf8* displayed first signs of filamentation already 30 min after exposure to serum whereas wild-type reference strain cells start filamentation only after 1 hour of exposure. Scale bars in the right lower corner of the pictures represent 7.5 µm.

(B) The activity of the Mkc1/Cek1 MAPK pathway was analyzed on protein level in a Western blot using an antibody specific for the phosphorylated portion of the two kinases. Wild-type and *try4 zfu2 zcf8* strains were grown to stationary phase in YPD at 30°C shaking. Hyphal transition was induced with 10% serum. Whole cell extracts were prepared at timepoint 0, after 30, 60 and 180 min and after overnight incubation and resolved by PAGE as described in chapter 2.3.9 and 4.3.12. Proteins were transferred to a PVDF membrane and the phosphorylated portion of Mkc1p and Cek1p was stained using a mouse monoclonal anti-Phospho-p44/42 MAPK (Erk1/2) (Thr202/Tyr204) antibody. As loading control actin was stained using a rabbit polyclonal anti-Actin antibody (lower panel). Mkc1p and Cek1p were earlier and higher phosphorylated in the mutant compared to the wild-type in response to serum, indicating an earlier and stronger activation of the Mkc1/Cek1 MAPK pathway.

(C) Quantification of the Western blot shown in (B). Plotted is the phosphorylated portion of Mkc1p in the wild-type and the triple deletion mutant based on the intensity of the signal obtained in the Western blot shown in (B). Notice the faster and heightened activity of the Mkc1/Cek1 MAPK pathway in the triple deletion mutant compared to the wild-type in response to serum.

Serum is known to activate several signal transduction pathways (i.e. MAP kinase and cAMP-PKA pathways) resulting in the induction of filament-specific genes. We evaluated the activity of the Mkc1/Cek1 MAPK pathways, major signaling cascades that are activated by phosphorylation in response to filamenting cues. The phosphorylation level of these two kinases was tested through western blot analysis in the triple deletion mutant *zfu2 try4 zcf8*. Both proteins, Mkc1 and Cek1, were phosphorylated at earlier time points and at higher levels compared to the wild-type (Figure 36B, C). Already 30 min after hyphal induction, phosphorylated Mkc1p was detected in the triple deletion mutant whereas in the wild-type a signal was detected only after 60 min. After 60 and 180 min the total level of phosphorylated Mkc1p was higher in the mutant compared to the wild-type. Cek1p was phosphorylated in the mutant after 60 min and in the wild-type only after 180 min. Thus, the hyperfilamentation phenotype of the triple mutant strain correlates with a faster and heightened response to filamenting cues such as serum.

4.4.3) Localization of *SHE3*-associated transcripts depends on *ZCF8*, *TRY4*, and *ZFU2*.

Among the top targets of regulation of *ZFU2*, *TRY4*, and *ZCF8* there was another gene of interest, *SHE3*. This gene encodes a protein which is part of an mRNA transport system in *C. albicans*. The She3p-dependent subcellular localization of mRNAs contributes to proper hyphal morphology and to specific aspects of hyphal function (Elson *et al.*, 2009). She3p transports a set of mRNAs from the nucleus to daughter cells and into tip cells of growing hyphae. Two thirds of the transcripts transported by She3p play roles in hyphal development in *C. albicans* (Elson *et al.*, 2009). To establish whether *TRY4*, *ZFU2*, and *ZCF8* impact mRNA transport via She3p, the localization of two mRNAs known to be targets of She3p was analyzed. To do so, I employed fluorescence *in situ* hybridization (FISH) (Zenklusen *et al.*, 2010). I first validated the technique in *C. albicans* establishing the localization of *ITS2*. *ITS2* is the internal transcribed spacer (ITS) between the 5.8 and 28S rRNA. In *S. cerevisiae* this rRNA is known to be located in a specific area of the nucleus (Zenklusen *et al.*, 2010). I established that *ITS2* is located to a specific area of the nucleus in *C. albicans* as well (Figure 37).

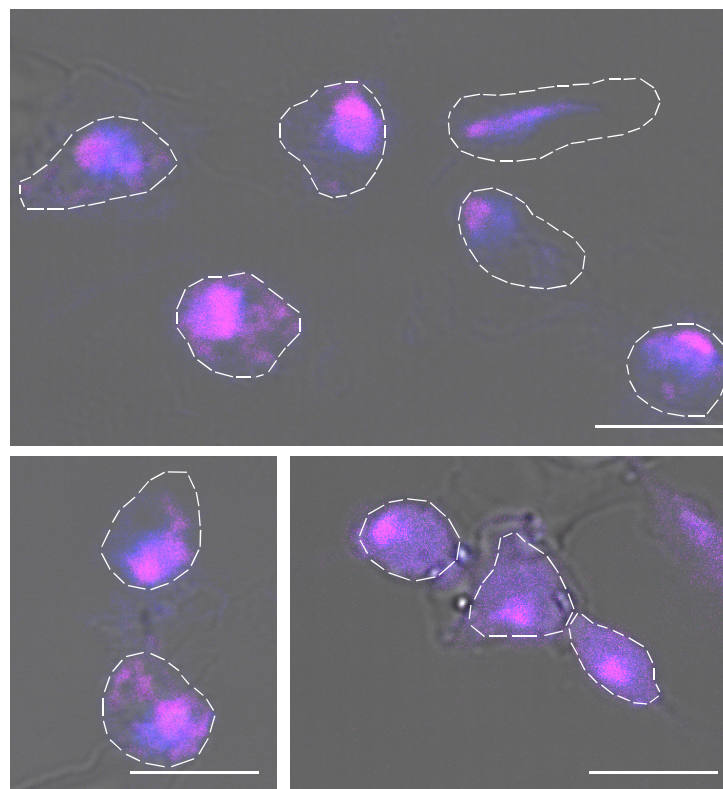


Figure 37: *ITS2* localizes in *C. albicans* to a specific area of the nucleus.

Shown are representative pictures of *C. albicans* cells after fluorescence *in situ* hybridization (FISH) of *ITS2*. Wild-type cells were grown to stationary phase in YPD liquid, spheroblasted, fixed and hybridized with an *ITS2* probe (Zenklusen *et al.*, 2010). Nuclei were stained using DAPI. *ITS2* localizes to a specific area of the nucleus of *C. albicans* cells as it was earlier shown for *S. cerevisiae* (Zenklusen *et al.*, 2010). Scale bars in the right lower corner of the pictures represent 2 μ m.

In a next step, FISH was used to analyze the localization of the *ASH1* mRNA, a target of the She3p mRNA transport machinery. *ASH1* was one of the first described mRNAs in *S. cerevisiae* to be distributed unequally in mother and daughter cells. Transport of *ASH1* mRNA into daughter cells ensures inhibition of mating in these newly formed cells. I compared the localization of *ASH1* mRNA in *C. albicans* wild-type and triple deletion mutant cells. In the wild-type reference strain *ASH1* mRNA was mainly detected in the tip of budding cells (Figure 38A) as it was previously shown (Elson *et al.*, 2009). In the triple deletion mutant *ASH1* mRNA was distributed equally in the cytoplasm of mother and daughter cells (Figure 38B). Moreover, the stronger signal detected in the mutant suggests that in total there is more *ASH1* mRNA present in these cells.

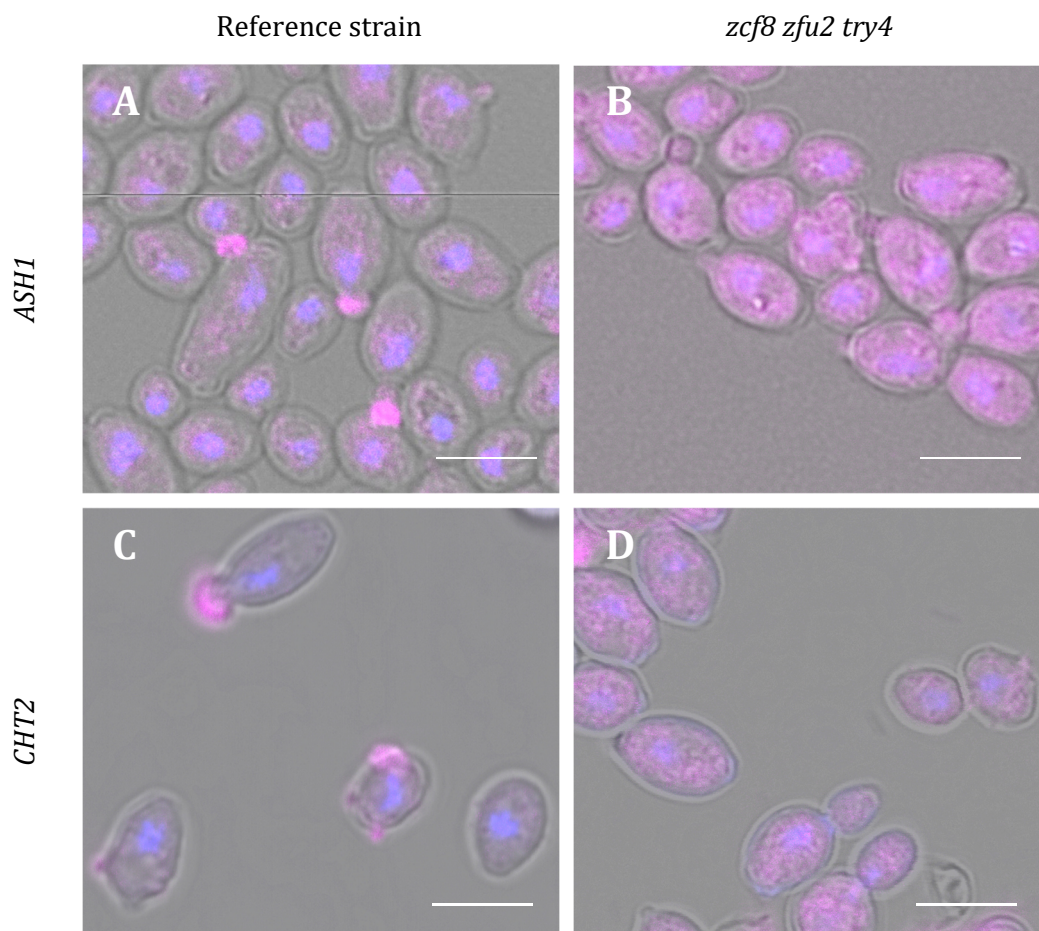


Figure 38: Deletion of the three regulators disturbs localization of *SHE3*-associated transcripts.

Representative pictures of *C. albicans* wild-type and triple deletion mutant cells after fluorescence *in situ* hybridization (FISH) of two *SHE3*-associated transcripts. (A+B) FISH of *ASH1* mRNA. (C+D) FISH of *CHT2* mRNA. Wild-type and mutant cells were grown 30 min in the presence of 10% serum at 30°C shaking, fixed, spheroblasted and hybridized. Signal of the FISH probes complementary to *ASH1* and *CHT2* mRNAs are shown in pink. Nuclei were stained using DAPI (shown in blue). Scale bars in the right lower corner of the pictures represent 5 µm.

(A) *ASH1* mRNA localizes in the wild-type reference strain to the tip of budding cells as previously described (Elson *et al.*, 2009).

(B) *ASH1* mRNA does not show a specific localization in triple deletion mutant cells and is equally distributed throughout the cytoplasm of mother and daughter cells. Stronger signal of the FISH probes indicates a higher total concentration of *ASH1* mRNA in these cells.

(C) *CHT2* mRNA localizes in the wild-type reference strain to the tip of budding cells as previously described (Elson *et al.*, 2009).

(D) *CHT2* mRNA does not show a specific localization in triple deletion mutant cells and is equally distributed throughout the cytoplasm of mother and daughter cells.

To further establish whether in the absence of *ZCF8*, *ZFU2*, and *TRY4* the mRNA transport mediated by She3p is disturbed, another target mRNA was chosen for FISH: *CHT2*. *CHT2* encodes a chitinase that is required in *C. albicans* for normal hyphal growth and impacts the chitin content of the cell wall. FISH was performed exactly as it was done for the *ASH1* mRNA and revealed similar results. The *CHT2* transcript is located to the tip of budding wild-type reference cells (Figure 38C) as for *ASH1* (Figure 38A) (Elson *et al.*, 2009). Deletion of *ZCF8*, *ZFU2*, and *TRY4* resulted in the elimination of this focalized pattern of localization; instead the mRNA was distributed throughout the cytoplasm of mother and daughter cells (Figure 38D). Mislocalization of the *ASH1* and *CHT2* transcripts in the triple deletion mutant cells indicates that the mRNA transport machinery depending on She3p is impaired when the transcriptional regulators *ZCF8*, *ZFU2*, and *TRY4* are absent. Transcriptomics uncovered *SHE3* as one of the top common targets of *ZCF8*, *ZFU2*, and *TRY4*. Fluorescence *in situ* hybridization revealed that the mRNA transport machinery depending on She3p is affected when all three regulators are absent. To see if this observation can indeed be connected to differences in the concentration of She3p itself in the cells, the protein was MYC-tagged and the level in the cells was analyzed in a Western blot. In response to serum, higher levels of She3p were detected in *try4 zfu2 zcf8* triple deletion cells than in wild-type cells (Figure 39A). Furthermore, immunostaining revealed that in addition to the total level of She3p in the cells also its localization in the cells was affected when the three transcriptional regulators were deleted (Figure 39B). In wild-

type cells She3p is located mainly in budding cells. In contrast in the triple mutant it shows equal distribution throughout the cytoplasm of all cells (Figure 39B).

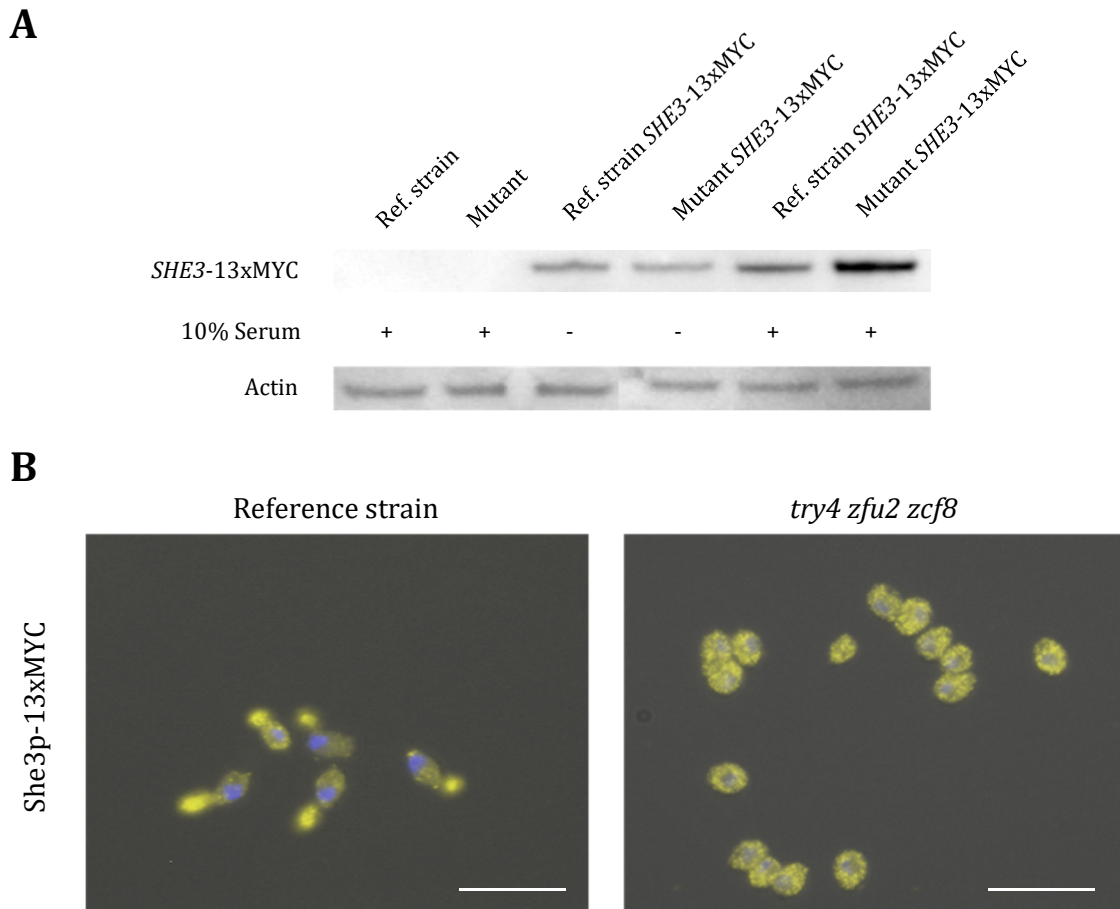


Figure 39: The level and localization of She3p is affected by the three regulators.

The She3p was tagged with 13 repeats of MYC in wild-type and triple mutant background to analyze its concentration using a Western blot and localization using an immunostaining in *C. albicans* wild-type and triple mutant cells.

(A) Wild-type and triple deletion mutant cells with and without MYC tagged She3p were grown in the pre- and absence of 10% serum. Whole cell extracts were prepared and resolved by PAGE as described in chapter 2.3.9 and 4.3.12. Proteins were transferred to a PVDF membrane and the MYC tag was stained using a mouse c-Myc Monoclonal Antibody. As loading control actin was stained using a rabbit polyclonal anti-Actin antibody (lower panel). Without MYC tag, no signal was detected. When She3p was MYC-tagged, there was no difference in its concentration when the cells were grown in the absence of serum. When MYC-tagged strains were grown in the presence of serum, there were higher levels of She3 protein present in the triple deletion mutant compared to the wild type reference.

(B) Wild-type and triple deletion mutant cells with and without *SHE3*-MYC tag were grown in the presence of 10% serum. Cells were fixed, spheroblasted and the MYC-tag was located using a mouse c-Myc Monoclonal Antibody and Alexa Fluor™ 488 goat anti-mouse secondary antibody. Untagged wild-type and mutant cells showed no signal. In wild-type cells containing the *SHE3*-MYC-tag She3p could be mainly located to budding cells whereas in mutant cells there was no specific localization of She3p. Scale bars in the right lower corner of the pictures represent 10 μ m.

Taken together, the results obtained through the analysis of the She3p-mRNA transport system in *C. albicans* indicates that the transcription regulators *ZCF8*, *ZFU2*, and *TRY4* influence, either directly or indirectly, this mRNA subcellular localization process.

4.4.4) *ZCF8*, *ZFU2*, and *TRY4* influence recognition by immune cells.

In the previous chapter (4.4.3), I showed that the *CHT2* transcript is mislocalized in *try4 zfu2 zcf8* triple deletion cells. As mentioned earlier, *CHT2* encodes a chitinase contributing to the chitin content of the cell wall. It was shown to process newly produced long chitin chains in small fragments that are incorporated into the cell wall close to the cell membrane (Sherrington *et al.*, 2017). Mislocalization of *CHT2* could therefore cause defects in chitin processing and incorporation into the cell wall resulting in abnormal exposure of this sugar in the cell surface. To establish whether the triple deletion mutant indeed displays alterations in chitin exposure, the accessibility of cell wall components was analyzed through specific cell wall stainings and FACS analysis in collaboration with the laboratory of Rebecca Hall at the University of Birmingham (UK) (Method description see (Sherrington *et al.*, 2017)). This analysis revealed that the triple deletion mutant displays increased exposure of chitin on the cell surface compared to the wild-type (Figure 40). By contrast, the glucan exposure was similar between wild-type and mutant cells (Figure 40).

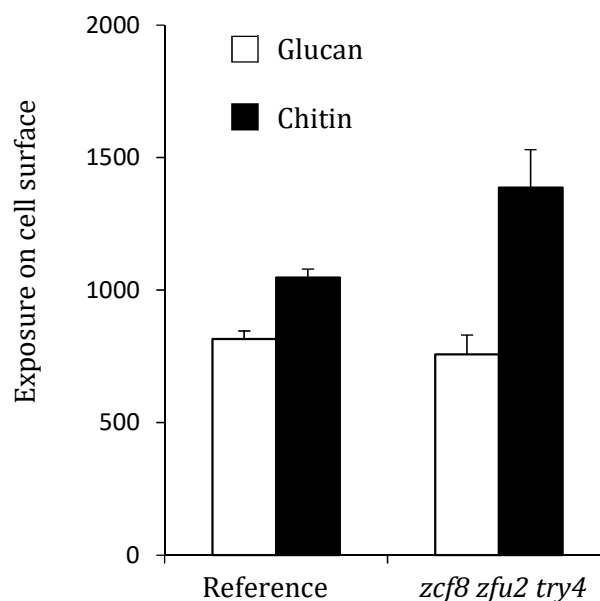
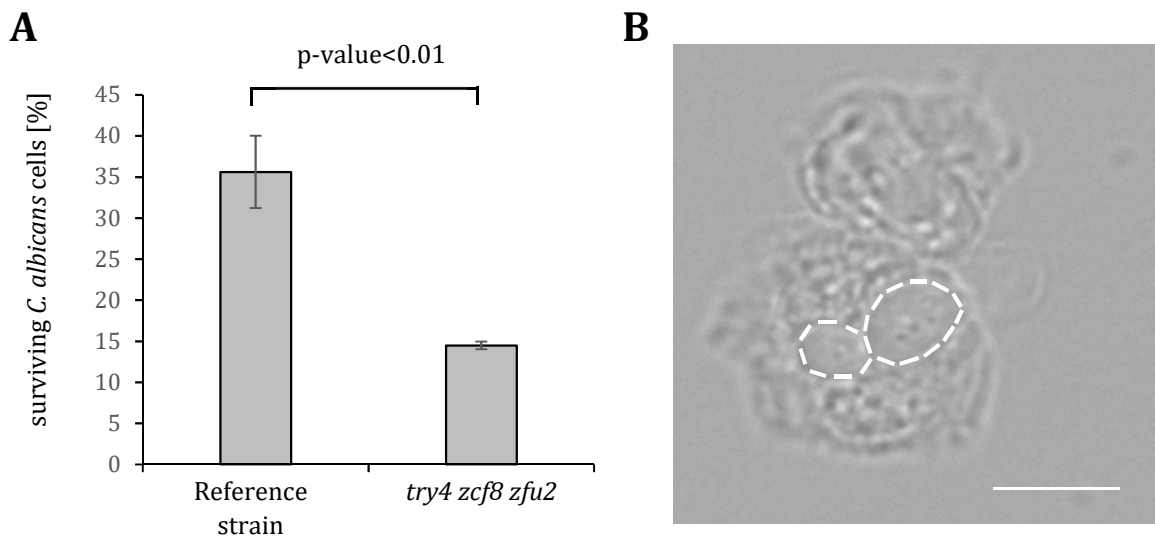


Figure 40: Deletion of the regulators induces cell wall rearrangements.

Graph depicting measurements of glucan and chitin exposed to *C. albicans* cell surface. Glucan and Chitin were stained with fluorescent dyes that cannot cross the cell wall and fluorescence level was determined via FACS analysis (performed by Rebecca Hall, detailed method description see (Sherrington *et al.*, 2017)). Experiments were conducted in three independent triplicates and shown is the average and the standard deviation. Glucan exposure to the cell surface was similar in both, wild-type and mutant cells (white bars), whereas there was more chitin exposed to the cell surface in triple deletion mutant compared to wild-type cells (black bars).

Since the first contact point of fungal and immune cells is the fungal cell wall, changes in its composition might influence recognition and killing by immune cells. Thus, the next obvious question was whether the changes in the *C. albicans* cell wall observed when the *ZCF8*, *ZFU2*, and *TRY4* are absent induces increased killing by immune cells. To test this idea human neutrophils were freshly isolated and incubated with *C. albicans* wild-type and *try4 zfu2 zcf8* triple deletion cells in a neutrophil killing assay. Neutrophils were chosen, since they are known to be the major *C. albicans* killer of the human immune system. This assay revealed that triple deletion mutant cells survive significantly less when incubated with human neutrophils than wild-type cells (Figure 41A, B).

**Figure 41: Mutant of all three regulators induces increased killing by immune cells.**

Resistance of *C. albicans* strains to neutrophils.

(A) Graph depicting percentages of surviving *C. albicans* cells after incubation with freshly isolated human neutrophils. Neutrophils were isolated from three different Donors and incubated with wild-type reference and triple deletion mutant cells for two hours in 24-well plates. Contents of each well were plated on YM agar and incubated 24 hours at 37°C. CFUs were counted and percentage of surviving *C. albicans* cells were determined via comparison to fungal cells incubated under the same conditions but without neutrophils. For each donor, the assay was conducted in

triplicate and the average survival (%) is plotted. In all donors, the triple deletion mutant was killed more by neutrophils than wild-type cells. Statistical analysis was performed using the Wilcoxon rank test for matched-pairs.

(B) Representative microscopy picture demonstrating the interaction of neutrophils and *C. albicans* cells. The lower neutrophil engulfed two fungal cells marked with white dotted lines. Scale bars in the right lower corner of the picture represent 5 μm .

Taken together, the results observed by analyzing the interaction of *C. albicans try4 zfu2 zcf8* triple deletion cells and host immune cells revealed that in the absence of the three transcription regulators fungal cells are better recognized and killed by neutrophils. This observation might at least in part be due to the increased exposure of chitin to its cell surface.

4.5) Discussion

In this chapter, I have further elucidated the role of the previously identified transcriptional regulators *ZCF8*, *ZFU2*, and *TRY4*. Transcriptome profiling illustrated that these regulators that are confirmed to contribute to the ability of *C. albicans* to colonize the GI tract of germ-free animals (Figure 23) and verified to be involved in the yeast-to-hyphal transition (Figure 25) at least partly control the same biological processes (Figure 33, Table 11). Furthermore, transcriptomics uncovered *FGR17*, a known regulator of hyphal induction, as one of the top common targets of *ZCF8*, *ZFU2*, and *TRY4* (Table 11). In its absence, *C. albicans* colonies display similar wrinkling as in the absence of *ZCF8*, *ZFU2*, and *TRY4* (Figure 34), which suggests that the hyperfilamentation observed in *zcf8*, *zfu2* and *try4* mutants might at least partially be due to changes in Fgr17p levels in the cells. A deletion mutant of all three regulators increased the previously observed hyperfilamentation phenotype (Figure 35), further implying that they act at least partly in concert. Earlier activity of two kinases involved in major signaling cascades (Figure 36) that govern the yeast-to-hyphal transition in *C. albicans* in the triple mutant might serve as an additional explanation for the observed hyperfilamentation phenotype. Using fluorescence in situ hybridization, I established that in the triple mutant, the *SHE3*-dependent mRNA transport is affected, which may cause changes in filamentation as well (Figure 38, Figure 39). Finally, alterations in the composition of the cell wall in the absence of the three regulators might elucidate an increased detection and killing by immune cells (Figure 40, Figure 41).

Transcriptome profiling of the three deletion mutants (Figure 33) clearly indicated that these transcription factors are at least partially involved in regulating the same biological processes. Phenotypic analysis revealed that one of these processes is filamentation. Simultaneous deletion of all three regulators increased the observed hyperfilamentation phenotype of each single mutant (Figure 35), further supporting the idea that the regulators function in concert. In *C. albicans*, hyphal transition is induced in response to a number of environmental cues, such as mammalian body temperature, CO₂, alkaline pH, and serum (Brown, 2002; Brown et al., 1999; Mitchell, 1998). The induction of hyphal formation is an intricately regulated process that involves activating or repressing various transcriptional regulators: Efg1 (Stoldt et al., 1997), Cph1 (Leberer et al., 1996; Liu et al., 1994), Cph2 (Lane et al., 2001b), Tec1 (Lane et al., 2001a), and Rim101 (Davis et al., 2000; Davis, 2009; El Barkani et al., 2000) are only some examples of transcriptional regulators

that positively regulate filamentation in *C. albicans*, all of them activating the expression of hyphal-specific genes (HSGs) in response to different external cues. Tup1 (Braun et al., 1997; Murad et al., 2001a), Nrg1 (Braun et al., 2001; Murad et al., 2001b), and Rfg1 (Kadosh et al., 2001) are some negative regulators of filamentation that repress the expression of HSGs under non-inducing conditions. In response to filamenting cues, these regulators are repressed to induce the expression of HSGs. Among the top targets of regulation of *ZCF8*, *ZFU2*, and *TRY4* is *FGR17* (Table 11), another transcriptional regulator demonstrated to influence hyphal formation but with contradictory results (Homann et al., 2009; Uhl et al., 2003). A deletion mutant of *FGR17* exhibited similar colony wrinkling to mutants of *ZCF8*, *ZFU2*, and *TRY4*, indicating hyperfilamentation (Figure 34). *FGR17* thus contributes to hyphal formation in *C. albicans* as a negative regulator, and its expression depends on the transcriptional regulators *ZCF8*, *ZFU2*, and *TRY4*.

Hyphal formation relies on cell wall restructuring and the transport of detrimental factors to the growing hyphae, among other factors. Another top target of *ZCF8*, *ZFU2*, and *TRY4* discovered via transcriptome analysis is *SHE3* (Table 11), part of an mRNA transport mechanism first described in *S. cerevisiae* (Jansen et al., 1996). It is connected to the motor protein Myo4, a type V myosin motor, and together with She2p a subset of mRNAs to bud tips along actin filaments (Munchow et al., 1999). A similar mechanism was described in *C. albicans* and connected to filamentation and invasive growth (Elson et al., 2009). In *C. albicans*, She3p transports a set of mRNAs, many of them encoding proteins that contribute to hyphal development, to the tips of growing hyphae (Elson et al., 2009). Even though participants and target mRNAs of this process have been identified, the mechanisms that regulate this process remain unclear. Fluorescence *in situ* hybridization established that in the absence of the transcriptional regulators *ZCF8*, *ZFU2*, and *TRY4*, She3p itself and two of its target mRNAs, *ASH1* and *CHT2*, are mislocalized (Figure 38, Figure 39). The mRNA of *ASH1* was one of the first described target mRNAs of She3p in *S. cerevisiae* and encodes a transcriptional repressor of *HO*, an endonuclease needed for mating-type interconversion (Jansen et al., 1996). The She-transport ensures the localization of this mRNA to daughter cells to prevent their mating-type switching (Jansen et al., 1996). In *C. albicans*, *ASH1* mRNA is a target of the She-transport as well (Elson et al., 2009), and it encodes a transcription factor required for WT virulence and filamentous growth on solid media (Inglis et al., 2002). *CHT2* mRNA, another target of She3p, encodes a chitinase known to be involved in cutting newly formed chitin chains before their

integration into the cell wall and is necessary for normal filamentous growth (Sherrington et al., 2017). The mislocalization of the transport protein She3 and two of its target mRNAs in the absence of *ZCF8*, *ZFU2*, and *TRY4* (Figure 38, Figure 39) might therefore cause the changes in filamentation observed in single and triple mutants. Changes in the concentration of She3p in mutant cells (Figure 39) further observed through Western blot analysis support this idea.

In addition to the top targets of *ZCF8*, *ZFU2*, and *TRY4*, a number of other genes regulate various cellular processes (Table 11). Several cell wall-related enzymes (*GLC3*, *BMT4*, *SEC20*, and *ACF2*) indicate a connection between the three regulators and the composition of the cell wall, even though standard cell wall staining revealed no difference in mannan or chitin content (data not shown). *ALS2*, encoding a GPI-linked surface adhesin, and *PGK1*, encoding a phosphoglycerate kinase, are known to be relevant during biofilm formation (Garcia-Sanchez et al., 2004; Green et al., 2004), assuming a role of *ZCF8*, *ZFU2*, and *TRY4* in this process. Biofilm formation is one of the major factors that contributes to the virulence of *C. albicans*. It is especially relevant in the hospital-acquired bloodstream infections with high mortality rates that are often transmitted through contaminated catheters. Another GO term relevant to the network is “response to oxidative stress.” *ASR1*, *ORF19.5525*, and *GPX2* encode genes with roles in the resistance of *C. albicans* against oxidative stress. Oxidative stress responses are vital in the colonization of the digestive tract (Flint et al., 2014), potentially contributing to the previously observed defects of mutants of the three regulators in gut colonization. The discrimination between direct targets of regulation of *ZCF8*, *ZFU2*, and *TRY4* and secondary effects, as well as further studies on their direct targets, should help to further understand the roles of these regulators in the abovementioned processes.

C. albicans' adaption to various environmental cues involves the selective activation and inactivation of several kinase pathways. One group of kinases that play critical roles in the response to external signals are mitogen-activated protein (MAP) kinases. The complex process of the yeast-to-hyphal transition in *C. albicans* comprises the activation of many MAP kinase pathways. In response to serum, the three transcriptional regulators studied here induce an earlier and heightened activation of two major MAPK pathways: the Cek1 and the Mkc1 MAPK pathways (Figure 36). Both are involved in hyphal formation in *C. albicans*. The Cek1 MAPK pathway was proved to regulate the switch from unicellular yeast to invasive hyphae and the hyphal growth rate (Csank et al., 1998). The Mkc1 MAPK

pathway is involved in regulating growth rate, cell viability, and mainly cell wall composition; however, disruptions of this pathway also decrease invasive growth on certain media and the length of the formed hyphae (Navarro-Garcia et al., 1998). Earlier and increased activation of these two pathways in the absence of *ZCF8*, *ZFU2*, and *TRY4* could cause a heightened filament growth rate and filament length, both aspects that were observed in phenotypic screenings (Figure 35). Even though numerous components of these pathways and transcriptional regulators that are induced or repressed through the activation of these cascades have been identified, less is known about what senses the external stimuli and how the cells decide which pathways must be activated to ensure signaling specificity. The results presented in this chapter indicate that the three studied transcriptional regulators negatively control the activity of the Cek1 and Mkc1 MAPK pathways in response to serum.

The interplay between *C. albicans* and the host immune system is largely mediated by elements of the fungal cell wall, including mannans, β -glucans, and chitin (Hall et al., 2013b). Transcriptome profiling already indicated a connection between *ZCF8*, *ZFU2*, and *TRY4* and the composition of *C. albicans*' cell wall (Table 11), but again, standard cell wall stainings and microscopy analysis disclosed no difference in mannan or chitin content in their absence. Nevertheless, studies on the She-dependent mRNA transport revealed a mislocalization of the *CHT2* mRNA when the three regulators were deleted simultaneously (Figure 38). The chitinase, encoded by *CHT2*, is anchored in the plasma membrane and cuts freshly produced long chitin chains before their incorporation into the cell wall. It was recently established that mutations in the *CHT2* gene lead to the exposure of chitin to the cell surface typically located close to the plasma membrane (Sherrington et al., 2017). The observed mislocalization of *CHT2* in the triple deletion mutant might therefore cause changes in the sugars exposed to the cell surface of the fungus. Sugar-specific stainings followed by FACS analysis confirmed that *ZCF8*, *ZFU2*, and *TRY4* indeed affect the exposure of chitin to the cell surface (Figure 40). Different components of the *C. albicans* cell wall are recognized by specific receptors (pattern recognition receptors [PRRs]) on the surface of innate immune cells (e.g., macrophages and neutrophils) (Bourgeois et al., 2010). Changes in the sugars exposed to the cell surface might thus cause changes in the recognition of the fungus by immune cells. An *in vitro* neutrophil killing assay suggested that in the absence of the three regulators, cells are better recognized and eliminated by neutrophils (Figure 41). *C. albicans* is such a

successful opportunistic pathogen because it can grow and proliferate under a wide range of different host conditions. One feature that allows its adaption to varying environments is the dynamic structure of its cell wall. It ensures the maintenance of cell shape, the protection and stability against environmental stresses, and especially the evasion of the immune system. All these functions require a complex network of regulation. The results presented here indicate that *ZCF8*, *ZFU2*, and *TRY4* contribute to the intricate regulated composition of the *C. albicans* cell wall and therefore influence its recognition by innate immune cells *in vitro*. However, further studies are needed to determine how changes in the sugars exposed to the cell surface caused by the three regulators impact *C. albicans*' growth *in vivo*.

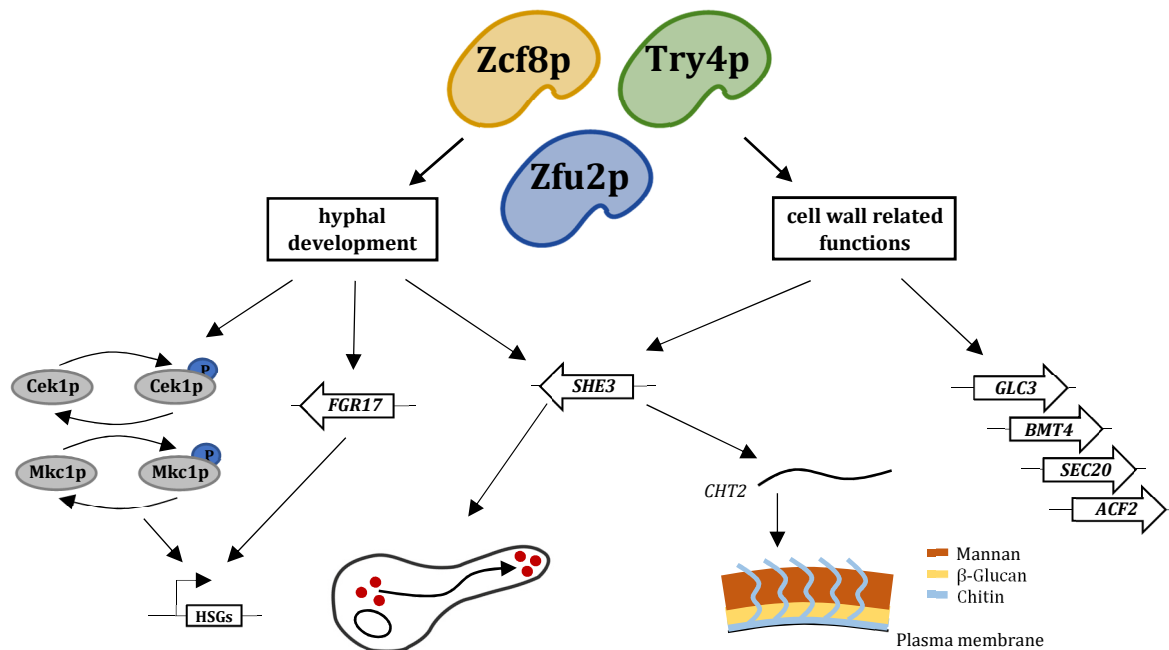


Figure 42: The transcriptional regulators *ZCF8*, *ZFU2*, and *TRY4* control various biological aspects in *C. albicans*.

Overview of the biological functions *ZCF8*, *ZFU2*, and *TRY4* govern in *C. albicans* based on the results presented in this chapter. Transcriptomics revealed a significant overlap in the target genes of all three regulators, indicating that they are to some extent involved in controlling the same biological functions. Based on the top common targets of regulation we identified the terms 'osmotic stress response', 'biofilm formation', 'hyphal development' and 'cell wall related functions'. Albeit the involvement in osmotic stress response and biofilm formation need to be confirmed, the contribution to hyphal development and the control of cell wall related functions could be verified through diverse *in vitro* experiments. Under certain *in vitro* growth conditions *C. albicans* cells hyperfilament in the absence of the three regulators, similarly to an *fgr17* mutant, one of the top common targets of regulation. In response to serum two major MAPK pathways

(Cek1, Mkc1) known to contribute to hyphal formation are earlier activated when all three regulators are deleted. Fluorescence *in situ* hybridization revealed that the regulators affect the *SHE3*-dependent mRNA transport previously shown to be involved in filamentation on *C. albicans*, analyzed because *SHE3* was another top common target of regulation. Changes in the exposure of chitin, a component of the cell wall typically located close to the membrane possibly due to the affected mRNA transport of *CHT2* via She3p, confirmed the contribution of the three regulators to the complex regulated composition of *C. albicans* cell wall.

Altogether, the analysis of the three transcriptional regulators *ZCF8*, *ZFU2*, and *TRY4* indicates that they influence multiple cellular processes. One of these processes is the response to filamenting cues (Figure 42). *ZCF8*, *ZFU2*, and *TRY4* are negative regulators of the yeast-to-filament transition. The negative effect on this morphological transition appears to be mediated at least partly by the transcriptional control of the transcriptional regulator *FGR17*, previously proved to influence hyphal formation, and by changes in the activity of two major kinase pathways. Furthermore, the regulators clearly played a role in the subcellular localization of the RNA-binding protein *SHE3* and the mRNAs that this protein transports. Another process the three regulators are involved in is the organization of the cell wall (Figure 42). Transcriptome profiling uncovered not only assorted cell wall-related enzymes as targets of regulation but also that the observed changes in the She-dependent mRNA transport affect the localization of *CHT2* mRNA, causing the exposure of chitin to the cell surface. These changes in the cell wall may lead to differences in the recognition of *C. albicans* triple mutant cells by innate immune cells.

5) Conclusion and Outlook

In this thesis, I have studied regulatory circuits that underlie host colonization by the eukaryotic member of the human microbiota, *Candida albicans*. *Candida albicans* is, on the one hand, the most prominent fungal species living in the human intestine and, on the other hand, a common cause of deep-seated, fatal infections. This organism is thus particularly suited to studying the biology of microbes that are harmless inhabitants of our mucosal surfaces but cause life-threatening human diseases as well. In the first part, I explored the contribution of a previously identified transcriptional regulator, *ZCF21*, to the pathogenicity of this fungus. Whole transcriptomics, susceptibility to cell wall-intercalating agents, changes in the overall structure, and an effect on the outcome of the interactions between *Candida* and host immune cells support the finding that this regulator is a key factor of the circuitry that dictates the overall composition and structure of *C. albicans*' cell surface. In the second part, I established that gnotobiotic mice mono-colonized with *C. albicans* represent a well-defined model system that can be used to study the commensal state of this fungus in the GI tract. First analyses of *C. albicans* colonizing this model system revealed that morphology and the ability to adhere are fundamental determinants of the persistence of this fungus in the digestive tract of these animals. In the final part, I further defined the roles of three previously undescribed regulators (*ZCF8*, *ZFU2*, and *TRY4*) in the commensal colonization of the GI tract of gnotobiotic mice by *C. albicans*. Transcriptome profiling and *in vitro* phenotypic analyses verified that these regulators control several processes that affect the yeast-to-hyphal transition, supporting the finding that the morphology plays a key role in the commensal colonization of the digestive tract of gnotobiotic mice. Overall, my dissertation unravels first how a transcriptional regulator promotes virulence by repressing the expression of its target genes and second which traits *C. albicans* requires to colonize the GI tract of gnotobiotic mice as a harmless commensal. It thus contributes new determinants of fungal commensalism and pathogenicity to the current understanding.

To date, most studies have focused on the pathogenicity of *C. albicans*—understandable since it is still considered one of the most prevalent human fungal pathogens, causing mucosal disease in healthy humans and life-threatening infections in immunocompromised individuals. These studies have uncovered numerous traits of this

fungus important for its virulence: phenotypic switching, adhesion to host cells, the secretion of hydrolytic enzymes, the modulation and evasion of the host immune system, and biofilm formation (Calderone et al., 2012; Chaffin et al., 1998; Cutler, 1991; Martinez et al., 1998; Naglik et al., 2003; Soll, 1992). The cell wall, being the outermost structure of *C. albicans* cells, is involved in many of these processes: enabling the release of hydrolytic enzymes, harboring many molecules important for adhesion, and being the first point of contact with host immune cells. It is therefore not surprising that this organelle is one of the most complexly regulated and dynamic structures in *C. albicans*. Various transcriptional regulators were previously described as controlling the cell wall composition: Bcr1p, for instance, controls the expression of cell surface adhesins and contributes thereby to adherence during biofilm formation (Nobile et al., 2006a). The ability to form biofilms enables the growth of *C. albicans* cells on surgical catheters, representing a high risk for the transfer of fungal cells to individuals undergoing surgery. Rim101p, another transcriptional regulator, controls the expression of several cell wall genes, affecting the pathogenicity of *C. albicans* cells during oropharyngeal candidiasis (Nobile et al., 2008). Moreover, Tup1p, which controls several secreted or cell surface proteins, is confirmed to be important during the process of filamentation and pathogenicity in *C. albicans*. Transcriptome analysis revealed that Zcf21p controls the expression of several genes encoding cell wall proteins and cell wall-modifying enzymes as well. The comparison to *in vitro* binding studies uncovered that it contributes to virulence almost exclusively through the downregulation of its direct target genes. The fact that *ZCF21* is transcribed at relatively high levels irrespective of media and growth conditions indicates that this regulator is constitutively expressed in the cell. I thus conclude that its role in generating the complex and dynamic composition and structure of the cell wall in *C. albicans* might be to limit the expression of cell wall components and thereby set a default state of their expression. Whenever these components are needed, other transcriptional regulators such as the ones described above may then induce their expression.

C. albicans, similar to other pathogenic fungi, faces a large assortment of stressful conditions while colonizing its mammalian host: nutrient limitation, antimicrobial peptides, oxidation, varying temperatures, and copper are only some of these stresses (Besold et al., 2016; Brown et al., 2009; Dantas Ada et al., 2015; Garcia-Santamarina et al., 2015; Hodgkinson et al., 2012; O'Meara et al., 2017). To mount a local or systemic

infection, this fungus developed tightly regulated mechanisms, enabling its survival under these harsh conditions. Temperature changes engender, for example, the activation of a diverse set of heat shock proteins (HSPs) (Franzmann et al., 2008; Mayer et al., 2012), facilitating the maintenance of protein homeostasis (Zuiderweg et al., 2017) or the stabilization of the folding of hundreds of proteins (Makhnevych et al., 2012; Taipale et al., 2010; Taipale et al., 2014). Nutrient acquisition is critical for living inside the host and causing disease. *C. albicans* can assimilate a wide range of nutrients in the mammalian host, non-fermentable carbon sources included (Vieira et al., 2010). To assimilate these alternative carbon sources, it induces the expression of specific transport proteins that facilitate the import of these substrates across the plasma membrane (Vieira et al., 2010). Copper is an essential metal in most cells, since it is an essential cofactor for many enzymes, but when it accumulates to levels beyond cellular needs, it can be toxic to invading microorganisms (Festa et al., 2012). *C. albicans* can decrease the copper uptake through the downregulation of copper importer (Marvin et al., 2004) and store excessive intracellular copper inside the vacuole to survive under high copper levels (Jo et al., 2008; Riggle et al., 2000; Weissman et al., 2000; Wysocki et al., 2010). The transcriptome analysis of this study indicates that *ZCF21* controls the expression of several genes in *C. albicans* connected to different stress responses: it regulates the expression of assorted transporters important to the uptake of essential nutrients (*OPT4*, *OPT2*, *HGT12*, *HGT16*, and *JEN2*) and the expression of various surface and cytoplasmic enzymes that bind to extracellular or intracellular copper (*SOD5*, *FET99*, *CUP1*, *FRE7*, *FRE30*, and *FET33*), thus regulating the copper level. All processes *C. albicans* requires to mount a systemic, disseminated infection are controlled by an overlapping set of transcriptional regulators. *RTG1*, *RTG3*, and *HMS1*, for instance, known to be crucial for systemic infections (Perez et al., 2013b), control the expression of genes involved in metabolism, as well as the yeast-to-filament transition. Similarly, *ZCF21* is involved in the regulation of cell surface remodeling but also controls the expression of nutrient acquisition and copper metabolism genes, implying that it may furthermore contribute to robust stress responses and metabolic flexibility.

Altogether, my results suggest that *ZCF21* controls different cellular processes in *C. albicans*, but all of them are conducive to the pathogenicity of this fungus inside its mammalian host. The most obvious effect of this regulator were alterations in the cell wall composition. More detailed analyses of the cell wall composition and the

interconnectedness with pathways known to control the organization of the cell wall should generate a more defined picture of *ZCF21*'s role in shaping the cell surface of *C. albicans*.

The human intestinal microbiome, known to be involved in metabolic, nutritional, physiological, and immunological processes (Bocci, 1992) and linked to several disease conditions (Lynch et al., 2016), comprises more than 1,000 different species (Rajilic-Stojanovic et al., 2014). The complexity of this human microbiome superorganism (Lederberg, 2000) is further increased through its variations within the human population (genetics, environment, and lifestyle). Studying any given member of the gut microbiota and its contributions to health and/or disease is therefore an intricate intention. One way to start dissecting the biology of a specific microorganism of the gut microbiota is to decrease the complexity to a minimum: one microorganism in a well-defined *in vivo* model. In this study, I demonstrated that gnotobiotic mice mono-colonized with *C. albicans* are a good model to use to start the analysis of traits important for this eukaryotic organism to colonize the mammalian GI tract. The animals revealed no overt signs of disease, and we yielded similar fungal loads as we did by using conventional antibiotic-treated mice possessing a residual undefined microflora commonly used to study gut colonization by *C. albicans in vivo*. We therefore conclude that *C. albicans* colonizes the digestive tract of gnotobiotic animals as a harmless commensal. Studying the commensal state of *C. albicans in vivo* in mono-colonized animals should allow the identification of traits that the fungus needs to colonize the GI tract and what might induce invasive proliferation in the fungus resulting in harmful diseases.

As a dimorphic organism, *C. albicans* can switch between different morphological forms. Known and well-studied environmental conditions produce distinct morphologies of this fungus: low temperatures, oxygen, acidic pH (four to six), and enriched media promote the yeast form (Braun et al., 1997; Odds, 1985, 1988); serum, a high temperature (37°C), a high ratio of CO₂ to O₂, neutral pH, and nutrient-poor media stimulate hyphal growth (Braun et al., 1997). We were therefore quite surprised to find *C. albicans* almost solely in its round-shaped yeast form colonizing the digestive tract of gnotobiotic animals. This phenomenon implies that in mono-colonized mice, the conditions present in the gut environment or some unknown host-derived factors seem to be able to overcome the strong filamentation inducers, 37°C and serum. We found three potential explanations as to why the yeast form is favored over the filamentous form in this model: First, the

filamentous form might induce a higher immune response or be more susceptible to immune factors, supported by the finding that a mutant of a well-established positive regulator of filamentation induced the release of the neutrophil-stimulating chemokine G-CSF (Granulocyte colony-stimulating factor) (Bohm et al., 2017). The filamentous form might hence induce an immune response and be cleared of the host. Second, the absence of other microbes might impact the metabolites available in the GI tract of germ-free animals. The yeast form might simply display a better fitness under these conditions. Third, in conventional animals, the fungus must face other competing and/or antagonistic microbes; to persist in such a complex ecosystem, the fungus may have to employ heterogeneous morphologies.

Hyphal formation is a complex process in *C. albicans* involving the induction of hyphal formation and the maintenance of hyphal growth. Both stages consist of various cellular mechanisms that underlie a highly connected network of regulation. Transcriptional regulators are known to control diverse processes important for *C. albicans* to stimulate and maintain hyphal growth: Efg1 (Stoldt et al., 1997), Cph1 (Leberer et al., 1996; Liu et al., 1994), Cph2 (Lane et al., 2001b), Tec1 (Lane et al., 2001a), and Rim101 (Davis et al., 2000; Davis, 2009; El Barkani et al., 2000) are only some examples of transcriptional regulators that positively regulate hypha-specific gene expression in *C. albicans*. Tup1 (Braun et al., 1997; Murad et al., 2001a), Nrg1 (Braun et al., 2001; Murad et al., 2001b), and Rfg1 (Kadosh et al., 2001) are known negative regulators of filamentation. A genetic screening of a transcription factor mutant library in gnotobiotic mice uncovered three transcriptional regulators (*ZCF8*, *ZFU2*, and *TRY4*) to be essential for the gut colonization of this animal model. *In vitro* phenotypic analysis indicated a connection between these three regulators and hyphal formation in *C. albicans*: under non-inducing conditions, mutants of the three regulators filament, suggesting that they are negative regulators of filamentation. Transcriptome analysis uncovered *FGR17* as one of the top common targets of regulation of *ZCF8*, *ZFU2*, and *TRY4*. *FGR17*, another transcriptional regulator, was previously proved to influence hyphal formation. Under non-inducing conditions, a deletion mutant of *FGR17* demonstrated similar colony wrinkling as mutants of *ZCF8*, *ZFU2*, and *TRY4*, indicating hyperfilamentation. *FGR17* thus leads to hyphal formation in *C. albicans*, as negative regulator and its expression depends on the presence of the transcriptional regulators *ZCF8*, *ZFU2*, and *TRY4*.

Upstream of many transcriptional regulators that control hyphal-specific gene expression are distinct signaling pathways that integrate environmental signals from numerous sources essential for hyphal formation. In response to serum, a strong filamentation inducer, Ras1, and the only adenylyl cyclase that *C. albicans* expresses, Cyr1, are activated (Fang et al., 2006). Through different signaling cascades, various transcriptional regulators that induce the expression of hyphal specific genes are activated or repressed. The activity of Efg1, for instance, is regulated through the pathway based on cyclic AMP (Sonneborn et al., 2000; Stoldt et al., 1997). Cph1's activity depends on a mitogen-activated protein kinase (MAPK) signaling pathway (Liu et al., 1994). I identified an earlier and heightened activation of two major MAPK pathways in a mutant of the three defined regulators in response to serum: the Cek1 and Mkc1 MAPK pathways. The Cek1 MAPK pathway was revealed to regulate the switch from unicellular yeast to invasive hyphae and the hyphal growth rate (Csank et al., 1998). The Mkc1 MAPK pathway is involved in regulating growth rate, cell viability, and mainly cell wall composition, but disruptions of this pathway also decrease invasive growth on certain media and the length of the formed hyphae (Navarro-Garcia et al., 1998). An earlier and heightened activation of these two pathways might therefore cause a heightened filament growth rate and filament length in *C. albicans* cells, both aspects that were observed in phenotypic screenings of the triple deletion mutant. However, further studies are required to define the contribution of *ZCF8*, *ZFU2*, and *TRY4* to these complex cascades.

Other processes important during hyphal formation in *C. albicans* are cell wall restructuring and the transport of detrimental factors to the growing hyphae. An mRNA transport mechanism in *C. albicans* was recently connected to the process of filamentation (Elson et al., 2009): the She-dependent mRNA transport mechanism, first described in *S. cerevisiae* (Jansen et al., 1996). Nevertheless, the mechanisms and factors that regulate the activity of this transport mechanism remain unclear. Under the top targets of *ZCF8*, *ZFU2*, and *TRY4* was *SHE3*, a gene involved in this transport mechanism. In *C. albicans*, She3p transports a set of mRNAs, many of them encoding proteins that are instrumental in hyphal development, to the tips of growing hyphae (Elson et al., 2009). Fluorescence *in situ* hybridization revealed that in the absence of the transcriptional regulators *ZCF8*, *ZFU2*, and *TRY4*, two of the target mRNAs of She3p, *ASH1* and *CHT2*, are mislocalized in growing hyphae. *ASH1* mRNA encodes a transcription factor required for WT virulence and filamentous growth on solid media (Inglis et al., 2002), while *CHT2* mRNA encodes a

chitinase known to be involved in cutting newly formed chitin chains before their integration into the cell wall and is necessary for normal filamentous growth (Sherrington et al., 2017). Mislocalization of the transport protein *SHE3* and two of its target mRNAs in the absence of *ZCF8*, *ZFU2*, and *TRY4* might therefore cause the changes in filamentation observed in single and triple mutants.

The fact that I found *C. albicans* almost exclusively in its yeast form in the GI tract of monocolonized mice suggests that the negative regulation of filamentation might be essential for the gut colonization of this mouse model. As described above, the transcriptional regulators *ZCF8*, *ZFU2*, and *TRY4*, unable to colonize the GI tract of monocolonized mice, contribute in at least three ways to hyphal formation in *C. albicans*. As a result, mutants of these regulators might be unable to remain in yeast form in this niche and thus cannot colonize it successfully.

In the intestine, a mucus layer separates the epithelium from colonizing microbes. Through its composition, this layer precludes the diffusion of microbial cells due to their size (Johansson et al., 2008), and the microbial cells hence do not get in contact with the epithelium. In conventional antibiotic-treated animals, it is known that *C. albicans* cells are only rarely located in close proximity to the mucus layer (Bohm et al., 2017). In monocolonized animals, I observed a different pattern of colonization: cells were located mostly in close proximity to the mucus layer. This could be because the intestinal mucus layer of germ-free animals is easier to penetrate than that of conventional animals (Johansson et al., 2015), or the underdeveloped immune system of germ-free animals might affect the distribution of *C. albicans* cells in the intestine (Vaishnava et al., 2011). Further studies are needed to conclude whether the mentioned mechanisms or others are the source of the altered distribution of *C. albicans* cells in gnotobiotic animals.

Adherence to mucus-containing surfaces was so far described to be essential only for gut colonization in several bacteria. The results described in this study suggest that *ZCF8*, *ZFU2*, and *TRY4* control similar functions in *C. albicans*. Mutants of the three identified regulators display reduced ability to bind to a surface containing mucin and to mucus-producing cells (Bohm et al., 2017). The fact that fungal cells are located in close proximity to the intestinal mucus layer in gnotobiotic animals supports the idea that *C. albicans* exhibits mechanisms to adhere to intestinal mucus and elaborates how the three regulators are conducive to gut colonization. The fact that mutants of these regulators display a gut colonization defect only in the absence of microbes and not in conventional

animals treated with antibiotics exhibiting a residual microbiota might reflect an effect of residual microbes themselves or, alternatively, of differences in the murine response to the presence of these microbes. Further studies are required to understand these effects, although it should again be stressed that mice are not natural hosts of *C. albicans*, and their indigenous flora might therefore not be relevant for gut colonization of the fungus.

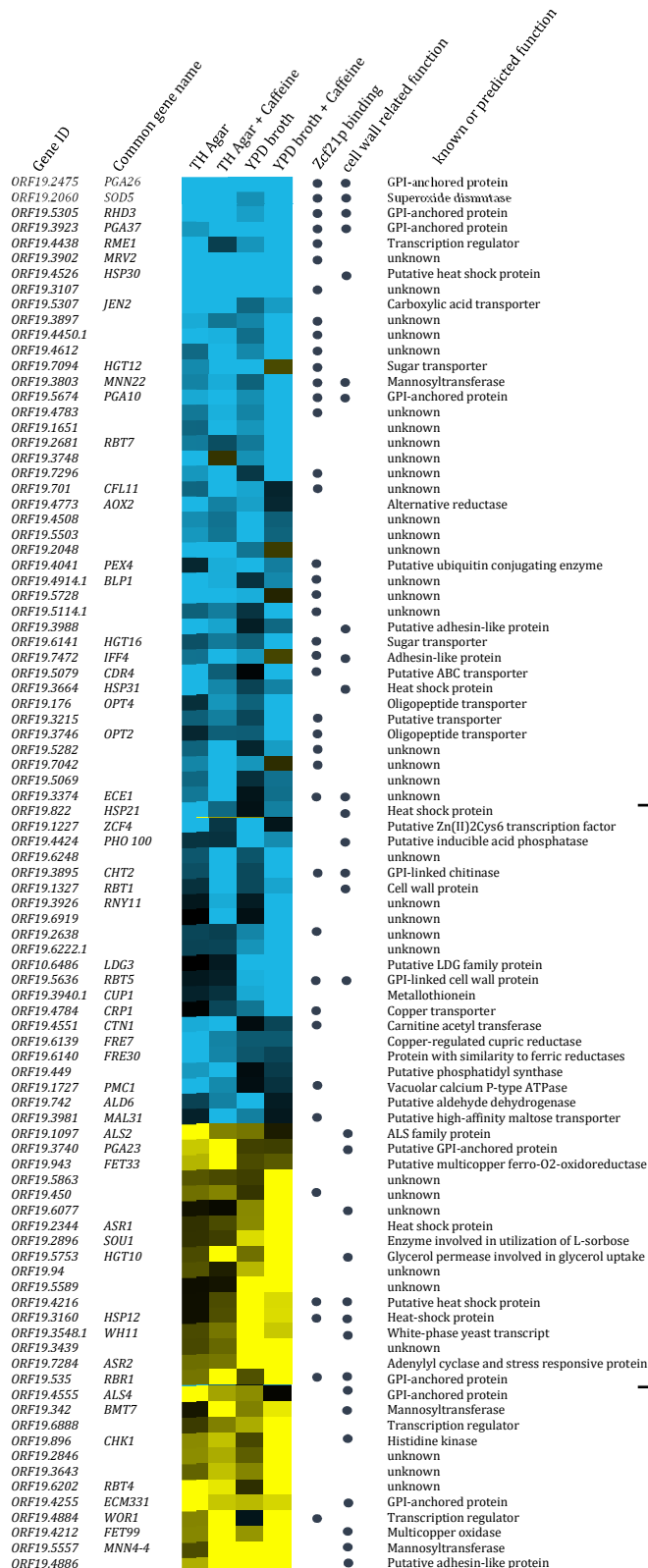
A crucial point in *C. albicans*' colonization of different niches throughout the human body is its evasion of detection by host immune cells. Because the cell wall is the first contact point of fungal and host cells, the composition of this structure mainly mediates the interplay between *C. albicans* and immune cells. Whole transcriptome analysis indicated a connection between *ZCF8*, *ZFU2*, and *TRY4* and the composition of the cell wall; the mislocalization of *CHT2* mRNA in the absence of the three regulators further supported this notion. Since standard cell wall stainings revealed no changes in the cell wall, we tested the exposure of certain cell wall components to the cell surface in a collaboration with Rebecca Hall, Birmingham, UK. This analysis disclosed that chitin, a sugar that is typically located close to the plasma membrane, is exposed to the cell surface in the absence *ZCF8*, *ZFU2*, and *TRY4*. An *in vitro* neutrophil killing assay confirmed that in the absence of the three regulators, cells are better recognized and eliminated by neutrophils. *C. albicans* is such a successful opportunistic pathogen because it can grow and proliferate under a wide range of different host conditions. One feature that allows its adaption to these various environments is the dynamic structure of its cell wall, which ensures the maintenance of cell shape, the protection and stability against environmental stresses, and especially the evasion of the immune system. All these functions require a complex network of regulation. The results presented here indicate that *ZCF8*, *ZFU2*, and *TRY4* are fundamental to the intricately regulated composition of the *C. albicans* cell wall and thus influence its recognition by innate immune cells *in vitro*. However, further studies are needed to determine how changes in the sugars exposed to the cell surface caused by the three regulators impact *C. albicans*' growth *in vivo*.

Overall, the results presented in this thesis add new aspects to both, *Candida albicans* pathogenicity and commensalism. On the one hand, I have clarified how a previously undescribed transcriptional regulator contributes to the virulence of the fungus through the downregulation of cell wall-related proteins; on the other hand, I have developed a complementary system to uncover new aspects of gut colonization by *C. albicans*: germ-free mice monocolonized with *C. albicans*. Using this model, we began to identify traits

that the fungus needs to colonize the GI tract. Further studies of *C. albicans* in this well-defined model system should help us to understand the biology of the fungus colonizing this niche and identify factors that induce invasive proliferation that results in harmful diseases.

6) Supporting Information

6.1) Supplementary Figures



37 genes showing >2-fold expression changes in 2 of 4 conditions

Figure S 1: Genes encoding ‘cell surface’ and ‘cell wall’ components are overrepresented in an enlarged set of ZCF21-target genes (Bohm *et al.*, 2016).

Heat map depicting 91 *C. albicans* genes that show significant differences in transcript levels based on our RNA-seq data. The genes included in this plot are those that showed >2-fold differences in at least two of four conditions investigated. The shade of blue to yellow in each square represent the $\log_2(wt/zcf21)$ numbers for each ORF based on their calculated FPKM values. Blue dots to the right denote that Zcf21p binds *in vivo* to the intergenic region upstream of the target gene (Perez *et al.*, 2013b) and/or that the gene encodes a protein that localizes to the cell membrane or cell wall. Gene Ontology analyses indicate that ‘cell surface’ and ‘cell wall’ are terms highly overrepresented in this dataset ($P = 9.18 \times 10^{-9}$).

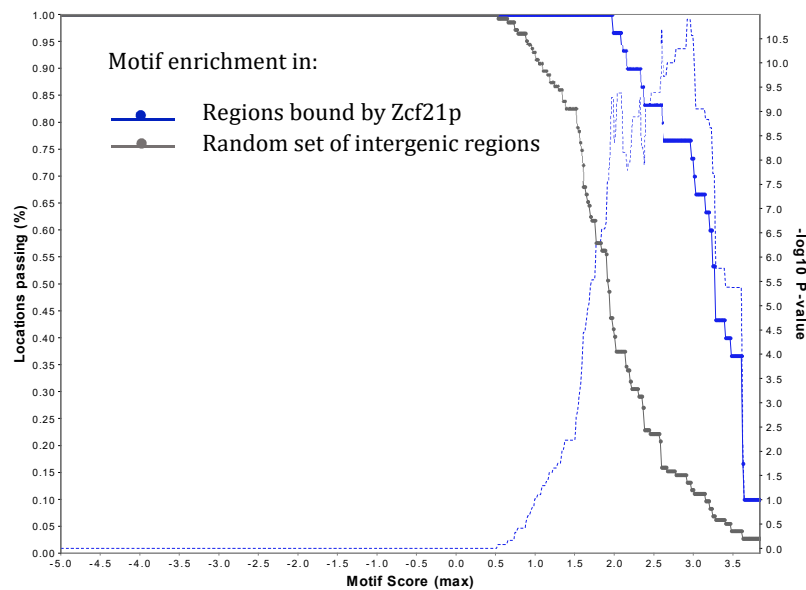


Figure S 2: Putative Zcf21p motif occurs preferentially in regions bound and controlled by the regulator (Bohm *et al.*, 2016).

(A) The frequency with which the DNA motif shown in Figure 7 occurs in regions bound by Zcf21p (solid blue line) versus in a set of random intergenic regions (solid grey line) was evaluated in MochiView using its “enrichment plot” function. The Zcf21p bound sequences include all 30 ChIP peaks (500 nt sequences centered in the midpoint of the peak) that occur in the intergenic regions upstream of the *ZCF21*-regulated transcripts identified by RNA-seq (Bohm *et al.*, 2016). The set of random intergenic regions is composed of 144 sequences, 500 nt in length each, generated randomly from the *C. albicans* genome. Note that the blue line runs to the right of the grey line indicating that at any motif score that one chooses as a cutoff, the set of Zcf21p-bound regions contains a higher proportion of matches to the motif than the set of random sequences. The dotted (light blue) line denotes the P-value distribution ($-\log_{10}$) across the motif scores.

6.2) Supplementary Tables

Table S 1: RNA Seq results

ID ORF	ORF name	wt FPKM	wt_caff FPKM	zcf21 FPKM	zcf21_caff FPKM	wt/zcf21	log2 (wt/zcf21)	wt_caff /zcf21_caff	log2 (wt_caff /zcf21_caff)	wt liq FPKM	wt liq_caff FPKM	zcf21 liq FPKM	zcf21 liq_caff FPKM	wt liq/zcf21 liq	log2 (wt liq /zcf21 liq)	wt liq_caff /zcf21 liq_caff	log2 (wt liq_caff /zcf21 liq_caff)
orf19.2475	PGA26	2.80	0.15	150.93	88.60	0.02	5.75	0.00	9.19	5.73	0.32	221.49	159.78	0.03	5.27	0.00	8.97
orf19.2060	SOD5	6.92	2.04	33.62	430.58	0.12	2.28	0.01	7.26	10.29	0.26	30.83	3.33	0.33	1.58	0.08	3.62
orf19.5305	RND3	44.10	9.87	369.82	180.67	0.12	3.07	0.05	4.19	622.42	87.46	2089.12	1155.93	0.30	1.75	0.08	3.72
orf19.2923	PGA37	0.56	0.69	1.77	7.09	0.32	1.66	0.10	3.36	3.76	1.02	15.63	15.65	0.24	2.06	0.07	3.94
orf19.4438	RME1	4.69	1.46	43.85	2.36	0.11	3.22	0.62	0.69	12.70	3.59	39.55	83.60	0.32	1.64	0.04	4.54
orf19.3902	MRV2	4.04	2.15	29.92	10.79	0.14	2.89	0.20	2.33	2.20	0.27	11.56	1.15	0.19	2.40	0.23	2.11
orf19.4526	HSP30	100.81	131.67	522.18	539.00	0.19	2.37	0.24	2.03	0.83	0.35	0.18	2.26	0.19	2.40	0.15	2.69
orf19.3107		1.52	1.44	7.02	7.62	0.22	2.20	0.19	2.41	2.10	1.43	11.81	7.89	0.18	2.49	0.20	2.31
orf19.5307	JEN2	0.66	0.55	5.96	3.91	0.11	3.18	0.14	2.84	0.49	0.03	1.07	0.10	0.46	1.13	0.30	1.72
orf19.3897		0.48	0.25	1.76	0.61	0.27	1.87	0.41	1.29	1.34	0.27	3.69	5.01	0.36	1.46	0.05	4.20
orf19.4450.1		143.76	180.77	850.95	696.20	0.17	2.57	0.26	1.95	654.32	12.46	1511.28	97.57	0.43	1.21	0.13	2.97
orf19.4612		3.11	1.90	6.91	17.52	0.45	1.15	0.11	3.20	1.63	1.18	4.58	8.39	0.36	1.49	0.14	2.83
orf19.7094	HGT12	2.11	0.09	6.05	0.96	0.35	1.52	0.09	3.50	0.14	0.01	2.50	0.01	0.06	4.11	1.50	-0.58
orf19.3803	MNN22	61.36	44.66	166.01	165.74	0.37	1.44	0.27	1.89	56.34	24.80	118.25	261.24	0.48	1.07	0.09	3.40
orf19.5674	PGA10	22.83	10.86	82.33	51.10	0.28	1.85	0.21	2.23	7.45	10.72	21.89	44.92	0.34	1.55	0.24	2.07
orf19.4783		1.97	1.85	4.99	7.04	0.40	1.31	0.26	1.23	1.21	1.27	3.31	9.50	0.37	1.45	0.13	2.91
orf19.1651		3.75	3.06	8.14	12.11	0.46	1.12	0.25	1.98	1.66	1.08	3.19	7.66	0.32	1.64	0.07	2.83
orf19.2681	RBT7	1.62	1.51	4.16	2.73	0.39	1.36	0.55	0.85	0.94	2.90	2.13	29.28	0.40	1.33	0.07	3.76
orf19.3748		0.56	0.15	3.95	2.77	0.15	2.78	1.32	0.41	0.24	0.85	0.71	8.53	0.33	1.59	0.10	3.32
orf19.7296		16.41	20.61	51.66	127.52	0.32	1.65	0.16	2.63	72.74	24.69	111.49	117.63	0.65	0.62	0.21	2.25
orf19.701	CFL11	0.27	0.16	0.59	2.26	0.46	1.12	0.07	3.02	0.04	0.15	0.15	0.20	0.29	1.81	0.76	0.39
orf19.4772	AOX2	18.73	94.16	149.79	252.02	0.13	3.00	0.37	1.42	16.06	260.97	541.13	350.46	0.30	1.75	0.74	0.43
orf19.4508		1.67	4.67	4.90	11.10	0.34	1.55	0.42	1.26	0.30	1.07	2.40	2.39	0.16	2.65	0.49	1.04
orf19.5502		0.26	0.69	0.83	1.66	0.32	1.66	0.10	2.45	37.32	1897.72	90.72	1371.43	0.41	1.29	1.38	-0.47
orf19.2048		76.61	125.68	656.52	698.97	0.12	3.10	0.18	1.90	19.42	35.51	107.99	92.78	0.18	2.49	0.38	1.39
orf19.4041	PEX4	8.93	3.91	11.99	14.55	0.74	0.43	0.27	1.90	145.42	17.58	211.81	49.56	0.69	0.54	0.35	1.50
orf19.4914.1	BLP1	319.09	366.60	1300.79	1368.97	0.25	2.02	0.25	2.01	0.02	0.24	0.08	0.20	0.27	1.91	1.22	-0.28
orf19.5728		0.44	0.15	2.21	0.60	0.20	2.32	0.38	1.38	3806.51	625.02	13729.40	4731.01	0.28	0.57	0.13	2.92
orf19.3988		30.81	6.29	195.94	21.88	0.16	2.67	0.29	1.80	1.81	2.11	2.27	4.64	0.80	0.33	0.46	1.14
orf19.6141	HGT16	3.65	3.53	6.73	8.94	0.54	0.88	0.39	1.34	7.97	1.99	15.95	11.81	0.49	1.02	0.16	2.64
orf19.7472	IF4	1.22	1.42	2.91	15.55	0.42	1.25	0.09	3.45	0.48	1.34	1.53	0.92	0.31	1.67	0.16	-0.55
orf19.5079	CDR4	55.27	86.47	227.94	177.27	0.24	2.04	0.49	1.04	91.06	30.06	94.24	191.94	0.97	0.05	0.16	2.66
orf19.3664	HSP31	8.92	17.62	36.10	49.32	0.25	2.02	0.36	1.49	2.66	1.14	4.42	3.08	0.60	0.74	0.37	1.43
orf19.176	OPT4	5.96	11.29	8.49	35.22	0.70	0.51	0.32	1.64	3.55	9.35	7.46	43.56	0.48	1.07	0.21	2.22
orf19.3215		180.97	144.61	372.60	378.43	0.49	1.04	0.38	1.39	270.43	116.89	461.45	525.42	0.59	0.77	0.22	2.17
orf19.3746	OPT2	9.56	15.30	12.76	31.54	0.75	0.42	0.48	1.04	5.10	15.44	10.36	112.11	0.49	1.02	0.14	2.86
orf19.5282		26.58	11.37	56.73	48.40	0.47	1.09	0.23	2.09	67.61	50.66	89.40	166.65	0.76	0.40	0.30	1.72
orf19.7042		1.26	1.17	3.48	6.40	0.36	1.47	0.18	2.45	1.34	119.58	4.19	93.45	0.32	1.64	1.28	-0.36
orf19.5069		2.62	4.76	5.75	22.67	0.46	1.13	0.21	2.25	7.05	7.02	10.06	16.69	0.70	0.51	0.42	1.25
orf19.3374	ECE1	3.09	36.92	7.70	175.53	0.40	1.32	0.21	2.25	0.84	0.61	0.98	1.41	0.86	0.23	0.43	1.22
orf19.822	HSP21	782.26	1167.71	3214.01	2955.68	0.24	2.04	0.45	1.15	23.71	17.18	27.13	45.44	0.87	0.19	0.38	1.40
orf19.1227	ZCF4	0.70	3.39	3.04	5.16	0.23	2.12	0.66	0.61	0.01	1.49	0.33	1.74	0.03	5.04	0.85	0.23
orf19.4424	PHO100	0.66	0.19	0.98	0.28	0.68	0.57	0.68	0.55	0.19	0.94	2.84	2.71	0.07	3.94	0.35	1.53
orf19.6248		0.41	0.59	0.79	2.65	0.52	0.95	0.22	2.18	0.86	1.74	1.63	10.75	0.53	0.93	0.16	2.63
orf19.3895	CHT2	235.76	14.04	430.06	83.81	0.55	0.87	0.17	2.58	1088.86	326.68	1892.56	1472.69	0.58	0.80	0.22	2.17
orf19.1327	RBT1	14.24	10.12	20.68	81.33	0.69	0.54	0.12	3.01	5.35	15.76	9.34	55.05	0.57	0.80	0.29	1.80
orf19.3926	RNY11	0.27	0.29	0.32	1.08	0.84	0.25	0.27	1.88	0.40	5.34	0.49	74.72	0.81	0.30	0.07	3.81
orf19.6919		0.01	0.13	0.01	0.58	1.00	0.00	0.22	2.20	0.25	0.31	0.28	2.23	0.89	0.17	0.14	2.83
orf19.2638		0.98	5.95	1.66	9.68	0.59	0.77	0.61	0.70	0.55	0.10	1.51	2.51	0.36	1.46	0.04	4.67
orf19.6222.1		12.94	39.08	21.60	66.15	0.60	0.74	0.59	0.76	43.51	43.81	134.25	341.78	0.32	1.63	0.13	2.96
orf19.6486	LDG3	0.01	0.23	0.01	0.28	1.00	0.00	0.82	0.29	0.22	0.24	1.00	2.32	0.22	2.17	0.10	3.27
orf19.5636	RBT5	2587.23	566.39	3098.72	723.66	0.83	0.26	0.78	0.35	8.16	165.69	31.03	1100.80	0.26	1.93	0.15	2.73
orf19.3940.1	CUP1	6533.43	1174.20	8463.07	17077.80	0.77	0.37	0.69	0.54	3806.51	10248.30	13729.40	44857.70	0.28	1.85	0.23	2.13
orf19.4784	CRP1	33.03	17.57	33.69	30.23	0.98	0.03	0.58	0.78	24.60	25.80	60.09	116.33	0.41	1.29	0.22	2.17
orf19.4551	CTN1	0.51	0.42	1.88	2.97	0.27	1.88	0.14	2.84	0.46	0.07	0.50	0.11	0.91	0.13	0.59	0.76
orf19.6139	FRE7	26.05	53.51	124.44	145.14	0.21	2.26	0.37	1.44	23.17	273.46	46.05	543.21	0.50	0.99	0.50	0.99
orf19.6140	FRE30	22.23	44.99	100.81	123.92	0.22	2.18	0.36	1.46	16.35	182.41	31.40	308.72	0.52	0.94	0.59	0.76
orf19.449		21.09	21.10	67.51	91.58	0.31	1.68	0.23	2.12	91.23	42.13	99.94	66.11	0.91	0.13	0.64	0.65
orf19.1277	PMCI	63.96	132.95	258.00	378.45	0.25	2.01	0.35	1.51	37.75	50.41	42.00	73.73	0.90	0.15	0.68	0.55
orf19.742	ALD6	6.28	4.59	10.39	12.26	0.60	0.73	0.37	1.42	2.74	1.00	15.64	1.24	0.18	2.51	0.81	0.31
orf19.3981	MAL31	22.01	6.13	28.34	38.42	0.78	0.36	0.16	2.65	3.66	0.30	9.69	0.36	0.38	1.40	0.83	0.26
orf19.1097	ALS2	535.31	925.84	112.16	455.44	4.77	-2.25	2.03	-1.02	55.28	99.74	29.01	85.49	1.91	-0.93	1.17	-0.22
orf19.3740	PGA23	8.80	38.85	2.94	8.20	3.00	-1.58	4.74	-2.24	8.28	118.16	5.79	83.93	1.43	-0.52	1.41	-0.49
orf19.943	FET3	109.00	100.21	40.67	6.99	2.68	-1.42	14.35	-3.84	471.74	408.09	313.59	250.09	1.50	-0.59	1.63	-0.71
orf19.5863		19.69	38.13	12.32	25.47	1.60	-0.68	1.50	-0.58	3.06	40.87	2.16	8.99	1.41	-0.50	4.55	-2.18
orf19.450		24.12	34.52	13.09	16.77	1.84	-0.88	2.06	-1.04	2.32	31.82	1.74	7.16	1.33	-0.42	4.44	-2.15
orf19.6077		41.43	38.43	37.28	36.49	1.11	-0.15	1.05	-0.07	76.34	34.89	36.22	8.41	2.11	-1.08	4.15	-2.05
orf19.2344	ASR1	47.10	47.67	35.98	31.70	1.31	-0.39	1.50	-0.59	22.54	240.56	10.62	47.12	2.12	-1.09	5.11	-2.35
orf19.2896	SOU1	89.03	108.30	67.66	77.08												

Table S 2: RNA Seq $p_{adj} < 0.1$

Gene name	Common name	TRY4	ZCF8	ZFU2	Description
orf19.101	<i>RIM9</i>	-0.41		-0.36	Protein required for alkaline pH response via the Rim101 signaling pathway; ortholog of <i>S. cerevisiae</i> Rim9 and <i>A. nidulans</i> pall; Spider biofilm induced
orf19.102		-0.48	-0.38		Protein of unknown function
orf19.1048	<i>IFD6</i>	-0.71		-0.45	Aldo-keto reductase; similar to aryl alcohol dehydrogenases; protein increase correlates with MDR1 overexpression (not CDR1 or CDR2) in fluconazole-resistant clinical isolates; farnesol regulated; possibly essential; Spider biofilm induced
orf19.105	<i>HAL22</i>		-0.42		Putative phosphoadenosine-5'-phosphate or 3'-phosphoadenosine 5'-phosphosulfate phosphatase; possible role in sulfur recycling; Hap43-repressed; F-12/CO2 biofilm induced
orf19.1075		-0.74	-0.47	-0.62	Protein of unknown function; Spider biofilm induced
orf19.1078	<i>HBR2</i>	-0.30			Putative alanine glyoxylate aminotransferase; regulated by Gcn4p and hemoglobin; stationary phase enriched protein
orf19.1082		-0.46	-0.48		Protein with an Alba DNA/RNA-binding protein domain; Spider biofilm induced
orf19.1083		-0.39	-0.49	-0.38	Putative protein of unknown function; macrophage-induced gene
orf19.1084	<i>CDC39</i>	-0.38	-0.33		Protein similar to <i>S. cerevisiae</i> Cdc39p, which is part of the CCR4-NOT transcription regulatory complex; transposon mutation affects filamentous growth
orf19.1085		-0.65	-0.61	-0.47	Protein of unknown function
orf19.1089	<i>PEX11</i>	-0.66	-0.46	-0.36	Putative peroxisomal membrane protein; role in fatty acid oxidation; expression is Tac1-regulated; Hms1p-dependent induction by geldamycin; Spider biofilm induced
orf19.109		-0.32			Probable mitochondrial tyrosyl-tRNA synthetase, based on conservation in other fungi
orf19.1091	<i>NOP8</i>	-0.30			Ortholog of <i>S. cerevisiae</i> Nop8; has a role in ribosomal large subunit biogenesis; rat catheter and Spider biofilm induced
orf19.1092		-0.34			Dolichol-P-Man dependent alpha(1-3) mannosyltransferase; role in the synthesis of dolichol-linked oligosaccharide donor for N-linked glycosylation of proteins; rat catheter biofilm repressed
orf19.1095	<i>GLE2</i>	-0.50	-0.43	-0.40	Putative nuclear pore complex; possibly an essential gene, disruptants not obtained by UAU1 method; rat catheter biofilm repressed
orf19.1097	<i>ALS2</i>	-0.80	-0.70	-0.77	ALS family protein; role in adhesion, biofilm formation, germ tube induction; expressed at infection of human buccal epithelial cells; putative GPI-anchor; induced by ketoconazole, low iron and at cell wall regeneration; regulated by Sfu1p
orf19.113	<i>CIP1</i>			-0.49	Possible oxidoreductase; transcript induced by cadmium but not other heavy metals, heat shock, yeast-hypha switch, oxidative stress (via Cap1), or macrophage interaction; stationary phase enriched protein; Spider biofilm induced
orf19.1149	<i>MRF1</i>	-0.42			Putative mitochondrial respiratory protein; induced by farnesol, benomyl, nitric oxide, core stress response; oxidative stress-induced via Cap1; stationary-phase enriched protein; Spider biofilm induced
orf19.1153	<i>GAD1</i>	-0.49			Putative glutamate decarboxylase; alkaline, macrophage-downregulated gene; amphotericin B induced; induced by Mnl1 under weak acid stress; stationary phase enriched protein; rat catheter biofilm repressed
orf19.117		-0.43	-0.42	-0.39	Protein of unknown function
orf19.1177		-0.39	-0.42	-0.39	Ortholog of <i>S. cerevisiae</i> Rtt106; histone chaperone that regulates chromatin structure in transcribed and silenced chromosomal regions; affects transcriptional elongation; Hap43-repressed; Spider biofilm repressed
orf19.1179		-0.43	-0.48		Protein of unknown function; induced in high iron; possibly subject to Kex2 processing; Hap43-repressed
orf19.118	<i>FAD2</i>		-0.35		Delta-12 fatty acid desaturase, involved in production of linoleic acid, which is a major component of membranes
orf19.1180		-0.53	-0.50	-0.44	Putative 2-aminoadipate transaminase; rat catheter and Spider biofilm repressed
orf19.1181			-0.41	-0.35	Protein of unknown function
orf19.1182		-0.51	-0.51	-0.50	Protein of unknown function
orf19.1183		-0.58	-0.54	-0.58	Protein of unknown function
orf19.1185			-0.36		Protein of unknown function
orf19.1186		-0.46	-0.36	-0.38	Protein of unknown function
orf19.1187	<i>CPH2</i>	-0.31			Myc-bHLH transcription factor; promotes hyphal growth; directly regulates Tec1 to induce hypha-specific genes; probably homodimeric, phosphorylated; required for colonization of the mouse GI tract; rat catheter and Spider biofilm induced
orf19.119		-0.55	-0.47		Protein of unknown function
orf19.1190	<i>STV1</i>	-0.33	-0.38	-0.34	Predicted subunit a of vacuolar proton-translocating ATPase V0 domain, Golgi isoform
orf19.1191		-0.32	-0.36	-0.34	Protein of unknown function
orf19.1192	<i>DNA2</i>			-0.38	Protein similar to <i>S. cerevisiae</i> Dna2p, which is a DNA replication factor involved in DNA repair; induced under hydroxyurea treatment
orf19.1193	<i>GNP1</i>		-0.31		Similar to asparagine and glutamine permease; fluconazole, caspofungin induced; regulated by Nrg1, Mig1, Tup1, Gcn2, Gcn4, and alkaline regulated by Rim101; repressed during chlamydospore formation; rat catheter, flow model biofilm induced
orf19.1198		-0.64	-0.47	-0.37	Predicted mitochondrial intermembrane space protein of unknown function; possibly an essential gene, disruptants not obtained by UAU1 method
orf19.1199	<i>NOP5</i>		-0.55	-0.35	Ortholog of <i>S. cerevisiae</i> Nop58; involved in pre-rRNA process; Tn mutation affects filamentous growth; macrophage/pseudohyphal-induced; physically interacts with TAP-tagged Nop1; Spider biofilm repressed
orf19.1200		-0.44	-0.51	-0.45	Protein of unknown function; Spider biofilm induced
orf19.1201		-0.46	-0.37	-0.36	Protein of unknown function
orf19.1202		-0.46			Protein of unknown function
orf19.1203	<i>SRO77</i>	-0.45	-0.38	-0.38	Protein with a predicted role in docking and fusion of post-Golgi vesicles with the plasma membrane; filament induced; fungal-specific (no human or murine homolog)
orf19.1203.1			-0.44	-0.35	Predicted dolichol-phosphate mannosyltransferase subunit; flow model and Spider biofilm repressed
orf19.1204		-0.45	-0.50	-0.42	Phosphorylated protein of unknown function; transcript is upregulated clinical isolates from HIV positive patients with oral candidiasis
orf19.121	<i>ARC18</i>	-0.64	-0.42	-0.34	Putative ARP2/3 complex subunit; mutation confers hypersensitivity to cytochalasin D
orf19.1210		-0.41	-0.38	-0.46	Protein of unknown function
orf19.1212		-0.58	-0.52	-0.39	Protein of unknown function
orf19.1214		-0.44	-0.63	-0.42	Protein of unknown function
orf19.1215		-0.53		-0.44	Protein of unknown function
orf19.1217		-0.43			Protein of unknown function
orf19.1220	<i>RVS167</i>	-0.38	-0.33	-0.34	SH3-domain- and BAR domain-containing protein involved in endocytosis; null mutant exhibits defects in hyphal growth, virulence, cell wall integrity, and actin patch localization; cosediments with phosphorylated Myo5p
orf19.1221	<i>ALG2</i>	-0.46	-0.36	-0.39	Putative mannosyltransferase involved in cell wall mannan biosynthesis; transcription is elevated in chk1, nik1, and sln1 homozygous null mutants
orf19.1224	<i>FRP3</i>	0.36			Putative ammonium transporter; upregulated in the presence of human neutrophils; fluconazole-downregulated; repressed by nitric oxide; Spider biofilm induced; rat catheter biofilm repressed
orf19.123	<i>RCN1</i>			-0.39	Protein involved in calcineurin-dependent signaling that controls stress response and virulence; inhibits calcineurin function
orf19.124	<i>CIC1</i>	-0.38	-0.50	-0.38	Putative proteasome-interacting protein; rat catheter biofilm induced
orf19.1240			0.29		Protein of unknown function
orf19.125	<i>EBP1</i>		-0.54	-0.41	NADPH oxidoreductase; interacts with phenolic substrates (17beta-estradiol); possible role in estrogen response; induced by oxidative, weak acid stress, NO, benomyl, GlcNAc, Cap1, Mnl1 induced; Hap43-repressed; rat catheter biofilm induced

Supporting Information

orf19.1253	<i>PHO4</i>		0,41		bHLH transcription factor of the myc-family; required for growth in medium lacking phosphate and for resistance to copper and Phloxine B; induced by Mnl1 under weak acid stress
orf19.1287			0,48		Protein of unknown function; flow model biofilm induced; Spider biofilm induced
orf19.130	<i>VPS15</i>	-0,56			Protein involved in retrograde endosome-to-Golgi protein transport; required for normal virulence
orf19.1308				1,58	Predicted membrane transporter, member of the drug:proton antiporter (14 spanner) (DHA2) family, major facilitator superfamily (MFS)
orf19.1309				1,08	Protein of unknown function
orf19.131.2		-0,41	-0,37		Protein of unknown function
orf19.1310				0,54	Protein of unknown function
orf19.1311	<i>SPO75</i>			0,42	Protein of unknown function
orf19.132		-0,31			Protein of unknown function
orf19.1326		-0,39	-0,49	-0,36	Protein of unknown function
orf19.1344		0,91			Protein of unknown function; fluconazole-induced; Spider biofilm induced
orf19.135	<i>EXO84</i>	-0,39	-0,43	-0,36	Predicted subunit of the exocyst complex, involved in exocytosis; localizes to a crescent on the surface of the hyphal tip
orf19.1350		-0,35			Protein with a thioredoxin domain; predicted role in cell redox homeostasis; rat catheter and Spider biofilm induced
orf19.1353		-0,43			Protein of unknown function; repressed by yeast-hypha switch; Ras1-regulated; oral infection induced; mutants defective in damage to oral epithelium; flow model biofilm induced; Spider biofilm induced
orf19.1354	<i>UCF1</i>	-0,38			Upregulated by cAMP in filamentous growth; induced in high iron, decreased upon yeast-hypha switch; downregulation correlates with clinical fluconazole resistance; Ras1-regulated; Hap43-repressed; flow model biofilm induced
orf19.136	<i>QDR3</i>			0,41	Predicted membrane transporter, member of the drug:proton antiporter (12 spanner) (DHA1) family, major facilitator superfamily (MFS); Hap43p-repressed gene
orf19.137		-0,44	-0,37		Putative transferase involved in phospholipid biosynthesis; induced by alpha pheromone in SpiderM medium
orf19.139	<i>TRA1</i>	-0,30			Subunit of the NuA4 histone acetyltransferase complex
orf19.1397		0,41			Protein of unknown function
orf19.1405	<i>PHO13</i>			0,38	Putative 4-nitrophenylphosphatase; Hap43p-repressed gene; transcription is regulated upon yeast-hyphal switch
orf19.1433		-0,43			Protein of unknown function; Hap43-repressed; colony morphology-related gene regulation by Ssn6; Spider biofilm induced
orf19.1439	<i>IPK1</i>	-0,50	-0,34	-0,37	Ortholog of <i>S. cerevisiae/S. pombe</i> Ipk1; an inositol pentakisphosphate 2-kinase, a nuclear protein required for synthesis of 1,2,3,4,5,6-hexakisphosphate; Spider biofilm induced
orf19.1479			0,35		Ortholog of the mitochondria localized <i>S. cerevisiae</i> Pib2 protein of unknown function; has a FYVE zinc finger domain; Spider biofilm induced
orf19.1481	<i>HAP42</i>		0,40		Predicted transcription factor; possibly an essential gene, disruptants not obtained by UAU1 method
orf19.1486			0,50		Protein with a life-span regulatory factor domain; regulated by Sef1, Sfu1, and Hap43; flow model biofilm induced; Spider biofilm induced
orf19.1490	<i>MSB2</i>		0,47	0,39	Mucin family adhesin-like protein; cell wall damage sensor; required for Cek1 phosphorylation by cell wall stress; Rim101-repressed; activation releases extracellular domain into medium; Spider biofilm induced
orf19.1509	<i>ROD1</i>		0,34		Protein similar to <i>S. cerevisiae</i> Rod1; a membrane protein with a role in drug tolerance; repressed by Rgt1; mutant is viable
orf19.1600			0,65	0,36	Protein of unknown function
orf19.1607	<i>ALR1</i>		0,30		Putative transporter of divalent cations; hyphal-induced expression; rat catheter biofilm induced
orf19.1614	<i>MEP1</i>	0,88	0,57	0,37	Ammonium permease; Mep1 more efficient permease than Mep2, Mep2 has additional regulatory role; 11 predicted transmembrane regions; low mRNA abundance; hyphal downregulated; flow model biofilm induced
orf19.1653			0,37	0,37	Protein of unknown function
orf19.1655.3			0,35		Protein of unknown function
orf19.1691		-0,58			Plasma-membrane-localized protein; filament induced; Hog1, ketoconazole, fluconazole and hypoxia-induced; regulated by Nrg1, Tup1, Upc2; induced by prostaglandins; flow model biofilm induced; rat catheter and Spider biofilm repressed
orf19.1715	<i>IRO1</i>	-0,47	-0,53	-0,47	Putative transcription factor; role in iron utilization, pathogenesis; both IRO1 and adjacent URA3 are mutated in strain CAI4; suppresses <i>S. cerevisiae</i> aft1 mutant low-iron growth defect; hyphal-induced; reports differ about iron regulation
orf19.1716	<i>URA3</i>	-0,71	-0,86	-0,69	Orotidine-5'-phosphate decarboxylase; pyrimidine biosynthesis; gene used as genetic marker; decreased expression when integrated at ectopic chromosomal locations can cause defects in hyphal growth and virulence; Spider biofilm repressed
orf19.1727	<i>PMC1</i>		0,40		Vacuolar calcium P-type ATPase; transcript regulated by calcineurin and fluconazole; mutant shows increased resistance to fluconazole, lithium; increased sensitivity to calcium; Spider biofilm induced
orf19.1770	<i>CYC1</i>		0,45	0,37	Cytochrome c; complements defects of <i>S. cerevisiae</i> cyc1 cyc7 double mutant; induced in high iron; alkaline repressed; repressed by nitric oxide; Hap43-dependent repression in low iron; regulated by Sef1, Sfu1
orf19.1795	<i>PUF3</i>		0,46		Ortholog of <i>S. cerevisiae</i> Puf3; mRNA-binding protein involved in RNA catabolism; mutant is viable
orf19.1842	<i>BUD5</i>		0,35		Predicted GTP/GDP exchange factor for Rsr1; rat catheter biofilm induced
orf19.1847	<i>ARO10</i>	-0,39	0,49		Aromatic decarboxylase; Ehrlich fusel oil pathway of aromatic alcohol biosynthesis; alkaline repressed; protein abundance affected by URA3 expression in CAI-4 strain; Spider biofilm induced
orf19.1862		-0,61			Possible stress protein; increased transcription associated with CDR1 and CDR2 overexpression or fluphenazine treatment; regulated by Sfu1, Nrg1, Tup1; stationary phase enriched protein; Spider biofilm induced
orf19.1868	<i>RNR22</i>		-0,34		Putative ribonucleoside diphosphate reductase; colony morphology-related gene regulation by Ssn6; transcript regulated by tyrosol and cell density; Hap43-repressed; Spider biofilm induced
orf19.1887			0,38	0,36	Protein of unknown function
orf19.1896	<i>SSC1</i>		0,36		Heat shock protein; at yeast-form cell surface, not hyphae; antigenic; Gcn4-regulated; induced by amino acid starvation (3-AT) or by adherence to polystyrene; macrophage-repressed; sumoylation target; possibly essential
orf19.1945	<i>AUR1</i>		0,33		Inositolphosphorylceramide (IPC) synthase; catalyzes the key step in sphingolipid biosynthesis; antifungal drug target; flow model biofilm induced; Spider biofilm induced
orf19.1960	<i>CLN3</i>	-0,34			G1 cyclin; depletion abolishes budding and causes hyphal growth defects; farnesol regulated, functional in <i>S. cerevisiae</i> ; possibly essential (UAU1 method); other biofilm induced; Spider biofilm induced
orf19.1964		0,41			Protein of unknown function; repressed by fluphenazine treatment; induced by benomyl treatment and in an RHE model; regulated by Nrg1, Tup1
orf19.1978	<i>GIT2</i>	0,36	0,59	0,40	Putative glycerophosphoinositol permease; fungal-specific; repressed by alpha pheromone in SpiderM medium; Hap43-repressed; Spider biofilm induced
orf19.1979	<i>GIT3</i>	0,44	0,55		Glycerophosphocholine permease; white cell specific transcript; fungal-specific; alkaline repressed; caspofungin, macrophage/pseudohyphal-repressed; flow model biofilm induced; Spider biofilm induced
orf19.1995	<i>MNN24</i>		0,45		Alpha-1,2-mannosyltransferase; required for normal cell wall mannan content
orf19.1996	<i>CHA1</i>		0,52	0,47	Similar to catabolic ser/thr dehydratases; repressed by Rim101; induced in low iron; regulated on white-opaque switch; filament induced; Tn mutation affects filamentation; flow model biofilm induced; Spider biofilm repressed
orf19.2003	<i>HNM1</i>			0,36	Putative choline/ethanolamine transporter; mutation confers hypersensitivity to toxic ergosterol analog; colony morphology-related gene regulation by Ssn6; clade-associated gene expression
orf19.2005	<i>REG1</i>		0,44		Putative protein phosphatase regulatory subunit; Hap43-repressed gene; macrophage/pseudohyphal-induced; possibly regulated upon hyphal formation; flow model biofilm induced
orf19.2006.1	<i>COX17</i>			0,35	Putative copper metallochaperone; Hap43p-repressed gene; rat catheter biofilm induced; Spider biofilm induced
orf19.2008				0,34	Protein of unknown function

orf19.2028	<i>MXR1</i>		-0,32		Putative methionine sulfoxide reductase; Plc1-regulated; induced by human neutrophils, flucytosine; macrophage regulated (gene induced, protein decreased); possibly adherence-induced; Spider biofilm induced
orf19.203	<i>STB3</i>		0,41		Putative SIN3-binding protein 3 homolog; caspofungin induced; macrophage/pseudohyphal-repressed; rat catheter biofilm induced
orf19.2048			0,71		Protein of unknown function; transcript positively regulated by Sfu1; Hap43 repressed; Spider biofilm induced
orf19.2076		-0,55			Protein of unknown function; S. pombe ortholog SPAC7D4.05 encodes a predicted hydrolase; Hap43-repressed; Spider biofilm induced
orf19.2108	<i>SOD6</i>		0,50	0,34	Copper- and zinc-containing superoxide dismutase; gene family includes SOD1, SOD4, SOD5, and SOD6; gene may contain an intron; Hap43-repressed; flow model and rat catheter biofilm induced
orf19.2125		-0,45			Protein of unknown function; GlcNAc-induced protein; Spider biofilm induced; rat catheter biofilm repressed
orf19.2128		-0,42	-0,51	-0,43	Protein of unknown function
orf19.2129		-0,38			Ortholog of <i>S. cerevisiae</i> Spo71; a meiosis-specific protein required for spore wall formation during sporulation in <i>S. cerevisiae</i> ; possibly an essential gene, disruptants not obtained by UAU1 method
orf19.2131			-0,36		Protein of unknown function
orf19.2132		-0,55	-0,53	-0,49	Protein of unknown function
orf19.2133	<i>LIP4</i>			-0,44	Secreted lipase, member of a differentially expressed lipase gene family with possible roles in nutrition and/or in creating an acidic microenvironment; expressed more strongly during mucosal infections than during systemic infections
orf19.2135	<i>TSM1</i>	-0,36	-0,30		Putative transcription initiation factor TFIIID subunit; transcript is upregulated in clinical isolates from HIV+ patients with oral candidiasis; Nrg1-regulated
orf19.2138	<i>ILS1</i>	-0,27	-0,37		Putative isoleucyl-tRNA synthetase, the target of drugs including the cyclic beta-amino acid icofungipen/PLD-118/BAY-10-8888 and mupirocin; protein present in exponential and stationary growth phase yeast cultures
orf19.2143		-0,35	-0,37		Protein of unknown function
orf19.2146	<i>HAT2</i>	-0,40	-0,44	-0,40	Putative Hat1-Hat2 histone acetyltransferase complex subunit; role in DNA damage repair and morphogenesis; mutations cause constitutive pseudohyphal growth, caspofungin sensitivity; rat catheter and Spider biofilm repressed
orf19.215			0,48		Component of a complex containing the Tor2p kinase; possible a role in regulation of cell growth; Spider biofilm induced
orf19.2150		-0,40	-0,49	-0,35	Putative ortholog of mammalian electron transfer flavoprotein complex subunit ETF-alpha; Spider biofilm repressed
orf19.2151	<i>NAG6</i>	-0,48	-0,43	-0,41	Protein required for wild-type mouse virulence and wild-type cycloheximide resistance; putative GTP-binding motif; similar to <i>S. cerevisiae</i> Yor165Wp; in gene cluster that encodes enzymes of GlcNAc catabolism; no human or murine homolog
orf19.2154	<i>HXX1</i>	-0,33	-0,39	-0,37	N-acetylglucosamine (GlcNAc) kinase; involved in GlcNAc utilization; required for wild-type hyphal growth and mouse virulence; GlcNAc-induced transcript; induced by alpha pheromone in SpiderM medium
orf19.2158	<i>NAG3</i>			-0,37	Putative MFS transporter; similar to Nag4; required for wild-type mouse virulence and cycloheximide resistance; in gene cluster that includes genes encoding enzymes of GlcNAc catabolism; Spider biofilm repressed
orf19.2163			-0,35		Protein of unknown function
orf19.2165			-0,49		Predicted hydrolase; induced by nitric oxide
orf19.2172	<i>ARA1</i>	-0,42			D-Arabinose dehydrogenase; dehydro-D-arabinono-1,4-lactone synthesis; active on D-arabinose, L-fucose, L-xylose, L-galactose; inhibited by metal ions, thiol group-specific reagents; induced on polystyrene adherence; Spider biofilm induced
orf19.2175		-0,33			Putative mitochondrial cell death effector; induced by nitric oxide; Spider biofilm induced; rat catheter biofilm repressed
orf19.2179	<i>SIT1</i>		-0,38		Transporter of ferrichrome siderophores, not ferrioxamine B; required for human epithelial cell invasion in vitro, not for mouse systemic infection; regulated by iron, Sfu1, Rfg1, Tup1, Hap43; rat catheter and Spider biofilm induced
orf19.2192	<i>GDH2</i>	0,33			Putative NAD-specific glutamate dehydrogenase; fungal-specific; transcript regulated by Nrg1, Mig1, Tup1, and Gcn4; stationary phase enriched protein; flow model biofilm induced; Spider biofilm induced
orf19.2199	<i>PHO86</i>	0,40			Putative endoplasmic reticulum protein; possibly adherence-induced
orf19.2241	<i>PST1</i>	-0,51			Putative 1,4-benzoquinone reductase; hyphal-induced; regulated by Cyr1, Ras1, Efg1, Nrg1, Rfg1, Tup1; Hap43-induced; Spider biofilm induced
orf19.2269		-0,41	-0,41		Putative 3-phosphoserine phosphatase; induced by benomyl or in azole-resistant strain that overexpresses MDR1; early-stage flow model biofilm induced; Spider biofilm repressed
orf19.2270	<i>SMF12</i>		0,52	0,38	Ortholog of <i>S. cerevisiae</i> Smf1; manganese transporter; Gcn4-regulated; Hap43, alkaline induced; caspofungin repressed; mutants are viable
orf19.2301			-0,38		Protein of unknown function
orf19.2344	<i>ASR1</i>	-1,35	-0,59	-0,62	Heat shock protein; transcript regulated by cAMP, osmotic stress, ciclopirox olamine, ketoconazole; repressed by Cyr1, Ras1; colony morphology-related regulated by Ssn6; stationary phase enriched; Hap43-induced; Spider biofilm induced
orf19.238	<i>CCP1</i>	-0,39			Cytochrome-c peroxidase N terminus; Rim101, alkaline pH repressed; induced in low iron or by macrophage interaction; oxygen-induced activity; regulated by Sef1, Sfu1, and Hap43; Spider biofilm induced; rat catheter biofilm repressed
orf19.2382			0,32		Protein similar to isoleucyl-tRNA synthetase; isoleucyl-tRNA synthetase is the target of drugs including the cyclic beta-amino acid icofungipen/PLD-118/BAY-10-8888 and mupirocin
orf19.2396	<i>IFR2</i>	-0,48			Zinc-binding dehydrogenase; induced by benomyl, ciclopirox olamine, alpha pheromone, Hap43; regulated by oxidative stress via Cap1, osmotic stress via Hog1; protein present in exponential and stationary phase; rat catheter biofilm repressed
orf19.2415			0,35		Protein of unknown function
orf19.2445				-0,38	Putative dicarboxylic amino acid permease; fungal-specific (no human or murine homolog); induced by alpha pheromone in SpiderM medium
orf19.2451	<i>PGA45</i>	0,65		0,45	Putative GPI-anchored cell wall protein; repressed in core caspofungin response; Hog1-induced; regulated by Ssn6; Mob2-dependent hyphal regulation; flow model biofilm induced
orf19.2452		0,35			Protein of unknown function; induced in high iron; repressed in core caspofungin response; ketoconazole-repressed; colony morphology-related gene regulation by Ssn6; possibly subject to Kex2 processing
orf19.2461	<i>PRN4</i>		-0,37		Protein with similarity to pirins; induced by benomyl treatment; flow model biofilm repressed
orf19.2501	<i>FLC1</i>		0,32		Protein involved in heme uptake; putative FAD transporter, similar to <i>S. cerevisiae</i> Flc1; regulated by iron; macrophage-induced; mutant defective in filamentous growth; Spider biofilm induced
orf19.251	<i>GLX3</i>	-0,52	-0,37		Glutathione-independent glyoxalase; binds human immunoglobulin E; alkaline, fluconazole, Hog1 repressed; hypoxia, oxidative stress via Cap1, Hap43 induced; stationary-phase enriched; rat catheter, Spider biofilm induced
orf19.2529.1				0,36	Protein of unknown function; Spider biofilm repressed
orf19.2531	<i>CSP37</i>	-0,43			Hyphal cell wall protein; role in progression of mouse systemic infection; predicted P-loop, divalent cation binding, N-glycosylation sites; expressed in yeast and hyphae; hyphal downregulated; stationary-phase enriched; GlcNAc-induced
orf19.2532	<i>PRS</i>		0,41		Putative prolyl-tRNA synthetase; monofunctional Class II synthetase; gene is constitutively expressed
orf19.2551	<i>MET6</i>	0,29			Essential 5-methyltetrahydropteroyltryglutamate-homocysteine methyltransferase (cobalamin-independent methionine synthase); antigenic in murine/human systemic infection; heat shock, estrogen, GCN-induced; Spider biofilm repressed
orf19.2608	<i>ADH5</i>	-0,37			Putative alcohol dehydrogenase; regulated by white-opaque switch; fluconazole-induced; antigenic in murine infection; regulated by Nrg1, Tup1; Hap43, macrophage repressed, flow model biofilm induced; Spider biofilm induced
orf19.2613	<i>ECM4</i>	-0,31			Cytoplasmic glutathione S-transferase; regulated by Nrg1, Tup1; induced in core stress response, in <i>cyr1</i> or <i>ras1</i> mutant (yeast or hyphal cells); Tn mutation affects filamentous growth; stationary phase enriched; Spider biofilm induced

Supporting Information

orf19.2670		-0,38			Protein of unknown function
orf19.2685	<i>PGA54</i>		0,38		GPI-anchored protein; Hog1-repressed; induced in <i>cyr1</i> or <i>efg1</i> mutant or in hyphae; colony morphology-related gene regulation by <i>Ssn6</i> ; induced in RHE model; mRNA binds <i>She3</i> ; regulated in Spider biofilms by <i>Tec1</i> , <i>Egf1</i> , <i>Ntd80</i> , <i>Rob1</i> , <i>Brg1</i>
orf19.2686				0,64	Protein of unknown function
orf19.2737		-0,61			Carbohydrate kinase domain-containing protein; Spider biofilm induced
orf19.2747	<i>RGT1</i>		0,46		Zn(II)2Cys6 transcription factor; transcriptional repressor involved in the regulation of glucose transporter genes; ortholog of <i>S. cerevisiae Rgt1</i> ; mutants display decreased colonization of mouse kidneys
orf19.2762	<i>AHP1</i>	-0,56	-0,53	-0,40	Alkyl hydroperoxide reductase; immunogenic; fluconazole-induced; amphotericin B, caspofungin, alkaline repressed; core stress response induced; <i>Ssk1/Nrg1/Tup1/Ssn6/Hog1</i> regulated; flow model biofilm induced; rat catheter biofilm repressed
orf19.2768	<i>AMS1</i>	-0,45			Putative alpha-mannosidase; transcript regulated by <i>Nrg1</i> ; induced during cell wall regeneration; flow model biofilm induced; Spider biofilm induced
orf19.2769		-0,39			Putative protease B inhibitor; hyphal-induced expression; <i>Cyr1p</i> - and <i>Ras1p</i> -repressed
orf19.2770.1	<i>SOD1</i>		-0,37		Cytosolic copper- and zinc-containing superoxide dismutase; role in protection from oxidative stress; required for full virulence; alkaline induced by <i>Rim101</i> ; induced by human blood; rat catheter, flow model and Spider biofilm repressed
orf19.2771	<i>BEM3</i>		0,39		Putative GTPase-activating protein (GAP) for Rho-type GTPase <i>Cdc42p</i> ; involved in cell signaling pathways that control cell polarity; similar to <i>S. cerevisiae Bem3p</i>
orf19.2809	<i>CTN3</i>		0,48		Peroxisomal carnitine acetyl transferase; no obvious metabolic, hyphal, virulence defects in <i>Ura+</i> strain; induced by macrophage engulfment, hyphal growth, starvation, nonfermentable carbon sources; rat catheter, Spider biofilm induced
orf19.2810	<i>AAP1</i>	0,47			Putative amino acid permease; fungal-specific; possibly essential, disruptants not obtained by UAU1 method; Spider biofilm induced
orf19.2823	<i>RFG1</i>		0,50		HMG domain transcriptional repressor of filamentous growth and hyphal genes; in <i>Tup1</i> -dependent and -independent pathways; binds DNA; transcript not regulated by oxygen or serum; not responsible for hypoxic repression; Spider biofilm induced
orf19.2839	<i>CIRT4B</i>	-0,48			Cirt family transposase; transcript repressed in an azole-resistant strain that overexpresses <i>CDR1</i> and <i>CDR2</i> ; <i>Hap43</i> -repressed; flow model biofilm induced
orf19.2841	<i>PGM2</i>	-0,31			Ortholog of <i>S. cerevisiae Pgm2</i> ; induced in planktonic culture; <i>Tye7p</i> -regulated; flow model biofilm induced; rat catheter biofilm repressed
orf19.2846		-0,63		-0,54	Protein of unknown function; <i>Hap43</i> -repressed; induced in core caspofungin response; regulated by yeast-hypha switch; Spider biofilm repressed
orf19.2896	<i>SOU1</i>	-0,67	-0,47		Enzyme involved in utilization of L-sorbose; has sorbitol dehydrogenase, fructose reductase, and sorbose reductase activities; NAD-binding site motif; transcriptional regulation affected by chromosome 5 copy number; <i>Hap43p</i> -induced gene
orf19.2943.5			0,44		Protein of unknown function
orf19.2971			0,38		Protein of unknown function
orf19.2990	<i>XOG1</i>		0,42	0,37	Exo-1,3-beta-glucanase; 5 glycosyl hydrolase family member; affects sensitivity to chitin and glucan synthesis inhibitors; not required for yeast-to-hypha transition or for virulence in mice; <i>Hap43</i> -induced; Spider biofilm induced
orf19.3007.2				-0,34	Protein of unknown function
orf19.3066	<i>ENG1</i>		0,30		Endo-1,3-beta-glucanase; ortholog of <i>S. cerevisiae Dse4</i> needed for cell separation; caspofungin, fluconazole repressed; repressed by alpha pheromone in SpiderM medium; flow model biofilm induced; rat catheter biofilm repressed
orf19.3127	<i>CZF1</i>	-0,50			Transcription factor; regulates white-opaque switch; hyphal growth regulator; expression in <i>S. cerevisiae</i> causes dominant-negative inhibition of pheromone response; required for yeast cell adherence to silicone; Spider biofilm induced
orf19.3139				0,72	Putative NADP-dependent oxidoreductase; <i>Hap43</i> -repressed; induced by benomyl treatment; oxidative stress-induced via <i>Cap1</i> ; rat catheter biofilm repressed
orf19.3150	<i>GRE2</i>	-0,41	-0,34	-0,43	Putative reductase; <i>Nrg1</i> and <i>Tup1</i> -regulated; benomyl- and hyphal-induced; macrophage/pseudohyphal-repressed; repressed by low iron; possibly involved in osmotic stress response; stationary phase enriched protein; Spider biofilm induced
orf19.3152	<i>AMO2</i>			-0,37	Protein similar to <i>A. niger</i> predicted peroxisomal copper amino oxidase; mutation confers hypersensitivity to toxic ergosterol analog; F-12/CO2 early biofilm induced
orf19.3153	<i>MSS4</i>		0,29		Phosphatidylinositol-4-phosphate 5-kinase; activity induced by phosphatidic acid (Pld1 product); macrophage/pseudohyphal-repressed; mRNA binds to <i>She3</i> , localized to yeast cell buds and hyphal tips; <i>Hap43</i> -induced; Spider biofilm induced
orf19.3171	<i>ACH1</i>	0,38	0,44	0,37	Acetyl-coA hydrolase; acetate utilization; nonessential; soluble protein in hyphae; antigenic in human; induced on polystyrene adherence; farnesol-, ketoconazole-induced; no human or murine homolog; stationary phase-enriched protein
orf19.320		-0,70	-0,44	-0,49	Predicted short chain dehydrogenase; Spider biofilm induced
orf19.3208	<i>DALS2</i>			3,35	Putative allantoinase; mutant is viable; similar but not orthologous to <i>S. cerevisiae Dal5</i>
orf19.3209	<i>FGR42</i>			-0,38	Protein lacking an ortholog in <i>S. cerevisiae</i> ; transposon mutation affects filamentous growth
orf19.3221	<i>CPA2</i>		0,51		Putative arginine-specific carbamoylphosphate synthetase; protein enriched in stationary phase yeast cultures; rat catheter biofilm induced; Spider biofilm induced
orf19.323			0,35		Putative haloacid dehalogenase; localized to plasma membrane
orf19.3256	<i>SLN1</i>		0,33		Histidine kinase involved in a two-component signaling pathway that regulates cell wall biosynthesis; mutants are sensitive to growth on H2O2 medium; rat catheter and Spider biofilm induced
orf19.33		-0,45	-0,29		Predicted ORF from Assembly 19; removed from Assembly 20; restored based on transcription data; similar to orf19.7550
orf19.334			0,74	0,42	Protein of unknown function; flow model biofilm induced; Spider biofilm induced; regulated by <i>Sef1</i> , <i>Sfu1</i> , and <i>Hap43</i>
orf19.335			0,40		<i>Sef1p</i> -, <i>Sfu1p</i> -, and <i>Hap43p</i> -regulated gene
orf19.3360			0,32		Protein of unknown function; flow model biofilm induced; Spider biofilm induced
orf19.3364			0,44		Protein of unknown function
orf19.3369	<i>MOH1</i>		0,40		Ortholog of <i>S. cerevisiae Moh1</i> , essential for stationary phase growth; induced by alpha pheromone in SpiderM medium and by <i>Mn11</i> under weak acid stress; possibly essential (UAU1 method); flow model biofilm induced; Spider biofilm induced
orf19.338		-0,30			Putative glycoside hydrolase; stationary phase enriched protein; <i>Hog1p</i> -downregulated; shows colony morphology-related gene regulation by <i>Ssn6p</i>
orf19.3391	<i>ADK1</i>	-0,44			Putative adenylate kinase; repressed in hyphae; macrophage-induced protein; adenylate kinase release used as marker for cell lysis; possibly essential (UAU1 method); flow model biofilm induced; rat catheter and Spider biofilm repressed
orf19.3392	<i>DOG1</i>	-0,60	-0,62	-0,43	Putative 2-deoxyglucose-6-phosphatase; haloacid dehalogenase hydrolase/phosphatase superfamily; similar to <i>S. cerevisiae Dog1</i> , <i>Dog2</i> , <i>Hor1</i> , <i>Rhr2</i> ; regulated by <i>Nrg1</i> , <i>Tup1</i> ; Spider biofilm repressed
orf19.3393		-0,33	-0,57	-0,37	Putative DEAD-box helicase; <i>Hap43</i> -induced; Spider biofilm induced
orf19.3396	<i>HCH1</i>	-0,44	-0,55		Ortholog of <i>S. cerevisiae Hch1</i> , a regulator of heat shock protein <i>Hsp90</i> ; regulated by <i>Gcn4</i> ; induced in response to amino acid starvation (3-aminotriazole treatment); mutants are viable
orf19.3399		-0,40	-0,47	-0,42	Protein of unknown function
orf19.34	<i>GIT1</i>	0,56			Glycerophosphoinositol permease; involved in utilization of glycerophosphoinositol as a phosphate source; <i>Rim101</i> -repressed; virulence-group-correlated expression
orf19.3400	<i>COQ3</i>	-0,51	-0,54	-0,40	Protein with a predicted role in coenzyme Q biosynthesis; transcriptionally induced by interaction with macrophages; possibly an essential gene, disruptants not obtained by UAU1 method
orf19.3401	<i>CTAI</i>	-0,41	-0,52	-0,42	Protein similar to <i>S. cerevisiae Mos10p</i> , which affects <i>S. cerevisiae</i> filamentous growth; activates transcription in 1-hybrid assay in <i>S. cerevisiae</i> ; protein levels increase under weak acid stress; nonessential
orf19.3402	<i>FPG1</i>	-0,39			Formamidopyrimidine DNA glycosylase, involved in repair of gamma-irradiated DNA; <i>Hap43p</i> -repressed gene

orf19.3405	<i>ZCF18</i>		-0.46	-0.40	Putative Zn(II)2Cys6 transcription factor; heterozygous null mutant displays sensitivity to virgineone and decreased colonization of mouse kidneys
orf19.3407	<i>RAD18</i>		-0.42	-0.37	Putative transcription factor with zinc finger DNA-binding motif; Hap43p-repressed gene
orf19.3409	<i>SEC12</i>	-0.41	-0.50	-0.43	Putative guanyl-nucleotide exchange factor; induced in high iron; Hap43-repressed
orf19.3411				-0.53	Protein of unknown function
orf19.3412	<i>ATG15</i>		-0.36	-0.38	Putative lipase; fungal-specific (no human or murine homolog); Hap43p-repressed gene
orf19.3414	<i>SUR7</i>	-0.39		-0.36	Protein required for normal cell wall, plasma membrane, cytoskeletal organization, endocytosis; localizes to eisosome subdomains of plasma membrane; four transmembrane motifs; mutant shows ectopic, chitin-rich cell wall; fluconazole-induced
orf19.3415.1	<i>RPL32</i>	-0.40	-0.54		Component of the large (60S) ribosomal subunit; Spider biofilm repressed
orf19.3417	<i>ACF2</i>	-0.55	-0.65	-0.55	Putative endo-1,3-beta-glucanase; fungal-specific (no human or murine homolog)
orf19.3423	<i>TIF3</i>	-0.28	-0.44		Putative translation initiation factor; genes encoding ribosomal subunits, translation factors, and tRNA synthetases are downregulated upon phagocytosis by murine macrophage
orf19.3426	<i>ANB1</i>	-0.40	-0.50	-0.37	Translation initiation factor eIF-5A; repressed in hyphae vs yeast cells; downregulated upon phagocytosis by murine macrophage; Hap43-induced; GlcNAc-induced protein; Spider biofilm repressed
orf19.3427				-0.41	Protein of unknown function
orf19.3428		-0.31			Protein of unknown function; flow model biofilm induced
orf19.3430		-0.37			Plasma membrane-associated protein; physically interacts with TAP-tagged Nop1p
orf19.3433	<i>OYE23</i>	-0.52		-0.65	Putative NADPH dehydrogenase; induced by nitric oxide, benomyl; oxidative stress-induced via Cap1; Hap43p-repressed; rat catheter biofilm induced
orf19.3438				-0.34	Protein of unknown function
orf19.3439			-0.37	-0.52	Protein of unknown function; Cyr1-repressed; rat catheter and Spider biofilm induced
orf19.344				0.35	Protein of unknown function; upregulated by fluphenazine treatment or in an azole-resistant strain that overexpresses CDR1 and CDR2; transcript possibly regulated by Tac1
orf19.3441	<i>FRP6</i>	-0.35			Putative ammonia transport protein; regulated by Nrg1 and Tup1; regulated by Ssn6; induced by human neutrophils
orf19.3442		-0.47	-0.48	-0.41	Putative oxidoreductase; Hap43-repressed gene
orf19.3443	<i>OYE2</i>	-0.60	-0.51	-0.56	Putative NADPH dehydrogenase; induced by nitric oxide; Spider biofilm induced
orf19.3445	<i>HOC1</i>	-0.44	-0.46	-0.43	Protein with similarity to mannosyltransferases; similar to <i>S. cerevisiae</i> Hoc1p and <i>C. albicans</i> Och1p
orf19.3446		-0.43	-0.39		Protein of unknown function
orf19.3447		-0.42	-0.37	-0.42	Protein of unknown function
orf19.3448		-0.46			Protein of unknown function; ketoconazole-repressed
orf19.3449		-0.34			Protein of unknown function
orf19.3450.1				-0.41	Protein of unknown function
orf19.3453			-0.36		Protein of unknown function
orf19.3455		-0.45		-0.35	Putative mitochondrial inner membrane magnesium transporter; possibly an essential gene, disruptants not obtained by UAU1 method
orf19.3456		-0.71	-0.63	-0.59	Protein with a predicted serine/threonine kinase and tyrosine kinase domain; possibly an essential gene, disruptants not obtained by UAU1 method
orf19.3457	<i>SWD3</i>	-0.50	-0.45	-0.40	Protein of unknown function
orf19.3458		-0.51	-0.60	-0.45	Protein of unknown function
orf19.3459		-0.52	-0.47	-0.47	Putative serine/threonine/tyrosine (dual-specificity) kinase; disruptants not obtained by UAU1 method
orf19.3460		-0.73		-0.52	Protein of unknown function; mRNA binds She3; transcript regulated upon yeast-hypha switch; induced in oralpharyngeal candidiasis
orf19.3462	<i>SAR1</i>	-0.46	-0.53	-0.40	Functional homolog of <i>S. cerevisiae</i> Sar1; which is required for ER-to-Golgi protein transport; binds GTP; similar to small GTPase superfamily proteins; gene has intron; Hap43-induced; rat catheter biofilm repressed
orf19.3463		-0.37	-0.51	-0.35	Putative GTPase; role in 60S ribosomal subunit biogenesis; Spider biofilm induced
orf19.3465	<i>RPL10A</i>	-0.34	-0.48		Predicted ribosomal protein; downregulated upon phagocytosis by murine macrophages; Hap43-induced; Spider biofilm repressed
orf19.3467	<i>SEC27</i>	-0.46	-0.41	-0.35	Protein of unknown function
orf19.3469		-0.43		-0.33	<i>S. cerevisiae</i> ortholog Stb1 has a role in regulation of MBF-specific transcription at Start; induced in a <i>cyr1</i> null mutant; Spider biofilm induced
orf19.3473		-0.36	-0.38	-0.40	Protein of unknown function
orf19.3474	<i>IPL1</i>			-0.41	Putative Aurora kinase; Hap43-induced; induced during planktonic growth; possibly an essential gene, disruptants not obtained by UAU1 method
orf19.3476	<i>HRR25</i>	-0.27			Predicted protein serine/threonine kinase; Spider biofilm induced
orf19.3477		-0.39	-0.44		Putative pseudouridine synthase; predicted role in snRNA pseudouridine synthesis, tRNA pseudouridine synthesis; Spider biofilm induced
orf19.3478	<i>NIP7</i>	-0.45	-0.58	-0.39	Putative nucleolar protein with role in ribosomal assembly; hyphal-induced; Hap43-induced; Spider biofilm induced
orf19.3480		-0.45			Protein of unknown function
orf19.3481		-0.30			Putative mitochondrial ATP-dependent RNA helicase of the DEAD-box family, transcription is activated in the presence of elevated CO ₂
orf19.3482		-0.49	-0.53	-0.52	Protein of unknown function
orf19.3483		-0.35			Putative phosphatidyl glycerol phospholipase C; Plc1-regulated; flow model biofilm induced; Spider biofilm induced
orf19.3496	<i>CHC1</i>	-0.43	-0.36	-0.37	Clathrin heavy chain; subunit of the major coat protein; role in intracellular protein transport and endocytosis; flow model and rat catheter biofilm repressed
orf19.3498				-0.35	Protein of unknown function
orf19.3501		-0.41		-0.40	<i>S. cerevisiae</i> ortholog Pxl1 localizes to sites of polarized growth and is required for selection and/or maintenance of polarized growth sites; Hog1p-repressed
orf19.3503		-0.51		-0.55	Protein of unknown function
orf19.3504	<i>RPL23A</i>		-0.42		Ribosomal protein; downregulated upon phagocytosis by murine macrophage; Hap43-induced; sumoylation target; Spider biofilm repressed
orf19.3506	<i>DBR1</i>			-0.35	Debranchase; homozygous mutant accumulates lariat intermediates of mRNA splicing; rat catheter biofilm repressed
orf19.3507	<i>MCR1</i>	-0.55	-0.47	-0.39	NADH-cytochrome-b5 reductase; soluble in hyphae; alkaline downregulated; farnesol, ketoconazole or flucytosine induced; protein present in exponential and stationary growth phase yeast; YNB biofilm induced; rat catheter biofilm repressed
orf19.3508		-0.60	-0.43	-0.46	Putative protein of unknown function; stationary phase enriched protein
orf19.3529	<i>ABP2</i>			0.33	Putative alpha-actinin-like protein; induced by alpha pheromone in SpiderM medium
orf19.3548.1	<i>WH11</i>	-0.38			White-phase yeast transcript; expression in opaques increases virulence/switching; mutant switches as WT; Hap43, hypoxia, ketoconazole induced; required for RPMI biofilm; Bcr1-induced in RPMI a/a biofilm; rat catheter, Spider biofilm induced
orf19.3563		0.44			Protein of unknown function
orf19.3575	<i>CDC19</i>		-0.27		Pyruvate kinase at yeast cell surface; Gcn4/Hog1/GlcNAc regulated; Hap43/polystyrene adherence induced; repressed by phagocytosis/farnesol; hyphal growth role; stationary phase enriched; flow model biofilm induced; Spider biofilm repressed
orf19.3603	<i>MFG1</i>		0.39		Regulator of filamentous growth; required for biofilm formation, virulence; interacts with Flo8 and Mss11
orf19.3618	<i>YWP1</i>		0.30		Secreted yeast wall protein; possible role in dispersal in host; mutation increases adhesion and biofilm formation; propeptide; growth phase, phosphate, Ssk1/Ssn6/Efg1/Efh1/Hap43 regulated; mRNA binds She3; flow and Spider biofilm repressed
orf19.3642	<i>SUN41</i>	-0.43	-0.48	-0.44	Cell wall glycosidase; role in biofilm formation and cell separation; possibly secreted; hypoxia, hyphal induced; caspofungin repressed; Efg1, Cph1 regulated; O-glycosylated, possible Kex2 substrate; 5'-UTR intron; Spider biofilm induced
orf19.3643				-0.42	Protein of unknown function; Hap43-repressed gene

Supporting Information

orf19.3644		-0,41	-0,38	-0,41	Protein of unknown function; Cyr1-repressed; rat catheter and Spider biofilm induced
orf19.3646	<i>CTR1</i>	-0,31	0,33		Copper transporter; transcribed in low copper; induced Mac1, Tye7, macrophage interaction, alkaline pH via Rim101; 17-beta-estradiol repressed; complements <i>S. cerevisiae</i> ctr1 ctr3 copper transport mutant; flow model/Spider biofilm induced
orf19.3647	<i>SEC8</i>	-0,46	-0,46	-0,37	Predicted subunit of the exocyst complex, involved in exocytosis; localizes to a crescent on the surface of the hyphal tip
orf19.3649		-0,64	-0,76	-0,54	Protein of unknown function
orf19.3651	<i>PGK1</i>	-0,81	-0,65	-0,49	Phosphoglycerate kinase; localizes to cell wall and cytoplasm; antigenic in murine/human infection; flow model biofilm, Hog1-, Hap43-, GCN-induced; repressed upon phagocytosis; repressed in Spider biofilms by Bcr1, Ndt80, Rob1, Brg1
orf19.3653	<i>FAT1</i>		-0,42		Predicted enzyme of sphingolipid biosynthesis; upregulated in biofilm
orf19.3656	<i>COX15</i>	-0,38			Cytochrome oxidase assembly protein; transcript regulated by Nrg1 and Tup1; alkaline repressed; Hap43-repressed; early-stage flow model biofilm induced; Spider biofilm repressed
orf19.3658				-0,38	Protein of unknown function
orf19.3659		-0,52	-0,42		Putative CTD phosphatase; role in dephosphorylation of RNA polymerase II C-terminal domain, transcription from RNA polymerase II promoter; flow model biofilm induced
orf19.3660		-0,45	-0,54	-0,39	Protein of unknown function
orf19.3664	<i>HSP31</i>	0,61	1,40	0,88	Putative 30 kda heat shock protein; repressed during the mating process; rat catheter biofilm induced
orf19.3668	<i>HGT2</i>	0,32			Putative MFS glucose transporter; 20 member <i>C. albicans</i> glucose transporter family; 12 probable membrane-spanning segments; expressed in rich medium with 2% glucose; rat catheter and Spider biofilm induced
orf19.3669	<i>SHA3</i>		0,46	0,33	Putative ser/thr kinase involved in glucose transport; Tn mutation affects filamentous growth; fluconazole-induced; ketoconazole-repressed; induced in by alpha pheromone in SpiderM; possibly essential; flow model biofilm induced
orf19.367	<i>CNH1</i>	0,32			Na ⁺ /H ⁺ antiporter; required for wild-type growth, cell morphology, and virulence in a mouse model of systemic infection; not transcriptionally regulated by NaCl; fungal-specific (no human or murine homolog)
orf19.3670	<i>GAL1</i>		0,33	0,34	Galactokinase; galactose, Mig1, Tup1, Hap43 regulated; fluconazole, ketoconazole-induced; stationary phase enriched protein; GlcNAc-induced protein; farnesol, hypoxia-repressed in biofilm; rat catheter and Spider biofilm induced
orf19.3672	<i>GAL10</i>			0,38	UDP-glucose 4-epimerase; galactose utilization; mutant has cell wall defects and increased filamentation; GlcNAc-, fluconazole- and ketoconazole-induced; stationary phase enriched protein; rat catheter and flow model biofilm induced
orf19.3675	<i>GAL7</i>		0,31	0,43	Putative galactose-1-phosphate uridylyl transferase; downregulated by hypoxia, upregulated by ketoconazole; macrophage/pseudohyphal-repressed
orf19.3682	<i>CWH8</i>	-0,32			Putative dolichyl pyrophosphate (Dol-P-P) phosphatase; ketoconazole-induced; expression is increased in a fluconazole-resistant isolate; clade-associated gene expression; Hap43p-induced gene
orf19.3707	<i>YHB1</i>	-0,63			Nitric oxide dioxygenase; acts in nitric oxide scavenging/detoxification; role in virulence in mouse; transcript activated by NO, macrophage interaction; Hap43, hypha repressed; mRNA binds She3
orf19.3733	<i>IDP2</i>		0,77	0,64	Isocitrate dehydrogenase; white-opaque switch regulated; morphology-regulation by Ssn6; protein in exponential and stationary phase yeast; Hap43-repressed; Spider biofilm repressed by Bcr1, Tec1, Ndt80, Rob1, Brg1; Spider biofilm induced
orf19.3740	<i>PGA23</i>	-0,66			Putative GPI-anchored protein of unknown function; Rim101-repressed; Cyr1-regulated; colony morphology-related gene regulation by Ssn6
orf19.3770	<i>ARG8</i>		0,42		Putative acetylornithine aminotransferase; Gcn2, Gcn4 regulated; rat catheter biofilm induced; Spider biofilm induced
orf19.3793			0,41		Protein of unknown function; mRNA binds She3; regulated by Nrg1; upregulated in a <i>cyr1</i> or <i>ras1</i> mutant
orf19.3803	<i>MNN2</i>		0,36		Alpha-1,2-mannosyltransferase; required for normal cell wall mannan; regulated by Tsa1, Tsa1B at 37 deg; repressed in core stress response; NO, Hog1 induced; confers sensitivity to cell wall perturbing agents; Spider biofilm repressed
orf19.3839	<i>SAP10</i>			-0,33	Secreted aspartyl protease; roles in adhesion, virulence (RHE model), cell surface integrity; distinct specificity from Sap9; at cell membrane and wall; GPI-anchored; induced in low iron; Tbf1-activated; Spider biofilm induced
orf19.3844	<i>MRP8</i>		-0,37		Mitochondrial ribosomal protein; ortholog of <i>S. cerevisiae</i> MRP8; transcript induced in hyphal form; mutant is viable; flow model and rat catheter biofilm repressed
orf19.385	<i>GCV2</i>	0,48	0,41	0,44	Glycine decarboxylase P subunit; protein of glycine catabolism; repressed by Efg1; Hog1-induced; induced by Rim101 at acid pH; transcript induced in elevated CO2; stationary phase enriched protein
orf19.3854			0,39		Ortholog of <i>S. cerevisiae</i> Sat4; amphotericin B induced; clade-associated gene expression; Spider biofilm induced
orf19.3869			0,32		Protein of unknown function; regulated by Tsa1, Tsa1B in minimal media at 37 degrees C; shows colony morphology-related gene regulation by Ssn6; Spider biofilm induced
orf19.3888	<i>PGI1</i>	-0,29			Glucose-6-phosphate isomerase; enzyme of glycolysis; antigenic; Efg1-regulated; induced upon adherence to polystyrene; repressed by phagocytosis, human neutrophils; flow model biofilm induced; rat catheter and Spider biofilm repressed
orf19.3895	<i>CHT2</i>	0,45	0,41		GPI-linked chitinase; required for normal filamentous growth; repressed in core caspofungin response; fluconazole, Cyr1, Efg1, pH-regulated; mRNA binds She3 and is localized to yeast-form buds and hyphal tips; Spider biofilm repressed
orf19.3932		-0,56		-0,37	Predicted RNA binding protein; stationary phase enriched; induced in core caspofungin response; induced by nitric oxide independent of Yhb1; repressed in <i>ssr1</i> null; ketoconazole, hypoxia induced; Spider biofilm induced
orf19.3932.1		-0,53		-0,51	Protein of unknown function
orf19.3988			1,54	0,99	Putative adhesin-like protein; induced by Mnl1 under weak acid stress; rat catheter and Spider biofilm induced
orf19.4056	<i>BRG1</i>		0,29		Transcription factor; recruits Hda1 to hypha-specific promoters; Tn mutation affects filamentation; Hap43-repressed; Spider and flow model biofilm induced; required for Spider biofilm formation; Bcr1-repressed in RPM1 a/a biofilms
orf19.4066			0,36		Putative glycerol-3-phosphate acyltransferase; Hog1-repressed
orf19.4082	<i>DDR48</i>	-0,71	-0,35		Immunogenic stress-associated protein; filamentation regulated; induced by benomyl/caspofungin/ketoconazole or in azole-resistant strain; Hog1, farnesol, alkaline repressed; stationary phase enriched; Spider, flow model biofilm induced
orf19.4110			0,37		Protein of unknown function
orf19.4192	<i>CDC14</i>		-0,40	-0,39	Protein involved in exit from mitosis and morphogenesis; ortholog of <i>S. cerevisiae</i> Cdc14p, which is a dual-specificity phosphatase and cell-cycle regulator; suppresses <i>S. cerevisiae</i> cdc15-lyt1, dbf2-2, and (partially) <i>tem1</i> mutant phenotypes
orf19.4192.1		-0,47	-0,60	-0,37	Protein of unknown function
orf19.4193		-0,47	-0,47		Protein of unknown function
orf19.4194		-0,50	-0,38	-0,36	Putative TFIIF complex subunit; possibly an essential gene, disruptants not obtained by UAU1 method
orf19.4195.1	<i>FCA1</i>	-0,49	-0,61		Cytosine deaminase; enzyme of pyrimidine salvage; functional homolog of <i>S. cerevisiae</i> Fcy1p; mutation is associated with resistance to flucytosine (5-FC) in a clinical isolate; hyphal downregulated; gene has intron
orf19.4201	<i>NHX1</i>		-0,35		Protein similar to <i>S. cerevisiae</i> Nhx1p, which is a Na ⁺ /H ⁺ exchanger required for intracellular sequestration of Na ⁺
orf19.4203		-0,48	-0,37		Protein of unknown function
orf19.4204		-0,38	-0,32		Protein of unknown function
orf19.4206		-0,44	-0,47	-0,37	Protein of unknown function
orf19.4207				-0,38	Predicted ORF from Assembly 19; removed from Assembly 20; restored based on comparative genome analysis
orf19.4208	<i>RAD52</i>	-0,44	-0,50	-0,52	Required for homologous DNA recombination, repair of UV- or MMS-damaged DNA, telomere length, UV-induced LOH; constitutive expression, MMS-induced; weakly complements <i>S. cerevisiae</i> rad52 mutant; slow growth, increased white-to-opaque switch

orf19.4209		-0,52	-0,58	-0,48	Protein of unknown function
orf19.4211			-0,44		Multicopper oxidase; for growth in low iron, prostaglandin E2 synthesis; ketoconazole/caspofungin/amphotericin B repressed; Sef1/Sfu1/Hap43 regulated; reports differ if functional homolog of ScFet3; rat catheter and Spider biofilm induced
orf19.4213				-0,34	Putative iron transport multicopper oxidase precursor; flucytosine induced; caspofungin repressed
orf19.4215	FET34	-0,34	-0,58	-0,33	Multicopper ferroxidase; induced by low iron, ciclopirox olamine, ketoconazole, hypoxia; alkaline induced by Rim101; repressed in fluconazole-resistant isolate; Sfu1, Hog1 repressed; complements <i>S. cerevisiae</i> fet3; Spider biofilm induced
orf19.4246		-0,58	-0,34		Protein with similarity to <i>S. cerevisiae</i> Ykr070w; Tn mutation affects filamentation; Hog1-repressed; colony morphology-related gene regulation by Ssn6p; induced during cell wall regeneration; possibly essential
orf19.4255	ECM331	-0,50	-0,74	-0,47	GPI-anchored protein; mainly at plasma membrane, also at cell wall; Hap43, caspofungin-induced; Plc1-regulated; Hog1, Rim101-repressed; colony morphology-related regulated by Ssn6; induced by ketoconazole and hypoxia
orf19.4274	PUT1		0,41		Putative proline oxidase; alkaline upregulated by Rim101; flow model biofilm induced; Spider biofilm induced
orf19.4309	GRP2	-0,29			Methylglyoxal reductase; regulation associated with azole resistance; induced in core stress response or by oxidative stress via Cap1, flufenazine, benomyl, by Hap43 or with long term fluconazole treatment; Spider biofilm induced
orf19.4317	GRE3	-0,33			Putative D-xylose reductase; antigenic in murine systemic infection; soluble protein in hyphae; induced by farnesol, macrophage interaction and by Mnl1 under weak acid stress; stationary-phase enriched protein; Spider biofilm induced
orf19.4369			0,36		Ortholog of <i>S. cerevisiae</i> Spp41; protein involved in negative regulation of expression of spliceosome components PRP4 and PRP3 in <i>S. cerevisiae</i> ; mutants are viable
orf19.4384	HXT5	-0,49			Putative sugar transporter; induced by ciclopirox olamine; Snf3-induced; alkaline repressed; colony morphology-related gene regulation by Ssn6; possibly essential gene
orf19.4393	CIT1		0,61	0,39	Citrate synthase; induced by phagocytosis; induced in high iron; Hog1-repressed; Efg1-regulated under yeast, not hyphal growth conditions; present in exponential and stationary phase; Spider biofilm repressed; rat catheter biofilm induced
orf19.4432	KSP1		0,40		Putative serine/threonine protein kinase; mRNA binds She3 and is localized to hyphal tips; mutation confers hypersensitivity to amphotericin B
orf19.4436	GPX3	-0,54			Putative glutathione peroxidase involved in Cap1p-dependent oxidative stress response, required for Cap1p oxidation in response to H2O2; planktonic growth-induced
orf19.4438	RME1		0,71		Zinc finger protein; controls meiosis in <i>S. cerevisiae</i> ; white-specific transcript; upregulation correlates with clinical development of fluconazole resistance; Upc2-regulated in hypoxia; flow model biofilm induced; Spider biofilm repressed
orf19.4443	YPD1		-0,48		Phosphohistidine intermediate protein in a phosphorelay signal transduction pathway; residue His69 is the phosphoacceptor histidine; predicted to be soluble and cytosolic; functional homolog of <i>S. cerevisiae</i> Ypd1p
orf19.4445			0,42	0,35	Protein of unknown function; Plc1p-regulated; expression induced early upon infection of reconstituted human epithelium (RHE), while expression of the <i>C. dubliniensis</i> ortholog is not; mutant is viable; Spider biofilm induced
orf19.4450.1			0,59		Protein conserved among the CTG-clade; 2 adjacent upstream SRE-1 elements; highly up-regulated in cecum-grown cells in a Cph2-dependent manner; Hap43-repressed; rat catheter, Spider and flow model biofilm induced
orf19.4456	GAP4		0,27		Putative amino acid permease; hyphal induced; regulated by Hap43, Gcn2 and Gcn4; colony morphology-related gene regulation by Ssnp; detected at plasma membrane of yeast and germ tube by mass spec; Spider biofilm induced
orf19.4457	BNI4		0,33		Protein required for wild-type cell wall chitin distribution, morphology, hyphal growth; not essential; similar to <i>S. cerevisiae</i> Bni4p (targeting subunit for Glc7p phosphatase, involved in bud-neck localization of chitin synthase III)
orf19.4475	KTR4	-0,43			Mannosyltransferase; induced during cell wall regeneration; fungal-specific (no human or murine homolog); Bcr1-repressed in RPM1 a/a biofilms
orf19.4476		-0,50		-0,51	Protein with a NADP-dependent oxidoreductase domain; transcript induced by ketoconazole; rat catheter and Spider biofilm induced
orf19.4477	CSH1	-0,75	-0,46	-0,62	Aldo-keto reductase; role in fibronectin adhesion, cell surface hydrophobicity; regulated by temperature, growth phase, benomyl, macrophage interaction; azole resistance associated; Spider biofilm induced; rat catheter biofilm repressed
orf19.4526	HSP30		1,79	1,06	Putative heat shock protein; fluconazole repressed; amphotericin B induced; Spider biofilm induced; rat catheter biofilm induced
orf19.4527	HGT1	0,33	0,35		High-affinity MFS glucose transporter; induced by progesterone, chloramphenicol, benomyl; likely essential for growth; protein newly produced during adaptation to the serum; rat catheter and Spider biofilm induced
orf19.4530.1		-0,34			Protein of unknown function; regulated by Nrg1, Tup1; Spider and flow model biofilm induced
orf19.4555	ALS4	-0,69	-0,64		GPI-anchored adhesin; role in adhesion, germ tube induction; growth, temperature regulated; expressed during infection of human buccal epithelial cells; repressed by vaginal contact; biofilm induced; repressed during chlamyospore formation
orf19.4557		-0,39			Protein of unknown function
orf19.4565	BGL2		-0,31		Cell wall 1,3-beta-glucosyltransferase; mutant has cell-wall and growth defects, but wild-type 1,3- or 1,6-beta-glucan content; antigenic; virulence role in mouse systemic infection; rat catheter biofilm induced
orf19.4583		0,50			Protein with a mitochondrial carrier protein domain; possibly an essential gene, disruptants not obtained by UAU1 method; Spider biofilm repressed
orf19.4593	RGA2		0,36		Putative GTPase-activating protein (GAP) for Rho-type GTPase Cdc42; involved in cell signaling pathways controlling cell polarity; induced by low-level peroxide stress; flow model biofilm induced
orf19.4599	PHO89	0,80	0,69	0,40	Putative phosphate permease; transcript regulated upon white-opaque switch; alkaline induced by Rim101; possibly adherence-induced; F-12/CO2 model, rat catheter and Spider biofilm induced
orf19.4609				0,49	Putative diene lactone hydrolase; protein abundance is affected by URA3 expression in the CAI-4 strain background; protein present in exponential and stationary growth phase yeast cultures; rat catheter biofilm repressed
orf19.4630	CPA1		0,36		Putative carbamoyl-phosphate synthase subunit; alkaline repressed; rat catheter, Spider and flow model biofilm induced
orf19.4645	BEM1		0,38		Protein required for wild-type budding, hyphal growth, and virulence in a mouse systemic infection; suppresses pseudohyphal and filamentous growth defects of various <i>S. cerevisiae</i> mutants and heat sensitivity of <i>S. cerevisiae</i> cdc24-4 mutant
orf19.4655	OPT6	-0,47			Putative oligopeptide transporter; fungal-specific (no human or murine homolog); expression of OPT6, OPT7, or OPT8 does not suppress defect of mutant lacking Opt1p, Opt2p, and Opt3p; alleles are nonidentical
orf19.4664	NAT4			-0,37	Putative histone acetyltransferase; involved in regulation of white-opaque switch; early-stage flow model biofilm induced; Spider biofilm induced
orf19.4666		-0,38	-0,47	-0,45	Protein of unknown function; hyphal-induced expression, regulated by Cyr1, Ras1, Efg1; Spider biofilm induced
orf19.467	WOR3	0,59	0,96	1,00	Transcription factor; modulator of white-opaque switch; induced in opaque cells; promoter bound by Wor1; overexpression at 25 degr shifts cells to opaque state; deletion stabilizes opaque cells at higher temperatures; Spider biofilm induced
orf19.4674.1	CRD2	-0,50			Metallothionein; for adaptation to growth in high copper; basal transcription is cadmium-repressed; Ssn6 regulated; complements copper sensitivity of an <i>S. cerevisiae</i> cup1 mutant; regulated by Sef1, Sfu1, and Hap43; Spider biofilm induced
orf19.4679	AGP2	-0,53			Amino acid permease; hyphal repressed; white-opaque switch regulated; induced in core caspofungin response, during cell wall regeneration, by flucytosine; regulated by Sef1, Sfu1, and Hap43; rat catheter and Spider biofilm induced
orf19.4682	HGT17			-0,39	Putative MFS family glucose transporter; 20 members in <i>C. albicans</i> ; 12 probable membrane-spanning segments; induced at low (0.2%, compared to 2%) glucose in rich media; Spider biofilm induced

Supporting Information

orf19.4688	<i>DAG7</i>	-0,51	-0,43		Secretory protein; a-specific, alpha-factor induced; mutation confers hypersensitivity to toxic ergosterol analog; fluconazole-induced; induced during chlamyospore formation in <i>C. albicans</i> and <i>C. dubliniensis</i>
orf19.4698	<i>PTC8</i>		0,39		Predicted type 2C protein phosphatase, ser/thr-specific; required for hyphal growth; transcript induced by stress; flow model biofilm induced; Spider biofilm induced
orf19.4716	<i>GDH3</i>		0,32		NADP-glutamate dehydrogenase; Nrg1, Plc1 regulated; hypha, hypoxia, Efg1-repressed; Rim101-induced at pH 8; GlcNAc, ciclopirox, ketoconazole induced; exp and stationary phase protein; Spider biofilm repressed; rat catheter biofilm induced
orf19.4752	<i>MSN4</i>		0,41		Zinc finger transcription factor; similar to <i>S. cerevisiae</i> Msn4, but not a significant stress response regulator in <i>C. albicans</i> ; partly complements STRE-activation defect of <i>S. cerevisiae</i> msn2 msn4 double mutant; flow model biofilm induced
orf19.4773	<i>AOX2</i>	0,53	0,97		Alternative oxidase; cyanide-resistant respiration; induced by antimycin A, oxidants; growth; Hap43, chlamyospore formation repressed; rat catheter, Spider biofilm induced; regulated in Spider biofilms by Bcr1, Tec1, Ndt80, Brg1
orf19.4775	<i>CTA8</i>		0,36		Essential transcription factor, mediates heat shock transcriptional induction; in the absence of heat stress, Cta8p levels are modulated by growth temperature to regulate basal expression of genes involved in protein folding
orf19.4777	<i>DAK2</i>	-0,58			Putative dihydroxyacetone kinase; repressed by yeast-hypha switch; fluconazole-induced; caspofungin repressed; protein enriched in stationary phase yeast cultures; flow model biofilm induced; rat catheter and Spider biofilm repressed
orf19.4779				0,47	Putative transporter; slightly similar to the Sit1p siderophore transporter; Gcn4p-regulated; fungal-specific; induced by Mn1p under weak acid stress
orf19.4784	<i>CRP1</i>		0,63	0,36	Copper transporter; CPx P1-type ATPase; mediates Cu resistance; similar to Menkes and Wilson disease proteins; copper-induced; Tbf1-activated; suppresses Cu sensitivity of <i>S. cerevisiae</i> cup1 mutant; flow model biofilm induced
orf19.4788	<i>ARG5,6</i>		0,44		Arginine biosynthetic enzyme; processed in <i>S. cerevisiae</i> into 2 polypeptides with acetylglutamate kinase (Arg6) activity and acetylglutamate-phosphate reductase (Arg5) activity; Gcn4 regulated; alkaline repressed; Spider biofilm induced
orf19.48	<i>RPM2</i>		0,44		Mitochondrial RNase P subunit; roles in nuclear transcription, cytoplasmic and mitochondrial RNA processing, mitochondrial translation; virulence-group-correlated expression; likely essential (JAU1 method); rat catheter biofilm induced
orf19.4818				0,42	Protein of unknown function; Spider biofilm induced
orf19.4864		-0,37			Protein of unknown function
orf19.4898		-0,46	-0,32		Putative protein of unknown function; induced by prostaglandins
orf19.4899	<i>GCA1</i>	-0,47			Extracellular/plasma membrane-associated glucoamylase; expressed in rat oral infection; regulated by carbohydrates, pH, galactose; promotes biofilm matrix formation; flow model biofilm induced; Bcr1 repressed in RPM1 a/a biofilms
orf19.4906			0,39		Putative adhesin-like protein; positively regulated by Tbf1; Spider biofilm induced
orf19.4907			0,77		Putative protein of unknown function; Hap43p-repressed gene; increased transcription is observed upon fluphenazine treatment; possibly transcriptionally regulated by Tac1p; induced by nitric oxide; fungal-specific (no human/murine homolog)
orf19.4909	<i>CBK1</i>		0,31		Ser/Thr kinase of cell wall integrity pathway; mutants show abnormal morphology and aggregation; Mob2p associated; required for wild-type hyphal growth and transcriptional regulation of cell-wall-associated genes
orf19.4914.1	<i>BLP1</i>	-0,52			Protein of unknown function, serum-induced
orf19.4929			0,34		Protein of unknown function
orf19.4932			0,34		Protein of unknown function
orf19.4940				0,34	Putative histidine permease; fungal-specific (no human or murine homolog); Hap43p-induced gene
orf19.4941	<i>TYE7</i>			0,34	bHLH transcription factor; control of glycolysis; required for biofilm formation; hyphally regulated by Cph1, Cyr1; flucytosine, Hog1 induced; amphotericin B, caspofungin repressed; induced in flow model biofilm and planktonic cultures
orf19.4943	<i>PSA2</i>	-0,68		-0,36	Mannose-1-phosphate guanyltransferase; Hap43, macrophage-repressed; stationary phase enriched protein; Spider biofilm induced; rat catheter biofilm repressed
orf19.4949			-0,31		Protein of unknown function
orf19.4980	<i>HSP70</i>	-0,37			Putative hsp70 chaperone; role in entry into host cells; heat-shock, amphotericin B, cadmium, ketoconazole-induced; surface localized in yeast and hyphae; antigenic in host; farnesol-downregulated in biofilm; Spider biofilm induced
orf19.5005	<i>OSM2</i>		0,38		Putative mitochondrial fumarate reductase; regulated by Ssn6p, Gcn2p, and Gcn4p; Hog1p-downregulated; stationary phase enriched protein; Hap43p-repressed gene
orf19.5025	<i>MET3</i>		-0,43		ATP sulfurylase; sulfate assimilation; repressed by Met, Cys, Sfu1, or in fluconazole-resistant isolate; Hog1, caspofungin, white phase-induced; induced on biofilm formation, even in presence of Met and Cys; Spider, F-12/CO2 biofilm induced
orf19.5031	<i>SSK1</i>	-0,32			Response regulator of two-component system; role in oxidative stress response, cell wall biosynthesis, virulence, hyphal growth on solid media; expressed in hyphae and yeast; peroxisomal targeting sequence (PTS1); Spider biofilm induced
orf19.5032	<i>SIM1</i>		-0,34		Adhesin-like protein; involved in cell wall maintenance, redundant with Sun41; possibly secreted; macrophage-repressed; repressed by Rim101, Cyr1, Ras1; Spider biofilm induced
orf19.5045	<i>PTP2</i>	-0,39			Predicted protein tyrosine phosphatase; involved in regulation of MAP kinase Hog1 activity; induced by Mn1 under weak acid stress; rat catheter and Spider biofilm induced
orf19.5054		-0,33			Putative quinolinate phosphoribosyl transferase, involved in NAD biosynthesis; Hap43p-repressed gene
orf19.5079	<i>CDR4</i>		0,57		Putative ABC transporter superfamily; fluconazole, Sfu1, Hog1, core stress response induced; caspofungin repressed; fluconazole resistance not affected by mutation or correlated with expression; rat catheter and flow model biofilm induced
orf19.5125				-0,35	Protein of unknown function; induced by ketoconazole; Spider, F-12/CO2 and flow model biofilm induced
orf19.5158		-0,50			Protein with similarity to a human gene associated with colon cancer and to orf19.5158; regulated by Gcn4, Cyr1; induced by amino acid starvation; macrophage-induced protein, macrophage-repressed; Spider biofilm induced
orf19.5163	<i>SFI1</i>		0,35		Putative centrin-binding protein; predicted role in spindle pole body duplication; induced by alpha pheromone in SpiderM medium; essential for growth
orf19.5227		-0,43			Chaperone component; involved in assembly of alpha subunits into the 20S proteasome; flow model biofilm induced
orf19.5285	<i>PST3</i>			0,34	Putative flavodoxin; YNB biofilm induced; stationary phase enriched protein; rat catheter and Spider biofilm repressed
orf19.5293		0,35			Protein of unknown function
orf19.5305	<i>RHD3</i>	0,53	0,38		GPI-anchored yeast-associated cell wall protein; induced in high iron; clade-associated gene expression; not essential for cell wall integrity; fluconazole-repressed; flow model and Spider biofilm repressed
orf19.5337	<i>UBC15</i>	0,44			Putative E2 ubiquitin-conjugating enzyme
orf19.5342.2				-0,36	Protein of unknown function; protein newly produced during adaptation to the serum
orf19.5383	<i>PMA1</i>	0,47	0,43	0,40	Plasma membrane H(+)-ATPase; highly expressed, comprises 20-40% of total plasma membrane protein; levels increase at stationary phase transition; fluconazole induced; caspofungin repressed; upregulated in RHE model; Spider biofilm repressed
orf19.54	<i>RHD1</i>	-0,35	-0,36	-0,44	Putative beta-mannosyltransferase required for the addition of beta-mannose to the acid-labile fraction of cell wall phosphopeptidomannan; 9-gene family member; regulated on yeast-hypha and white-opaque switches; Spider biofilm repressed
orf19.5417	<i>DOT5</i>	-0,33	-0,31		Putative nuclear thiol peroxidase; alkaline downregulated; sumoylation target; Spider and flow model biofilm induced
orf19.542	<i>HXK2</i>	-0,32			Hexokinase II; antigenic in humans; repressed by human neutrophils; Efg1-regulated; fluconazole-induced; gene regulation by Ssn6; present in exponential and stationary growth phase; flow model biofilm induced; Spider biofilm repressed

orf19.5431		-0,48			Protein of unknown function; Hap43-repressed; Spider biofilm induced
orf19.5455		0,43			Protein of unknown function
orf19.5510			-0,33		Protein of unknown function
orf19.5514				-0,46	Ortholog of <i>S. pombe</i> SPC550.08, an N-acetyltransferase; transcript induced during growth in the mouse cecum
orf19.5515		-0,37			Protein of unknown function
orf19.5516		-0,47	-0,43		Protein of unknown function
orf19.5517			-0,60	-0,37	Similar to alcohol dehydrogenases; induced by benomyl treatment, nitric oxide; induced in core stress response; oxidative stress-induced via Cap1; Spider biofilm repressed
orf19.5518		-0,51	-0,50	-0,33	Protein of unknown function; Spider biofilm induced
orf19.5519	<i>GCV1</i>	-0,53	-0,44		Putative T subunit of glycine decarboxylase; transcript negatively regulated by Sfu1; Spider biofilm repressed
orf19.5521	<i>ISA1</i>	-0,52			Putative mitochondrial iron-sulfur protein; alkaline repressed; induced in high iron; regulated by Sef1, Sfu1, Hap43; Spider biofilm induced
orf19.5522		-0,57	-0,51		Protein of unknown function
orf19.5525		-0,82	-0,62	-0,48	Putative oxidoreductase; protein levels affected by URA3 expression in CAI-4 strain background; Efg1, Efh1 regulated; Rgt1-repressed; protein present in exponential and stationary growth phase yeast; rat catheter biofilm repressed
orf19.5526	<i>SEC20</i>	-0,66	-0,57	-0,49	Essential protein; similar to <i>S. cerevisiae</i> Sec20p; depletion causes membrane accumulation and drug sensitivity; expression regulated by growth phase; O-mannosylation regulates proteolysis; does not complement <i>S. cerevisiae</i> sec20-1 mutant
orf19.5530	<i>NAB3</i>		-0,36	-0,34	Putative nuclear polyadenylated RNA-binding protein; flucytosine repressed
orf19.5531	<i>CDC37</i>	-0,51	-0,48	-0,42	Chaperone for Crk1p; interacts with Crk1p kinase domain and with Sti1p; putative phosphorylation site at Ser14; functional homolog of <i>S. cerevisiae</i> Cdc37p; likely to be essential for growth; regulated by Gcn2p and Gcn4p
orf19.5533		-0,35			Protein of unknown function
orf19.5534			-0,37	-0,40	Protein with a predicted role in mitotic spindle elongation, vesicle-mediated transport; flow model biofilm induced
orf19.5535			-0,38		Predicted membrane transporter, member of the anion:cation symporter (ACS) family, major facilitator superfamily (MFS)
orf19.5539		-0,61	-0,49	-0,41	Protein of unknown function
orf19.5541			-0,31		Protein with similarity to <i>S. pombe</i> Nrd1p; transcription induced upon induction of hyphal growth; regulated by Cph1p, Efg1p, Cph2p; low-level expression; alkaline upregulated; fungal-specific (no human or murine homolog)
orf19.5544	<i>SAC6</i>	-0,57	-0,52	-0,51	Fimbrin; actin filament bundling protein; transcript regulated by Nrg1 and Mig1; protein level decreases in stationary phase
orf19.5547		-0,40	-0,39		Protein of unknown function; Hap43-repressed gene
orf19.5548	<i>LYS14</i>			-0,34	Zn(II)2Cys6 transcription factor; has similarity to <i>S. cerevisiae</i> Lys14, which is a transcription factor involved in the regulation of lysine biosynthesis genes
orf19.5550	<i>MRT4</i>	-0,40	-0,64	-0,35	Putative mRNA turnover protein; Hap43-induced; mutation confers hypersensitivity to tubercidin (7-deazaadenosine); rat catheter biofilm induced
orf19.5551	<i>MIF2</i>	-0,44	-0,40	-0,39	Centromere-associated protein; similar to CENP-C proteins; Cse4p and Mif2p colocalize at <i>C. albicans</i> centromeres
orf19.5552		-0,50	-0,46	-0,43	Putative transcriptional regulator of ribonucleotide reductase genes; Spider biofilm induced
orf19.5553		-0,62	-0,58	-0,47	Protein of unknown function
orf19.5555		-0,41	-0,32		Protein of unknown function
orf19.5558	<i>RBF1</i>		0,37		Transcription factor; glutamine-rich activation domain; binds RPG-box DNA sequences; predominantly nuclear; mutation causes accelerated induction of filamentous growth; antigenic during human oral infection; Sko1p-repressed
orf19.5559	<i>RAV2</i>	-0,48	-0,47	-0,35	Protein similar to <i>S. cerevisiae</i> Rav2; a regulator of (H ⁺)-ATPase in vacuolar membrane; transposon mutation affects filamentous growth
orf19.5561	<i>STE23</i>		-0,45	-0,39	Ortholog of <i>S. cerevisiae</i> Ste23 metalloprotease; role in N-terminal processing of pro-a-factor to the mature form; Tn mutation affects filamentous growth; Spider biofilm induced
orf19.5563	<i>RNH1</i>	-0,39	-0,63	-0,40	Ribonuclease H (RNase H); hyphal-induced; flucytosine induced; similar to orf19.5564 (see Locus History); possibly essential (UAU1 method); rat catheter biofilm induced; flow model biofilm repressed
orf19.5564		-0,44	-0,53		Protein of unknown function
orf19.5566		-0,40	-0,46		Protein of unknown function
orf19.5567	<i>POP4</i>	-0,37	-0,43		Ortholog of <i>S. cerevisiae</i> Pop4; a subunit of both RNase MRP and nuclear RNase P; filament induced; regulated by Nrg1, Tup1; likely essential, based on UAU1 strategy; rat catheter and Spider biofilm induced
orf19.5568	<i>VPS51</i>			-0,35	Protein with a role in vacuolar function; null mutant has defect in damaging oral epithelial and vascular endothelial cells; required for normal hyphal growth and stress resistance; induced in presence of host oral or vascular cells
orf19.5569		-0,39	-0,35	-0,37	Protein of unknown function
orf19.5574		-0,55	-0,52	-0,46	Protein of unknown function
orf19.5578				-0,33	Protein of unknown function
orf19.5579				-0,37	Protein with a predicted double-strand break repair domain; Hap43-repressed gene
orf19.5580	<i>TEL1</i>	-0,45	-0,34	-0,37	Protein of unknown function
orf19.5584	<i>PEP3</i>	-0,50	-0,47	-0,40	Peptidase; activity useful for strain identification by multilocus enzyme electrophoresis (MLEE); clade-associated gene expression
orf19.5585	<i>SAP5</i>			-0,42	Secreted aspartyl proteinase; sap4,5,6 triple null defective in utilization of protein as N source; virulence role effected by URA3; expressed during infection; mRNA localized to hyphal tip via She3; rat catheter and Spider biofilm induced
orf19.5586			-0,42	-0,46	Protein of unknown function
orf19.5587		-0,58		-0,53	Protein of unknown function; transcript is upregulated in clinical isolates from HIV+ patients with oral candidiasis
orf19.5595	<i>SHE3</i>	-0,56	-0,59	-0,57	mRNA-binding protein that localizes specific mRNAs to daughter yeast cells and to hyphal tips; required for normal filamentation and host epithelial cell damage; ortholog of <i>S. cerevisiae</i> She3 but target mRNAs differs
orf19.5596		-0,42			Protein of unknown function
orf19.5597	<i>POL5</i>	-0,41	-0,41		Putative DNA Polymerase phi; F-12/CO2 early biofilm induced
orf19.5597.1				-0,34	Protein of unknown function
orf19.5599	<i>MDL2</i>	-0,38	-0,33	-0,34	Putative mitochondrial, half-size MDR-subfamily ABC transporter
orf19.5601				-0,39	Protein of unknown function
orf19.5604	<i>MDR1</i>			-0,55	Plasma membrane MDR/MFS multidrug efflux pump; methotrexate is preferred substrate; overexpression in drug-resistant clinical isolates confers fluconazole resistance; repressed in young biofilms; rat catheter biofilm induced
orf19.5607		-0,48	-0,43		Protein of unknown function
orf19.5608		-0,40	-0,46		RNA polymerase III subunit; Spider biofilm induced
orf19.5612	<i>BMT4</i>	-0,45	-0,70	-0,63	Beta-mannosyltransferase; for elongation of beta-mannose chains on the acid-labile fraction of cell wall phosphopeptidomannan; 9-gene family member; regulated by Tsa1, Tsa1B; flow model biofilm induced; rat catheter biofilm repressed
orf19.5614		-0,91	-0,83	-0,73	Putative ribonuclease H1; possibly an essential gene, disruptants not obtained by UAU1 method; flow model biofilm induced; Spider biofilm induced
orf19.5615	<i>AYR2</i>	-0,40	-0,33		Putative NADPH-dependent 1-acyl dihydroxyacetone phosphate reductase; shows colony morphology-related gene regulation by Ssn6p
orf19.5617		-0,33			Protein of unknown function
orf19.5618		-0,63	-0,44	-0,47	Protein of unknown function
orf19.5619		-0,54	-0,42	-0,46	Protein of unknown function; induced by alpha pheromone in SpiderM medium; Spider biofilm induced

Supporting Information

orf19.5620		-0.82	-0.67	-0.53	Stationary phase enriched protein; Gcn4-regulated; induced by amino acid starvation (3-AT), benomyl or in azole-resistant strain that overexpresses MDR1; flow model biofilm induced; rat catheter biofilm repressed; overlaps orf19.5621
orf19.5621		-0.56	-0.40	-0.42	Putative protein of unknown function; mutation confers hypersensitivity to amphotericin B; overlaps orf19.5621
orf19.5622	<i>GLC3</i>	-0.94	-0.94	-0.82	Putative 1,4-glucan branching enzyme; fluconazole-induced; colony morphology-related gene regulation by Ssn6; stationary phase enriched protein
orf19.5623	<i>ARP4</i>	-0.54	-0.51	-0.42	Subunit of the NuA4 histone acetyltransferase complex
orf19.5626		-0.70	-0.45	-0.48	Protein of unknown function; Plc1-regulated; induced by Mnl1 under weak acid stress; flow model biofilm induced
orf19.5627		-0.53	-0.52	-0.44	<i>S. cerevisiae</i> ortholog Hek2/Khd1 is a putative RNA binding protein involved in the asymmetric localization of ASH1 mRNA; Hap43-induced gene
orf19.5629	<i>QCR7</i>	-0.48	-0.45		Putative ubiquinol-cytochrome-c reductase, subunit 7; Hap43p-repressed gene
orf19.5630	<i>APA2</i>	-0.46	-0.39		Putative ATP adenyltransferase II; regulated by Gcn4; repressed by amino acid starvation (3-AT); induced by prostaglandins; Hap43-repressed; Spider biofilm repressed
orf19.5634	<i>FRP1</i>	0.49			Ferric reductase; alkaline-induced by Rim101; iron-chelation-induced by CCAAT-binding factor; fluconazole-repressed; ciclopirox-, hypoxia-, Hap43-induced; colony morphology-related regulation by Ssn6; Spider and flow model biofilm induced
orf19.5635	<i>PGA7</i>	0.37			GPI-linked hyphal surface antigen; induced by ciclopirox olamine, ketoconazole, Rim101 at pH 8; Hap43, fluconazole; flow model biofilm induced; Spider biofilm induced; required for RPMI biofilm in a/a biofilm
orf19.5636	<i>RBT5</i>	0.35			GPI-linked cell wall protein; hemoglobin utilization; Rfg1, Rim101, Tbf1, Fe regulated; Sfu1, Hog1, Tup1, serum, alkaline pH, antifungal drugs, geldamycin repressed; Hap43 induced; required for RPMI biofilms; Spider biofilm induced
orf19.5686		-0.54			Protein of unknown function; Spider biofilm induced
orf19.5701		-0.48			Protein of unknown function
orf19.5702		-0.41			Protein of unknown function
orf19.5704		-0.31			Protein of unknown function
orf19.5705	<i>NAM2</i>	-0.36			Mitochondrial leucyl-tRNA synthetase
orf19.5711			-0.38		Putative phosphatidylinositol transfer protein; possibly an essential gene, disruptants not obtained by UAU1 method
orf19.5713	<i>YMX6</i>			1.11	Putative NADH dehydrogenase; macrophage-downregulated gene; induced by nitric oxide; rat catheter biofilm induced
orf19.5718		-0.55	-0.56	-0.58	Protein of unknown function
orf19.5720				-0.34	Predicted membrane transporter, member of the monocarboxylate porter (MCP) family, major facilitator superfamily (MFS); ketoconazole or caspofungin repressed; Spider biofilm induced
orf19.5723	<i>POX1</i>		-0.43	-0.35	Predicted acyl-CoA oxidase; regulated upon white-opaque switch; upregulated upon phagocytosis; Spider biofilm induced
orf19.5727		-0.49			Protein of unknown function
orf19.5728				0.62	Putative cytochrome P450; Spider biofilm induced
orf19.5729	<i>FGR17</i>	-0.72	-0.58	-0.57	Putative DNA-binding transcription factor; has zinc cluster DNA-binding motif; lacks an ortholog in <i>S. cerevisiae</i> ; transposon mutation affects filamentous growth; Hap43p-repressed gene
orf19.5731	<i>PAD1</i>		-0.47	-0.36	Putative phenylacrylic acid decarboxylase; repressed by Rgt1p
orf19.5732	<i>NOG2</i>	-0.36	-0.39	-0.36	Putative nucleolar GTPase; repressed by prostaglandins; Hap43-induced, rat catheter and Spider biofilm induced
orf19.5734	<i>POP2</i>	-0.53	-0.48	-0.45	Component of the Ccr4-Pop2 mRNA deadenylase; heterozygous null mutant exhibits resistance to parnafungin and cordycepin in the <i>C. albicans</i> fitness test
orf19.5735	<i>CDC50</i>	-0.37	-0.46	-0.39	Putative endosomal protein; induced by Mnl1p under weak acid stress
orf19.5736	<i>ALS5</i>	-0.51		-0.36	ALS family adhesin; highly variable; expression in <i>S. cerevisiae</i> causes adhesion to human epithelium, endothelium or ECM, endothelial invasiveness by endocytosis and, at high abundance, ECM-induced aggregation; can form amyloid fibrils
orf19.5742	<i>ALS9</i>	-0.63	-0.40	-0.46	ALS family cell-surface glycoprotein; expressed during infection of human epithelial cells; confers laminin adhesion to <i>S. cerevisiae</i> ; highly variable; putative GPI-anchor; Hap43-repressed
orf19.5746	<i>ALA1</i>	-0.38	-0.43	-0.38	Alanyl-tRNA synthetase; translational regulation generates cytoplasmic and mitochondrial forms; Gcn4p-regulated; repressed by amino acid starvation (3-AT); translation-related genes downregulated upon phagocytosis by murine macrophages
orf19.5747		-0.43			Protein of unknown function
orf19.5749	<i>SBA1</i>	-0.51	-0.43	-0.35	Similar to co-chaperones; induced in high iron; farnesol-, heavy metal (cadmium) stress-induced; protein level decreases in stationary phase cultures; Hap43-repressed
orf19.5750	<i>SHM2</i>	-0.29	-0.45		Cytoplasmic serine hydroxymethyltransferase; complements glycine auxotrophy of <i>S. cerevisiae</i> shm1 shm2 gly1-1 mutant; antigenic; farnesol-upregulated in biofilm; stationary-phase enriched protein; rat catheter and Spider biofilm repressed
orf19.5751	<i>ORM1</i>	-0.40	-0.33	-0.35	Putative endoplasmic reticulum membrane protein; Hap43p-repressed gene; mutation confers hypersensitivity to aureobasidin A
orf19.5752		-0.42	-0.47	-0.46	Protein of unknown function
orf19.5754		-0.48			Putative membrane protein with a predicted role in zinc ion homeostasis; Hap43-induced; fluconazole-induced; rat catheter and Spider biofilm induced
orf19.5757		-0.61	-0.51	-0.51	Protein of unknown function
orf19.5758	<i>SAL6</i>		-0.33		Putative protein phosphatase of the Type 1 family; serine/threonine-specific; similar to <i>S. cerevisiae</i> Ppq1; mutant has virulence defect; Spider biofilm induced
orf19.5760	<i>IHD1</i>		0.43		GPI-anchored protein; alkaline, hypha-induced; regulated by Nrg1, Rfg1, Tup1 and Tsa1, Tsa1B in minimal media at 37; oropharyngeal candidiasis induced; Spider biofilm induced; regulated in Spider biofilms by Tec1, Efg1, Ndt80, Rob1, Brg1
orf19.5763		-0.63	-0.52	-0.45	Protein of unknown function
orf19.5764	<i>SKI8</i>	-0.52	-0.63	-0.50	Protein of unknown function
orf19.5765	<i>NUP82</i>	-0.59	-0.57	-0.50	Linker nucleoporin of the nuclear pore complex; role in mRNA export from nucleus, protein import into nucleus, ribosomal large subunit export from nucleus, ribosomal small subunit export from nucleus; rat catheter biofilm repressed
orf19.5767		-0.57	-0.48	-0.39	Protein of unknown function
orf19.5768	<i>SNF4</i>	-0.56	-0.56	-0.50	Transcription factor; ortholog of <i>S. cerevisiae</i> Snf4; caspofungin repressed; transposon mutation affects filamentation
orf19.5771	<i>PBP2</i>	-0.38	-0.46	-0.36	Putative RNA binding protein; transcript regulated by Nrg1, Mig1, and Tup1
orf19.5772		-0.40	-0.39	-0.34	Protein of unknown function
orf19.5773		-0.56	-0.52	-0.47	Putative dipeptidyl-peptidase III; protein detected by mass spec in exponential and stationary phase cultures; Hog1p-induced; clade-associated gene expression
orf19.5784	<i>AMO1</i>	0.69			Putative peroxisomal copper amine oxidase
orf19.5785				0.72	Protein of unknown function; upregulated in a <i>cyr1</i> or <i>ras1</i> null mutant; induced by nitric oxide
orf19.5806	<i>ALD5</i>			0.38	NAD-aldehyde dehydrogenase; decreased expression in fluconazole-resistant isolate, or in hyphae; biofilm induced; fluconazole-downregulated; protein abundance is affected by URA3 expression in the CAI-4 strain; stationary phase enriched
orf19.5818	<i>SUR2</i>	-0.36			Putative ceramide hydroxylase; predicted enzyme of sphingolipid biosynthesis; regulated by Tsa1, Tsa1B under H2O2 stress conditions; Spider and flow model biofilm induced
orf19.5820	<i>UGA6</i>	-0.55		-0.34	Putative GABA-specific permease; decreased transcription is observed upon benomyl treatment or in an azole-resistant strain that overexpresses MDR1
orf19.5843	<i>SRR1</i>	-0.46			Two-component system response regulator; involved in stress response; Plc1-regulated; upregulated in <i>cyr1</i> null mutant; flow model biofilm induced; Spider biofilm induced

orf19.5863		-0,63		-0,41	Protein of unknown function
orf19.5867	<i>WSC1</i>		0,46		Putative cell wall component; transcript upregulated in <i>cyr1</i> mutant (yeast or hyphae); Spider and flow model biofilm induced
orf19.5908	<i>TEC1</i>		0,40		TEA/ATTS transcription factor; white cell pheromone response, hyphal gene regulation; required for Spider and RPMI biofilm formation; regulates BCR1; Cph2 regulated transcript; alkaline, rat catheter, Spider, flow model biofilm induced
orf19.5949	<i>FAS2</i>	0,31			Alpha subunit of fatty-acid synthase; required for virulence in mouse systemic infection and rat oropharyngeal infection models; regulated by Efg1; fluconazole-induced; amphotericin B repressed; flow model and Spider biofilm repressed
orf19.5960	<i>NCE102</i>		0,41		Non classical protein export protein; localized to plasma membrane; Hap43-induced gene; flow model biofilm induced; Spider biofilm induced
orf19.5989			-0,34		Putative cleavage factor I subunit; required for the cleavage and polyadenylation of pre-mRNA 3' ends; Spider biofilm repressed
orf19.5992	<i>WOR2</i>		0,38		Zn(II)2Cys6 transcription factor; regulator of white-opaque switching; required for maintenance of opaque state; Hap43-induced
orf19.6003		0,55	0,72	0,50	Protein of unknown function; role in intracellular signal transduction; Spider biofilm induced
orf19.6065		-0,36			RNA polymerase II holoenzyme/mediator subunit; regulated by Mig1, Tup1; amphotericin B, caspofungin repressed; protein present in exponential and stationary growth phase yeast; Hap43-repressed; Spider biofilm repressed
orf19.6073	<i>HMX1</i>	0,67		0,36	Heme oxygenase; utilization of hemin iron; transcript induced by heat, low iron, or hemin; repressed by Efg1; induced by low iron; upregulated by Rim101 at pH 8; Hap43-induced; Spider and flow model biofilm induced
orf19.6077				-0,37	Putative protein of unknown function; shows colony morphology-related gene regulation by Ssn6p
orf19.6078	<i>POL93</i>		0,54	0,38	Predicted ORF in retrotransposon Tca8 with similarity to the Pol region of retrotransposons encoding reverse transcriptase, protease and integrase; downregulated in response to ciclopirox olamine; F-12/CO2 early biofilm induced
orf19.6079			0,47	0,36	Predicted ORF in retrotransposon Tca8 with similarity to the Gag region encoding nucleocapsid-like protein; repressed by ciclopirox olamine; filament induced; regulated by Rfg1, Tup1; overlaps orf19.6078.1
orf19.6081	<i>PHR2</i>		-0,58		Glycosidase; role in vaginal not systemic infection (low pH not neutral); low pH, high iron, fluconazole, Hap43-induced; Rim101-repressed at pH8; rat catheter biofilm induced; Bcr1-repressed in RPMI a/a biofilms
orf19.610	<i>EFG1</i>		0,34		bHLH transcription factor; required for white-phase cell type, RPMI and Spider biofilm formation, hyphal growth, cell-wall gene regulation; roles in adhesion, virulence; Cph1 and Efg1 have role in host cytokine response; binds E-box
orf19.6116	<i>GLK4</i>	-0,39			Putative glucokinase; decreased expression in hyphae compared to yeast-form cells
orf19.6139	<i>FRE7</i>		0,71		Copper-regulated cupric reductase; repressed by ciclopirox olamine or 17-beta-estradiol; induced by alkaline conditions or interaction with macrophage; Spider biofilm induced
orf19.6140	<i>FRE30</i>		0,59		Protein with similarity to ferric reductases; downregulated in response to amphotericin B, estradiol, or ciclopirox olamine, and upregulated by interaction with macrophage; un-merged from orf19.6139 in a revision of Assembly 21
orf19.6141	<i>HGT16</i>	0,50			Putative glucose transporter of the major facilitator superfamily; the <i>C. albicans</i> glucose transporter family comprises 20 members; 12 probable membrane-spanning segments; gene has intron; expressed in rich medium with 2% glucose
orf19.6165	<i>KGD1</i>	0,32	0,30		Putative 2-oxoglutarate dehydrogenase; regulated by Efg1 under yeast but not hyphal growth conditions; transcript induced in an RHE model of oral candidiasis; stationary phase enriched protein; Hap43-repressed; rat catheter biofilm induced
orf19.6197	<i>DHH1</i>	0,40	0,47	0,41	Putative RNA helicase
orf19.6202	<i>RBT4</i>	-0,91	-0,77	-0,68	Pry family protein; required for virulence in mouse systemic/rabbit corneal infections; not filamentation; mRNA binds She3, is localized to hyphal tips; Hap43-induced; in both yeast and hyphal culture supernatants; Spider biofilm induced
orf19.6229	<i>CAT1</i>	-0,42		-0,46	Catalase; resistance to oxidative stress, neutrophils, peroxide; role in virulence; regulated by iron, ciclopirox, fluconazole, carbon source, pH, Rim101, Ssn6, Hog1, Hap43, Sfu1, Sef1, farnesol, core stress response; Spider biofilm induced
orf19.6245		-0,40			Protein of unknown function; regulated by osmotic stress via Hog1 and oxidative stress (Hog1- and Cap1-independent); induced by alpha pheromone in SpiderM medium; Spider biofilm induced
orf19.6276			0,36		Protein of unknown function; rat catheter biofilm repressed
orf19.6311		0,65			Protein of unknown function; Hap43-induced; rat catheter and Spider biofilm induced
orf19.6318				0,43	Protein of unknown function
orf19.6322	<i>ARD</i>	-0,42	-0,48		D-arabitol dehydrogenase, NAD-dependent (ArDH); enzyme of D-arabitol and D-arabinose catabolism; D-arabitol is a marker for active infection in humans; rat catheter and Spider biofilm induced
orf19.6324	<i>VID27</i>	-0,29	-0,45	-0,33	Protein similar to <i>S. cerevisiae</i> Vid27p; transposon mutation affects filamentous growth; mutation confers hypersensitivity to toxic ergosterol analog; fungal-specific (no human or murine homolog)
orf19.6326			-0,37		Protein of unknown function
orf19.6327	<i>HET1</i>	-0,46	-0,56	-0,45	Putative sphingolipid transfer protein; involved in localization of glucosylceramide which is important for virulence; Spider biofilm repressed
orf19.6328		-0,42	-0,46	-0,36	Putative protein of the mitochondrial intermembrane space; predicted role in acetate utilization and gluconeogenesis; Spider biofilm repressed
orf19.6329			-0,42	-0,43	Protein of unknown function; opaque-specific transcript; fluconazole-repressed; induced in <i>cyr1</i> mutant and in oropharyngeal candidiasis; Spider biofilm induced
orf19.6336	<i>PGA25</i>	-0,41	-0,39		Putative GPI-anchored adhesin-like protein; fluconazole-downregulated; induced in oropharyngeal candidiasis; Spider biofilm induced
orf19.6337	<i>TLO13</i>		-0,53	-0,36	Member of a family of telomere-proximal genes of unknown function; may be spliced in vivo; overlaps orf19.6337.1, which is a region annotated as blocked reading frame
orf19.6341			-0,34	-0,35	Protein of unknown function
orf19.638	<i>FDH1</i>		0,66	0,45	Formate dehydrogenase; oxidizes formate to CO2; Mig1 regulated; induced by macrophages; fluconazole-repressed; repressed by Efg1 in yeast, not hyphal conditions; stationary phase enriched; rat catheter and Spider biofilm induced
orf19.6385	<i>ACO1</i>	0,28	0,36		Aconitase; induced in high iron; 2 upstream CCAAT motifs; amino acid starvation (3-AT), amphotericin B, phagocytosis, farnesol induced; Hap43, fluconazole-repressed; Gcn4-regulated; antigenic in infection; flow and Spider biofilm repressed
orf19.6387	<i>HSP104</i>		0,36		Heat-shock protein; roles in biofilm and virulence; complements chaperone, prion activity in <i>S. cerevisiae</i> ; guanidine-insensitive; heat shock/stress induced; repressed in farnesol-treated biofilm; sumoylation target; Spider biofilm induced
orf19.6408		0,47			Putative DnaJ-like heat shock/chaperone; Hap43-repressed; Spider and F-12/CO2 biofilm induced
orf19.6459	<i>DPP3</i>	-0,45	-0,37	-0,48	Protein similar to <i>S. cerevisiae</i> pyrophosphate phosphatase Dpp1; required for farnesol biosynthesis; repressed by 17-beta-estradiol, ethynyl estradiol; Spider biofilm induced
orf19.6481	<i>YPS7</i>		0,37		Putative aspartic-type endopeptidase with limited ability to degrade alpha pheromone; mutants show increased sensitivity to alpha pheromone
orf19.6489	<i>FMP45</i>		0,54		Predicted membrane protein induced during mating; mutation confers hypersensitivity to toxic ergosterol analog, to amphotericin B; alkaline repressed; repressed by alpha pheromone in SpiderM medium; rat catheter, Spider biofilm induced
orf19.655	<i>PHO84</i>		0,58	0,42	High-affinity phosphate transporter; transcript regulated by white-opaque switch; Hog1, ciclopirox olamine or alkaline induced; caspofungin, stress repressed; upregulated in RHE model; Spider and flow model biofilm induced, Hap43-induced
orf19.657	<i>SAM2</i>	0,30			S-adenosylmethionine synthetase; localizes to surface of hyphae, not yeast cells; alkaline, Hog1-induced; farnesol-downregulated; F-12/CO2 early biofilm induced; Spider biofilm repressed
orf19.6577	<i>FLU1</i>			0,63	Multidrug efflux pump of the plasma membrane; MDR family member of the MFS (major facilitator superfamily) of transporters; involved in histatin 5 efflux; fungal-specific (no human/murine homolog)

Supporting Information

orf19.6595	<i>RTA4</i>	-0,49			Protein similar to <i>S. cerevisiae</i> Rsb1p, involved in fatty acid transport; transposon mutation affects filamentous growth; alkaline downregulated; caspofungin induced; possibly an essential gene; Hap43p-repressed
orf19.6601.1	<i>YKE2</i>	-0,41			Possible heterohexameric Gim/prefoldin protein complex subunit; role in folding alpha-tubulin, beta-tubulin, and actin; transcript induced by yeast-to-hypha switch; regulated by Nrg1, Tup1; Spider and flow model biofilm induced
orf19.6604		-0,38			Ortholog of <i>S. cerevisiae</i> Pba1 that is involved in 20S proteasome assembly; upregulated in a <i>cyr1</i> null mutant; contains a 5' UTR intron
orf19.6637		-0,36			Predicted glycosyl hydrolase; hypoxia induced; flow model biofilm induced
orf19.6639			0,37		Ortholog of <i>S. cerevisiae</i> Mdm36; mitochondrial distribution and morphology protein; Hap43-repressed gene
orf19.6640	<i>TPS1</i>	-0,55			Trehalose-6-phosphate synthase; role in hyphal growth and virulence in mouse systemic infection; induced in presence of human neutrophils; macrophage/pseudohyphal-repressed after 16h; stationary phase enriched protein; Hap43-repressed
orf19.6656			0,34		Spermidine transporter; induced in strains from HIV patients with oral candidiasis; alkaline repressed; amphotericin B induced; colony morphology regulated by Ssn6; reduced oral epithelial cell damage by mutant; Spider biofilm induced
orf19.6658		-0,43	-0,42	-0,41	Stationary phase enriched protein; predicted ORF from Assembly 19; removed from Assembly 20; subsequently reinstated in Assembly 21 based on comparative genome analysis
orf19.6688			0,44		Protein of unknown function; expression decreases by benomyl treatment or in an azole-resistant strain overexpressing MDR1; Spider biofilm induced
orf19.670.2		0,47		0,62	Protein of unknown function; hypoxia, Hap43-repressed; ketoconazole induced; induced in oropharyngeal candidiasis; 16h flow model biofilm repressed, late-stage flow model biofilm induced; rat catheter and Spider biofilm induced
orf19.6705			0,51		Putative guanyl nucleotide exchange factor with Sec7 domain; required for normal filamentous growth; regulated by yeast-hyphal switch; filament induced; regulated by Nrg1, Tup1, Mob2, Hap43; mRNA binds She3; Spider biofilm induced
orf19.6720			-0,31		P-Loop domain-containing protein of unknown function; transposon mutation affects filamentous growth; Spider biofilm induced
orf19.6724	<i>FUM12</i>		0,32		Putative fumarate hydratase; enzyme of citric acid cycle; fluconazole, Efg1 repressed; induced in high iron; protein present in exponential and stationary growth phase
orf19.6734	<i>TCC1</i>		0,35		Putative transcription factor/corepressor; regulation of filamentation and virulence; interacts with Tup1; regulates hypha-specific gene expression; contains 4 tetratricopeptide repeat (TPR) motifs; flucytosine repressed; Tbp1-induced
orf19.675			0,33		Cell wall protein; induced in core stress response and core caspofungin response; iron-regulated; amphotericin B, ketoconazole, and hypoxia induced; regulated by Cyr1, Ssn6; induced in oropharyngeal candidiasis; Spider biofilm repressed
orf19.6770			0,41		protein with ENTH Epsin domain, N-terminal; Spider biofilm repressed
orf19.6782	<i>BMT1</i>		0,42		Beta-mannosyltransferase, required for addition of the 1st beta-mannose residue to acid-stable fraction of cell wall phosphopeptidomannan; 9-gene family member; mutants induce higher levels of inflammatory cytokines in mouse dendritic cells
orf19.6783			0,31		Putative geranylgeranyltransferase regulatory component
orf19.6805			0,41		Protein of unknown function; Spider biofilm induced
orf19.6816		-0,61	-0,37		Putative xylose and arabinose reductase; flow model biofilm induced; Spider biofilm repressed
orf19.6824	<i>TRY6</i>		0,65		Helix-loop-helix transcription factor; regulator of yeast form adherence; required for yeast cell adherence to silicone substrate; Spider and F-12/CO2 biofilm induced; repressed by alpha pheromone in SpiderM medium
orf19.6834.10	<i>TAR1</i>		0,63	-0,59	Ortholog of <i>S. cerevisiae</i> Tar1p; Transcript Antisense to Ribosomal RNA; encoded within the 25S rRNA gene on the opposite strand; induced by Tbf1
orf19.684		-0,36	-0,37	-0,34	Putative transcription factor with zinc finger DNA-binding motif; heterozygous null mutant exhibits hypersensitivity to parnafungin and cordycepin in the <i>C. albicans</i> fitness test
orf19.6844	<i>ICL1</i>		0,45		Isocitrate lyase; glyoxylate cycle enzyme; required for virulence in mice; induced upon phagocytosis by macrophage; farnesol regulated; Pex5-dependent peroxisomal localization; stationary phase enriched; rat catheter, Spider biofilm induced
orf19.6852.1		-0,44			Protein of unknown function; Spider biofilm induced
orf19.686		-0,50	-0,45	-0,35	Protein of unknown function; regulated by Nrg1
orf19.687		-0,52	-0,53	-0,45	Protein of unknown function
orf19.687.1	<i>RPL25</i>	-0,38	-0,54		Putative rRNA-binding ribosomal protein component of the 60S ribosomal subunit; Hap43-induced; colony morphology-related gene regulated by Ssn6
orf19.688		-0,37			Mitochondrial ribosomal protein of the small subunit; <i>S. cerevisiae</i> ortholog is essential for viability; Spider biofilm repressed
orf19.6882	<i>OSM1</i>	-0,51			Putative flavoprotein subunit of fumarate reductase; soluble protein in hyphae; caspofungin repressed; stationary phase enriched protein; flow model biofilm induced; Spider biofilm repressed
orf19.6888		-0,59	-0,52	0,61	Zn(II)2Cys6 domain transcription factor; regulated by Mig1 and Tup1; rat catheter and Spider biofilm induced
orf19.692			-0,59	-0,60	Protein of unknown function; Hap43-repressed gene; rat catheter and Spider biofilm induced
orf19.6984				0,48	Protein of unknown function
orf19.7020			0,34		Protein similar to <i>S. cerevisiae</i> Kex1p, which is a pheromone-processing peptidase; possible Kex2p substrate
orf19.7022		-0,41			Protein of unknown function
orf19.7053	<i>GAC1</i>		0,30		Putative regulatory subunit of ser/thr phosphoprotein phosphatase 1; fluconazole-induced; caspofungin repressed; transcript induced by Mnl1 under weak acid stress; regulated by Nrg1, Tup1; Spider and flow model biofilm induced
orf19.7077		0,39	0,64	0,46	Putative ferric reductase; induced by Mac1 under copper starvation; Plc1-regulated; Rim101-repressed
orf19.7085			0,35		Protein of unknown function; induced in core stress response; induced by cadmium stress via Hog1; oxidative stress-induced via Cap1; induced by Mnl1 under weak acid stress; macrophage-repressed; rat catheter and Spider biofilm induced
orf19.7094	<i>HGT12</i>	0,39			Glucose, fructose, mannose transporter; major facilitator superfamily; role in macrophage-induced hyphal growth; detected at germ tube plasma membrane by mass spectrometry; Snf3p-induced; 12 probable transmembrane segments
orf19.7111.1	<i>SOD3</i>		0,42		Cytosolic manganese-containing superoxide dismutase; protects against oxidative stress; repressed by ciclopirox olamine, induced during stationary phase when SOD1 expression is low; Hap43-repressed; Spider and flow model biofilm induced
orf19.7112	<i>FRP2</i>	0,49			Putative ferric reductase; alkaline induced by Rim101; fluconazole-downregulated; upregulated in the presence of human neutrophils; possibly adherence-induced; regulated by Sef1, Sfu1, and Hap43
orf19.717	<i>HSP60</i>		0,45	0,36	Heat shock protein; soluble in hyphae; regulated by Nrg1 and by iron; induced in high iron; heavy metal (cadmium) stress-induced; sumoylation target; protein present in exponential and stationary phase cells; Hap43-repressed
orf19.7214		-0,72	-0,40	-0,41	Glucan 1,3-beta-glucosidase; regulated by Nrg1, Tup1 and possibly Tac1; induced by NO and during cell wall regeneration; stationary phase enriched; possibly essential (UAU1 method); F-12/CO2 early biofilm induced; flow biofilm repressed
orf19.7218	<i>RBE1</i>	0,43	0,44	0,38	Pry family cell wall protein; Rim101, Efg1, Ssn6, alkaline repressed; O-glycosylation; no GPI anchor predicted; ketoconazol induced; regulated by Sef1, Sfu1, Hap4; flow model biofilm induced; rat catheter and Spider biofilm repressed
orf19.7247	<i>RIM101</i>		0,34		Transcription factor; alkaline pH response; required for alkaline-induced hyphal growth; role in virulence in mice; activated by C-terminal proteolytic cleavage; mediates both positive and negative regulation; Spider biofilm induced
orf19.7251	<i>WSC4</i>			0,34	Putative cell wall integrity and stress response subunit 4 precursor; transcription is specific to white cell type
orf19.7284	<i>ASR2</i>	-0,88	-0,50	-0,53	Adenyl cyclase and stress responsive protein; induced in <i>cyr1</i> or <i>ras1</i> mutant; stationary phase enriched protein; Spider biofilm induced

orf19.7288		-0,49			Protein with predicted oxidoreductase and dehydrogenase domains; Hap43-repressed; Spider biofilm induced
orf19.7296			-0,54	-0,52	Putative cation conductance protein; similar to stomatin mechanoreception protein; plasma-membrane localized; induced by Rgt1; rat catheter and Spider biofilm induced
orf19.73		-0,62	-0,46	-0,44	Putative metalloprotease; associates with ribosomes and is involved in ribosome biogenesis; Spider biofilm induced
orf19.7310		-0,51			Protein with a role in directing meiotic recombination events to homologous chromatids; induced by ciclopirox olamine; positively regulated by Sfu1; Hog1, fluconazole-repressed; Hap43-induced; Spider biofilm induced
orf19.7319	<i>SUC1</i>			-0,37	Zinc-finger transcription factor; regulates alpha-glucosidase expression; complements <i>S. cerevisiae</i> suc2 for sucrose utilization and mal13 maltase defect; required for yeast cell adherence to silicone substrate; rat catheter biofilm induced
orf19.7337			0,48		Protein with a nischarin related domain and leucine rich repeats; Spider biofilm induced
orf19.734	<i>GLK1</i>	-0,45			Putative glucokinase; transcript regulated upon yeast-hyphal switch; Efg1 regulated; fluconazole-induced; induced in core stress response; colony morphology-related gene regulation by Ssn6; GlcNAc-induced protein
orf19.7392	<i>DED1</i>	0,28			Predicted ATP-dependent RNA helicase; RNA strand annealing activity; Spider biofilm induced
orf19.74	<i>SEC5</i>	-0,49		-0,36	Predicted exocyst component; ortholog of <i>S. cerevisiae</i> Sec5p; merged with orf19.75 in Assembly 21
orf19.740	<i>HAP41</i>		0,44	0,40	Putative Hap4-like transcription factor; Hap43-repressed; not required for response to low iron; induced by Mnl1 under weak acid stress; Spider biofilm induced
orf19.7411	<i>OAC1</i>	0,59			Putative mitochondrial inner membrane transporter; rat catheter biofilm induced
orf19.7436	<i>AAF1</i>		0,44		Possible regulatory protein; possible adhesin-like; Glu-rich domain; production in <i>S. cerevisiae</i> increases endothelial cell adherence and flocculence; flow model biofilm, alkaline or caspofungin induced
orf19.7445		0,32	0,42	0,38	Ortholog of <i>S.c. Vid24</i> ; a peripheral membrane protein located at Vid (vacuole import and degradation) vesicles; regulated by Sef1, Sfu1, and Hap43; Spider biofilm induced
orf19.7504		-0,36	-0,38		Ortholog of <i>S. cerevisiae</i> Rts3; a component of the protein phosphatase type 2A complex; Plc1-regulated; induced in core caspofungin response; Spider biofilm induced
orf19.7514	<i>PCK1</i>			0,48	Phosphoenolpyruvate carboxykinase; glucose, C-source, yeast-hypha, Hap43 regulated; fluconazole, phagocytosis, H2O2, oral candidiasis, Spider/rat catheter/flow model biofilm induced; repressed in biofilm by Bcr1, Tec1, Ndt80, Rob1, Brg1
orf19.7522			-0,36		Protein with a pyridoxal phosphate-dependent transferase domain; Hap43-repressed; mutation confers hypersensitivity to amphotericin B; Spider biofilm repressed
orf19.753	<i>MNN15</i>	-0,40			Putative alpha-1,3-mannosyltransferase; predicted role in protein O-linked glycosylation; Spider biofilm induced
orf19.7561	<i>DEF1</i>		0,28		RNA polymerase II regulator; role in filamentation, epithelial cell escape, dissemination in RHE model; induced by fluconazole, high cell density; Efg1/hyphal regulated; role in adhesion, hyphal growth on solid media; Spider biofilm induced
orf19.7567				-0,33	Protein of unknown function; induced by alpha pheromone in SpiderM medium
orf19.7583	<i>ZCF39</i>		-0,34		Zn(II)2Cys6 transcription factor; mutants are viable; filament induced; required for yeast cell adherence to silicone substrate; Spider biofilm induced
orf19.7585	<i>INO1</i>	-0,42		-0,46	Inositol-1-phosphate synthase; antigenic in human; repressed by farnesol in biofilm or by caspofungin; upstream inositol/choline regulatory element; glycosylation predicted; rat catheter, flow model induced; Spider biofilm repressed
orf19.76	<i>SPB1</i>	-0,39	-0,55	-0,41	Putative AdoMet-dependent methyltransferase; Hap43-induced; repressed by prostaglandins; possibly essential gene, disruptants not obtained by UAU1 method; Spider biofilm induced
orf19.7610	<i>PTP3</i>	-0,34			Putative protein tyrosine phosphatase; hypha induced; alkaline induced; regulated by Efg1, Ras1, cAMP pathways; mutants are viable; Spider biofilm induced; rat catheter biofilm repressed; flow model biofilm repressed
orf19.7612	<i>CTM1</i>	-0,37			Putative cytochrome c lysine methyltransferase; regulated by Gcn2 and Gcn4; transcript induced by Mnl1 under weak acid stress; early-stage flow model biofilm induced
orf19.7648				0,35	Protein of unknown function
orf19.7676	<i>XYL2</i>	-0,40			D-xylulose reductase; immunogenic in mice; soluble protein in hyphae; induced by caspofungin, fluconazole, Hog1 and during cell wall regeneration; Mnl1-induced in weak acid stress; stationary phase enriched; flow model biofilm induced
orf19.802	<i>UGA1</i>	0,31		0,36	Putative GABA transaminase; transcription regulated by Mig1 and Tup1; stationary phase enriched protein; rat catheter and Spider biofilm induced
orf19.822	<i>HSP21</i>		0,52		Small heat shock protein; role in stress response and virulence; fluconazole-downregulated; induced in <i>cyr1</i> or <i>ras1</i> mutant; stationary phase enriched protein; detected in some, not all, biofilm extracts; Spider biofilm induced
orf19.84	<i>CAN3</i>	-0,43	-0,43	-0,64	Predicted amino acid transmembrane transporter; transcript regulated by white-opaque switch; Hap43-repressed gene
orf19.85	<i>GPX2</i>	-0,65	-0,52	-0,65	Similar to glutathione peroxidase; induced in high iron; alkaline induced by Rim101; induced by alpha factor or interaction with macrophage; regulated by Efg1; caspofungin repressed; Spider biofilm induced
orf19.86		-0,38			Putative glutathione peroxidase; induced by peroxide, exposure to neutrophils and macrophage blood fractions; repressed during infection of macrophages; Spider biofilm induced; flow model biofilm repressed
orf19.866	<i>RAD32</i>		-0,36		Protein similar to <i>S. cerevisiae</i> protein with role in nucleotide excision repair; down-regulation associated with azole resistance; Hap43p-repressed gene
orf19.868	<i>ADAEC</i>	-0,44			Protein of unknown function; transcription is specific to white cell type
orf19.871			0,33		Protein of unknown function
orf19.88	<i>ILV5</i>		-0,55	-0,34	Ketol-acid reductoisomerase; antigenic; regulated by Gcn4; GlcNAc, amino acid starvation (3-AT)-induced; macrophage-repressed protein; protein present in exponential and stationary phase; flow model and Spider biofilm repressed
orf19.882	<i>HSP78</i>		0,42		Heat-shock protein; regulated by macrophage response, Nrg1, Mig1, Gcn2, Gcn4, Mnl1p; heavy metal (cadmium) stress-induced; stationary phase enriched protein; rat catheter and Spider biofilm induced
orf19.89	<i>PEX7</i>		-0,76	-0,55	Protein of unknown function
orf19.896	<i>CHK1</i>	-0,37			Histidine kinase; 2-component signaling, cell wall synthesis; hyphal growth defect; avirulent in mouse, not rat vaginal infection; phagocytosis rate increased; Spider biofilm induced; required for RPM1 biofilm; Bcr1-induced in a biofilm
orf19.90		-0,66	-0,61	-0,58	Protein of unknown function
orf19.903	<i>GPM1</i>		-0,29		Phosphoglycerate mutase; surface protein that binds host complement Factor H and FHL-1; antigenic; fluconazole, or amino acid starvation (3-AT) induced, farnesol-repressed; Hap43, flow model biofilm induced; Spider biofilm repressed
orf19.909	<i>STP4</i>		0,43		C2H2 transcription factor; induced in core caspofungin response; colony morphology-related gene regulation by Ssn6; induced by 17-beta-estradiol, ethynyl estradiol; rat catheter and Spider biofilm induced
orf19.91		-0,50		-0,36	Protein of unknown function; flow model biofilm induced; Hap43-repressed
orf19.918	<i>CDR11</i>		0,51		Putative transporter of PDR subfamily of ABC family; Gcn4-regulated; induced by Rim101 at pH 8; Spider biofilm induced
orf19.92		-0,52	-0,49	-0,42	Protein with a predicted thioredoxin-like domain; Hap43-repressed; induced by prostaglandins
orf19.921	<i>HMS1</i>		0,46		hLh domain Myc-type transcript factor; required for morphogenesis induced by elevated temperature or Hsp90 compromise; acts downstream of Pcl1; Spider biofilm induced
orf19.932			0,48	0,48	Putative aminophospholipid translocase (flippase); merged with orf19.2226 in Assembly 21; possibly an essential gene, disruptants not obtained by UAU1 method
orf19.938		0,52		0,60	Protein of unknown function
orf19.94		-0,59	-0,54	-0,56	Protein of unknown function; Spider biofilm induced
orf19.944	<i>IFG3</i>	-0,38			Putative D-amino acid oxidase; Spider biofilm induced
orf19.96	<i>TOP1</i>	-0,32	-0,47	-0,40	DNA topoisomerase I; required for wild-type growth and for wild-type mouse virulence; sensitive to camptothecin; induced upon adherence to polystyrene; rat catheter biofilm induced

Supporting Information

orf19.979	<i>FAS1</i>	0,30			Beta subunit of fatty-acid synthase; multifunctional enzyme; Hap43, fluconazole-induced; amphotericin B, caspofungin repressed; macrophage/pseudohyphal-induced; flow model and Spider biofilm repressed
orf19.984	<i>PHO8</i>	0,50			Putative repressible vacuolar alkaline phosphatase; Rim101-induced transcript; regulated by Tsa1, Tsa1B in minimal media at 37 deg; possibly adherence-induced
orf19.99	<i>HAL21</i>	-0,63	-0,82	-0,57	Putative phosphoadenosine-5'-phosphate or 3'-phosphoadenosine 5'-phosphosulfate phosphatase; possible role in sulfur recycling; ortholog of <i>S. cerevisiae</i> Met22; predicted Kex2 substrate; F-12/CO2 biofilm induced
orf19.999	<i>GCA2</i>	-0,48			Predicted extracellular glucoamylase; induced by ketoconazole; possibly essential, disruptants not obtained by UAU1 method; promotes biofilm matrix formation; Spider biofilm induced; Bcr1-induced in RPM1 a/a biofilms

Table S 3: RNA seq $p_{adj} < 0.05$

Gene name	Common name	TRY4	ZFU2	ZCF8	Description
orf19.101	<i>RIM9</i>			-0,36	Protein required for alkaline pH response via the Rim101 signaling pathway; ortholog of <i>S. cerevisiae</i> Rim9 and <i>A. nidulans</i> pall; Spider biofilm induced
orf19.102		-0,48			Protein of unknown function
orf19.1048	<i>IFD6</i>	-0,71		-0,45	Aldo-keto reductase; similar to aryl alcohol dehydrogenases; protein increase correlates with MDR1 overexpression (not CDR1 or CDR2) in fluconazole-resistant clinical isolates; farnesol regulated; possibly essential; Spider biofilm induced
orf19.105	<i>HAL22</i>		-0,42		Putative phosphoadenosine-5'-phosphate or 3'-phosphoadenosine 5'-phosphosulfate phosphatase; possible role in sulfur recycling; Hap43-repressed; F-12/CO2 biofilm induced
orf19.1075		-0,74	-0,47	-0,62	Protein of unknown function; Spider biofilm induced
orf19.1083			-0,49	-0,38	Putative protein of unknown function; macrophage-induced gene
orf19.1084	<i>CDC39</i>	-0,38	-0,33		Protein similar to <i>S. cerevisiae</i> Cdc39p, which is part of the CCR4-NOT transcription regulatory complex; transposon mutation affects filamentous growth
orf19.1085		-0,65	-0,61	-0,47	Protein of unknown function
orf19.1089	<i>PEX11</i>	-0,66	-0,46	-0,36	Putative peroxisomal membrane protein; role in fatty acid oxidation; expression is Tac1-regulated; Hms1p-dependent induction by geldamycin; Spider biofilm induced
orf19.1095	<i>GLE2</i>	-0,50	-0,43	-0,40	Putative nuclear pore complex; possibly an essential gene, disruptants not obtained by UAU1 method; rat catheter biofilm repressed
orf19.1097	<i>ALS2</i>	-0,80	-0,70	-0,77	ALS family protein; role in adhesion, biofilm formation, germ tube induction; expressed at infection of human buccal epithelial cells; putative GPI-anchor; induced by ketoconazole, low iron and at cell wall regeneration; regulated by Sfu1p
orf19.113	<i>CIP1</i>			-0,49	Possible oxidoreductase; transcript induced by cadmium but not other heavy metals, heat shock, yeast-hypha switch, oxidative stress (via Cap1), or macrophage interaction; stationary phase enriched protein; Spider biofilm induced
orf19.1149	<i>MRF1</i>	-0,42			Putative mitochondrial respiratory protein; induced by farnesol, benomyl, nitric oxide, core stress response; oxidative stress-induced via Cap1; stationary-phase enriched protein; Spider biofilm induced
orf19.1153	<i>GAD1</i>	-0,49			Putative glutamate decarboxylase; alkaline, macrophage-downregulated gene; amphotericin B induced; induced by Mn1 under weak acid stress; stationary phase enriched protein; rat catheter biofilm repressed
orf19.117		-0,43	-0,42	-0,39	Protein of unknown function
orf19.1177		-0,39	-0,42	-0,39	Ortholog of <i>S. cerevisiae</i> Rtt106; histone chaperone that regulates chromatin structure in transcribed and silenced chromosomal regions; affects transcriptional elongation; Hap43-repressed; Spider biofilm repressed
orf19.1179		-0,43	-0,48		Protein of unknown function; induced in high iron; possibly subject to Kex2 processing; Hap43-repressed
orf19.118	<i>FAD2</i>		-0,35		Delta-12 fatty acid desaturase, involved in production of linoleic acid, which is a major component of membranes
orf19.1180		-0,53	-0,50	-0,44	Putative 2-aminoadipate transaminase; rat catheter and Spider biofilm repressed
orf19.1181				-0,35	Protein of unknown function
orf19.1182		-0,51	-0,51	-0,50	Protein of unknown function
orf19.1183		-0,58	-0,54	-0,58	Protein of unknown function
orf19.1185			-0,36		Protein of unknown function
orf19.1186		-0,46		-0,38	Protein of unknown function
orf19.119		-0,55			Protein of unknown function
orf19.1190	<i>STV1</i>		-0,38	-0,34	Predicted subunit a of vacuolar proton-translocating ATPase V0 domain, Golgi isoform
orf19.1191			-0,36	-0,34	Protein of unknown function
orf19.1192	<i>DNA2</i>			-0,38	Protein similar to <i>S. cerevisiae</i> Dna2p, which is a DNA replication factor involved in DNA repair; induced under hydroxyurea treatment
orf19.1193	<i>GNP1</i>		-0,31		Similar to asparagine and glutamine permease; fluconazole, caspofungin induced; regulated by Nrg1, Mig1, Tup1, Gcn2, Gcn4, and alkaline regulated by Rim101; repressed during chlamyospore formation; rat catheter, flow model biofilm induced
orf19.1198		-0,64	-0,47	-0,37	Predicted mitochondrial intermembrane space protein of unknown function; possibly an essential gene, disruptants not obtained by UAU1 method
orf19.1199	<i>NOP5</i>		-0,55	-0,35	Ortholog of <i>S. cerevisiae</i> Nop58; involved in pre-rRNA process; Tn mutation affects filamentous growth; macrophage/pseudohyphal-induced; physically interacts with TAP-tagged Nop1; Spider biofilm repressed
orf19.1200		-0,44	-0,51	-0,45	Protein of unknown function; Spider biofilm induced
orf19.1201		-0,46	-0,37	-0,36	Protein of unknown function
orf19.1202		-0,46			Protein of unknown function
orf19.1203	<i>SRO77</i>	-0,45	-0,38	-0,38	Protein with a predicted role in docking and fusion of post-Golgi vesicles with the plasma membrane; filament induced; fungal-specific (no human or murine homolog)
orf19.1203.1			-0,44	-0,35	Predicted dolichol-phosphate mannosyltransferase subunit; flow model and Spider biofilm repressed
orf19.1204		-0,45	-0,50	-0,42	Phosphorylated protein of unknown function; transcript is upregulated clinical isolates from HIV positive patients with oral candidiasis
orf19.121	<i>ARC18</i>	-0,64		-0,34	Putative ARP2/3 complex subunit; mutation confers hypersensitivity to cytochalasin D
orf19.1210		-0,41	-0,38	-0,46	Protein of unknown function
orf19.1212		-0,58	-0,52	-0,39	Protein of unknown function
orf19.1214		-0,44	-0,63	-0,42	Protein of unknown function
orf19.1215		-0,53		-0,44	Protein of unknown function
orf19.1217		-0,43			Protein of unknown function
orf19.1220	<i>RVS167</i>	-0,38	-0,33	-0,34	SH3-domain- and BAR domain-containing protein involved in endocytosis; null mutant exhibits defects in hyphal growth, virulence, cell wall integrity, and actin patch localization; cosediments with phosphorylated Myo5p
orf19.1221	<i>ALG2</i>	-0,46		-0,39	Putative mannosyltransferase involved in cell wall mannan biosynthesis; transcription is elevated in <i>chk1</i> , <i>nik1</i> , and <i>sln1</i> homozygous null mutants
orf19.1224	<i>FRP3</i>	0,36			Putative ammonium transporter; upregulated in the presence of human neutrophils; fluconazole-downregulated; repressed by nitric oxide; Spider biofilm induced; rat catheter biofilm repressed
orf19.123	<i>RCN1</i>			-0,39	Protein involved in calcineurin-dependent signaling that controls stress response and virulence; inhibits calcineurin function
orf19.124	<i>CIC1</i>	-0,38	-0,50	-0,38	Putative proteasome-interacting protein; rat catheter biofilm induced
orf19.125	<i>EBP1</i>		-0,54	-0,41	NADPH oxidoreductase; interacts with phenolic substrates (17beta-estradiol); possible role in estrogen response; induced by oxidative, weak acid stress, NO, benomyl, GlcNAc; Cap1, Mnl1 induced; Hap43-repressed; rat catheter biofilm induced

orf19.1253	<i>PHO4</i>		0,41		bHLH transcription factor of the myc-family; required for growth in medium lacking phosphate and for resistance to copper and Phloxine B; induced by Mnl1 under weak acid stress
orf19.1287			0,48		Protein of unknown function; flow model biofilm induced; Spider biofilm induced
orf19.130	<i>VPS15</i>	-0,56			Protein involved in retrograde endosome-to-Golgi protein transport; required for normal virulence
orf19.1308				1,58	Predicted membrane transporter, member of the drug:proton antiporter (14 spanner) (DHA2) family, major facilitator superfamily (MFS)
orf19.1309				1,08	Protein of unknown function
orf19.131.2		-0,41	-0,37		Protein of unknown function
orf19.1310				0,54	Protein of unknown function
orf19.1311	<i>SPO75</i>			0,42	Protein of unknown function
orf19.1326			-0,49	-0,36	Protein of unknown function
orf19.1344		0,91			Protein of unknown function; fluconazole-induced; Spider biofilm induced
orf19.135	<i>EXO84</i>	-0,39	-0,43	-0,36	Predicted subunit of the exocyst complex, involved in exocytosis; localizes to a crescent on the surface of the hyphal tip
orf19.1353		-0,43			Protein of unknown function; repressed by yeast-hypha switch; Ras1-regulated; oral infection induced; mutants defective in damage to oral epithelium; flow model biofilm induced; Spider biofilm induced
orf19.1354	<i>UCF1</i>	-0,38			Upregulated by cAMP in filamentous growth; induced in high iron, decreased upon yeast-hypha switch; downregulation correlates with clinical fluconazole resistance; Ras1-regulated; Hap43-repressed; flow model biofilm induced
orf19.136	<i>QDR3</i>			0,41	Predicted membrane transporter, member of the drug:proton antiporter (12 spanner) (DHA1) family, major facilitator superfamily (MFS); Hap43p-repressed gene
orf19.137		-0,44			Putative transferase involved in phospholipid biosynthesis; induced by alpha pheromone in SpiderM medium
orf19.1405	<i>PHO13</i>			0,38	Putative 4-nitrophenylphosphatase; Hap43p-repressed gene; transcription is regulated upon yeast-hyphal switch
orf19.1433		-0,43			Protein of unknown function; Hap43-repressed; colony morphology-related gene regulation by Ssn6; Spider biofilm induced
orf19.1439	<i>IPK1</i>	-0,50		-0,37	Ortholog of <i>S. cerevisiae</i> / <i>S. pombe</i> <i>IpK1</i> ; an inositol pentakisphosphate 2-kinase, a nuclear protein required for synthesis of 1,2,3,4,5,6-hexakisphosphate; Spider biofilm induced
orf19.1486			0,50		Protein with a life-span regulatory factor domain; regulated by Sef1, Sfu1, and Hap43; flow model biofilm induced; Spider biofilm induced
orf19.1490	<i>MSB2</i>		0,47	0,39	Mucin family adhesin-like protein; cell wall damage sensor; required for Cek1 phosphorylation by cell wall stress; Rim101-repressed; activation releases extracellular domain into medium; Spider biofilm induced
orf19.1509	<i>ROD1</i>		0,34		Protein similar to <i>S. cerevisiae</i> <i>Rod1</i> ; a membrane protein with a role in drug tolerance; repressed by Rgt1; mutant is viable
orf19.1600			0,65	0,36	Protein of unknown function
orf19.1614	<i>MEP1</i>	0,88	0,57	0,37	Ammonium permease; Mep1 more efficient permease than Mep2, Mep2 has additional regulatory role; 11 predicted transmembrane regions; low mRNA abundance; hyphal downregulated; flow model biofilm induced
orf19.1653				0,37	Protein of unknown function
orf19.1691		-0,58			Plasma-membrane-localized protein; filament induced; Hog1, ketoconazole, fluconazole and hypoxia-induced; regulated by Nrg1, Tup1, Upc2; induced by prostaglandins; flow model biofilm induced; rat catheter and Spider biofilm repressed
orf19.1715	<i>IRO1</i>	-0,47	-0,53	-0,47	Putative transcription factor; role in iron utilization, pathogenesis; both IRO1 and adjacent URA3 are mutated in strain CA14; suppresses <i>S. cerevisiae</i> <i>aft1</i> mutant low-iron growth defect; hyphal-induced; reports differ about iron regulation
orf19.1716	<i>URA3</i>	-0,71	-0,86	-0,69	Orotidine-5'-phosphate decarboxylase; pyrimidine biosynthesis; gene used as genetic marker; decreased expression when integrated at ectopic chromosomal locations can cause defects in hyphal growth and virulence; Spider biofilm repressed
orf19.1727	<i>PMC1</i>		0,40		Vacuolar calcium P-type ATPase; transcript regulated by calcineurin and fluconazole; mutant shows increased resistance to fluconazole, lithium; increased sensitivity to calcium; Spider biofilm induced
orf19.1770	<i>CYC1</i>		0,45	0,37	Cytochrome c; complements defects of <i>S. cerevisiae</i> <i>cyc1 cyc7</i> double mutant; induced in high iron; alkaline repressed; repressed by nitric oxide; Hap43-dependent repression in low iron; regulated by Sef1, Sfu1
orf19.1795	<i>PUF3</i>		0,46		Ortholog of <i>S. cerevisiae</i> <i>Puf3</i> ; mRNA-binding protein involved in RNA catabolism; mutant is viable
orf19.1842	<i>BUD5</i>		0,35		Predicted GTP/GDP exchange factor for Rsr1; rat catheter biofilm induced
orf19.1847	<i>ARO10</i>		0,49		Aromatic decarboxylase; Ehrlich fusel oil pathway of aromatic alcohol biosynthesis; alkaline repressed; protein abundance affected by URA3 expression in CA1-4 strain; Spider biofilm induced
orf19.1862		-0,61			Possible stress protein; increased transcription associated with CDR1 and CDR2 overexpression or fluphenazine treatment; regulated by Sfu1, Nrg1, Tup1; stationary phase enriched protein; Spider biofilm induced
orf19.1887				0,36	Protein of unknown function
orf19.1896	<i>SSC1</i>		0,36		Heat shock protein; at yeast-form cell surface, not hyphae; antigenic; Gcn4-regulated; induced by amino acid starvation (3-AT) or by adherence to polystyrene; macrophage-repressed; sumoylation target; possibly essential
orf19.1945	<i>AUR1</i>		0,33		Inositolphosphorylceramide (IPC) synthase; catalyzes the key step in sphingolipid biosynthesis; antifungal drug target; flow model biofilm induced; Spider biofilm induced
orf19.1960	<i>CLN3</i>	-0,34			G1 cyclin; depletion abolishes budding and causes hyphal growth defects; farnesol regulated, functional in <i>S. cerevisiae</i> ; possibly essential (UAU1 method); other biofilm induced; Spider biofilm induced
orf19.1964		0,41			Protein of unknown function; repressed by fluphenazine treatment; induced by benomyl treatment and in an RHE model; regulated by Nrg1, Tup1
orf19.1978	<i>GIT2</i>	0,36	0,59	0,40	Putative glycerophosphoinositol permease; fungal-specific; repressed by alpha pheromone in SpiderM medium; Hap43-repressed; Spider biofilm induced
orf19.1979	<i>GIT3</i>	0,44	0,55		Glycerophosphocholine permease; white cell specific transcript; fungal-specific; alkaline repressed; caspofungin, macrophage/pseudohyphal-repressed; flow model biofilm induced; Spider biofilm induced
orf19.1995	<i>MNN24</i>		0,45		Alpha-1,2-mannosyltransferase; required for normal cell wall mannan content
orf19.1996	<i>CHA1</i>		0,52	0,47	Similar to catabolic ser/thr dehydratases; repressed by Rim101; induced in low iron; regulated on white-opaque switch; filament induced; Tn mutation affects filamentation; flow model biofilm induced; Spider biofilm repressed
orf19.2003	<i>HNM1</i>			0,36	Putative choline/ethanolamine transporter; mutation confers hypersensitivity to toxic ergosterol analog; colony morphology-related gene regulation by Ssn6; clade-associated gene expression
orf19.2005	<i>REG1</i>		0,44		Putative protein phosphatase regulatory subunit; Hap43-repressed gene; macrophage/pseudohyphal-induced; possibly regulated upon hyphal formation; flow model biofilm induced
orf19.2006.1	<i>COX17</i>			0,35	Putative copper metallochaperone; Hap43p-repressed gene; rat catheter biofilm induced; Spider biofilm induced
orf19.2008				0,34	Protein of unknown function
orf19.2048			0,71		Protein of unknown function; transcript positively regulated by Sfu1; Hap43 repressed; Spider biofilm induced
orf19.2076		-0,55			Protein of unknown function; <i>S. pombe</i> ortholog SPAC7D4.05 encodes a predicted hydrolase; Hap43-repressed; Spider biofilm induced
orf19.2108	<i>SOD6</i>		0,50	0,34	Copper- and zinc-containing superoxide dismutase; gene family includes SOD1, SOD4, SOD5, and SOD6; gene may contain an intron; Hap43-repressed; flow model and rat catheter biofilm induced
orf19.2128		-0,42	-0,51	-0,43	Protein of unknown function
orf19.2131			-0,36		Protein of unknown function
orf19.2132		-0,55	-0,53	-0,49	Protein of unknown function
orf19.2133	<i>LIP4</i>			-0,44	Secreted lipase, member of a differentially expressed lipase gene family with possible roles in nutrition and/or in creating an acidic microenvironment; expressed more strongly during mucosal infections than during systemic infections
orf19.2135	<i>TSM1</i>	-0,36			Putative transcription initiation factor TFIIID subunit; transcript is upregulated in clinical isolates from HIV+ patients with oral candidiasis; Nrg1-regulated

Supporting Information

orf19.2138	<i>ILS1</i>		-0,37		Putative isoleucyl-tRNA synthetase, the target of drugs including the cyclic beta-amino acid icofungipen/PLD-118/BAY-10-8888 and mupirocin; protein present in exponential and stationary growth phase yeast cultures
orf19.2143		-0,35	-0,37		Protein of unknown function
orf19.2146	<i>HAT2</i>	-0,40	-0,44	-0,40	Putative Hat1-Hat2 histone acetyltransferase complex subunit; role in DNA damage repair and morphogenesis; mutations cause constitutive pseudohyphal growth, caspofungin sensitivity; rat catheter and Spider biofilm repressed
orf19.215			0,48		Component of a complex containing the Tor2p kinase; possible a role in regulation of cell growth; Spider biofilm induced
orf19.2150		-0,40	-0,49	-0,35	Putative ortholog of mammalian electron transfer flavoprotein complex subunit ETF-alpha; Spider biofilm repressed
orf19.2151	<i>NAG6</i>	-0,48	-0,43	-0,41	Protein required for wild-type mouse virulence and wild-type cycloheximide resistance; putative GTP-binding motif; similar to <i>S. cerevisiae</i> Yor165Wp; in gene cluster that encodes enzymes of GlcNAc catabolism; no human or murine homolog
orf19.2154	<i>HXK1</i>		-0,39	-0,37	N-acetylglucosamine (GlcNAc) kinase; involved in GlcNAc utilization; required for wild-type hyphal growth and mouse virulence; GlcNAc-induced transcript; induced by alpha pheromone in SpiderM medium
orf19.2158	<i>NAG3</i>			-0,37	Putative MFS transporter; similar to Nag4; required for wild-type mouse virulence and cycloheximide resistance; in gene cluster that includes genes encoding enzymes of GlcNAc catabolism; Spider biofilm repressed
orf19.2163			-0,35		Protein of unknown function
orf19.2165			-0,49		Predicted hydrolase; induced by nitric oxide
orf19.2172	<i>ARA1</i>	-0,42			D-Arabinose dehydrogenase; dehydro-D-arabinono-1,4-lactone synthesis; active on D-arabinose, L-fucose, L-xylose, L-galactose; inhibited by metal ions, thiol group-specific reagents; induced on polystyrene adherence; Spider biofilm induced
orf19.2175		-0,33			Putative mitochondrial cell death effector; induced by nitric oxide; Spider biofilm induced; rat catheter biofilm repressed
orf19.2179	<i>SIT1</i>		-0,38		Transporter of ferrichrome siderophores, not ferrioxamine B; required for human epithelial cell invasion in vitro, not for mouse systemic infection; regulated by iron, Sfu1, Rfg1, Tup1, Hap43; rat catheter and Spider biofilm induced
orf19.2192	<i>GDH2</i>	0,33			Putative NAD-specific glutamate dehydrogenase; fungal-specific; transcript regulated by Nrg1, Mig1, Tup1, and Gcn4; stationary phase enriched protein; flow model biofilm induced; Spider biofilm induced
orf19.2199	<i>PHO86</i>	0,40			Putative endoplasmic reticulum protein; possibly adherence-induced
orf19.2241	<i>PST1</i>	-0,51			Putative 1,4-benzoquinone reductase; hyphal-induced; regulated by Cyr1, Ras1, Efg1, Nrg1, Rfg1, Tup1; Hap43-induced; Spider biofilm induced
orf19.2269		-0,41	-0,41		Putative 3-phosphoserine phosphatase; induced by benomyl or in azole-resistant strain that overexpresses MDR1; early-stage flow model biofilm induced; Spider biofilm repressed
orf19.2270	<i>SMF12</i>		0,52	0,38	Ortholog of <i>S. cerevisiae</i> Smf1; manganese transporter; Gcn4-regulated; Hap43, alkaline induced; caspofungin repressed; mutants are viable
orf19.2344	<i>ASR1</i>	-1,35	-0,59	-0,62	Heat shock protein; transcript regulated by cAMP, osmotic stress, ciclopirox olamine, ketoconazole; repressed by Cyr1, Ras1; colony morphology-related regulated by Ssn6; stationary phase enriched; Hap43-induced; Spider biofilm induced
orf19.238	<i>CCP1</i>	-0,39			Cytochrome-c peroxidase N terminus; Rim101, alkaline pH repressed; induced in low iron or by macrophage interaction; oxygen-induced activity; regulated by Sef1, Sfu1, and Hap43; Spider biofilm induced; rat catheter biofilm repressed
orf19.2396	<i>IFR2</i>	-0,48			Zinc-binding dehydrogenase; induced by benomyl, ciclopirox olamine, alpha pheromone, Hap43; regulated by oxidative stress via Cap1, osmotic stress via Hog1; protein present in exponential and stationary phase; rat catheter biofilm repressed
orf19.2445				-0,38	Putative dicarboxylic amino acid permease; fungal-specific (no human or murine homolog); induced by alpha pheromone in SpiderM medium
orf19.2451	<i>PGA45</i>	0,65		0,45	Putative GPI-anchored cell wall protein; repressed in core caspofungin response; Hog1-induced; regulated by Ssn6; Mob2-dependent hyphal regulation; flow model biofilm induced
orf19.251	<i>GLX3</i>	-0,52	-0,37		Glutathione-independent glyoxalase; binds human immunoglobulin E; alkaline, fluconazole, Hog1 repressed; hypoxia, oxidative stress via Cap1, Hap43 induced; stationary-phase enriched; rat catheter, Spider biofilm induced
orf19.2529.1				0,36	Protein of unknown function; Spider biofilm repressed
orf19.2531	<i>CSP37</i>	-0,43			Hyphal cell wall protein; role in progression of mouse systemic infection; predicted P-loop, divalent cation binding, N-glycosylation sites; expressed in yeast and hyphae; hyphal downregulated; stationary-phase enriched; GlcNAc-induced
orf19.2613	<i>ECM4</i>	-0,31			Cytoplasmic glutathione S-transferase; regulated by Nrg1, Tup1; induced in core stress response, in <i>cyr1</i> or <i>ras1</i> mutant (yeast or hyphal cells); Tn mutation affects filamentous growth; stationary phase enriched; Spider biofilm induced
orf19.2686				0,64	Protein of unknown function
orf19.2737		-0,61			Carbohydrate kinase domain-containing protein; Spider biofilm induced
orf19.2747	<i>RGT1</i>		0,46		Zn(II)2Cys6 transcription factor; transcriptional repressor involved in the regulation of glucose transporter genes; ortholog of <i>S. cerevisiae</i> Rgt1; mutants display decreased colonization of mouse kidneys
orf19.2762	<i>AHP1</i>	-0,56	-0,53	-0,40	Alkyl hydroperoxide reductase; immunogenic; fluconazole-induced; amphotericin B, caspofungin, alkaline repressed; core stress response induced; Ssk1/Nrg1/Tup1/Ssn6/Hog1 regulated; flow model biofilm induced; rat catheter biofilm repressed
orf19.2768	<i>AMS1</i>	-0,45			Putative alpha-mannosidase; transcript regulated by Nrg1; induced during cell wall regeneration; flow model biofilm induced; Spider biofilm induced
orf19.2769		-0,39			Putative protease B inhibitor; hyphal-induced expression; Cyr1p- and Ras1p-repressed
orf19.2770.1	<i>SOD1</i>		-0,37		Cytosolic copper- and zinc-containing superoxide dismutase; role in protection from oxidative stress; required for full virulence; alkaline induced by Rim101; induced by human blood; rat catheter, flow model and Spider biofilm repressed
orf19.2771	<i>BEM3</i>		0,39		Putative GTPase-activating protein (GAP) for Rho-type GTPase Cdc42p; involved in cell signaling pathways that control cell polarity; similar to <i>S. cerevisiae</i> Bem3p
orf19.2809	<i>CTN3</i>		0,48		Peroxisomal carnitine acetyl transferase; no obvious metabolic, hyphal, virulence defects in Ura+ strain; induced by macrophage engulfment, hyphal growth, starvation, nonfermentable carbon sources; rat catheter, Spider biofilm induced
orf19.2823	<i>RFG1</i>		0,50		HMG domain transcriptional repressor of filamentous growth and hyphal genes; in Tup1-dependent and -independent pathways; binds DNA; transcript not regulated by oxygen or serum; not responsible for hypoxic repression; Spider biofilm induced
orf19.2839	<i>CIRT4B</i>	-0,48			Cirt family transposase; transcript repressed in an azole-resistant strain that overexpresses CDR1 and CDR2; Hap43-repressed; flow model biofilm induced
orf19.2846		-0,63		-0,54	Protein of unknown function; Hap43-repressed; induced in core caspofungin response; regulated by yeast-hypha switch; Spider biofilm repressed
orf19.2896	<i>SOU1</i>	-0,67	-0,47		Enzyme involved in utilization of L-sorbose; has sorbitol dehydrogenase, fructose reductase, and sorbose reductase activities; NAD-binding site motif; transcriptional regulation affected by chromosome 5 copy number; Hap43p-induced gene
orf19.2990	<i>XOG1</i>		0,42	0,37	Exo-1,3-beta-glucanase; 5 glycosyl hydrolase family member; affects sensitivity to chitin and glucan synthesis inhibitors; not required for yeast-to-hypha transition or for virulence in mice; Hap43-induced; Spider biofilm induced
orf19.3007.2				-0,34	Protein of unknown function
orf19.3127	<i>CZF1</i>	-0,50			Transcription factor; regulates white-opaque switch; hyphal growth regulator; expression in <i>S. cerevisiae</i> causes dominant-negative inhibition of pheromone response; required for yeast cell adherence to silicone; Spider biofilm induced
orf19.3139				0,72	Putative NADP-dependent oxidoreductase; Hap43-repressed; induced by benomyl treatment; oxidative stress-induced via Cap1; rat catheter biofilm repressed

orf19.3150	<i>GRE2</i>	-0,41		-0,43	Putative reductase; Nrg1 and Tup1-regulated; benomyl- and hyphal-induced; macrophage/pseudohyphal-repressed; repressed by low iron; possibly involved in osmotic stress response; stationary phase enriched protein; Spider biofilm induced
orf19.3152	<i>AMO2</i>			-0,37	Protein similar to <i>A. niger</i> predicted peroxisomal copper amino oxidase; mutation confers hypersensitivity to toxic ergosterol analog; F-12/CO2 early biofilm induced
orf19.3171	<i>ACH1</i>	0,38	0,44	0,37	Acetyl-coA hydrolase; acetate utilization; nonessential; soluble protein in hyphae; antigenic in human; induced on polystyrene adherence; farnesol-, ketoconazole-induced; no human or murine homolog; stationary phase-enriched protein
orf19.320		-0,70	-0,44	-0,49	Predicted short chain dehydrogenase; Spider biofilm induced
orf19.3208	<i>DAL52</i>			3,35	Putative allantoinase permease; mutant is viable; similar but not orthologous to <i>S. cerevisiae</i> Dal5
orf19.3209	<i>FGR42</i>			-0,38	Protein lacking an ortholog in <i>S. cerevisiae</i> ; transposon mutation affects filamentous growth
orf19.3221	<i>CPA2</i>		0,51		Putative arginine-specific carbamoylphosphate synthetase; protein enriched in stationary phase yeast cultures; rat catheter biofilm induced; Spider biofilm induced
orf19.33		-0,45			Predicted ORF from Assembly 19; removed from Assembly 20; restored based on transcription data; similar to orf19.7550
orf19.334			0,74	0,42	Protein of unknown function; flow model biofilm induced; Spider biofilm induced; regulated by Sef1, Sfu1, and Hap43
orf19.3364			0,44		Protein of unknown function
orf19.338		-0,30			Putative glycoside hydrolase; stationary phase enriched protein; Hog1p-downregulated; shows colony morphology-related gene regulation by Ssn6p
orf19.3391	<i>ADK1</i>	-0,44			Putative adenylate kinase; repressed in hyphae; macrophage-induced protein; adenylate kinase release used as marker for cell lysis; possibly essential (UAU1 method); flow model biofilm induced; rat catheter and Spider biofilm repressed
orf19.3392	<i>DOG1</i>	-0,60	-0,62	-0,43	Putative 2-deoxyglucose-6-phosphatase; haloacid dehalogenase hydrolase/phosphatase superfamily; similar to <i>S. cerevisiae</i> Dog1, Dog2, Hor1, Rhr2; regulated by Nrg1, Tup1; Spider biofilm repressed
orf19.3393		-0,33	-0,57	-0,37	Putative DEAD-box helicase; Hap43-induced; Spider biofilm induced
orf19.3396	<i>HCH1</i>	-0,44	-0,55		Ortholog of <i>S. cerevisiae</i> Hch1, a regulator of heat shock protein Hsp90; regulated by Gcn4; induced in response to amino acid starvation (3-aminotriazole treatment); mutants are viable
orf19.3399		-0,40	-0,47	-0,42	Protein of unknown function
orf19.34	<i>GIT1</i>	0,56			Glycerophosphoinositol permease; involved in utilization of glycerophosphoinositol as a phosphate source; Rim101-repressed; virulence-group-correlated expression
orf19.3400	<i>COQ3</i>	-0,51	-0,54	-0,40	Protein with a predicted role in coenzyme Q biosynthesis; transcriptionally induced by interaction with macrophages; possibly an essential gene, disruptants not obtained by UAU1 method
orf19.3401	<i>CTA1</i>	-0,41	-0,52	-0,42	Protein similar to <i>S. cerevisiae</i> Mos10p, which affects <i>S. cerevisiae</i> filamentous growth; activates transcription in 1-hybrid assay in <i>S. cerevisiae</i> ; protein levels increase under weak acid stress; nonessential
orf19.3402	<i>FPG1</i>	-0,39			Formamidopyrimidine DNA glycosylase, involved in repair of gamma-irradiated DNA; Hap43p-repressed gene
orf19.3405	<i>ZCF18</i>			-0,40	Putative Zn(II)2Cys6 transcription factor; heterozygous null mutant displays sensitivity to virgineone and decreased colonization of mouse kidneys
orf19.3407	<i>RAD18</i>			-0,37	Putative transcription factor with zinc finger DNA-binding motif; Hap43p-repressed gene
orf19.3409	<i>SEC12</i>	-0,41	-0,50	-0,43	Putative guanyl-nucleotide exchange factor; induced in high iron; Hap43-repressed
orf19.3411				-0,53	Protein of unknown function
orf19.3412	<i>ATG15</i>			-0,38	Putative lipase; fungal-specific (no human or murine homolog); Hap43p-repressed gene
orf19.3414	<i>SUR7</i>	-0,39		-0,36	Protein required for normal cell wall, plasma membrane, cytoskeletal organization, endocytosis; localizes to eisosome subdomains of plasma membrane; four transmembrane motifs; mutant shows ectopic, chitin-rich cell wall; fluconazole-induced
orf19.3415.1	<i>RPL32</i>	-0,40	-0,54		Component of the large (60S) ribosomal subunit; Spider biofilm repressed
orf19.3417	<i>ACF2</i>	-0,55	-0,65	-0,55	Putative endo-1,3-beta-glucanase; fungal-specific (no human or murine homolog)
orf19.3423	<i>TIF3</i>		-0,44		Putative translation initiation factor; genes encoding ribosomal subunits, translation factors, and tRNA synthetases are downregulated upon phagocytosis by murine macrophage
orf19.3426	<i>ANB1</i>	-0,40	-0,50	-0,37	Translation initiation factor eIF-5A; repressed in hyphae vs yeast cells; downregulated upon phagocytosis by murine macrophage; Hap43-induced; GlnAc-induced protein; Spider biofilm repressed
orf19.3427				-0,41	Protein of unknown function
orf19.3428		-0,31			Protein of unknown function; flow model biofilm induced
orf19.3430		-0,37			Plasma membrane-associated protein; physically interacts with TAP-tagged Nop1p
orf19.3433	<i>OYE23</i>	-0,52		-0,65	Putative NADPH dehydrogenase; induced by nitric oxide, benomyl; oxidative stress-induced via Cap1; Hap43p-repressed; rat catheter biofilm induced
orf19.3438				-0,34	Protein of unknown function
orf19.3439			-0,37	-0,52	Protein of unknown function; Cyr1-repressed; rat catheter and Spider biofilm induced
orf19.344				0,35	Protein of unknown function; upregulated by fluphenazine treatment or in an azole-resistant strain that overexpresses CDR1 and CDR2; transcript possibly regulated by Tac1
orf19.3441	<i>FRP6</i>	-0,35			Putative ammonia transport protein; regulated by Nrg1 and Tup1; regulated by Ssn6; induced by human neutrophils
orf19.3442		-0,47	-0,48	-0,41	Putative oxidoreductase; Hap43-repressed gene
orf19.3443	<i>OYE2</i>	-0,60	-0,51	-0,56	Putative NADPH dehydrogenase; induced by nitric oxide; Spider biofilm induced
orf19.3445	<i>HOC1</i>	-0,44	-0,46	-0,43	Protein with similarity to mannosyltransferases; similar to <i>S. cerevisiae</i> Hoc1p and <i>C. albicans</i> Och1p
orf19.3446		-0,43			Protein of unknown function
orf19.3447		-0,42		-0,42	Protein of unknown function
orf19.3448		-0,46			Protein of unknown function; ketoconazole-repressed
orf19.3449		-0,34			Protein of unknown function
orf19.3450.1				-0,41	Protein of unknown function
orf19.3455		-0,45		-0,35	Putative mitochondrial inner membrane magnesium transporter; possibly an essential gene, disruptants not obtained by UAU1 method
orf19.3456		-0,71	-0,63	-0,59	Protein with a predicted serine/threonine kinase and tyrosine kinase domain; possibly an essential gene, disruptants not obtained by UAU1 method
orf19.3457	<i>SWD3</i>	-0,50		-0,40	Protein of unknown function
orf19.3458		-0,51	-0,60	-0,45	Protein of unknown function
orf19.3459		-0,52	-0,47	-0,47	Putative serine/threonine/tyrosine (dual-specificity) kinase; disruptants not obtained by UAU1 method
orf19.3460		-0,73		-0,52	Protein of unknown function; mRNA binds She3; transcript regulated upon yeast-hypha switch; induced in oralpharyngeal candidiasis
orf19.3462	<i>SAR1</i>	-0,46	-0,53	-0,40	Functional homolog of <i>S. cerevisiae</i> Sar1; which is required for ER-to-Golgi protein transport; binds GTP; similar to small GTPase superfamily proteins; gene has intron; Hap43-induced; rat catheter biofilm repressed
orf19.3463		-0,37	-0,51	-0,35	Putative GTPase; role in 60S ribosomal subunit biogenesis; Spider biofilm induced
orf19.3465	<i>RPL10A</i>	-0,34	-0,48		Predicted ribosomal protein; downregulated upon phagocytosis by murine macrophages; Hap43-induced; Spider biofilm repressed
orf19.3467	<i>SEC27</i>	-0,46	-0,41	-0,35	Protein of unknown function
orf19.3469		-0,43		-0,33	<i>S. cerevisiae</i> ortholog Stb1 has a role in regulation of MBF-specific transcription at Start; induced in a <i>cyr1</i> null mutant; Spider biofilm induced
orf19.3473				-0,40	Protein of unknown function
orf19.3474	<i>IPL1</i>			-0,41	Putative Aurora kinase; Hap43-induced; induced during planktonic growth; possibly an essential gene, disruptants not obtained by UAU1 method
orf19.3477		-0,39	-0,44		Putative pseudouridine synthase; predicted role in snRNA pseudouridine synthesis, tRNA pseudouridine synthesis; Spider biofilm induced
orf19.3478	<i>NIP7</i>	-0,45	-0,58	-0,39	Putative nucleolar protein with role in ribosomal assembly; hyphal-induced; Hap43-induced; Spider biofilm induced
orf19.3480		-0,45			Protein of unknown function
orf19.3482		-0,49	-0,53	-0,52	Protein of unknown function

Supporting Information

orf19.3496	<i>CHC1</i>	-0,43	-0,36	-0,37	Clathrin heavy chain; subunit of the major coat protein; role in intracellular protein transport and endocytosis; flow model and rat catheter biofilm repressed
orf19.3498				-0,35	Protein of unknown function
orf19.3501		-0,41		-0,40	<i>S. cerevisiae</i> ortholog Pxl1 localizes to sites of polarized growth and is required for selection and/or maintenance of polarized growth sites; Hog1p-repressed
orf19.3503		-0,51		-0,55	Protein of unknown function
orf19.3504	<i>RPL23A</i>		-0,42		Ribosomal protein; downregulated upon phagocytosis by murine macrophage; Hap43-induced; sumoylation target; Spider biofilm repressed
orf19.3506	<i>DBR1</i>			-0,35	Debranchase; homozygous mutant accumulates lariat intermediates of mRNA splicing; rat catheter biofilm repressed
orf19.3507	<i>MCR1</i>	-0,55	-0,47	-0,39	NADH-cytochrome-b5 reductase; soluble in hyphae; alkaline downregulated; farnesol, ketoconazole or flucytosine induced; protein present in exponential and stationary growth phase yeast; YNB biofilm induced; rat catheter biofilm repressed
orf19.3508		-0,60	-0,43	-0,46	Putative protein of unknown function; stationary phase enriched protein
orf19.3529	<i>ABP2</i>			0,33	Putative alpha-actinin-like protein; induced by alpha pheromone in SpiderM medium
orf19.3548.1	<i>WH11</i>	-0,38			White-phase yeast transcript; expression in opaques increases virulence/switching; mutant switches as WT; Hap43, hypoxia, ketoconazol induced; required for RPMI biofilm; Bcr1-induced in RPMI a/a biofilm; rat catheter, Spider biofilm induced
orf19.3603	<i>MFG1</i>		0,39		Regulator of filamentous growth; required for biofilm formation, virulence; interacts with Flo8 and Mss11
orf19.3642	<i>SUN41</i>	-0,43	-0,48	-0,44	Cell wall glycosidase; role in biofilm formation and cell separation; possibly secreted; hypoxia, hyphal induced; caspofungin repressed; Efg1, Cph1 regulated; O-glycosylated, possible Kex2 substrate; 5'-UTR intron; Spider biofilm induced
orf19.3643				-0,42	Protein of unknown function; Hap43-repressed gene
orf19.3644		-0,41	-0,38	-0,41	Protein of unknown function; Cyr1-repressed; rat catheter and Spider biofilm induced
orf19.3646	<i>CTR1</i>		0,33		Copper transporter; transcribed in low copper; induced Mac1, Tye7, macrophage interaction, alkaline pH via Rim101; 17-beta-estradiol repressed; complements <i>S. cerevisiae</i> ctr1 ctr3 copper transport mutant; flow model/Spider biofilm induced
orf19.3647	<i>SEC8</i>	-0,46	-0,46	-0,37	Predicted subunit of the exocyst complex, involved in exocytosis; localizes to a crescent on the surface of the hyphal tip
orf19.3649		-0,64	-0,76	-0,54	Protein of unknown function
orf19.3651	<i>PGK1</i>	-0,81	-0,65	-0,49	Phosphoglycerate kinase; localizes to cell wall and cytoplasm; antigenic in murine/human infection; flow model biofilm, Hog1-, Hap43-, GCN-induced; repressed upon phagocytosis; repressed in Spider biofilms by Bcr1, Ndt80, Rob1, Brg1
orf19.3653	<i>FAT1</i>		-0,42		Predicted enzyme of sphingolipid biosynthesis; upregulated in biofilm
orf19.3656	<i>COX15</i>	-0,38			Cytochrome oxidase assembly protein; transcript regulated by Nrg1 and Tup1; alkaline repressed; Hap43-repressed; early-stage flow model biofilm induced; Spider biofilm repressed
orf19.3658				-0,38	Protein of unknown function
orf19.3659		-0,52			Putative CTD phosphatase; role in dephosphorylation of RNA polymerase II C-terminal domain, transcription from RNA polymerase II promoter; flow model biofilm induced
orf19.3660		-0,45	-0,54	-0,39	Protein of unknown function
orf19.3664	<i>HSP31</i>	0,61	1,40	0,88	Putative 30 kda heat shock protein; repressed during the mating process; rat catheter biofilm induced
orf19.3668	<i>HGT2</i>	0,32			Putative MFS glucose transporter; 20 member <i>C. albicans</i> glucose transporter family; 12 probable membrane-spanning segments; expressed in rich medium with 2% glucose; rat catheter and Spider biofilm induced
orf19.3669	<i>SHA3</i>		0,46	0,33	Putative ser/thr kinase involved in glucose transport; Tn mutation affects filamentous growth; fluconazole-induced; ketoconazole-repressed; induced in by alpha pheromone in SpiderM; possibly essential; flow model biofilm induced
orf19.367	<i>CNH1</i>	0,32			Na ⁺ /H ⁺ antiporter; required for wild-type growth, cell morphology, and virulence in a mouse model of systemic infection; not transcriptionally regulated by NaCl; fungal-specific (no human or murine homolog)
orf19.3670	<i>GAL1</i>		0,33	0,34	Galactokinase; galactose, Mig1, Tup1, Hap43 regulated; fluconazole, ketoconazole-induced; stationary phase enriched protein; GlcNAc-induced protein; farnesol, hypoxia-repressed in biofilm; rat catheter and Spider biofilm induced
orf19.3672	<i>GAL10</i>			0,38	UDP-glucose 4-epimerase; galactose utilization; mutant has cell wall defects and increased filamentation; GlcNAc-, fluconazole- and ketoconazole-induced; stationary phase enriched protein; rat catheter and flow model biofilm induced
orf19.3675	<i>GAL7</i>			0,43	Putative galactose-1-phosphate uridyl transferase; downregulated by hypoxia, upregulated by ketoconazole; macrophage/pseudohyphal-repressed
orf19.3707	<i>YHB1</i>	-0,63			Nitric oxide dioxygenase; acts in nitric oxide scavenging/detoxification; role in virulence in mouse; transcript activated by NO, macrophage interaction; Hap43, hypha repressed; mRNA binds She3
orf19.3733	<i>IDP2</i>		0,77	0,64	Isocitrate dehydrogenase; white-opaque switch regulated; morphology-regulation by Ssn6; protein in exponential and stationary phase yeast; Hap43-repressed; Spider biofilm repressed by Bcr1, Tec1, Ndt80, Rob1, Brg1; Spider biofilm induced
orf19.3740	<i>PGA23</i>	-0,66			Putative GPI-anchored protein of unknown function; Rim101-repressed; Cyr1-regulated; colony morphology-related gene regulation by Ssn6
orf19.3770	<i>ARG8</i>		0,42		Putative acetylornithine aminotransferase; Gcn2, Gcn4 regulated; rat catheter biofilm induced; Spider biofilm induced
orf19.3803	<i>MNN22</i>		0,36		Alpha-1,2-mannosyltransferase; required for normal cell wall mannan; regulated by Tsa1, Tsa1B at 37 deg; repressed in core stress response; NO, Hog1 induced; confers sensitivity to cell wall perturbing agents; Spider biofilm repressed
orf19.3839	<i>SAP10</i>			-0,33	Secreted aspartyl protease; roles in adhesion, virulence (RHE model), cell surface integrity; distinct specificity from Sap9; at cell membrane and wall; GPI-anchored; induced in low iron; Tbf1-activated; Spider biofilm induced
orf19.385	<i>GCV2</i>	0,48	0,41	0,44	Glycine decarboxylase P subunit; protein of glycine catabolism; repressed by Efg1; Hog1-induced; induced by Rim101 at acid pH; transcript induced in elevated CO2; stationary phase enriched protein
orf19.3854			0,39		Ortholog of <i>S. cerevisiae</i> Sat4; amphotericin B induced; clade-associated gene expression; Spider biofilm induced
orf19.3895	<i>CHT2</i>	0,45	0,41		GPI-linked chitinase; required for normal filamentous growth; repressed in core caspofungin response; fluconazole, Cyr1, Efg1, pH-regulated; mRNA binds She3 and is localized to yeast-form buds and hyphal tips; Spider biofilm repressed
orf19.3932		-0,56		-0,37	Predicted RNA binding protein; stationary phase enriched; induced in core caspofungin response; induced by nitric oxide independent of Yhb1; repressed in <i>ssr1</i> null; ketoconazole, hypoxia induced; Spider biofilm induced
orf19.3932.1		-0,53		-0,51	Protein of unknown function
orf19.3988			1,54	0,99	Putative adhesin-like protein; induced by Mnl1 under weak acid stress; rat catheter and Spider biofilm induced
orf19.4066			0,36		Putative glycerol-3-phosphate acyltransferase; Hog1-repressed
orf19.4082	<i>DDR48</i>	-0,71	-0,35		Immunogenic stress-associated protein; filamentation regulated; induced by benomyl/caspofungin/ketoconazole or in azole-resistant strain; Hog1, farnesol, alkaline repressed; stationary phase enriched; Spider, flow model biofilm induced
orf19.4192	<i>CDC14</i>		-0,40	-0,39	Protein involved in exit from mitosis and morphogenesis; ortholog of <i>S. cerevisiae</i> Cdc14p, which is a dual-specificity phosphatase and cell-cycle regulator; suppresses <i>S. cerevisiae</i> <i>cdc15-lyt1</i> , <i>dbf2-2</i> , and (partially) <i>tem1</i> mutant phenotypes
orf19.4192.1		-0,47	-0,60	-0,37	Protein of unknown function
orf19.4193		-0,47	-0,47		Protein of unknown function
orf19.4194		-0,50		-0,36	Putative TFIIF complex subunit; possibly an essential gene, disruptants not obtained by UAU1 method
orf19.4195.1	<i>FCA1</i>	-0,49	-0,61		Cytosine deaminase; enzyme of pyrimidine salvage; functional homolog of <i>S. cerevisiae</i> Fcy1p; mutation is associated with resistance to flucytosine (5-FC) in a clinical isolate; hyphal downregulated; gene has intron
orf19.4203		-0,48	-0,37		Protein of unknown function
orf19.4204		-0,38			Protein of unknown function

orf19.4206		-0,44	-0,47	-0,37	Protein of unknown function
orf19.4207				-0,38	Predicted ORF from Assembly 19; removed from Assembly 20; restored based on comparative genome analysis
orf19.4208	<i>RAD52</i>	-0,44	-0,50	-0,52	Required for homologous DNA recombination, repair of UV- or MMS-damaged DNA, telomere length, UV-induced LOH; constitutive expression, MMS-induced; weakly complements <i>S. cerevisiae</i> rad52 mutant; slow growth, increased white-to-opaque switch
orf19.4209		-0,52	-0,58	-0,48	Protein of unknown function
orf19.4211			-0,44		Multicopper oxidase; for growth in low iron, prostaglandin E2 synthesis; ketoconazole/caspofungin/amphotericin B repressed; Sef1/Sfu1/Hap43 regulated; reports differ if functional homolog of ScFet3; rat catheter and Spider biofilm induced
orf19.4213				-0,34	Putative iron transport multicopper oxidase precursor; flucytosine induced; caspofungin repressed
orf19.4215	<i>FET34</i>	-0,34	-0,58	-0,33	Multicopper ferroxidase; induced by low iron, ciclopirox olamine, ketoconazole, hypoxia; alkaline induced by Rim101; repressed in fluconazole-resistant isolate; Sfu1, Hog1 repressed; complements <i>S. cerevisiae</i> fet3; Spider biofilm induced
orf19.4246		-0,58	-0,34		Protein with similarity to <i>S. cerevisiae</i> Ykr070w; Tn mutation affects filamentation; Hog1-repressed; colony morphology-related gene regulation by Ssn6p; induced during cell wall regeneration; possibly essential
orf19.4255	<i>ECM331</i>	-0,50	-0,74	-0,47	GPI-anchored protein; mainly at plasma membrane, also at cell wall; Hap43, caspofungin-induced; Plc1-regulated; Hog1, Rim101-repressed; colony morphology-related regulated by Ssn6; induced by ketoconazole and hypoxia
orf19.4274	<i>PUT1</i>		0,41		Putative proline oxidase; alkaline upregulated by Rim101; flow model biofilm induced; Spider biofilm induced
orf19.4384	<i>HXT5</i>	-0,49			Putative sugar transporter; induced by ciclopirox olamine; Snf3-induced; alkaline repressed; colony morphology-related gene regulation by Ssn6; possibly essential gene
orf19.4393	<i>CIT1</i>		0,61	0,39	Citrate synthase; induced by phagocytosis; induced in high iron; Hog1-repressed; Efg1-regulated under yeast, not hyphal growth conditions; present in exponential and stationary phase; Spider biofilm repressed; rat catheter biofilm induced
orf19.4432	<i>KSP1</i>		0,40		Putative serine/threonine protein kinase; mRNA binds She3 and is localized to hyphal tips; mutation confers hypersensitivity to amphotericin B
orf19.4436	<i>GPX3</i>	-0,54			Putative glutathione peroxidase involved in Cap1p-dependent oxidative stress response, required for Cap1p oxidation in response to H2O2; planktonic growth-induced
orf19.4438	<i>RME1</i>		0,71		Zinc finger protein; controls meiosis in <i>S. cerevisiae</i> ; white-specific transcript; upregulation correlates with clinical development of fluconazole resistance; Upc2-regulated in hypoxia; flow model biofilm induced; Spider biofilm repressed
orf19.4443	<i>YPD1</i>		-0,48		Phosphohistidine intermediate protein in a phosphorelay signal transduction pathway; residue His69 is the phosphoacceptor histidine; predicted to be soluble and cytosolic; functional homolog of <i>S. cerevisiae</i> Ypd1p
orf19.4445			0,42	0,35	Protein of unknown function; Plc1p-regulated; expression induced early upon infection of reconstituted human epithelium (RHE), while expression of the <i>C. dubliniensis</i> ortholog is not; mutant is viable; Spider biofilm induced
orf19.4450.1			0,59		Protein conserved among the CTG-clade; 2 adjacent upstream SRE-1 elements; highly up-regulated in cecum-grown cells in a Cph2-dependent manner; Hap43-repressed; rat catheter, Spider and flow model biofilm induced
orf19.4475	<i>KTR4</i>	-0,43			Mannosyltransferase; induced during cell wall regeneration; fungal-specific (no human or murine homolog); Bcr1-repressed in RPM1 a/a biofilms
orf19.4476				-0,51	Protein with a NADP-dependent oxidoreductase domain; transcript induced by ketoconazole; rat catheter and Spider biofilm induced
orf19.4477	<i>CSH1</i>	-0,75	-0,46	-0,62	Aldo-keto reductase; role in fibronectin adhesion, cell surface hydrophobicity; regulated by temperature, growth phase, benomyl, macrophage interaction; azole resistance associated; Spider biofilm induced; rat catheter biofilm repressed
orf19.4526	<i>HSP30</i>		1,79	1,06	Putative heat shock protein; fluconazole repressed; amphotericin B induced; Spider biofilm induced; rat catheter biofilm induced
orf19.4527	<i>HGT1</i>	0,33	0,35		High-affinity MFS glucose transporter; induced by progesterone, chloramphenicol, benomyl; likely essential for growth; protein newly produced during adaptation to the serum; rat catheter and Spider biofilm induced
orf19.4530.1		-0,34			Protein of unknown function; regulated by Nrg1, Tup1; Spider and flow model biofilm induced
orf19.4555	<i>ALS4</i>	-0,69	-0,64		GPI-anchored adhesin; role in adhesion, germ tube induction; growth, temperature regulated; expressed during infection of human buccal epithelial cells; repressed by vaginal contact; biofilm induced; repressed during chlamyospore formation
orf19.4557		-0,39			Protein of unknown function
orf19.4565	<i>BGL2</i>		-0,31		Cell wall 1,3-beta-glucosyltransferase; mutant has cell-wall and growth defects, but wild-type 1,3- or 1,6-beta-glucan content; antigenic; virulence role in mouse systemic infection; rat catheter biofilm induced
orf19.4593	<i>RGA2</i>		0,36		Putative GTPase-activating protein (GAP) for Rho-type GTPase Cdc42; involved in cell signaling pathways controlling cell polarity; induced by low-level peroxide stress; flow model biofilm induced
orf19.4599	<i>PHO89</i>	0,80	0,69	0,40	Putative phosphate permease; transcript regulated upon white-opaque switch; alkaline induced by Rim101; possibly adherence-induced; F-12/CO2 model, rat catheter and Spider biofilm induced
orf19.4609				0,49	Putative diene lactone hydrolase; protein abundance is affected by URA3 expression in the CAI-4 strain background; protein present in exponential and stationary growth phase yeast cultures; rat catheter biofilm repressed
orf19.4645	<i>BEM1</i>		0,38		Protein required for wild-type budding, hyphal growth, and virulence in a mouse systemic infection; suppresses pseudohyphal and filamentous growth defects of various <i>S. cerevisiae</i> mutants and heat sensitivity of <i>S. cerevisiae</i> cdc24-4 mutant
orf19.4655	<i>OPT6</i>	-0,47			Putative oligopeptide transporter; fungal-specific (no human or murine homolog); expression of OPT6, OPT7, or OPT8 does not suppress defect of mutant lacking Opt1p, Opt2p, and Opt3p; alleles are nonidentical
orf19.4664	<i>NAT4</i>			-0,37	Putative histone acetyltransferase; involved in regulation of white-opaque switch; early-stage flow model biofilm induced; Spider biofilm induced
orf19.4666			-0,47	-0,45	Protein of unknown function; hyphal-induced expression, regulated by Cyr1, Ras1, Efg1; Spider biofilm induced
orf19.467	<i>WOR3</i>	0,59	0,96	1,00	Transcription factor; modulator of white-opaque switch; induced in opaque cells; promoter bound by Wor1; overexpression at 25 degr shifts cells to opaque state; deletion stabilizes opaque cells at higher temperatures; Spider biofilm induced
orf19.4674.1	<i>CRD2</i>	-0,50			Metallothionein; for adaptation to growth in high copper; basal transcription is cadmium-repressed; Ssn6 regulated; complements copper sensitivity of an <i>S. cerevisiae</i> cup1 mutant; regulated by Sef1, Sfu1, and Hap43; Spider biofilm induced
orf19.4679	<i>AGP2</i>	-0,53			Amino acid permease; hyphal repressed; white-opaque switch regulated; induced in core caspofungin response, during cell wall regeneration, by flucytosine; regulated by Sef1, Sfu1, and Hap43; rat catheter and Spider biofilm induced
orf19.4682	<i>HGT17</i>			-0,39	Putative MFS family glucose transporter; 20 members in <i>C. albicans</i> ; 12 probable membrane-spanning segments; induced at low (0.2%, compared to 2%) glucose in rich media; Spider biofilm induced
orf19.4688	<i>DAG7</i>	-0,51	-0,43		Secretory protein; a-specific, alpha-factor induced; mutation confers hypersensitivity to toxic ergosterol analog; fluconazole-induced; induced during chlamyospore formation in <i>C. albicans</i> and <i>C. dubliniensis</i>
orf19.4698	<i>PTC8</i>		0,39		Predicted type 2C protein phosphatase, ser/thr-specific; required for hyphal growth; transcript induced by stress; flow model biofilm induced; Spider biofilm induced
orf19.4752	<i>MSN4</i>		0,41		Zinc finger transcription factor; similar to <i>S. cerevisiae</i> Msn4, but not a significant stress response regulator in <i>C. albicans</i> ; partly complements STRE-activation defect of <i>S. cerevisiae</i> msn2 msn4 double mutant; flow model biofilm induced
orf19.4773	<i>AOX2</i>	0,53	0,97		Alternative oxidase; cyanide-resistant respiration; induced by antimycin A, oxidants; growth; Hap43, chlamyospore formation repressed; rat catheter, Spider biofilm induced; regulated in Spider biofilms by Bcr1, Tec1, Ndt80, Brg1

Supporting Information

orf19.4775	<i>CTA8</i>		0,36		Essential transcription factor, mediates heat shock transcriptional induction; in the absence of heat stress, Cta8p levels are modulated by growth temperature to regulate basal expression of genes involved in protein folding
orf19.4777	<i>DAK2</i>	-0,58			Putative dihydroxyacetone kinase; repressed by yeast-hypha switch; fluconazole-induced; caspofungin repressed; protein enriched in stationary phase yeast cultures; flow model biofilm induced; rat catheter and Spider biofilm repressed
orf19.4779				0,47	Putative transporter; slightly similar to the Sit1p siderophore transporter; Gcn4p-regulated; fungal-specific; induced by Mnl1p under weak acid stress
orf19.4784	<i>CRP1</i>		0,63	0,36	Copper transporter; CPx P1-type ATPase; mediates Cu resistance; similar to Menkes and Wilson disease proteins; copper-induced; Tbf1-activated; suppresses Cu sensitivity of <i>S. cerevisiae</i> cup1 mutant; flow model biofilm induced
orf19.4788	<i>ARG5,6</i>		0,44		Arginine biosynthetic enzyme; processed in <i>S. cerevisiae</i> into 2 polypeptides with acetylglutamate kinase (Arg6) activity and acetylglutamate-phosphate reductase (Arg5) activity; Gcn4 regulated; alkaline repressed; Spider biofilm induced
orf19.48	<i>RPM2</i>		0,44		Mitochondrial RNase P subunit; roles in nuclear transcription, cytoplasmic and mitochondrial RNA processing, mitochondrial translation; virulence-group-correlated expression; likely essential (UAI1 method); rat catheter biofilm induced
orf19.4898		-0,46			Putative protein of unknown function; induced by prostaglandins
orf19.4899	<i>GCA1</i>	-0,47			Extracellular/plasma membrane-associated glucoamylase; expressed in rat oral infection; regulated by carbohydrates, pH, galactose; promotes biofilm matrix formation; flow model biofilm induced; Bcr1 repressed in RPM1 a/a biofilms
orf19.4906			0,39		Putative adhesin-like protein; positively regulated by Tbf1; Spider biofilm induced
orf19.4907				0,77	Putative protein of unknown function; Hap43p-repressed gene; increased transcription is observed upon fluphenazine treatment; possibly transcriptionally regulated by Tac1p; induced by nitric oxide; fungal-specific (no human/murine homolog)
orf19.4914.1	<i>BLP1</i>	-0,52			Protein of unknown function, serum-induced
orf19.4932				0,34	Protein of unknown function
orf19.4940				0,34	Putative histidine permease; fungal-specific (no human or murine homolog); Hap43p-induced gene
orf19.4941	<i>TYE7</i>			0,34	bHLH transcription factor; control of glycolysis; required for biofilm formation; hyphally regulated by Cph1, Cyr1; flucytosine, Hog1 induced; amphotericin B, caspofungin repressed; induced in flow model biofilm and planktonic cultures
orf19.4943	<i>PSA2</i>	-0,68		-0,36	Mannose-1-phosphate guanyltransferase; Hap43, macrophage-repressed; stationary phase enriched protein; Spider biofilm induced; rat catheter biofilm repressed
orf19.4980	<i>HSP70</i>	-0,37			Putative hsp70 chaperone; role in entry into host cells; heat-shock, amphotericin B, cadmium, ketoconazole-induced; surface localized in yeast and hyphae; antigenic in host; farnesol-downregulated in biofilm; Spider biofilm induced
orf19.5005	<i>OSM2</i>		0,38		Putative mitochondrial fumarate reductase; regulated by Ssn6p, Gcn2p, and Gcn4p; Hog1p-downregulated; stationary phase enriched protein; Hap43p-repressed gene
orf19.5025	<i>MET3</i>		-0,43		ATP sulfurlyase; sulfate assimilation; repressed by Met, Cys, Sfu1, or in fluconazole-resistant isolate; Hog1, caspofungin, white phase-induced; induced on biofilm formation, even in presence of Met and Cys; Spider, F-12/CO2 biofilm induced
orf19.5031	<i>SSK1</i>	-0,32			Response regulator of two-component system; role in oxidative stress response, cell wall biosynthesis, virulence, hyphal growth on solid media; expressed in hyphae and yeast; peroxisomal targeting sequence (PTS1); Spider biofilm induced
orf19.5032	<i>SIM1</i>		-0,34		Adhesin-like protein; involved in cell wall maintenance, redundant with Sun41; possibly secreted; macrophage-repressed; repressed by Rim101, Cyr1, Ras1; Spider biofilm induced
orf19.5045	<i>PTP2</i>	-0,39			Predicted protein tyrosine phosphatase; involved in regulation of MAP kinase Hog1 activity; induced by Mnl1 under weak acid stress; rat catheter and Spider biofilm induced
orf19.5079	<i>CDR4</i>		0,57		Putative ABC transporter superfamily; fluconazole, Sfu1, Hog1, core stress response induced; caspofungin repressed; fluconazole resistance not affected by mutation or correlated with expression; rat catheter and flow model biofilm induced
orf19.5125				-0,35	Protein of unknown function; induced by ketoconazole; Spider, F-12/CO2 and flow model biofilm induced
orf19.5158		-0,50			Protein with similarity to a human gene associated with colon cancer and to orf19.5158; regulated by Gcn4, Cyr1; induced by amino acid starvation; macrophage-induced protein, macrophage-repressed; Spider biofilm induced
orf19.5227		-0,43			Chaperone component; involved in assembly of alpha subunits into the 20S proteasome; flow model biofilm induced
orf19.5285	<i>PST3</i>			0,34	Putative flavodoxin; YNB biofilm induced; stationary phase enriched protein; rat catheter and Spider biofilm repressed
orf19.5293		0,35			Protein of unknown function
orf19.5305	<i>RHD3</i>	0,53			GPI-anchored yeast-associated cell wall protein; induced in high iron; clade-associated gene expression; not essential for cell wall integrity; fluconazole-repressed; flow model and Spider biofilm repressed
orf19.5337	<i>UBC15</i>	0,44			Putative E2 ubiquitin-conjugating enzyme
orf19.5342.2				-0,36	Protein of unknown function; protein newly produced during adaptation to the serum
orf19.5383	<i>PMA1</i>	0,47	0,43	0,40	Plasma membrane H(+)-ATPase; highly expressed, comprises 20-40% of total plasma membrane protein; levels increase at stationary phase transition; fluconazole induced; caspofungin repressed; upregulated in RHE model; Spider biofilm repressed
orf19.54	<i>RHD1</i>	-0,35	-0,36	-0,44	Putative beta-mannosyltransferase required for the addition of beta-mannose to the acid-labile fraction of cell wall phosphopeptidomannan; 9-gene family member; regulated on yeast-hypha and white-opaque switches; Spider biofilm repressed
orf19.5417	<i>DOT5</i>	-0,33			Putative nuclear thiol peroxidase; alkaline downregulated; sumoylation target; Spider and flow model biofilm induced
orf19.5431		-0,48			Protein of unknown function; Hap43-repressed; Spider biofilm induced
orf19.5455		0,43			Protein of unknown function
orf19.5510				-0,33	Protein of unknown function
orf19.5514				-0,46	Ortholog of <i>S. pombe</i> SPCC550.08, an N-acetyltransferase; transcript induced during growth in the mouse cecum
orf19.5515		-0,37			Protein of unknown function
orf19.5516		-0,47	-0,43		Protein of unknown function
orf19.5517			-0,60	-0,37	Similar to alcohol dehydrogenases; induced by benomyl treatment, nitric oxide; induced in core stress response; oxidative stress-induced via Cap1; Spider biofilm repressed
orf19.5518		-0,51	-0,50	-0,33	Protein of unknown function; Spider biofilm induced
orf19.5519	<i>GCV1</i>	-0,53	-0,44		Putative T subunit of glycine decarboxylase; transcript negatively regulated by Sfu1; Spider biofilm repressed
orf19.5521	<i>ISA1</i>	-0,52			Putative mitochondrial iron-sulfur protein; alkaline repressed; induced in high iron; regulated by Sef1, Sfu1, Hap43; Spider biofilm induced
orf19.5522		-0,57	-0,51		Protein of unknown function
orf19.5525		-0,82	-0,62	-0,48	Putative oxidoreductase; protein levels affected by URA3 expression in CAI-4 strain background; Efg1, Efh1 regulated; Rgt1-repressed; protein present in exponential and stationary growth phase yeast; rat catheter biofilm repressed
orf19.5526	<i>SEC20</i>	-0,66	-0,57	-0,49	Essential protein; similar to <i>S. cerevisiae</i> Sec20p; depletion causes membrane accumulation and drug sensitivity; expression regulated by growth phase; O-mannosylation regulates proteolysis; does not complement <i>S. cerevisiae</i> sec20-1 mutant
orf19.5530	<i>NAB3</i>		-0,36	-0,34	Putative nuclear polyadenylated RNA-binding protein; flucytosine repressed
orf19.5531	<i>CDC37</i>	-0,51	-0,48	-0,42	Chaperone for Crk1p; interacts with Crk1p kinase domain and with Sti1p; putative phosphorylation site at Ser14; functional homolog of <i>S. cerevisiae</i> Cdc37p; likely to be essential for growth; regulated by Gcn2p and Gcn4p

orf19.5534				-0,40	Protein with a predicted role in mitotic spindle elongation, vesicle-mediated transport; flow model biofilm induced
orf19.5539		-0,61	-0,49	-0,41	Protein of unknown function
orf19.5544	<i>SAC6</i>	-0,57	-0,52	-0,51	Fimbrin; actin filament bundling protein; transcript regulated by Nrg1 and Mig1; protein level decreases in stationary phase
orf19.5547		-0,40	-0,39		Protein of unknown function; Hap43-repressed gene
orf19.5548	<i>LYS14</i>			-0,34	Zn(II)Cys6 transcription factor; has similarity to <i>S. cerevisiae</i> Lys14, which is a transcription factor involved in the regulation of lysine biosynthesis genes
orf19.5550	<i>MRT4</i>	-0,40	-0,64	-0,35	Putative mRNA turnover protein; Hap43-induced; mutation confers hypersensitivity to tubercidin (7-deazaadenosine); rat catheter biofilm induced
orf19.5551	<i>MIF2</i>	-0,44	-0,40	-0,39	Centromere-associated protein; similar to CENP-C proteins; Cse4p and Mif2p colocalize at <i>C. albicans</i> centromeres
orf19.5552		-0,50	-0,46	-0,43	Putative transcriptional regulator of ribonucleotide reductase genes; Spider biofilm induced
orf19.5553		-0,62	-0,58	-0,47	Protein of unknown function
orf19.5555		-0,41			Protein of unknown function
orf19.5559	<i>RAV2</i>	-0,48	-0,47	-0,35	Protein similar to <i>S. cerevisiae</i> Rav2; a regulator of (H ⁺)-ATPase in vacuolar membrane; transposon mutation affects filamentous growth
orf19.5561	<i>STE23</i>		-0,45	-0,39	Ortholog of <i>S. cerevisiae</i> Ste23 metalloprotease; role in N-terminal processing of pro-a-factor to the mature form; Tn mutation affects filamentous growth; Spider biofilm induced
orf19.5563	<i>RNH1</i>		-0,63	-0,40	Ribonuclease H (RNase H); hyphal-induced; flucytosine induced; similar to orf19.5564 (see Locus History); possibly essential (UAU1 method); rat catheter biofilm induced; flow model biofilm repressed
orf19.5564		-0,44	-0,53		Protein of unknown function
orf19.5566		-0,40	-0,46		Protein of unknown function
orf19.5568	<i>VPS51</i>			-0,35	Protein with a role in vacuolar function; null mutant has defect in damaging oral epithelial and vascular endothelial cells; required for normal hyphal growth and stress resistance; induced in presence of host oral or vascular cells
orf19.5569		-0,39	-0,35	-0,37	Protein of unknown function
orf19.5574		-0,55	-0,52	-0,46	Protein of unknown function
orf19.5578				-0,33	Protein of unknown function
orf19.5579				-0,37	Protein with a predicted double-strand break repair domain; Hap43-repressed gene
orf19.5580	<i>TEL1</i>	-0,45		-0,37	Protein of unknown function
orf19.5584	<i>PEP3</i>	-0,50	-0,47	-0,40	Peptidase; activity useful for strain identification by multilocus enzyme electrophoresis (MLEE); clade-associated gene expression
orf19.5585	<i>SAP5</i>			-0,42	Secreted aspartyl proteinase; sap4,5,6 triple null defective in utilization of protein as N source; virulence role effected by URA3; expressed during infection; mRNA localized to hyphal tip via She3; rat catheter and Spider biofilm induced
orf19.5586				-0,46	Protein of unknown function
orf19.5587		-0,58		-0,53	Protein of unknown function; transcript is upregulated in clinical isolates from HIV+ patients with oral candidiasis
orf19.5595	<i>SHE3</i>	-0,56	-0,59	-0,57	mRNA-binding protein that localizes specific mRNAs to daughter yeast cells and to hyphal tips; required for normal filamentation and host epithelial cell damage; ortholog of <i>S. cerevisiae</i> She3 but target mRNAs differs
orf19.5596		-0,42			Protein of unknown function
orf19.5597	<i>POL5</i>	-0,41	-0,41		Putative DNA Polymerase phi; F-12/CO2 early biofilm induced
orf19.5599	<i>MDL2</i>	-0,38		-0,34	Putative mitochondrial, half-size MDR-subfamily ABC transporter
orf19.5601				-0,39	Protein of unknown function
orf19.5604	<i>MDR1</i>			-0,55	Plasma membrane MDR/MFS multidrug efflux pump; methotrexate is preferred substrate; overexpression in drug-resistant clinical isolates confers fluconazole resistance; repressed in young biofilms; rat catheter biofilm induced
orf19.5607		-0,48	-0,43		Protein of unknown function
orf19.5608		-0,40	-0,46		RNA polymerase III subunit; Spider biofilm induced
orf19.5612	<i>BMT4</i>	-0,45	-0,70	-0,63	Beta-mannosyltransferase; for elongation of beta-mannose chains on the acid-labile fraction of cell wall phosphopeptidomannan; 9-gene family member; regulated by Tsa1, Tsa1B; flow model biofilm induced; rat catheter biofilm repressed
orf19.5614		-0,91	-0,83	-0,73	Putative ribonuclease H1; possibly an essential gene, disruptants not obtained by UAU1 method; flow model biofilm induced; Spider biofilm induced
orf19.5615	<i>AYR2</i>	-0,40			Putative NADPH-dependent 1-acyl dihydroxyacetone phosphate reductase; shows colony morphology-related gene regulation by Ssn6p
orf19.5618		-0,63	-0,44	-0,47	Protein of unknown function
orf19.5619		-0,54	-0,42	-0,46	Protein of unknown function; induced by alpha pheromone in SpiderM medium; Spider biofilm induced
orf19.5620		-0,82	-0,67	-0,53	Stationary phase enriched protein; Gcn4-regulated; induced by amino acid starvation (3-AT), benomyl or in azole-resistant strain that overexpresses MDR1; flow model biofilm induced; rat catheter biofilm repressed; overlaps orf19.5621
orf19.5621		-0,56	-0,40	-0,42	Putative protein of unknown function; mutation confers hypersensitivity to amphotericin B; overlaps orf19.5621
orf19.5622	<i>GLC3</i>	-0,94	-0,94	-0,82	Putative 1,4-glucan branching enzyme; fluconazole-induced; colony morphology-related gene regulation by Ssn6; stationary phase enriched protein
orf19.5623	<i>ARP4</i>	-0,54	-0,51	-0,42	Subunit of the NuA4 histone acetyltransferase complex
orf19.5626		-0,70	-0,45	-0,48	Protein of unknown function; Plc1-regulated; induced by Mnl1 under weak acid stress; flow model biofilm induced
orf19.5627		-0,53	-0,52	-0,44	<i>S. cerevisiae</i> ortholog Hek2/Khd1 is a putative RNA binding protein involved in the asymmetric localization of ASH1 mRNA; Hap43-induced gene
orf19.5629	<i>QCR7</i>	-0,48	-0,45		Putative ubiquinol-cytochrome-c reductase, subunit 7; Hap43p-repressed gene
orf19.5630	<i>APA2</i>	-0,46	-0,39		Putative ATP adenyllyltransferase II; regulated by Gcn4; repressed by amino acid starvation (3-AT); induced by prostaglandins; Hap43-repressed; Spider biofilm repressed
orf19.5634	<i>FRP1</i>	0,49			Ferric reductase; alkaline-induced by Rim101; iron-chelation-induced by CCAAT-binding factor; fluconazole-repressed; ciclopirox-, hypoxia-, Hap43-induced; colony morphology-related regulation by Ssn6; Spider and flow model biofilm induced
orf19.5636	<i>RBT5</i>	0,35			GPI-linked cell wall protein; hemoglobin utilization; Rfg1, Rim101, Tbf1, Fe regulated; Sfu1, Hog1, Tup1, serum, alkaline pH, antifungal drugs, geldamycin repressed; Hap43 induced; required for RPMI biofilms; Spider biofilm induced
orf19.5686		-0,54			Protein of unknown function; Spider biofilm induced
orf19.5702		-0,41			Protein of unknown function
orf19.5705	<i>NAM2</i>	-0,36			Mitochondrial leucyl-tRNA synthetase
orf19.5713	<i>YMX6</i>			1,11	Putative NADH dehydrogenase; macrophage-downregulated gene; induced by nitric oxide; rat catheter biofilm induced
orf19.5718		-0,55	-0,56	-0,58	Protein of unknown function
orf19.5720				-0,34	Predicted membrane transporter, member of the monocarboxylate porter (MCP) family, major facilitator superfamily (MFS); ketoconazole or caspofungin repressed; Spider biofilm induced
orf19.5723	<i>POX1</i>		-0,43	-0,35	Predicted acyl-CoA oxidase; regulated upon white-opaque switch; upregulated upon phagocytosis; Spider biofilm induced
orf19.5727		-0,49			Protein of unknown function
orf19.5728				0,62	Putative cytochrome P450; Spider biofilm induced
orf19.5729	<i>FGR17</i>	-0,72	-0,58	-0,57	Putative DNA-binding transcription factor; has zinc cluster DNA-binding motif; lacks an ortholog in <i>S. cerevisiae</i> ; transposon mutation affects filamentous growth; Hap43p-repressed gene
orf19.5731	<i>PAD1</i>			-0,36	Putative phenylacrylic acid decarboxylase; repressed by Rgt1p

Supporting Information

orf19.5732	<i>NOG2</i>	-0,36		-0,36	Putative nucleolar GTPase; repressed by prostaglandins; Hap43-induced, rat catheter and Spider biofilm induced
orf19.5734	<i>POP2</i>	-0,53	-0,48	-0,45	Component of the Ccr4-Pop2 mRNA deadenylase; heterozygous null mutant exhibits resistance to parnafungin and cordycepin in the <i>C. albicans</i> fitness test
orf19.5735	<i>CDC50</i>		-0,46	-0,39	Putative endosomal protein; induced by Mnl1p under weak acid stress
orf19.5736	<i>ALS5</i>	-0,51		-0,36	ALS family adhesin; highly variable; expression in <i>S. cerevisiae</i> causes adhesion to human epithelium, endothelium or ECM, endothelial invasiveness by endocytosis and, at high abundance, ECM-induced aggregation; can form amyloid fibrils
orf19.5742	<i>ALS9</i>	-0,63	-0,40	-0,46	ALS family cell-surface glycoprotein; expressed during infection of human epithelial cells; confers laminin adhesion to <i>S. cerevisiae</i> ; highly variable; putative GPI-anchor; Hap43-repressed
orf19.5746	<i>ALA1</i>	-0,38	-0,43	-0,38	Alanyl-tRNA synthetase; translational regulation generates cytoplasmic and mitochondrial forms; Gcn4p-regulated; repressed by amino acid starvation (3-AT); translation-related genes downregulated upon phagocytosis by murine macrophages
orf19.5747		-0,43			Protein of unknown function
orf19.5749	<i>SBA1</i>	-0,51	-0,43	-0,35	Similar to co-chaperones; induced in high iron; farnesol-, heavy metal (cadmium) stress-induced; protein level decreases in stationary phase cultures; Hap43-repressed
orf19.5750	<i>SHM2</i>		-0,45		Cytoplasmic serine hydroxymethyltransferase; complements glycine auxotrophy of <i>S. cerevisiae</i> shm1 shm2 gly1-1 mutant; antigenic; farnesol-upregulated in biofilm; stationary-phase enriched protein; rat catheter and Spider biofilm repressed
orf19.5751	<i>ORM1</i>	-0,40		-0,35	Putative endoplasmic reticulum membrane protein; Hap43p-repressed gene; mutation confers hypersensitivity to aureobasidin A
orf19.5752		-0,42	-0,47	-0,46	Protein of unknown function
orf19.5754		-0,48			Putative membrane protein with a predicted role in zinc ion homeostasis; Hap43-induced; fluconazole-induced; rat catheter and Spider biofilm induced
orf19.5757		-0,61	-0,51	-0,51	Protein of unknown function
orf19.5758	<i>SAL6</i>		-0,33		Putative protein phosphatase of the Type 1 family; serine/threonine-specific; similar to <i>S. cerevisiae</i> Ppq1; mutant has virulence defect; Spider biofilm induced
orf19.5760	<i>IHD1</i>		0,43		GPI-anchored protein; alkaline, hypha-induced; regulated by Nrg1, Rfg1, Tup1 and Tsa1, Tsa1B in minimal media at 37; oropharyngeal candidiasis induced ; Spider biofilm induced; regulated in Spider biofilms by Tec1, Efg1, Ndt80, Rob1, Brg1
orf19.5763		-0,63	-0,52	-0,45	Protein of unknown function
orf19.5764	<i>SKI8</i>	-0,52	-0,63	-0,50	Protein of unknown function
orf19.5765	<i>NUP82</i>	-0,59	-0,57	-0,50	Linker nucleoporin of the nuclear pore complex; role in mRNA anexport from nucleus, protein import into nucleus, ribosomal large subunit export from nucleus, ribosomal small subunit export from nucleus; rat catheter biofilm repressed
orf19.5767		-0,57	-0,48	-0,39	Protein of unknown function
orf19.5768	<i>SNF4</i>	-0,56	-0,56	-0,50	Transcription factor; ortholog of <i>S. cerevisiae</i> Snf4; caspofungin repressed; transposon mutation affects filamentation
orf19.5771	<i>PBP2</i>	-0,38	-0,46	-0,36	Putative RNA binding protein; transcript regulated by Nrg1, Mig1, and Tup1
orf19.5772		-0,40	-0,39	-0,34	Protein of unknown function
orf19.5773		-0,56	-0,52	-0,47	Putative dipeptidyl-peptidase III; protein detected by mass spec in exponential and stationary phase cultures; Hog1p-induced; clade-associated gene expression
orf19.5784	<i>AMO1</i>	0,69			Putative peroxisomal copper amine oxidase
orf19.5785				0,72	Protein of unknown function; upregulated in a <i>cyr1</i> or <i>ras1</i> null mutant; induced by nitric oxide
orf19.5806	<i>ALD5</i>			0,38	NAD-aldehyde dehydrogenase; decreased expression in fluconazole-resistant isolate, or in hyphae; biofilm induced; fluconazole-downregulated; protein abundance is affected by URA3 expression in the CAI-4 strain; stationary phase enriched
orf19.5820	<i>UGA6</i>	-0,55		-0,34	Putative GABA-specific permease; decreased transcription is observed upon benomyl treatment or in an azole-resistant strain that overexpresses MDR1
orf19.5843	<i>SRR1</i>	-0,46			Two-component system response regulator; involved in stress response; Plc1-regulated; upregulated in <i>cyr1</i> null mutant; flow model biofilm induced; Spider biofilm induced
orf19.5863		-0,63		-0,41	Protein of unknown function
orf19.5867	<i>WSC1</i>		0,46		Putative cell wall component; transcript upregulated in <i>cyr1</i> mutant (yeast or hyphae); Spider and flow model biofilm induced
orf19.5949	<i>FAS2</i>	0,31			Alpha subunit of fatty-acid synthase; required for virulence in mouse systemic infection and rat oropharyngeal infection models; regulated by Efg1; fluconazole-induced; amphotericin B repressed; flow model and Spider biofilm repressed
orf19.5960	<i>NCE102</i>		0,41		Non classical protein export protein; localized to plasma membrane; Hap43-induced gene; flow model biofilm induced; Spider biofilm induced
orf19.5989			-0,34		Putative cleavage factor I subunit; required for the cleavage and polyadenylation of pre-mRNA 3' ends; Spider biofilm repressed
orf19.6003		0,55	0,72	0,50	Protein of unknown function; role in intracellular signal transduction; Spider biofilm induced
orf19.6065		-0,36			RNA polymerase II holoenzyme/mediator subunit; regulated by Mig1, Tup1; amphotericin B, caspofungin repressed; protein present in exponential and stationary growth phase yeast; Hap43-repressed; Spider biofilm repressed
orf19.6073	<i>HMX1</i>	0,67		0,36	Heme oxygenase; utilization of heme iron; transcript induced by heat, low iron, or heme; repressed by Efg1; induced by low iron; upregulated by Rim101 at pH 8; Hap43-induced; Spider and flow model biofilm induced
orf19.6077				-0,37	Putative protein of unknown function; shows colony morphology-related gene regulation by Ssn6p
orf19.6078	<i>POL93</i>		0,54	0,38	Predicted ORF in retrotransposon Tca8 with similarity to the Pol region of retrotransposons encoding reverse transcriptase, protease and integrase; downregulated in response to ciclopirox olamine; F-12/CO2 early biofilm induced
orf19.6079			0,47	0,36	Predicted ORF in retrotransposon Tca8 with similarity to the Gag region encoding nucleocapsid-like protein; repressed by ciclopirox olamine; filament induced; regulated by Rfg1, Tup1; overlaps orf19.6078.1
orf19.6081	<i>PHR2</i>		-0,58		Glycosidase; role in vaginal not systemic infection (low pH not neutral); low pH, high iron, fluconazole, Hap43-induced; Rim101-repressed at pH8; rat catheter biofilm induced; Bcr1-repressed in RPMI a/a biofilms
orf19.610	<i>EFG1</i>		0,34		bHLH transcription factor; required for white-phase cell type, RPMI and Spider biofilm formation, hyphal growth, cell-wall gene regulation; roles in adhesion, virulence; Cph1 and Efg1 have role in host cytokine response; binds E-box
orf19.6139	<i>FRE7</i>		0,71		Copper-regulated cupric reductase; repressed by ciclopirox olamine or 17-beta-estradiol; induced by alkaline conditions or interaction with macrophage; Spider biofilm induced
orf19.6140	<i>FRE30</i>		0,59		Protein with similarity to ferric reductases; downregulated in response to amphotericin B, estradiol, or ciclopirox olamine, and upregulated by interaction with macrophage; un-merged from orf19.6139 in a revision of Assembly 21
orf19.6165	<i>KGD1</i>	0,32			Putative 2-oxoglutarate dehydrogenase; regulated by Efg1 under yeast but not hyphal growth conditions; transcript induced in an RHE model of oral candidiasis; stationary phase enriched protein; Hap43-repressed; rat catheter biofilm induced
orf19.6197	<i>DHH1</i>	0,40	0,47	0,41	Putative RNA helicase
orf19.6202	<i>RBT4</i>	-0,91	-0,77	-0,68	Pry family protein; required for virulence in mouse systemic/rabbit corneal infections; not filamentation; mRNA binds She3, is localized to hyphal tips; Hap43-induced; in both yeast and hyphal culture supernatants; Spider biofilm induced
orf19.6229	<i>CAT1</i>	-0,42		-0,46	Catalase; resistance to oxidative stress, neutrophils, peroxide; role in virulence; regulated by iron, ciclopirox, fluconazole, carbon source, pH, Rim101, Ssn6, Hog1, Hap43, Sfu1, Sef1, farnesol, core stress response; Spider biofilm induced
orf19.6245		-0,40			Protein of unknown function; regulated by osmotic stress via Hog1 and oxidative stress (Hog1- and Cap1-independent); induced by alpha pheromone in SpiderM medium; Spider biofilm induced
orf19.6311		0,65			Protein of unknown function; Hap43-induced; rat catheter and Spider biofilm induced
orf19.6318				0,43	Protein of unknown function

orf19.6322	<i>ARD</i>	-0,42	-0,48		D-arabitol dehydrogenase, NAD-dependent (ArDH); enzyme of D-arabitol and D-arabinose catabolism; D-arabitol is a marker for active infection in humans; rat catheter and Spider biofilm induced
orf19.6324	<i>VID27</i>		-0,45	-0,33	Protein similar to <i>S. cerevisiae</i> Vid27p; transposon mutation affects filamentous growth; mutation confers hypersensitivity to toxic ergosterol analog; fungal-specific (no human or murine homolog)
orf19.6327	<i>HET1</i>	-0,46	-0,56	-0,45	Putative sphingolipid transfer protein; involved in localization of glucosylceramide which is important for virulence; Spider biofilm repressed
orf19.6328			-0,46	-0,36	Putative protein of the mitochondrial intermembrane space; predicted role in acetate utilization and gluconeogenesis; Spider biofilm repressed
orf19.6329				-0,43	Protein of unknown function; opaque-specific transcript; fluconazole-repressed; induced in <i>cyr1</i> mutant and in oralpharyngeal candidiasis; Spider biofilm induced
orf19.6336	<i>PGA25</i>	-0,41			Putative GPI-anchored adhesin-like protein; fluconazole-downregulated; induced in oralpharyngeal candidiasis; Spider biofilm induced
orf19.6337	<i>TLO13</i>		-0,53	-0,36	Member of a family of telomere-proximal genes of unknown function; may be spliced in vivo; overlaps orf19.6337.1, which is a region annotated as blocked reading frame
orf19.6341				-0,35	Protein of unknown function
orf19.638	<i>FDH1</i>		0,66	0,45	Formate dehydrogenase; oxidizes formate to CO ₂ ; Mig1 regulated; induced by macrophages; fluconazole-repressed; repressed by Efg1 in yeast, not hyphal conditions; stationary phase enriched; rat catheter and Spider biofilm induced
orf19.6385	<i>ACO1</i>		0,36		Aconitase; induced in high iron; 2 upstream CCAAT motifs; amino acid starvation (3-AT), amphotericin B, phagocytosis, farnesol induced; Hap43, fluconazole-repressed; Gcn4-regulated; antigenic in infection; flow and Spider biofilm repressed
orf19.6387	<i>HSP104</i>		0,36		Heat-shock protein; roles in biofilm and virulence; complements chaperone, prion activity in <i>S. cerevisiae</i> ; guanidine-insensitive; heat shock/stress induced; repressed in farnesol-treated biofilm; sumoylation target; Spider biofilm induced
orf19.6408		0,47			Putative DnaJ-like heat shock/chaperone; Hap43-repressed; Spider and F-12/CO ₂ biofilm induced
orf19.6459	<i>DPP3</i>	-0,45		-0,48	Protein similar to <i>S. cerevisiae</i> pyrophosphate phosphatase Dpp1; required for farnesol biosynthesis; repressed by 17-beta-estradiol, ethynyl estradiol; Spider biofilm induced
orf19.6489	<i>FMP45</i>		0,54		Predicted membrane protein induced during mating; mutation confers hypersensitivity to toxic ergosterol analog, to amphotericin B; alkaline repressed; repressed by alpha pheromone in SpiderM medium; rat catheter, Spider biofilm induced
orf19.655	<i>PHO84</i>		0,58	0,42	High-affinity phosphate transporter; transcript regulated by white-opaque switch; Hog1, ciclopirox olamine or alkaline induced; caspofungin, stress repressed; upregulated in RHE model; Spider and flow model biofilm induced, Hap43-induced
orf19.657	<i>SAM2</i>	0,30			S-adenosylmethionine synthetase; localizes to surface of hyphae, not yeast cells; alkaline, Hog1-induced; farnesol-downregulated; F-12/CO ₂ early biofilm induced; Spider biofilm repressed
orf19.6577	<i>FLU1</i>			0,63	Multidrug efflux pump of the plasma membrane; MDR family member of the MFS (major facilitator superfamily) of transporters; involved in histatin 5 efflux; fungal-specific (no human/murine homolog)
orf19.6595	<i>RTA4</i>	-0,49			Protein similar to <i>S. cerevisiae</i> Rsb1p, involved in fatty acid transport; transposon mutation affects filamentous growth; alkaline downregulated; caspofungin induced; possibly an essential gene; Hap43p-repressed
orf19.6601.1	<i>YKE2</i>	-0,41			Possible heterohexameric Gim/prefoldin protein complex subunit; role in folding alpha-tubulin, beta-tubulin, and actin; transcript induced by yeast-to-hypha switch; regulated by Nrg1, Tup1; Spider and flow model biofilm induced
orf19.6604		-0,38			Ortholog of <i>S. cerevisiae</i> Pba1 that is involved in 20S proteasome assembly; upregulated in a <i>cyr1</i> null mutant; contains a 5' UTR intron
orf19.6637		-0,36			Predicted glycosyl hydrolase; hypoxia induced; flow model biofilm induced
orf19.6639			0,37		Ortholog of <i>S. cerevisiae</i> Mdm36; mitochondrial distribution and morphology protein; Hap43-repressed gene
orf19.6640	<i>TPS1</i>	-0,55			Trehalose-6-phosphate synthase; role in hyphal growth and virulence in mouse systemic infection; induced in presence of human neutrophils; macrophage/pseudohyphal-repressed after 16h; stationary phase enriched protein; Hap43-repressed
orf19.6658		-0,43	-0,42	-0,41	Stationary phase enriched protein; predicted ORF from Assembly 19; removed from Assembly 20; subsequently reinstated in Assembly 21 based on comparative genome analysis
orf19.6688			0,44		Protein of unknown function; expression decreases by benomyl treatment or in an azole-resistant strain overexpressing MDR1; Spider biofilm induced
orf19.670.2		0,47		0,62	Protein of unknown function; hypoxia, Hap43-repressed; ketoconazole induced; induced in oralpharyngeal candidiasis; 16h flow model biofilm repressed, late-stage flow model biofilm induced; rat catheter and Spider biofilm induced
orf19.6705			0,51		Putative guanyl nucleotide exchange factor with Sec7 domain; required for normal filamentous growth; regulated by yeast-hyphal switch; filament induced; regulated by Nrg1, Tup1, Mob2, Hap43; mRNA binds She3; Spider biofilm induced
orf19.6770			0,41		protein with ENTH Epsin domain, N-terminal; Spider biofilm repressed
orf19.6782	<i>BMT1</i>		0,42		Beta-mannosyltransferase, required for addition of the 1st beta-mannose residue to acid-stable fraction of cell wall phosphopeptidomannan; 9-gene family member; mutants induce higher levels of inflammatory cytokines in mouse dendritic cells
orf19.6816		-0,61			Putative xylose and arabinose reductase; flow model biofilm induced; Spider biofilm repressed
orf19.6824	<i>TRY6</i>		0,65		Helix-loop-helix transcription factor; regulator of yeast form adherence; required for yeast cell adherence to silicone substrate; Spider and F-12/CO ₂ biofilm induced; repressed by alpha pheromone in SpiderM medium
orf19.6834.10	<i>TAR1</i>		0,63	-0,59	Ortholog of <i>S. cerevisiae</i> Tar1p; Transcript Antisense to Ribosomal RNA; encoded within the 25S rRNA gene on the opposite strand; induced by Tbf1
orf19.684		-0,36		-0,34	Putative transcription factor with zinc finger DNA-binding motif; heterozygous null mutant exhibits hypersensitivity to parnafungin and cordycepin in the <i>C. albicans</i> fitness test
orf19.6844	<i>ICL1</i>		0,45		Isocitrate lyase; glyoxylate cycle enzyme; required for virulence in mice; induced upon phagocytosis by macrophage; farnesol regulated; Pex5-dependent peroxisomal localization; stationary phase enriched; rat catheter, Spider biofilm induced
orf19.6852.1		-0,44			Protein of unknown function; Spider biofilm induced
orf19.686		-0,50	-0,45	-0,35	Protein of unknown function; regulated by Nrg1
orf19.687		-0,52	-0,53	-0,45	Protein of unknown function
orf19.687.1	<i>RPL25</i>	-0,38	-0,54		Putative rRNA-binding ribosomal protein component of the 60S ribosomal subunit; Hap43-induced; colony morphology-related gene regulation by Ssn6
orf19.688		-0,37			Mitochondrial ribosomal protein of the small subunit; <i>S. cerevisiae</i> ortholog is essential for viability; Spider biofilm repressed
orf19.6882	<i>OSM1</i>	-0,51			Putative flavoprotein subunit of fumarate reductase; soluble protein in hyphae; caspofungin repressed; stationary phase enriched protein; flow model biofilm induced; Spider biofilm repressed
orf19.6888		-0,59	-0,52	0,61	Zn(II)2Cys6 domain transcription factor; regulated by Mig1 and Tup1; rat catheter and Spider biofilm induced
orf19.692			-0,59	-0,60	Protein of unknown function; Hap43-repressed gene; rat catheter and Spider biofilm induced
orf19.6984				0,48	Protein of unknown function
orf19.7020			0,34		Protein similar to <i>S. cerevisiae</i> Kex1p, which is a pheromone-processing peptidase; possible Kex2p substrate
orf19.7022		-0,41			Protein of unknown function
orf19.7077		0,39	0,64	0,46	Putative ferric reductase; induced by Mac1 under copper starvation; Plc1-regulated; Rim101-repressed
orf19.7111.1	<i>SOD3</i>		0,42		Cytosolic manganese-containing superoxide dismutase; protects against oxidative stress; repressed by ciclopirox olamine, induced during stationary phase when SOD1 expression is low; Hap43-repressed; Spider and flow model biofilm induced
orf19.7112	<i>FRP2</i>	0,49			Putative ferric reductase; alkaline induced by Rim101; fluconazole-downregulated; upregulated in the presence of human neutrophils; possibly adherence-induced; regulated by Sef1, Sfu1, and Hap43
orf19.717	<i>HSP60</i>		0,45	0,36	Heat shock protein; soluble in hyphae; regulated by Nrg1 and by iron; induced in high iron; heavy metal (cadmium) stress-induced; sumoylation target; protein present in exponential and stationary phase cells; Hap43-repressed

Supporting Information

orf19.7214		-0,72	-0,40	-0,41	Glucan 1,3-beta-glucosidase; regulated by Nrg1, Tup1 and possibly Tac1; induced by NO and during cell wall regeneration; stationary phase enriched; possibly essential (UAU1 method); F-12/CO2 early biofilm induced; flow biofilm repressed
orf19.7218	<i>RBE1</i>	0,43	0,44	0,38	Pry family cell wall protein; Rim101, Efg1, Ssn6, alkaline repressed; O-glycosylation; no GPI anchor predicted; ketoconazol induced; regulated by Sef1, Sfu1, Hap4; flow model biofilm induced; rat catheter and Spider biofilm repressed
orf19.7247	<i>RIM101</i>		0,34		Transcription factor; alkaline pH response; required for alkaline-induced hyphal growth; role in virulence in mice; activated by C-terminal proteolytic cleavage; mediates both positive and negative regulation; Spider biofilm induced
orf19.7251	<i>WSC4</i>			0,34	Putative cell wall integrity and stress response subunit 4 precursor; transcription is specific to white cell type
orf19.7284	<i>ASR2</i>	-0,88	-0,50	-0,53	Adenylyl cyclase and stress responsive protein; induced in <i>cyr1</i> or <i>ras1</i> mutant; stationary phase enriched protein; Spider biofilm induced
orf19.7288		-0,49			Protein with predicted oxidoreductase and dehydrogenase domains; Hap43-repressed; Spider biofilm induced
orf19.7296			-0,54	-0,52	Putative cation conductance protein; similar to stomatin mechanoreception protein; plasma-membrane localized; induced by Rgt1; rat catheter and Spider biofilm induced
orf19.73		-0,62	-0,46	-0,44	Putative metalloprotease; associates with ribosomes and is involved in ribosome biogenesis; Spider biofilm induced
orf19.7310		-0,51			Protein with a role in directing meiotic recombination events to homologous chromatids; induced by ciclopirox olamine; positively regulated by Sfu1; Hog1, fluconazole-repressed; Hap43-induced; Spider biofilm induced
orf19.7319	<i>SUC1</i>			-0,37	Zinc-finger transcription factor; regulates alpha-glucosidase expression; complements <i>S. cerevisiae</i> <i>suc2</i> for sucrose utilization and <i>mal13</i> maltase defect; required for yeast cell adherence to silicone substrate; rat catheter biofilm induced
orf19.7337			0,48		Protein with a nischarin related domain and leucine rich repeats; Spider biofilm induced
orf19.734	<i>GLK1</i>	-0,45			Putative glucokinase; transcript regulated upon yeast-hyphal switch; Efg1 regulated; fluconazole-induced; induced in core stress response; colony morphology-related gene regulation by Ssn6; GlcNAc-induced protein
orf19.74	<i>SEC5</i>	-0,49		-0,36	Predicted exocyst component; ortholog of <i>S. cerevisiae</i> Sec5p; merged with orf19.75 in Assembly 21
orf19.740	<i>HAP41</i>		0,44	0,40	Putative Hap4-like transcription factor; Hap43-repressed; not required for response to low iron; induced by Mnl1 under weak acid stress; Spider biofilm induced
orf19.7411	<i>OAC1</i>	0,59			Putative mitochondrial inner membrane transporter; rat catheter biofilm induced
orf19.7436	<i>AAF1</i>		0,44		Possible regulatory protein; possible adhesin-like; Glu-rich domain; production in <i>S. cerevisiae</i> increases endothelial cell adherence and flocculence; flow model biofilm, alkaline or caspofungin induced
orf19.7445			0,42	0,38	Ortholog of <i>S.c. Vid24</i> ; a peripheral membrane protein located at Vid (vacuole import and degradation) vesicles; regulated by Sef1, Sfu1, and Hap43; Spider biofilm induced
orf19.7504		-0,36	-0,38		Ortholog of <i>S. cerevisiae</i> Rts3; a component of the protein phosphatase type 2A complex; Plc1-regulated; induced in core caspofungin response; Spider biofilm induced
orf19.7514	<i>PCK1</i>			0,48	Phosphoenolpyruvate carboxykinase; glucose, C-source, yeast-hypha, Hap43 regulated; fluconazole, phagocytosis, H2O2, oral candidiasis, Spider/rat catheter/flow model biofilm induced; repressed in biofilm by Bcr1, Tec1, Ndt80, Rob1, Brg1
orf19.753	<i>MNN15</i>	-0,40			Putative alpha-1,3-mannosyltransferase; predicted role in protein O-linked glycosylation; Spider biofilm induced
orf19.7567				-0,33	Protein of unknown function; induced by alpha pheromone in SpiderM medium
orf19.7585	<i>INO1</i>			-0,46	Inositol-1-phosphate synthase; antigenic in human; repressed by farnesol in biofilm or by caspofungin; upstream inositol/choline regulatory element; glycosylation predicted; rat catheter, flow model induced; Spider biofilm repressed
orf19.76	<i>SPB1</i>	-0,39	-0,55	-0,41	Putative AdoMet-dependent methyltransferase; Hap43-induced; repressed by prostaglandins; possibly essential gene, disruptants not obtained by UAU1 method; Spider biofilm induced
orf19.7610	<i>PTP3</i>	-0,34			Putative protein tyrosine phosphatase; hypha induced; alkaline induced; regulated by Efg1, Ras1, cAMP pathways; mutants are viable; Spider biofilm induced; rat catheter biofilm repressed; flow model biofilm repressed
orf19.7612	<i>CTM1</i>	-0,37			Putative cytochrome c lysine methyltransferase; regulated by Gcn2 and Gcn4; transcript induced by Mnl1 under weak acid stress; early-stage flow model biofilm induced
orf19.7648				0,35	Protein of unknown function
orf19.7676	<i>XYL2</i>	-0,40			D-xylulose reductase; immunogenic in mice; soluble protein in hyphae; induced by caspofungin, fluconazole, Hog1 and during cell wall regeneration; Mnl1-induced in weak acid stress; stationary phase enriched; flow model biofilm induced
orf19.802	<i>UGA1</i>			0,36	Putative GABA transaminase; transcription regulated by Mig1 and Tup1; stationary phase enriched protein; rat catheter and Spider biofilm induced
orf19.822	<i>HSP21</i>		0,52		Small heat shock protein; role in stress response and virulence; fluconazole-downregulated; induced in <i>cyr1</i> or <i>ras1</i> mutant; stationary phase enriched protein; detected in some, not all, biofilm extracts; Spider biofilm induced
orf19.84	<i>CAN3</i>	-0,43	-0,43	-0,64	Predicted amino acid transmembrane transporter; transcript regulated by white-opaque switch; Hap43-repressed gene
orf19.85	<i>GPX2</i>	-0,65	-0,52	-0,65	Similar to glutathione peroxidase; induced in high iron; alkaline induced by Rim101; induced by alpha factor or interaction with macrophage; regulated by Efg1; caspofungin repressed; Spider biofilm induced
orf19.86		-0,38			Putative glutathione peroxidase; induced by peroxide, exposure to neutrophils and macrophage blood fractions; repressed during infection of macrophages; Spider biofilm induced; flow model biofilm repressed
orf19.868	<i>ADAEC</i>	-0,44			Protein of unknown function; transcription is specific to white cell type
orf19.88	<i>ILV5</i>		-0,55	-0,34	Ketol-acid reductoisomerase; antigenic; regulated by Gcn4; GlcNAc, amino acid starvation (3-AT)-induced; macrophage-repressed protein; protein present in exponential and stationary phase; flow model and Spider biofilm repressed
orf19.882	<i>HSP78</i>		0,42		Heat-shock protein; regulated by macrophage response, Nrg1, Mig1, Gcn2, Gcn4, Mnl1p; heavy metal (cadmium) stress-induced; stationary phase enriched protein; rat catheter and Spider biofilm induced
orf19.89	<i>PEX7</i>		-0,76	-0,55	Protein of unknown function
orf19.896	<i>CHK1</i>	-0,37			Histidine kinase; 2-component signaling, cell wall synthesis; hyphal growth defect; avirulent in mouse, not rat vaginal infection; phagocytosis rate increased; Spider biofilm induced; required for RPM1 biofilm; Bcr1-induced in a/a biofilm
orf19.90		-0,66	-0,61	-0,58	Protein of unknown function
orf19.909	<i>STP4</i>		0,43		C2H2 transcription factor; induced in core caspofungin response; colony morphology-related gene regulation by Ssn6; induced by 17-beta-estradiol, ethynyl estradiol; rat catheter and Spider biofilm induced
orf19.91		-0,50		-0,36	Protein of unknown function; flow model biofilm induced; Hap43-repressed
orf19.918	<i>CDR11</i>		0,51		Putative transporter of PDR subfamily of ABC family; Gcn4-regulated; induced by Rim101 at pH 8; Spider biofilm induced
orf19.92		-0,52	-0,49	-0,42	Protein with a predicted thioredoxin-like domain; Hap43-repressed; induced by prostaglandins
orf19.921	<i>HMS1</i>		0,46		hLh domain Myc-type transcription factor; required for morphogenesis induced by elevated temperature or Hsp90 compromise; acts downstream of Pcl1; Spider biofilm induced
orf19.932			0,48	0,48	Putative aminophospholipid translocase (flippase); merged with orf19.2226 in Assembly 21; possibly an essential gene, disruptants not obtained by UAU1 method
orf19.938				0,60	Protein of unknown function
orf19.94		-0,59	-0,54	-0,56	Protein of unknown function; Spider biofilm induced
orf19.96	<i>TOP1</i>	-0,32	-0,47	-0,40	DNA topoisomerase I; required for wild-type growth and for wild-type mouse virulence; sensitive to camptothecin; induced upon adherence to polystyrene; rat catheter biofilm induced
orf19.979	<i>FAS1</i>	0,30			Beta subunit of fatty-acid synthase; multifunctional enzyme; Hap43, fluconazole-induced; amphotericin B, caspofungin repressed; macrophage/pseudohyphal-induced; flow model and Spider biofilm repressed
orf19.984	<i>PHO8</i>	0,50			Putative repressible vacuolar alkaline phosphatase; Rim101-induced transcript; regulated by Tsa1, Tsa1B in minimal media at 37 deg; possibly adherence-induced

orf19.99	<i>HAL21</i>	-0,63	-0,82	-0,57	Putative phosphoadenosine-5'-phosphate or 3'-phosphoadenosine 5'-phosphosulfate phosphatase; possible role in sulfur recycling; ortholog of <i>S. cerevisiae</i> Met22; predicted Kex2 substrate; F-12/CO2 biofilm induced
orf19.999	<i>GCA2</i>	-0,48			Predicted extracellular glucoamylase; induced by ketoconazole; possibly essential, disruptants not obtained by UAU1 method; promotes biofilm matrix formation; Spider biofilm induced; Bcr1-induced in RPM1 a/a biofilms

Table S 4: RNA seq $p_{adj} < 0.01$

Gene name	Common name	<i>TRY4</i>	<i>ZFU2</i>	<i>ZCF8</i>	Description
orf19.102		-0,48			Protein of unknown function
orf19.1048	<i>IFD6</i>	-0,71		-0,45	Aldo-keto reductase; similar to aryl alcohol dehydrogenases; protein increase correlates with MDR1 overexpression (not CDR1 or CDR2) in fluconazole-resistant clinical isolates; farnesol regulated; possibly essential; Spider biofilm induced
orf19.1075		-0,74		-0,62	Protein of unknown function; Spider biofilm induced
orf19.1083				-0,38	Putative protein of unknown function; macrophage-induced gene
orf19.1084	<i>CDC39</i>	-0,38			Protein similar to <i>S. cerevisiae</i> Cdc39p, which is part of the CCR4-NOT transcription regulatory complex; transposon mutation affects filamentous growth
orf19.1085		-0,65	-0,61	-0,47	Protein of unknown function
orf19.1089	<i>PEX11</i>	-0,66	-0,46	-0,36	Putative peroxisomal membrane protein; role in fatty acid oxidation; expression is Tac1-regulated; Hms1p-dependent induction by geldamycin; Spider biofilm induced
orf19.1095	<i>GLE2</i>	-0,50	-0,43	-0,40	Putative nuclear pore complex; possibly an essential gene, disruptants not obtained by UAU1 method; rat catheter biofilm repressed
orf19.1097	<i>ALS2</i>	-0,80	-0,70	-0,77	ALS family protein; role in adhesion, biofilm formation, germ tube induction; expressed at infection of human buccal epithelial cells; putative GPI-anchor; induced by ketoconazole, low iron and at cell wall regeneration; regulated by Sfu1p
orf19.113	<i>CIP1</i>			-0,49	Possible oxidoreductase; transcript induced by cadmium but not other heavy metals, heat shock, yeast-hypha switch, oxidative stress (via Cap1), or macrophage interaction; stationary phase enriched protein; Spider biofilm induced
orf19.1149	<i>MRF1</i>	-0,42			Putative mitochondrial respiratory protein; induced by farnesol, benomyl, nitric oxide, core stress response; oxidative stress-induced via Cap1; stationary-phase enriched protein; Spider biofilm induced
orf19.1153	<i>GAD1</i>	-0,49			Putative glutamate decarboxylase; alkaline, macrophage-downregulated gene; amphoterin B induced; induced by Mnl1 under weak acid stress; stationary phase enriched protein; rat catheter biofilm repressed
orf19.117		-0,43	-0,42	-0,39	Protein of unknown function
orf19.1177				-0,39	Ortholog of <i>S. cerevisiae</i> Rtt106; histone chaperone that regulates chromatin structure in transcribed and silenced chromosomal regions; affects transcriptional elongation; Hap43-repressed; Spider biofilm repressed
orf19.1179		-0,43	-0,48		Protein of unknown function; induced in high iron; possibly subject to Kex2 processing; Hap43-repressed
orf19.1180		-0,53	-0,50	-0,44	Putative 2-aminoadipate transaminase; rat catheter and Spider biofilm repressed
orf19.1182		-0,51	-0,51	-0,50	Protein of unknown function
orf19.1183		-0,58	-0,54	-0,58	Protein of unknown function
orf19.1186				-0,38	Protein of unknown function
orf19.119		-0,55			Protein of unknown function
orf19.1190	<i>STV1</i>			-0,34	Predicted subunit a of vacuolar proton-translocating ATPase V0 domain, Golgi isoform
orf19.1191				-0,34	Protein of unknown function
orf19.1192	<i>DNA2</i>			-0,38	Protein similar to <i>S. cerevisiae</i> Dna2p, which is a DNA replication factor involved in DNA repair; induced under hydroxyurea treatment
orf19.1198		-0,64		-0,37	Predicted mitochondrial intermembrane space protein of unknown function; possibly an essential gene, disruptants not obtained by UAU1 method
orf19.1199	<i>NOP5</i>		-0,55	-0,35	Ortholog of <i>S. cerevisiae</i> Nop58; involved in pre-rRNA process; Tn mutation affects filamentous growth; macrophage/pseudohyphal-induced; physically interacts with TAP-tagged Nop1; Spider biofilm repressed
orf19.1200			-0,51	-0,45	Protein of unknown function; Spider biofilm induced
orf19.1201		-0,46		-0,36	Protein of unknown function
orf19.1203	<i>SRO77</i>	-0,45		-0,38	Protein with a predicted role in docking and fusion of post-Golgi vesicles with the plasma membrane; filament induced; fungal-specific (no human or murine homolog)
orf19.1203.1				-0,35	Predicted dolichol-phosphate mannosyltransferase subunit; flow model and Spider biofilm repressed
orf19.1204			-0,50	-0,42	Phosphorylated protein of unknown function; transcript is upregulated clinical isolates from HIV positive patients with oral candidiasis
orf19.121	<i>ARC18</i>	-0,64			Putative ARP2/3 complex subunit; mutation confers hypersensitivity to cytochalasin D
orf19.1210		-0,41		-0,46	Protein of unknown function
orf19.1212		-0,58	-0,52	-0,39	Protein of unknown function
orf19.1214		-0,44	-0,63	-0,42	Protein of unknown function
orf19.1215				-0,44	Protein of unknown function
orf19.1217		-0,43			Protein of unknown function
orf19.1220	<i>RVS167</i>	-0,38		-0,34	SH3-domain- and BAR domain-containing protein involved in endocytosis; null mutant exhibits defects in hyphal growth, virulence, cell wall integrity, and actin patch localization; cosediments with phosphorylated Myo5p
orf19.1221	<i>ALG2</i>	-0,46		-0,39	Putative mannosyltransferase involved in cell wall mannan biosynthesis; transcription is elevated in <i>chk1</i> , <i>nik1</i> , and <i>sln1</i> homozygous null mutants
orf19.123	<i>RCN1</i>			-0,39	Protein involved in calcineurin-dependent signaling that controls stress response and virulence; inhibits calcineurin function
orf19.124	<i>CIC1</i>	-0,38	-0,50	-0,38	Putative proteasome-interacting protein; rat catheter biofilm induced
orf19.125	<i>EBP1</i>			-0,41	NADPH oxidoreductase; interacts with phenolic substrates (17beta-estradiol); possible role in estrogen response; induced by oxidative, weak acid stress, NO, benomyl, GlcNAc; Cap1, Mnl1 induced; Hap43-repressed; rat catheter biofilm induced
orf19.130	<i>VPS15</i>	-0,56			Protein involved in retrograde endosome-to-Golgi protein transport; required for normal virulence
orf19.1308				1,58	Predicted membrane transporter, member of the drug:proton antiporter (14 spanner) (DHA2) family, major facilitator superfamily (MFS)
orf19.1309				1,08	Protein of unknown function
orf19.1310				0,54	Protein of unknown function
orf19.1311	<i>SPO75</i>			0,42	Protein of unknown function
orf19.1344		0,91			Protein of unknown function; fluconazole-induced; Spider biofilm induced
orf19.135	<i>EXO84</i>			-0,36	Predicted subunit of the exocyst complex, involved in exocytosis; localizes to a crescent on the surface of the hyphal tip
orf19.1353		-0,43			Protein of unknown function; repressed by yeast-hypha switch; Ras1-regulated; oral infection induced; mutants defective in damage to oral epithelium; flow model biofilm induced; Spider biofilm induced
orf19.136	<i>QDR3</i>			0,41	Predicted membrane transporter, member of the drug:proton antiporter (12 spanner) (DHA1) family, major facilitator superfamily (MFS); Hap43p-repressed gene
orf19.1439	<i>IPK1</i>	-0,50		-0,37	Ortholog of <i>S. cerevisiae</i> / <i>S. pombe</i> <i>Ipk1</i> ; an inositol pentakisphosphate 2-kinase, a nuclear protein required for synthesis of 1,2,3,4,5,6-hexakisphosphate; Spider biofilm induced
orf19.1486			0,50		Protein with a life-span regulatory factor domain; regulated by Sef1, Sfu1, and Hap43; flow model biofilm induced; Spider biofilm induced

Supporting Information

orf19.1490	<i>MSB2</i>		0,47	0,39	Mucin family adhesin-like protein; cell wall damage sensor; required for Cek1 phosphorylation by cell wall stress; Rim101-repressed; activation releases extracellular domain into medium; Spider biofilm induced
orf19.1600			0,65	0,36	Protein of unknown function
orf19.1614	<i>MEP1</i>	0,88	0,57	0,37	Ammonium permease; Mep1 more efficient permease than Mep2, Mep2 has additional regulatory role; 11 predicted transmembrane regions; low mRNA abundance; hyphal downregulated; flow model biofilm induced
orf19.1653				0,37	Protein of unknown function
orf19.1691		-0,58			Plasma-membrane-localized protein; filament induced; Hog1, ketoconazole, fluconazole and hypoxia-induced; regulated by Nrg1, Tup1, Upc2; induced by prostaglandins; flow model biofilm induced; rat catheter and Spider biofilm repressed
orf19.1715	<i>IRO1</i>	-0,47	-0,53	-0,47	Putative transcription factor; role in iron utilization, pathogenesis; both IRO1 and adjacent URA3 are mutated in strain CA14; suppresses <i>S. cerevisiae</i> aft1 mutant low-iron growth defect; hyphal-induced; reports differ about iron regulation
orf19.1716	<i>URA3</i>	-0,71	-0,86	-0,69	Orotidine-5'-phosphate decarboxylase; pyrimidine biosynthesis; gene used as genetic marker; decreased expression when integrated at ectopic chromosomal locations can cause defects in hyphal growth and virulence; Spider biofilm repressed
orf19.1727	<i>PMC1</i>		0,40		Vacuolar calcium P-type ATPase; transcript regulated by calcineurin and fluconazole; mutant shows increased resistance to fluconazole, lithium; increased sensitivity to calcium; Spider biofilm induced
orf19.1770	<i>CYC1</i>		0,45	0,37	Cytochrome c; complements defects of <i>S. cerevisiae</i> cyc1 cyc7 double mutant; induced in high iron; alkaline repressed; repressed by nitric oxide; Hap43-dependent repression in low iron; regulated by Sef1, Sfu1
orf19.1795	<i>PUF3</i>		0,46		Ortholog of <i>S. cerevisiae</i> Puf3; mRNA-binding protein involved in RNA catabolism; mutant is viable
orf19.1847	<i>ARO10</i>		0,49		Aromatic decarboxylase; Ehrlich fusel oil pathway of aromatic alcohol biosynthesis; alkaline repressed; protein abundance affected by URA3 expression in CAI-4 strain; Spider biofilm induced
orf19.1862		-0,61			Possible stress protein; increased transcription associated with CDR1 and CDR2 overexpression or fluphenazine treatment; regulated by Sfu1, Nrg1, Tup1; stationary phase enriched protein; Spider biofilm induced
orf19.1887				0,36	Protein of unknown function
orf19.1978	<i>GIT2</i>		0,59	0,40	Putative glycerophosphoinositol permease; fungal-specific; repressed by alpha pheromone in SpiderM medium; Hap43-repressed; Spider biofilm induced
orf19.1979	<i>GIT3</i>		0,55		Glycerophosphocholine permease; white cell specific transcript; fungal-specific; alkaline repressed; caspofungin, macrophage/pseudohyphal-repressed; flow model biofilm induced; Spider biofilm induced
orf19.1996	<i>CHA1</i>		0,52	0,47	Similar to catabolic ser/thr dehydratases; repressed by Rim101; induced in low iron; regulated on white-opaque switch; filament induced; Tn mutation affects filamentation; flow model biofilm induced; Spider biofilm repressed
orf19.2003	<i>HNM1</i>			0,36	Putative choline/ethanolamine transporter; mutation confers hypersensitivity to toxic ergosterol analog; colony morphology-related gene regulation by Ssn6; clade-associated gene expression
orf19.2008				0,34	Protein of unknown function
orf19.2048			0,71		Protein of unknown function; transcript positively regulated by Sfu1; Hap43 repressed; Spider biofilm induced
orf19.2076		-0,55			Protein of unknown function; <i>S. pombe</i> ortholog SPAC7D4.05 encodes a predicted hydrolase; Hap43-repressed; Spider biofilm induced
orf19.2128			-0,51	-0,43	Protein of unknown function
orf19.2132		-0,55	-0,53	-0,49	Protein of unknown function
orf19.2133	<i>LIP4</i>			-0,44	Secreted lipase, member of a differentially expressed lipase gene family with possible roles in nutrition and/or in creating an acidic microenvironment; expressed more strongly during mucosal infections than during systemic infections
orf19.2138	<i>ILS1</i>		-0,37		Putative isoleucyl-tRNA synthetase, the target of drugs including the cyclic beta-amino acid icofungipen/PLD-118/BAY-10-8888 and mupirocin; protein present in exponential and stationary growth phase yeast cultures
orf19.2146	<i>HAT2</i>			-0,40	Putative Hat1-Hat2 histone acetyltransferase complex subunit; role in DNA damage repair and morphogenesis; mutations cause constitutive pseudohyphal growth, caspofungin sensitivity; rat catheter and Spider biofilm repressed
orf19.215			0,48		Component of a complex containing the Tor2p kinase; possible a role in regulation of cell growth; Spider biofilm induced
orf19.2150		-0,40	-0,49	-0,35	Putative ortholog of mammalian electron transfer flavoprotein complex subunit ETF-alpha; Spider biofilm repressed
orf19.2151	<i>NAG6</i>	-0,48	-0,43	-0,41	Protein required for wild-type mouse virulence and wild-type cycloheximide resistance; putative GTP-binding motif, similar to <i>S. cerevisiae</i> Yor165Wp; in gene cluster that encodes enzymes of GlcNAc catabolism; no human or murine homolog
orf19.2154	<i>HXK1</i>			-0,37	N-acetylglucosamine (GlcNAc) kinase; involved in GlcNAc utilization; required for wild-type hyphal growth and mouse virulence; GlcNAc-induced transcript; induced by alpha pheromone in SpiderM medium
orf19.2165			-0,49		Predicted hydrolase; induced by nitric oxide
orf19.2179	<i>SIT1</i>		-0,38		Transporter of ferrichrome siderophores, not ferrioxamine B; required for human epithelial cell invasion in vitro, not for mouse systemic infection; regulated by iron, Sfu1, Rfg1, Tup1, Hap43; rat catheter and Spider biofilm induced
orf19.2241	<i>PST1</i>	-0,51			Putative 1,4-benzoquinone reductase; hyphal-induced; regulated by Cyr1, Ras1, Efg1, Nrg1, Rfg1, Tup1; Hap43-induced; Spider biofilm induced
orf19.2270	<i>SMF12</i>		0,52	0,38	Ortholog of <i>S. cerevisiae</i> Smf1; manganese transporter; Gcn4-regulated; Hap43, alkaline induced; caspofungin repressed; mutants are viable
orf19.2344	<i>ASR1</i>	-1,35	-0,59	-0,62	Heat shock protein; transcript regulated by cAMP, osmotic stress, ciclopirox olamine, ketoconazole; repressed by Cyr1, Ras1; colony morphology-related regulated by Ssn6; stationary phase enriched; Hap43-induced; Spider biofilm induced
orf19.238	<i>CCP1</i>	-0,39			Cytochrome-c peroxidase N terminus; Rim101, alkaline pH repressed; induced in low iron or by macrophage interaction; oxygen-induced activity; regulated by Sef1, Sfu1, and Hap43; Spider biofilm induced; rat catheter biofilm repressed
orf19.2396	<i>IFR2</i>	-0,48			Zinc-binding dehydrogenase; induced by benomyl, ciclopirox olamine, alpha pheromone, Hap43; regulated by oxidative stress via Cap1, osmotic stress via Hog1; protein present in exponential and stationary phase; rat catheter biofilm repressed
orf19.2451	<i>PGA45</i>	0,65		0,45	Putative GPI-anchored cell wall protein; repressed in core caspofungin response; Hog1-induced; regulated by Ssn6; Mob2-dependent hyphal regulation; flow model biofilm induced
orf19.251	<i>GLX3</i>	-0,52			Glutathione-independent glyoxalase; binds human immunoglobulin E; alkaline, fluconazole, Hog1 repressed; hypoxia, oxidative stress via Cap1, Hap43 induced; stationary-phase enriched; rat catheter, Spider biofilm induced
orf19.2529.1				0,36	Protein of unknown function; Spider biofilm repressed
orf19.2531	<i>CSP37</i>	-0,43			Hyphal cell wall protein; role in progression of mouse systemic infection; predicted P-loop, divalent cation binding, N-glycosylation sites; expressed in yeast and hyphae; hyphal downregulated; stationary-phase enriched; GlcNAc-induced
orf19.2686				0,64	Protein of unknown function
orf19.2737		-0,61			Carbohydrate kinase domain-containing protein; Spider biofilm induced
orf19.2762	<i>AHP1</i>	-0,56	-0,53	-0,40	Alkyl hydroperoxide reductase; immunogenic; fluconazole-induced; amphotericin B, caspofungin, alkaline repressed; core stress response induced; Ssk1/Nrg1/Tup1/Ssn6/Hog1 regulated; flow model biofilm induced; rat catheter biofilm repressed
orf19.2768	<i>AMS1</i>	-0,45			Putative alpha-mannosidase; transcript regulated by Nrg1; induced during cell wall regeneration; flow model biofilm induced; Spider biofilm induced
orf19.2823	<i>RFG1</i>		0,50		HMG domain transcriptional repressor of filamentous growth and hyphal genes; in Tup1-dependent and -independent pathways; binds DNA; transcript not regulated by oxygen or serum; not responsible for hypoxic repression; Spider biofilm induced
orf19.2839	<i>CIRT4B</i>	-0,48			Cirt family transposase; transcript repressed in an azole-resistant strain that overexpresses CDR1 and CDR2; Hap43-repressed; flow model biofilm induced

orf19.2846		-0,63		-0,54	Protein of unknown function; Hap43-repressed; induced in core caspofungin response; regulated by yeast-hypha switch; Spider biofilm repressed
orf19.2896	<i>SOU1</i>	-0,67	-0,47		Enzyme involved in utilization of L-sorbose; has sorbitol dehydrogenase, fructose reductase, and sorbose reductase activities; NAD-binding site motif; transcriptional regulation affected by chromosome 5 copy number; Hap43p-induced gene
orf19.2990	<i>XOG1</i>		0,42	0,37	Exo-1,3-beta-glucanase; 5 glycosyl hydrolase family member; affects sensitivity to chitin and glucan synthesis inhibitors; not required for yeast-to-hypha transition or for virulence in mice; Hap43-induced; Spider biofilm induced
orf19.3127	<i>CZF1</i>	-0,50			Transcription factor; regulates white-opaque switch; hyphal growth regulator; expression in <i>S. cerevisiae</i> causes dominant-negative inhibition of pheromone response; required for yeast cell adherence to silicone; Spider biofilm induced
orf19.3139				0,72	Putative NADP-dependent oxidoreductase; Hap43-repressed; induced by benomyl treatment; oxidative stress-induced via Cap1; rat catheter biofilm repressed
orf19.3150	<i>GRE2</i>			-0,43	Putative reductase; Nrg1 and Tup1-regulated; benomyl- and hyphal-induced; macrophage/pseudohyphal-repressed; repressed by low iron; possibly involved in osmotic stress response; stationary phase enriched protein; Spider biofilm induced
orf19.3152	<i>AMO2</i>			-0,37	Protein similar to <i>A. niger</i> predicted peroxisomal copper amino oxidase; mutation confers hypersensitivity to toxic ergosterol analog; F-12/CO2 early biofilm induced
orf19.3171	<i>ACH1</i>	0,38	0,44	0,37	Acetyl-coA hydrolase; acetate utilization; nonessential; soluble protein in hyphae; antigenic in human; induced on polystyrene adherence; farnesol-, ketoconazole-induced; no human or murine homolog; stationary phase-enriched protein
orf19.320		-0,70		-0,49	Predicted short chain dehydrogenase; Spider biofilm induced
orf19.3208	<i>DAL52</i>			3,35	Putative allantoinase; mutant is viable; similar but not orthologous to <i>S. cerevisiae</i> Dal5
orf19.3209	<i>FGR42</i>			-0,38	Protein lacking an ortholog in <i>S. cerevisiae</i> ; transposon mutation affects filamentous growth
orf19.3221	<i>CPA2</i>		0,51		Putative arginine-specific carbamoylphosphate synthetase; protein enriched in stationary phase yeast cultures; rat catheter biofilm induced; Spider biofilm induced
orf19.33		-0,45			Predicted ORF from Assembly 19; removed from Assembly 20; restored based on transcription data; similar to orf19.7550
orf19.334			0,74	0,42	Protein of unknown function; flow model biofilm induced; Spider biofilm induced; regulated by Sef1, Sfu1, and Hap43
orf19.3391	<i>ADK1</i>	-0,44			Putative adenylate kinase; repressed in hyphae; macrophage-induced protein; adenylate kinase release used as marker for cell lysis; possibly essential (UAU1 method); flow model biofilm induced; rat catheter and Spider biofilm repressed
orf19.3392	<i>DOG1</i>	-0,60	-0,62	-0,43	Putative 2-deoxyglucose-6-phosphatase; haloacid dehalogenase hydrolase/phosphatase superfamily; similar to <i>S. cerevisiae</i> Dog1, Dog2, Hor1, Rhr2; regulated by Nrg1, Tup1; Spider biofilm repressed
orf19.3393			-0,57	-0,37	Putative DEAD-box helicase; Hap43-induced; Spider biofilm induced
orf19.3396	<i>HCH1</i>	-0,44	-0,55		Ortholog of <i>S. cerevisiae</i> Hch1, a regulator of heat shock protein Hsp90; regulated by Gcn4; induced in response to amino acid starvation (3-aminotriazole treatment); mutants are viable
orf19.3399		-0,40	-0,47	-0,42	Protein of unknown function
orf19.3400	<i>COQ3</i>	-0,51	-0,54	-0,40	Protein with a predicted role in coenzyme Q biosynthesis; transcriptionally induced by interaction with macrophages; possibly an essential gene, disruptants not obtained by UAU1 method
orf19.3401	<i>CTA1</i>		-0,52	-0,42	Protein similar to <i>S. cerevisiae</i> Mos10p, which affects <i>S. cerevisiae</i> filamentous growth; activates transcription in 1-hybrid assay in <i>S. cerevisiae</i> ; protein levels increase under weak acid stress; nonessential
orf19.3405	<i>ZCF18</i>			-0,40	Putative Zn(II)2Cys6 transcription factor; heterozygous null mutant displays sensitivity to virgineone and decreased colonization of mouse kidneys
orf19.3407	<i>RAD18</i>			-0,37	Putative transcription factor with zinc finger DNA-binding motif; Hap43p-repressed gene
orf19.3409	<i>SEC12</i>	-0,41	-0,50	-0,43	Putative guanyl-nucleotide exchange factor; induced in high iron; Hap43-repressed
orf19.3411				-0,53	Protein of unknown function
orf19.3412	<i>ATG15</i>			-0,38	Putative lipase; fungal-specific (no human or murine homolog); Hap43p-repressed gene
orf19.3414	<i>SUR7</i>	-0,39		-0,36	Protein required for normal cell wall, plasma membrane, cytoskeletal organization, endocytosis; localizes to eisosome subdomains of plasma membrane; four transmembrane motifs; mutant shows ectopic, chitin-rich cell wall; fluconazole-induced
orf19.3415.1	<i>RPL32</i>	-0,40	-0,54		Component of the large (60S) ribosomal subunit; Spider biofilm repressed
orf19.3417	<i>ACF2</i>	-0,55	-0,65	-0,55	Putative endo-1,3-beta-glucanase; fungal-specific (no human or murine homolog)
orf19.3423	<i>TIF3</i>		-0,44		Putative translation initiation factor; genes encoding ribosomal subunits, translation factors, and tRNA synthetases are downregulated upon phagocytosis by murine macrophage
orf19.3426	<i>ANB1</i>	-0,40	-0,50	-0,37	Translation initiation factor eIF-5A; repressed in hyphae vs yeast cells; downregulated upon phagocytosis by murine macrophage; Hap43-induced; GlcNAc-induced protein; Spider biofilm repressed
orf19.3427				-0,41	Protein of unknown function
orf19.3433	<i>OYE23</i>			-0,65	Putative NADPH dehydrogenase; induced by nitric oxide, benomyl; oxidative stress-induced via Cap1; Hap43p-repressed; rat catheter biofilm induced
orf19.3439				-0,52	Protein of unknown function; upregulated by fluphenazine treatment or in an azole-resistant strain that overexpresses CDR1 and CDR2; transcript possibly regulated by Tac1
orf19.344				0,35	Protein of unknown function; Cyr1-repressed; rat catheter and Spider biofilm induced
orf19.3442		-0,47	-0,48	-0,41	Putative oxidoreductase; Hap43-repressed gene
orf19.3443	<i>OYE2</i>	-0,60	-0,51	-0,56	Putative NADPH dehydrogenase; induced by nitric oxide; Spider biofilm induced
orf19.3445	<i>HOC1</i>	-0,44	-0,46	-0,43	Protein with similarity to mannosyltransferases; similar to <i>S. cerevisiae</i> Hoc1p and <i>C. albicans</i> Och1p
orf19.3447				-0,42	Protein of unknown function
orf19.3450.1				-0,41	Protein of unknown function
orf19.3456		-0,71	-0,63	-0,59	Protein with a predicted serine/threonine kinase and tyrosine kinase domain; possibly an essential gene, disruptants not obtained by UAU1 method
orf19.3457	<i>SWD3</i>			-0,40	Protein of unknown function
orf19.3458		-0,51	-0,60	-0,45	Protein of unknown function
orf19.3459		-0,52	-0,47	-0,47	Putative serine/threonine/tyrosine (dual-specificity) kinase; disruptants not obtained by UAU1 method
orf19.3460		-0,73		-0,52	Protein of unknown function; mRNA binds She3; transcript regulated upon yeast-hypha switch; induced in oropharyngeal candidiasis
orf19.3462	<i>SAR1</i>	-0,46	-0,53	-0,40	Functional homolog of <i>S. cerevisiae</i> Sar1; which is required for ER-to-Golgi protein transport; binds GTP; similar to small GTPase superfamily proteins; gene has intron; Hap43-induced; rat catheter biofilm repressed
orf19.3463		-0,37	-0,51	-0,35	Putative GTPase; role in 60S ribosomal subunit biogenesis; Spider biofilm induced
orf19.3465	<i>RPL10A</i>		-0,48		Predicted ribosomal protein; downregulated upon phagocytosis by murine macrophages; Hap43-induced; Spider biofilm repressed
orf19.3467	<i>SEC27</i>	-0,46	-0,41	-0,35	Protein of unknown function
orf19.3469		-0,43			<i>S. cerevisiae</i> ortholog Stb1 has a role in regulation of MBF-specific transcription at Start; induced in a <i>cyr1</i> null mutant; Spider biofilm induced
orf19.3473				-0,40	Protein of unknown function
orf19.3474	<i>IPL1</i>			-0,41	Putative Aurora kinase; Hap43-induced; induced during planktonic growth; possibly an essential gene, disruptants not obtained by UAU1 method
orf19.3477		-0,39			Putative pseudouridine synthase; predicted role in snRNA pseudouridine synthesis, tRNA pseudouridine synthesis; Spider biofilm induced
orf19.3478	<i>NIP7</i>	-0,45	-0,58	-0,39	Putative nucleolar protein with role in ribosomal assembly; hyphal-induced; Hap43-induced; Spider biofilm induced
orf19.3480		-0,45			Protein of unknown function
orf19.3482		-0,49	-0,53	-0,52	Protein of unknown function
orf19.3496	<i>CHC1</i>	-0,43		-0,37	Clathrin heavy chain; subunit of the major coat protein; role in intracellular protein transport and endocytosis; flow model and rat catheter biofilm repressed

Supporting Information

orf19.3501				-0,40	S. cerevisiae ortholog Pxl1 localizes to sites of polarized growth and is required for selection and/or maintenance of polarized growth sites; Hog1p-repressed
orf19.3503				-0,55	Protein of unknown function
orf19.3504	RPL23A		-0,42		Ribosomal protein; downregulated upon phagocytosis by murine macrophage; Hap43-induced; sumoylation target; Spider biofilm repressed
orf19.3507	MCR1	-0,55	-0,47	-0,39	NADH-cytochrome-b5 reductase; soluble in hyphae; alkaline downregulated; farnesol, ketoconazole or flucytosine induced; protein present in exponential and stationary growth phase yeast; YNB biofilm induced; rat catheter biofilm repressed
orf19.3508		-0,60		-0,46	Putative protein of unknown function; stationary phase enriched protein
orf19.3548.1	WH11	-0,38			White-phase yeast transcript; expression in opaques increases virulence/switching; mutant switches as WT; Hap43, hypoxia, ketoconazol induced; required for RPM1 biofilm; Bcr1-induced in RPM1 a/a biofilm; rat catheter, Spider biofilm induced
orf19.3642	SUN41	-0,43	-0,48	-0,44	Cell wall glycosidase; role in biofilm formation and cell separation; possibly secreted; hypoxia, hyphal induced; caspofungin repressed; Efg1, Cph1 regulated; O-glycosylated, possible Kex2 substrate; 5'-UTR intron; Spider biofilm induced
orf19.3643				-0,42	Protein of unknown function; Hap43-repressed gene
orf19.3644		-0,41		-0,41	Protein of unknown function; Cyr1-repressed; rat catheter and Spider biofilm induced
orf19.3647	SEC8	-0,46	-0,46	-0,37	Predicted subunit of the exocyst complex, involved in exocytosis; localizes to a crescent on the surface of the hyphal tip
orf19.3649		-0,64	-0,76	-0,54	Protein of unknown function
orf19.3651	PGK1	-0,81	-0,65	-0,49	Phosphoglycerate kinase; localizes to cell wall and cytoplasm; antigenic in murine/human infection; flow model biofilm, Hog1-, Hap43-, GCN-induced; repressed upon phagocytosis; repressed in Spider biofilms by Bcr1, Ndt80, Rob1, Brg1
orf19.3653	FAT1		-0,42		Predicted enzyme of sphingolipid biosynthesis; upregulated in biofilm
orf19.3658				-0,38	Protein of unknown function
orf19.3659		-0,52			Putative CTD phosphatase; role in dephosphorylation of RNA polymerase II C-terminal domain, transcription from RNA polymerase II promoter; flow model biofilm induced
orf19.3660			-0,54	-0,39	Protein of unknown function
orf19.3664	HSP31	0,61	1,40	0,88	Putative 30 kda heat shock protein; repressed during the mating process; rat catheter biofilm induced
orf19.3669	SHA3		0,46		Putative ser/thr kinase involved in glucose transport; Tn mutation affects filamentous growth; fluconazole-induced; ketoconazole-repressed; induced in by alpha pheromone in SpiderM; possibly essential; flow model biofilm induced
orf19.3672	GAL10			0,38	UDP-glucose 4-epimerase; galactose utilization; mutant has cell wall defects and increased filamentation; GlcNAc-, fluconazole- and ketoconazole-induced; stationary phase enriched protein; rat catheter and flow model biofilm induced
orf19.3675	GAL7			0,43	Putative galactose-1-phosphate uridyl transferase; downregulated by hypoxia, upregulated by ketoconazole; macrophage/pseudohyphal-repressed
orf19.3707	YHB1	-0,63			Nitric oxide dioxygenase; acts in nitric oxide scavenging/detoxification; role in virulence in mouse; transcript activated by NO, macrophage interaction; Hap43, hypha repressed; mRNA binds She3
orf19.3733	IDP2		0,77	0,64	Isocitrate dehydrogenase; white-opaque switch regulated; morphology-regulation by Ssn6; protein in exponential and stationary phase yeast; Hap43-repressed; Spider biofilm repressed by Bcr1, Tec1, Ndt80, Rob1, Brg1; Spider biofilm induced
orf19.3740	PGA23	-0,66			Putative GPI-anchored protein of unknown function; Rim101-repressed; Cyr1-regulated; colony morphology-related gene regulation by Ssn6
orf19.385	GCV2	0,48		0,44	Glycine decarboxylase P subunit; protein of glycine catabolism; repressed by Efg1; Hog1-induced; induced by Rim101 at acid pH; transcript induced in elevated CO2; stationary phase enriched protein
orf19.3895	CHT2	0,45	0,41		GPI-linked chitinase; required for normal filamentous growth; repressed in core caspofungin response; fluconazole, Cyr1, Efg1, pH-regulated; mRNA binds She3 and is localized to yeast-form buds and hyphal tips; Spider biofilm repressed
orf19.3932		-0,56		-0,37	Predicted RNA binding protein; stationary phase enriched; induced in core caspofungin response; induced by nitric oxide independent of Yhb1; repressed in ssr1 null; ketoconazole, hypoxia induced; Spider biofilm induced
orf19.3932.1				-0,51	Protein of unknown function
orf19.3988			1,54	0,99	Putative adhesin-like protein; induced by Mnl1 under weak acid stress; rat catheter and Spider biofilm induced
orf19.4082	DDR48	-0,71			Immunogenic stress-associated protein; filamentation regulated; induced by benomyl/caspofungin/ketoconazole or in azole-resistant strain; Hog1, farnesol, alkaline repressed; stationary phase enriched; Spider, flow model biofilm induced
orf19.4192	CDC14			-0,39	Protein involved in exit from mitosis and morphogenesis; ortholog of S. cerevisiae Cdc14p, which is a dual-specificity phosphatase and cell-cycle regulator; suppresses S. cerevisiae cdc15-lyt1, dbf2-2, and (partially) tem1 mutant phenotypes
orf19.4192.1		-0,47	-0,60	-0,37	Protein of unknown function
orf19.4194		-0,50			Putative TFIID complex subunit; possibly an essential gene, disruptants not obtained by UAU1 method
orf19.4195.1	FCA1	-0,49	-0,61		Cytosine deaminase; enzyme of pyrimidine salvage; functional homolog of S. cerevisiae Fcy1p; mutation is associated with resistance to flucytosine (5-FC) in a clinical isolate; hyphal downregulated; gene has intron
orf19.4203		-0,48			Protein of unknown function
orf19.4206				-0,37	Protein of unknown function
orf19.4208	RAD52		-0,50	-0,52	Required for homologous DNA recombination, repair of UV- or MMS-damaged DNA, telomere length, UV-induced LOH; constitutive expression, MMS-induced; weakly complements S. cerevisiae rad52 mutant; slow growth, increased white-to-opaque switch
orf19.4209		-0,52	-0,58	-0,48	Protein of unknown function
orf19.4211			-0,44		Multicopper oxidase; for growth in low iron, prostaglandin E2 synthesis; ketoconazole/caspofungin/amphotericin B repressed; Sef1/Sfu1/Hap43 regulated; reports differ if functional homolog of ScFet3; rat catheter and Spider biofilm induced
orf19.4215	FET34		-0,58		Multicopper ferroxidase; induced by low iron, ciclopirox olamine, ketoconazole, hypoxia; alkaline induced by Rim101; repressed in fluconazole-resistant isolate; Sfu1, Hog1 repressed; complements S. cerevisiae fet3; Spider biofilm induced
orf19.4246		-0,58			Protein with similarity to S. cerevisiae Ykr070w; Tn mutation affects filamentation; Hog1-repressed; colony morphology-related gene regulation by Ssn6p; induced during cell wall regeneration; possibly essential
orf19.4255	ECM331		-0,74	-0,47	GPI-anchored protein; mainly at plasma membrane, also at cell wall; Hap43, caspofungin-induced; Plc1-regulated; Hog1, Rim101-repressed; colony morphology-related regulated by Ssn6; induced by ketoconazole and hypoxia
orf19.4274	PUT1		0,41		Putative proline oxidase; alkaline upregulated by Rim101; flow model biofilm induced; Spider biofilm induced
orf19.4393	CIT1		0,61	0,39	Citrate synthase; induced by phagocytosis; induced in high iron; Hog1-repressed; Efg1-regulated under yeast, not hyphal growth conditions; present in exponential and stationary phase; Spider biofilm repressed; rat catheter biofilm induced
orf19.4436	GPX3	-0,54			Putative glutathione peroxidase involved in Cap1p-dependent oxidative stress response, required for Cap1p oxidation in response to H2O2; planktonic growth-induced
orf19.4438	RME1		0,71		Zinc finger protein; controls meiosis in S. cerevisiae; white-specific transcript; upregulation correlates with clinical development of fluconazole resistance; Upc2-regulated in hypoxia; flow model biofilm induced; Spider biofilm repressed
orf19.4445			0,42	0,35	Protein of unknown function; Plc1p-regulated; expression induced early upon infection of reconstituted human epithelium (RHE), while expression of the C. dubliniensis ortholog is not; mutant is viable; Spider biofilm induced
orf19.4450.1			0,59		Protein conserved among the CTG-clade; 2 adjacent upstream SRE-1 elements; highly up-regulated in cecum-grown cells in a Cph2-dependent manner; Hap43-repressed; rat catheter, Spider and flow model biofilm induced

orf19.4475	<i>KTR4</i>	-0,43			Mannosyltransferase; induced during cell wall regeneration; fungal-specific (no human or murine homolog); Bcr1-repressed in RPM1 a/a biofilms
orf19.4476				-0,51	Protein with a NADP-dependent oxidoreductase domain; transcript induced by ketoconazole; rat catheter and Spider biofilm induced
orf19.4477	<i>CSH1</i>	-0,75	-0,46	-0,62	Aldo-keto reductase; role in fibronectin adhesion, cell surface hydrophobicity; regulated by temperature, growth phase, benomyl, macrophage interaction; azole resistance associated; Spider biofilm induced; rat catheter biofilm repressed
orf19.4526	<i>HSP30</i>		1,79	1,06	Putative heat shock protein; fluconazole repressed; amphotericin B induced; Spider biofilm induced; rat catheter biofilm induced
orf19.4555	<i>ALS4</i>	-0,69	-0,64		GPI-anchored adhesin; role in adhesion, germ tube induction; growth, temperature regulated; expressed during infection of human buccal epithelial cells; repressed by vaginal contact; biofilm induced; repressed during chlamydospore formation
orf19.4599	<i>PHO89</i>	0,80	0,69	0,40	Putative phosphate permease; transcript regulated upon white-opaque switch; alkaline induced by Rim101; possibly adherence-induced; F-12/CO2 model, rat catheter and Spider biofilm induced
orf19.4609				0,49	Putative dienelectone hydrolase; protein abundance is affected by URA3 expression in the CAI-4 strain background; protein present in exponential and stationary growth phase yeast cultures; rat catheter biofilm repressed
orf19.4666				-0,45	Protein of unknown function; hyphal-induced expression, regulated by Cyr1, Ras1, Efg1; Spider biofilm induced
orf19.467	<i>WOR3</i>	0,59	0,96	1,00	Transcription factor; modulator of white-opaque switch; induced in opaque cells; promoter bound by Wor1; overexpression at 25 degr shifts cells to opaque state; deletion stabilizes opaque cells at higher temperatures; Spider biofilm induced
orf19.4679	<i>AGP2</i>	-0,53			Amino acid permease; hyphal repressed; white-opaque switch regulated; induced in core caspofungin response, during cell wall regeneration, by flucytosine; regulated by Sef1, Sfu1, and Hap43; rat catheter and Spider biofilm induced
orf19.4682	<i>HGT17</i>			-0,39	Putative MFS family glucose transporter; 20 members in <i>C. albicans</i> ; 12 probable membrane-spanning segments; induced at low (0.2%, compared to 2%) glucose in rich media; Spider biofilm induced
orf19.4688	<i>DAG7</i>	-0,51	-0,43		Secretory protein; a-specific, alpha-factor induced; mutation confers hypersensitivity to toxic ergosterol analog; fluconazole-induced; induced during chlamydospore formation in <i>C. albicans</i> and <i>C. dubliniensis</i>
orf19.4773	<i>AOX2</i>	0,53	0,97		Alternative oxidase; cyanide-resistant respiration; induced by antimycin A, oxidants; growth; Hap43, chlamydospore formation repressed; rat catheter, Spider biofilm induced; regulated in Spider biofilms by Bcr1, Tec1, Ndt80, Brg1
orf19.4777	<i>DAK2</i>	-0,58			Putative dihydroxyacetone kinase; repressed by yeast-hypha switch; fluconazole-induced; caspofungin repressed; protein enriched in stationary phase yeast cultures; flow model biofilm induced; rat catheter and Spider biofilm repressed
orf19.4779				0,47	Putative transporter; slightly similar to the Sit1p siderophore transporter; Gcn4p-regulated; fungal-specific; induced by Mnl1p under weak acid stress
orf19.4784	<i>CRP1</i>		0,63	0,36	Copper transporter; CPx P1-type ATPase; mediates Cu resistance; similar to Menkes and Wilson disease proteins; copper-induced; Tbf1-activated; suppresses Cu sensitivity of <i>S. cerevisiae</i> cup1 mutant; flow model biofilm induced
orf19.4788	<i>ARG5,6</i>		0,44		Arginine biosynthetic enzyme; processed in <i>S. cerevisiae</i> into 2 polypeptides with acetylglutamate kinase (Arg6) activity and acetylglutamate-phosphate reductase (Arg5) activity; Gcn4 regulated; alkaline repressed; Spider biofilm induced
orf19.48	<i>RPM2</i>		0,44		Mitochondrial RNase P subunit; roles in nuclear transcription, cytoplasmic and mitochondrial RNA processing, mitochondrial translation; virulence-group-correlated expression; likely essential (UAU1 method); rat catheter biofilm induced
orf19.4898		-0,46			Putative protein of unknown function; induced by prostaglandins
orf19.4899	<i>GCA1</i>	-0,47			Extracellular/plasma membrane-associated glucoamylase; expressed in rat oral infection; regulated by carbohydrates, pH, galactose; promotes biofilm matrix formation; flow model biofilm induced; Bcr1 repressed in RPM1 a/a biofilms
orf19.4907			0,77		Putative protein of unknown function; Hap43p-repressed gene; increased transcription is observed upon fluphenazine treatment; possibly transcriptionally regulated by Tac1p; induced by nitric oxide; fungal-specific (no human/murine homolog)
orf19.4914.1	<i>BLP1</i>	-0,52			Protein of unknown function, serum-induced
orf19.4940				0,34	Putative histidine permease; fungal-specific (no human or murine homolog); Hap43p-induced gene
orf19.4941	<i>TYE7</i>			0,34	bHLH transcription factor; control of glycolysis; required for biofilm formation; hyphally regulated by Cph1, Cyr1, flucytosine, Hog1 induced; amphotericin B, caspofungin repressed; induced in flow model biofilm and planktonic cultures
orf19.4943	<i>PSA2</i>	-0,68			Mannose-1-phosphate guanyltransferase; Hap43, macrophage-repressed; stationary phase enriched protein; Spider biofilm induced; rat catheter biofilm repressed
orf19.5025	<i>MET3</i>		-0,43		ATP sulfurlyase; sulfate assimilation; repressed by Met, Cys, Sfu1, or in fluconazole-resistant isolate; Hog1, caspofungin, white phase-induced; induced on biofilm formation, even in presence of Met and Cys; Spider, F-12/CO2 biofilm induced
orf19.5079	<i>CDR4</i>		0,57		Putative ABC transporter superfamily; fluconazole, Sfu1, Hog1, core stress response induced; caspofungin repressed; fluconazole resistance not affected by mutation or correlated with expression; rat catheter and flow model biofilm induced
orf19.5125				-0,35	Protein of unknown function; induced by ketoconazole; Spider, F-12/CO2 and flow model biofilm induced
orf19.5158		-0,50			Protein with similarity to a human gene associated with colon cancer and to orf19.5158; regulated by Gcn4, Cyr1; induced by amino acid starvation; macrophage-induced protein, macrophage-repressed; Spider biofilm induced
orf19.5285	<i>PST3</i>			0,34	Putative flavodoxin; YNB biofilm induced; stationary phase enriched protein; rat catheter and Spider biofilm repressed
orf19.5305	<i>RHD3</i>	0,53			GPI-anchored yeast-associated cell wall protein; induced in high iron; clade-associated gene expression; not essential for cell wall integrity; fluconazole-repressed; flow model and Spider biofilm repressed
orf19.5383	<i>PMA1</i>	0,47	0,43	0,40	Plasma membrane H(+)-ATPase; highly expressed, comprises 20-40% of total plasma membrane protein; levels increase at stationary phase transition; fluconazole induced; caspofungin repressed; upregulated in RHE model; Spider biofilm repressed
orf19.54	<i>RHD1</i>			-0,44	Putative beta-mannosyltransferase required for the addition of beta-mannose to the acid-labile fraction of cell wall phosphopeptidomannan; 9-gene family memebr; regulated on yeast-hypha and white-opaque switches; Spider biofilm repressed
orf19.5431		-0,48			Protein of unknown function; Hap43-repressed; Spider biofilm induced
orf19.5455		0,43			Protein of unknown function
orf19.5514				-0,46	Ortholog of <i>S. pombe</i> SPCC550.08, an N-acetyltransferase; transcript induced during growth in the mouse cecum
orf19.5516		-0,47	-0,43		Protein of unknown function
orf19.5517			-0,60	-0,37	Similar to alcohol dehydrogenases; induced by benomyl treatment, nitric oxide; induced in core stress response; oxidative stress-induced via Cap1; Spider biofilm repressed
orf19.5518		-0,51			Protein of unknown function; Spider biofilm induced
orf19.5519	<i>GCV1</i>	-0,53	-0,44		Putative T subunit of glycine decarboxylase; transcript negatively regulated by Sfu1; Spider biofilm repressed
orf19.5521	<i>ISA1</i>	-0,52			Putative mitochondrial iron-sulfur protein; alkaline repressed; induced in high iron; regulated by Sef1, Sfu1, Hap43; Spider biofilm induced
orf19.5522		-0,57	-0,51		Protein of unknown function
orf19.5525		-0,82	-0,62	-0,48	Putative oxidoreductase; protein levels affected by URA3 expression in CAI-4 strain background; Efg1, Efh1 regulated; Rgt1-repressed; protein present in exponential and stationary growth phase yeast; rat catheter biofilm repressed

Supporting Information

orf19.5526	<i>SEC20</i>	-0,66	-0,57	-0,49	Essential protein; similar to <i>S. cerevisiae</i> Sec20p; depletion causes membrane accumulation and drug sensitivity; expression regulated by growth phase; O-mannosylation regulates proteolysis; does not complement <i>S. cerevisiae</i> sec20-1 mutant
orf19.5530	<i>NAB3</i>			-0,34	Putative nuclear polyadenylated RNA-binding protein; flucytosine repressed
orf19.5531	<i>CDC37</i>	-0,51	-0,48	-0,42	Chaperone for Crk1p; interacts with Crk1p kinase domain and with Sti1p; putative phosphorylation site at Ser14; functional homolog of <i>S. cerevisiae</i> Cdc37p; likely to be essential for growth; regulated by Gcn2p and Gcn4p
orf19.5534				-0,40	Protein with a predicted role in mitotic spindle elongation, vesicle-mediated transport; flow model biofilm induced
orf19.5539		-0,61		-0,41	Protein of unknown function
orf19.5544	<i>SAC6</i>	-0,57	-0,52	-0,51	Fimbrin; actin filament bundling protein; transcript regulated by Nrg1 and Mig1; protein level decreases in stationary phase
orf19.5550	<i>MRT4</i>	-0,40	-0,64	-0,35	Putative mRNA turnover protein; Hap43-induced; mutation confers hypersensitivity to tubercidin (7-deazaadenosine); rat catheter biofilm induced
orf19.5551	<i>MIF2</i>	-0,44		-0,39	Centromere-associated protein; similar to CENP-C proteins; Cse4p and Mif2p colocalize at <i>C. albicans</i> centromeres
orf19.5552		-0,50	-0,46	-0,43	Putative transcriptional regulator of ribonucleotide reductase genes; Spider biofilm induced
orf19.5553		-0,62	-0,58	-0,47	Protein of unknown function
orf19.5561	<i>STE23</i>		-0,45	-0,39	Ortholog of <i>S. cerevisiae</i> Ste23 metalloprotease; role in N-terminal processing of pro-a-factor to the mature form; Tn mutation affects filamentous growth; Spider biofilm induced
orf19.5563	<i>RNH1</i>		-0,63	-0,40	Ribonuclease H (RNase H); hyphal-induced; flucytosine induced; similar to orf19.5564 (see Locus History); possibly essential (UAU1 method); rat catheter biofilm induced; flow model biofilm repressed
orf19.5564			-0,53		Protein of unknown function
orf19.5569		-0,39		-0,37	Protein of unknown function
orf19.5574		-0,55	-0,52	-0,46	Protein of unknown function
orf19.5580	<i>TEL1</i>	-0,45		-0,37	Protein of unknown function
orf19.5584	<i>PEP3</i>			-0,40	Peptidase; activity useful for strain identification by multilocus enzyme electrophoresis (MLEE); clade-associated gene expression
orf19.5585	<i>SAP5</i>			-0,42	Secreted aspartyl proteinase; sap4,5,6 triple null defective in utilization of protein as N source; virulence role effected by URA3; expressed during infection; mRNA localized to hyphal tip via She3; rat catheter and Spider biofilm induced
orf19.5586				-0,46	Protein of unknown function
orf19.5587				-0,53	Protein of unknown function; transcript is upregulated in clinical isolates from HIV+ patients with oral candidiasis
orf19.5595	<i>SHE3</i>	-0,56	-0,59	-0,57	mRNA-binding protein that localizes specific mRNAs to daughter yeast cells and to hyphal tips; required for normal filamentation and host epithelial cell damage; ortholog of <i>S. cerevisiae</i> She3 but target mRNAs differs
orf19.5597	<i>POL5</i>	-0,41			Putative DNA Polymerase phi; F-12/CO2 early biofilm induced
orf19.5599	<i>MDL2</i>			-0,34	Putative mitochondrial, half-size MDR-subfamily ABC transporter
orf19.5601				-0,39	Protein of unknown function
orf19.5604	<i>MDR1</i>			-0,55	Plasma membrane MDR/MFS multidrug efflux pump; methotrexate is preferred substrate; overexpression in drug-resistant clinical isolates confers fluconazole resistance; repressed in young biofilms; rat catheter biofilm induced
orf19.5607		-0,48			Protein of unknown function
orf19.5612	<i>BMT4</i>	-0,45	-0,70	-0,63	Beta-mannosyltransferase; for elongation of beta-mannose chains on the acid-labile fraction of cell wall phosphopeptidomannan; 9-gene family member; regulated by Tsa1, Tsa1B; flow model biofilm induced; rat catheter biofilm repressed
orf19.5614		-0,91	-0,83	-0,73	Putative ribonuclease H1; possibly an essential gene, disruptants not obtained by UAU1 method; flow model biofilm induced; Spider biofilm induced
orf19.5618		-0,63	-0,44	-0,47	Protein of unknown function
orf19.5619		-0,54		-0,46	Protein of unknown function; induced by alpha pheromone in SpiderM medium; Spider biofilm induced
orf19.5620		-0,82	-0,67	-0,53	Stationary phase enriched protein; Gcn4-regulated; induced by amino acid starvation (3-AT), benomyl or in azole-resistant strain that overexpresses MDR1; flow model biofilm induced; rat catheter biofilm repressed; overlaps orf19.5621
orf19.5621		-0,56		-0,42	Putative protein of unknown function; mutation confers hypersensitivity to amphotericin B; overlaps orf19.5621
orf19.5622	<i>GLC3</i>	-0,94	-0,94	-0,82	Putative 1,4-glucan branching enzyme; fluconazole-induced; colony morphology-related gene regulation by Ssn6; stationary phase enriched protein
orf19.5623	<i>ARP4</i>	-0,54	-0,51	-0,42	Subunit of the NuA4 histone acetyltransferase complex
orf19.5626		-0,70	-0,45	-0,48	Protein of unknown function; Plc1-regulated; induced by Mnl1 under weak acid stress; flow model biofilm induced
orf19.5627		-0,53	-0,52	-0,44	<i>S. cerevisiae</i> ortholog Hek2/Khd1 is a putative RNA binding protein involved in the asymmetric localization of ASH1 mRNA; Hap43-induced gene
orf19.5629	<i>QCR7</i>	-0,48	-0,45		Putative ubiquinol-cytochrome-c reductase, subunit 7; Hap43p-repressed gene
orf19.5630	<i>APA2</i>	-0,46			Putative ATP adenyllyltransferase II; regulated by Gcn4; repressed by amino acid starvation (3-AT); induced by prostaglandins; Hap43-repressed; Spider biofilm repressed
orf19.5634	<i>FRP1</i>	0,49			Ferric reductase; alkaline-induced by Rim101; iron-chelation-induced by CCAAT-binding factor; fluconazole-repressed; ciclopirox-, hypoxia-, Hap43-induced; colony morphology-related regulation by Ssn6; Spider and flow model biofilm induced
orf19.5686		-0,54			Protein of unknown function; Spider biofilm induced
orf19.5702		-0,41			Protein of unknown function
orf19.5713	<i>YMX6</i>			1,11	Putative NADH dehydrogenase; macrophage-downregulated gene; induced by nitric oxide; rat catheter biofilm induced
orf19.5718		-0,55	-0,56	-0,58	Protein of unknown function
orf19.5723	<i>POX1</i>			-0,35	Predicted acyl-CoA oxidase; regulated upon white-opaque switch; upregulated upon phagocytosis; Spider biofilm induced
orf19.5728				0,62	Putative cytochrome P450; Spider biofilm induced
orf19.5729	<i>FGR17</i>	-0,72	-0,58	-0,57	Putative DNA-binding transcription factor; has zinc cluster DNA-binding motif; lacks an ortholog in <i>S. cerevisiae</i> ; transposon mutation affects filamentous growth; Hap43p-repressed gene
orf19.5734	<i>POP2</i>	-0,53	-0,48	-0,45	Component of the Ccr4-Pop2 mRNA deadenylase; heterozygous null mutant exhibits resistance to parnafungin and cordycepin in the <i>C. albicans</i> fitness test
orf19.5735	<i>CDC50</i>			-0,39	Putative endosomal protein; induced by Mnl1p under weak acid stress
orf19.5736	<i>ALS5</i>	-0,51		-0,36	ALS family adhesin; highly variable; expression in <i>S. cerevisiae</i> causes adhesion to human epithelium, endothelium or ECM, endothelial invasiveness by endocytosis and, at high abundance, ECM-induced aggregation; can form amyloid fibrils
orf19.5742	<i>ALS9</i>	-0,63		-0,46	ALS family cell-surface glycoprotein; expressed during infection of human epithelial cells; confers laminin adhesion to <i>S. cerevisiae</i> ; highly variable; putative GPI-anchor; Hap43-repressed
orf19.5746	<i>ALA1</i>	-0,38	-0,43	-0,38	Alanyl-tRNA synthetase; translational regulation generates cytoplasmic and mitochondrial forms; Gcn4p-regulated; repressed by amino acid starvation (3-AT); translation-related genes downregulated upon phagocytosis by murine macrophages
orf19.5747		-0,43			Protein of unknown function
orf19.5749	<i>SBA1</i>	-0,51	-0,43	-0,35	Similar to co-chaperones; induced in high iron; farnesol-, heavy metal (cadmium) stress-induced; protein level decreases in stationary phase cultures; Hap43-repressed
orf19.5750	<i>SHM2</i>		-0,45		Cytoplasmic serine hydroxymethyltransferase; complements glycine auxotrophy of <i>S. cerevisiae</i> shm1 shm2 gly1-1 mutant; antigenic; farnesol-upregulated in biofilm; stationary-phase enriched protein; rat catheter and Spider biofilm repressed
orf19.5752				-0,46	Protein of unknown function

orf19.5754		-0,48			Putative membrane protein with a predicted role in zinc ion homeostasis; Hap43-induced; fluconazole-induced; rat catheter and Spider biofilm induced
orf19.5757		-0,61	-0,51	-0,51	Protein of unknown function
orf19.5760	<i>IHD1</i>		0,43		GPI-anchored protein; alkaline, hypha-induced; regulated by Nrg1, Rfg1, Tup1 and Tsa1, Tsa1B in minimal media at 37; oralpharyngeal candidiasis induced; Spider biofilm induced; regulated in Spider biofilms by Tec1, Efg1, Ndt80, Rob1, Brg1
orf19.5763		-0,63		-0,45	Protein of unknown function
orf19.5764	<i>SKI8</i>	-0,52	-0,63	-0,50	Protein of unknown function
orf19.5765	<i>NUP82</i>	-0,59	-0,57	-0,50	Linker nucleoporin of the nuclear pore complex; role in mRNA anexport from nucleus, protein import into nucleus, ribosomal large subunit export from nucleus, ribosomal small subunit export from nucleus; rat catheter biofilm repressed
orf19.5767		-0,57		-0,39	Protein of unknown function
orf19.5768	<i>SNF4</i>	-0,56	-0,56	-0,50	Transcription factor; ortholog of <i>S. cerevisiae</i> Snf4; caspofungin repressed; transposon mutation affects filamentation
orf19.5771	<i>PBP2</i>	-0,38	-0,46	-0,36	Putative RNA binding protein; transcript regulated by Nrg1, Mig1, and Tup1
orf19.5773		-0,56	-0,52	-0,47	Putative dipeptidyl-peptidase III; protein detected by mass spec in exponential and stationary phase cultures; Hog1p-induced; clade-associated gene expression
orf19.5784	<i>AMO1</i>	0,69			Putative peroxisomal copper amine oxidase
orf19.5785				0,72	Protein of unknown function; upregulated in a <i>cyr1</i> or <i>ras1</i> null mutant; induced by nitric oxide
orf19.5806	<i>ALD5</i>			0,38	NAD-aldehyde dehydrogenase; decreased expression in fluconazole-resistant isolate, or in hyphae; biofilm induced; fluconazole-downregulated; protein abundance is affected by URA3 expression in the CAI-4 strain; stationary phase enriched
orf19.5843	<i>SRR1</i>	-0,46			Two-component system response regulator; involved in stress response; Plc1-regulated; upregulated in <i>cyr1</i> null mutant; flow model biofilm induced; Spider biofilm induced
orf19.5863		-0,63		-0,41	Protein of unknown function
orf19.5867	<i>WSC1</i>		0,46		Putative cell wall component; transcript upregulated in <i>cyr1</i> mutant (yeast or hyphae); Spider and flow model biofilm induced
orf19.5960	<i>NCE102</i>		0,41		Non classical protein export protein; localized to plasma membrane; Hap43-induced gene; flow model biofilm induced; Spider biofilm induced
orf19.6003		0,55	0,72	0,50	Protein of unknown function; role in intracellular signal transduction; Spider biofilm induced
orf19.6073	<i>HMX1</i>	0,67			Heme oxygenase; utilization of heme iron; transcript induced by heat, low iron, or hemein; repressed by Efg1; induced by low iron; upregulated by Rim101 at pH 8; Hap43-induced; Spider and flow model biofilm induced
orf19.6077				-0,37	Putative protein of unknown function; shows colony morphology-related gene regulation by Ssn6p
orf19.6078	<i>POL93</i>		0,54	0,38	Predicted ORF in retrotransposon Tca8 with similarity to the Pol region of retrotransposons encoding reverse transcriptase, protease and integrase; downregulated in response to ciclopirox olamine; F-12/CO2 early biofilm induced
orf19.6079			0,47	0,36	Predicted ORF in retrotransposon Tca8 with similarity to the Gag region encoding nucleocapsid-like protein; repressed by ciclopirox olamine; filament induced; regulated by Rfg1, Tup1; overlaps orf19.6078.1
orf19.6081	<i>PHR2</i>		-0,58		Glycosidase; role in vaginal not systemic infection (low pH not neutral); low pH, high iron, fluconazole, Hap43-induced; Rim101-repressed at pH8; rat catheter biofilm induced; Bcr1-repressed in RPM1 a/a biofilms
orf19.6139	<i>FRE7</i>		0,71		Copper-regulated cupric reductase; repressed by ciclopirox olamine or 17-beta-estradiol; induced by alkaline conditions or interaction with macrophage; Spider biofilm induced
orf19.6140	<i>FRE30</i>		0,59		Protein with similarity to ferric reductases; downregulated in response to amphotericin B, estradiol, or ciclopirox olamine, and upregulated by interaction with macrophage; un-merged from orf19.6139 in a revision of Assembly 21
orf19.6197	<i>DHH1</i>			0,41	Putative RNA helicase
orf19.6202	<i>RBT4</i>	-0,91	-0,77	-0,68	Pry family protein; required for virulence in mouse systemic/rabbit corneal infections; not filamentation; mRNA binds She3, is localized to hyphal tips; Hap43-induced; in both yeast and hyphal culture supernatants; Spider biofilm induced
orf19.6229	<i>CAT1</i>	-0,42		-0,46	Catalase; resistance to oxidative stress, neutrophils, peroxide; role in virulence; regulated by iron, ciclopirox, fluconazole, carbon source, pH, Rim101, Ssn6, Hog1, Hap43, Sfu1, Sef1, farnesol, core stress response; Spider biofilm induced
orf19.6245		-0,40			Protein of unknown function; regulated by osmotic stress via Hog1 and oxidative stress (Hog1- and Cap1-independent); induced by alpha pheromone in SpiderM medium; Spider biofilm induced
orf19.6311		0,65			Protein of unknown function; Hap43-induced; rat catheter and Spider biofilm induced
orf19.6318				0,43	Protein of unknown function
orf19.6322	<i>ARD</i>	-0,42	-0,48		D-arabitol dehydrogenase, NAD-dependent (ArDH); enzyme of D-arabitol and D-arabinose catabolism; D-arabitol is a marker for active infection in humans; rat catheter and Spider biofilm induced
orf19.6324	<i>VID27</i>		-0,45	-0,33	Protein similar to <i>S. cerevisiae</i> Vid27p; transposon mutation affects filamentous growth; mutation confers hypersensitivity to toxic ergosterol analog; fungal-specific (no human or murine homolog)
orf19.6327	<i>HET1</i>	-0,46	-0,56	-0,45	Putative sphingolipid transfer protein; involved in localization of glucosylceramide which is important for virulence; Spider biofilm repressed
orf19.6329				-0,43	Protein of unknown function; opaque-specific transcript; fluconazole-repressed; induced in <i>cyr1</i> mutant and in oralpharyngeal candidiasis; Spider biofilm induced
orf19.6341				-0,35	Protein of unknown function
orf19.638	<i>FDH1</i>		0,66	0,45	Formate dehydrogenase; oxidizes formate to CO2; Mig1 regulated; induced by macrophages; fluconazole-repressed; repressed by Efg1 in yeast, not hyphal conditions; stationary phase enriched; rat catheter and Spider biofilm induced
orf19.6459	<i>DPP3</i>			-0,48	Protein similar to <i>S. cerevisiae</i> pyrophosphate phosphatase Dpp1; required for farnesol biosynthesis; repressed by 17-beta-estradiol, ethynyl estradiol; Spider biofilm induced
orf19.6489	<i>FMP45</i>		0,54		Predicted membrane protein induced during mating; mutation confers hypersensitivity to toxic ergosterol analog, to amphotericin B; alkaline repressed; repressed by alpha pheromone in SpiderM medium; rat catheter, Spider biofilm induced
orf19.655	<i>PHO84</i>		0,58	0,42	High-affinity phosphate transporter; transcript regulated by white-opaque switch; Hog1, ciclopirox olamine or alkaline induced; caspofungin, stress repressed; upregulated in RHE model; Spider and flow model biofilm induced, Hap43-induced
orf19.6577	<i>FLU1</i>			0,63	Multidrug efflux pump of the plasma membrane; MDR family member of the MFS (major facilitator superfamily) of transporters; involved in histatin 5 efflux; fungal-specific (no human/murine homolog)
orf19.6640	<i>TPS1</i>	-0,55			Trehalose-6-phosphate synthase; role in hyphal growth and virulence in mouse systemic infection; induced in presence of human neutrophils; macrophage/pseudohyphal-repressed after 16h; stationary phase enriched protein; Hap43-repressed
orf19.6658		-0,43		-0,41	Stationary phase enriched protein; predicted ORF from Assembly 19; removed from Assembly 20; subsequently reinstated in Assembly 21 based on comparative genome analysis
orf19.6688			0,44		Protein of unknown function; expression decreases by benomyl treatment or in an azole-resistant strain overexpressing MDR1; Spider biofilm induced
orf19.670.2			0,47	0,62	Protein of unknown function; hypoxia, Hap43-repressed; ketoconazole induced; induced in oralpharyngeal candidiasis; 16h flow model biofilm repressed, late-stage flow model biofilm induced; rat catheter and Spider biofilm induced
orf19.6705			0,51		Putative guanyl nucleotide exchange factor with Sec7 domain; required for normal filamentous growth; regulated by yeast-hyphal switch; filament induced; regulated by Nrg1, Tup1, Mob2, Hap43; mRNA binds She3; Spider biofilm induced
orf19.6816		-0,61			Putative xylose and arabinose reductase; flow model biofilm induced; Spider biofilm repressed
orf19.6824	<i>TRY6</i>		0,65		Helix-loop-helix transcription factor; regulator of yeast form adherence; required for yeast cell adherence to silicone substrate; Spider and F-12/CO2 biofilm induced; repressed by alpha pheromone in SpiderM medium
orf19.6834.10	<i>TAR1</i>		0,63	-0,59	Ortholog of <i>S. cerevisiae</i> Tar1p; Transcript Antisense to Ribosomal RNA; encoded within the 25S rRNA gene on the opposite strand; induced by Tbf1

Supporting Information

orf19.6844	<i>ICL1</i>		0,45		Isocitrate lyase; glyoxylate cycle enzyme; required for virulence in mice; induced upon phagocytosis by macrophage; farnesol regulated; Pex5-dependent peroxisomal localization; stationary phase enriched; rat catheter, Spider biofilm induced
orf19.686		-0,50	-0,45	-0,35	Protein of unknown function; regulated by <i>Nrg1</i>
orf19.687				-0,45	Protein of unknown function
orf19.687.1	<i>RPL25</i>	-0,38	-0,54		Putative rRNA-binding ribosomal protein component of the 60S ribosomal subunit; Hap43-induced; colony morphology-related gene regulation by <i>Ssn6</i>
orf19.6882	<i>OSM1</i>	-0,51			Putative flavoprotein subunit of fumarate reductase; soluble protein in hyphae; caspofungin repressed; stationary phase enriched protein; flow model biofilm induced; Spider biofilm repressed
orf19.6888		-0,59	-0,52	0,61	Zn(II)2Cys6 domain transcription factor; regulated by <i>Mig1</i> and <i>Tup1</i> ; rat catheter and Spider biofilm induced
orf19.692			-0,59	-0,60	Protein of unknown function; Hap43-repressed gene; rat catheter and Spider biofilm induced
orf19.6984				0,48	Protein of unknown function
orf19.7077			0,64	0,46	Putative ferric reductase; induced by <i>Mac1</i> under copper starvation; <i>Plc1</i> -regulated; <i>Rim101</i> -repressed
orf19.7111.1	<i>SOD3</i>		0,42		Cytosolic manganese-containing superoxide dismutase; protects against oxidative stress; repressed by ciclopirox olamine, induced during stationary phase when <i>SOD1</i> expression is low; Hap43-repressed; Spider and flow model biofilm induced
orf19.717	<i>HSP60</i>		0,45	0,36	Heat shock protein; soluble in hyphae; regulated by <i>Nrg1</i> and by iron; induced in high iron; heavy metal (cadmium) stress-induced; sumoylation target; protein present in exponential and stationary phase cells; Hap43-repressed
orf19.7214		-0,72		-0,41	Glucan 1,3-beta-glucosidase; regulated by <i>Nrg1</i> , <i>Tup1</i> and possibly <i>Tac1</i> ; induced by NO and during cell wall regeneration; stationary phase enriched; possibly essential (UAU1 method); F-12/CO2 early biofilm induced; flow biofilm repressed
orf19.7218	<i>RBE1</i>			0,38	Pry family cell wall protein; <i>Rim101</i> , <i>Efg1</i> , <i>Ssn6</i> , alkaline repressed; O-glycosylation; no GPI anchor predicted; ketoconazol induced; regulated by <i>Sef1</i> , <i>Sfu1</i> , <i>Hap4</i> ; flow model biofilm induced; rat catheter and Spider biofilm repressed
orf19.7284	<i>ASR2</i>	-0,88	-0,50	-0,53	Adenylyl cyclase and stress responsive protein; induced in <i>cyr1</i> or <i>ras1</i> mutant; stationary phase enriched protein; Spider biofilm induced
orf19.7288		-0,49			Protein with predicted oxidoreductase and dehydrogenase domains; Hap43-repressed; Spider biofilm induced
orf19.7296				-0,52	Putative cation conductance protein; similar to stomatin mechanoreception protein; plasma-membrane localized; induced by <i>Rgt1</i> ; rat catheter and Spider biofilm induced
orf19.73		-0,62	-0,46	-0,44	Putative metalloprotease; associates with ribosomes and is involved in ribosome biogenesis; Spider biofilm induced
orf19.7310		-0,51			Protein with a role in directing meiotic recombination events to homologous chromatids; induced by ciclopirox olamine; positively regulated by <i>Sfu1</i> ; <i>Hog1</i> , fluconazole-repressed; Hap43-induced; Spider biofilm induced
orf19.7319	<i>SUC1</i>			-0,37	Zinc-finger transcription factor; regulates alpha-glucosidase expression; complements <i>S. cerevisiae</i> <i>suc2</i> for sucrose utilization and <i>mal13</i> maltase defect; required for yeast cell adherence to silicone substrate; rat catheter biofilm induced
orf19.7337			0,48		Protein with a nischarin related domain and leucine rich repeats; Spider biofilm induced
orf19.734	<i>GLK1</i>	-0,45			Putative glucokinase; transcript regulated upon yeast-hyphal switch; <i>Efg1</i> regulated; fluconazole-induced; induced in core stress response; colony morphology-related gene regulation by <i>Ssn6</i> ; GlcNAc-induced protein
orf19.74	<i>SEC5</i>	-0,49		-0,36	Predicted exocyst component; ortholog of <i>S. cerevisiae</i> <i>Sec5p</i> ; merged with orf19.75 in Assembly 21
orf19.740	<i>HAP41</i>		0,44	0,40	Putative Hap4-like transcription factor; Hap43-repressed; not required for response to low iron; induced by <i>Mnl1</i> under weak acid stress; Spider biofilm induced
orf19.7436	<i>AAF1</i>		0,44		Possible regulatory protein; possible adhesin-like; Glu-rich domain; production in <i>S. cerevisiae</i> increases endothelial cell adherence and flocculence; flow model biofilm, alkaline or caspofungin induced
orf19.7445				0,38	Ortholog of <i>S. Vid24</i> ; a peripheral membrane protein located at <i>Vid</i> (vacuole import and degradation) vesicles; regulated by <i>Sef1</i> , <i>Sfu1</i> , and <i>Hap43</i> ; Spider biofilm induced
orf19.7514	<i>PCK1</i>			0,48	Phosphoenolpyruvate carboxykinase; glucose, C-source, yeast-hypha, Hap43 regulated; fluconazole, phagocytosis, H2O2, oral candidiasis, Spider/rat catheter/flow model biofilm induced; repressed in biofilm by <i>Bcr1</i> , <i>Tec1</i> , <i>Ndt80</i> , <i>Rob1</i> , <i>Brg1</i>
orf19.7585	<i>INO1</i>			-0,46	Inositol-1-phosphate synthase; antigenic in human; repressed by farnesol in biofilm or by caspofungin; upstream inositol/choline regulatory element; glycosylation predicted; rat catheter, flow model induced; Spider biofilm repressed
orf19.76	<i>SPB1</i>	-0,39	-0,55	-0,41	Putative AdoMet-dependant methyltransferase; Hap43-induced; repressed by prostaglandins; possibly essential gene, disruptants not obtained by UAU1 method; Spider biofilm induced
orf19.802	<i>UGA1</i>			0,36	Putative GABA transaminase; transcription regulated by <i>Mig1</i> and <i>Tup1</i> ; stationary phase enriched protein; rat catheter and Spider biofilm induced
orf19.822	<i>HSP21</i>		0,52		Small heat shock protein; role in stress response and virulence; fluconazole-downregulated; induced in <i>cyr1</i> or <i>ras1</i> mutant; stationary phase enriched protein; detected in some, not all, biofilm extracts; Spider biofilm induced
orf19.84	<i>CAN3</i>	-0,43		-0,64	Predicted amino acid transmembrane transporter; transcript regulated by white-opaque switch; Hap43-repressed gene
orf19.85	<i>GPX2</i>	-0,65	-0,52	-0,65	Similar to glutathione peroxidase; induced in high iron; alkaline induced by <i>Rim101</i> ; induced by alpha factor or interaction with macrophage; regulated by <i>Efg1</i> ; caspofungin repressed; Spider biofilm induced
orf19.868	<i>ADAEC</i>	-0,44			Protein of unknown function; transcription is specific to white cell type
orf19.88	<i>ILV5</i>		-0,55		Ketol-acid reductoisomerase; antigenic; regulated by <i>Gcn4</i> ; GlcNAc, amino acid starvation (3-AT)-induced; macrophage-repressed protein; protein present in exponential and stationary phase; flow model and Spider biofilm repressed
orf19.882	<i>HSP78</i>		0,42		Heat-shock protein; regulated by macrophage response, <i>Nrg1</i> , <i>Mig1</i> , <i>Gcn2</i> , <i>Gcn4</i> , <i>Mnl1p</i> ; heavy metal (cadmium) stress-induced; stationary phase enriched protein; rat catheter and Spider biofilm induced
orf19.89	<i>PEX7</i>		-0,76	-0,55	Protein of unknown function
orf19.90		-0,66	-0,61	-0,58	Protein of unknown function
orf19.91		-0,50		-0,36	Protein of unknown function; flow model biofilm induced; Hap43-repressed
orf19.918	<i>CDR11</i>		0,51		Putative transporter of PDR subfamily of ABC family; <i>Gcn4</i> -regulated; induced by <i>Rim101</i> at pH 8; Spider biofilm induced
orf19.92		-0,52	-0,49	-0,42	Protein with a predicted thioredoxin-like domain; Hap43-repressed; induced by prostaglandins
orf19.921	<i>HMS1</i>		0,46		hLh domain Myc-type transcription factor; required for morphogenesis induced by elevated temperature or <i>Hsp90</i> compromise; acts downstream of <i>Pcl1</i> ; Spider biofilm induced
orf19.932			0,48	0,48	Putative aminophospholipid translocase (flippase); merged with orf19.2226 in Assembly 21; possibly an essential gene, disruptants not obtained by UAU1 method
orf19.938				0,60	Protein of unknown function
orf19.94		-0,59	-0,54	-0,56	Protein of unknown function; Spider biofilm induced
orf19.96	<i>TOP1</i>		-0,47	-0,40	DNA topoisomerase I; required for wild-type growth and for wild-type mouse virulence; sensitive to camptothecin; induced upon adherence to polystyrene; rat catheter biofilm induced
orf19.99	<i>HAL21</i>	-0,63	-0,82	-0,57	Putative phosphoadenosine-5'-phosphate or 3'-phosphoadenosine 5'-phosphosulfate phosphatase; possible role in sulfur recycling; ortholog of <i>S. cerevisiae</i> <i>Met22</i> ; predicted <i>Kex2</i> substrate; F-12/CO2 biofilm induced

7) References

- Akaike, H. (1973). Information Theory and an Extension of the Maximum Likelihood Principle. In P. E., T. K., & K. G. (Eds.), *Selected Papers of Hirotugu Akaike*. (pp. 199-213). New York: Springer.
- Akpan, A., & Morgan, R. (2002). Oral candidiasis. *Postgrad Med J*, 78(922), 455-459. doi:10.1136/pmj.78.922.455
- Alexopoulos, C. J., Mims, C. W., & Blackwell, M. (1996). *Introductory Mycology* (Vol. 4th): John Wiley & Sons.
- Anders, S., Pyl, P. T., & Huber, W. (2015). HTSeq--a Python framework to work with high-throughput sequencing data. *Bioinformatics*, 31(2), 166-169. doi:10.1093/bioinformatics/btu638
- Askew, C., Sellam, A., Epp, E., Hogues, H., Mullick, A., Nantel, A., & Whiteway, M. (2009). Transcriptional regulation of carbohydrate metabolism in the human pathogen *Candida albicans*. *PLoS Pathog*, 5(10), e1000612. doi:10.1371/journal.ppat.1000612
- Backhed, F., & Crawford, P. A. (2010). Coordinated regulation of the metabolome and lipidome at the host-microbial interface. *Biochim Biophys Acta*, 1801(3), 240-245. doi:10.1016/j.bbali.2009.09.009
- Barr, D. J. S. (2001). Chytridiomycota. In D. J. McLaughlin, E. G. McLaughlin, & P. A. Lemke (Eds.), *Systematics and Evolution: The Mycota* (Vol. 7A). Berlin, Heidelberg: Springer.
- Bashirullah, A., Cooperstock, R. L., & Lipshitz, H. D. (1998). RNA localization in development. *Annu Rev Biochem*, 67, 335-394. doi:10.1146/annurev.biochem.67.1.335
- Bashirullah, A., Halsell, S. R., Cooperstock, R. L., Kloc, M., Karaiskakis, A., Fisher, W. W., . . . Lipshitz, H. D. (1999). Joint action of two RNA degradation pathways controls the timing of maternal transcript elimination at the midblastula transition in *Drosophila melanogaster*. *EMBO J*, 18(9), 2610-2620. doi:10.1093/emboj/18.9.2610
- Bastidas, R. J., Heitman, J., & Cardenas, M. E. (2009). The protein kinase Tor1 regulates adhesin gene expression in *Candida albicans*. *PLoS Pathog*, 5(2), e1000294. doi:10.1371/journal.ppat.1000294
- Bates, S., Hughes, H. B., Munro, C. A., Thomas, W. P., MacCallum, D. M., Bertram, G., . . . Gow, N. A. (2006). Outer chain N-glycans are required for cell wall integrity and virulence of *Candida albicans*. *J Biol Chem*, 281(1), 90-98. doi:10.1074/jbc.M510360200
- Benjamini, Y., Drai, D., Elmer, G., Kafkafi, N., & Golani, I. (2001). Controlling the false discovery rate in behavior genetics research. *Behav Brain Res*, 125(1-2), 279-284.
- Besold, A. N., Culbertson, E. M., & Culotta, V. C. (2016). The Yin and Yang of copper during infection. *J Biol Inorg Chem*, 21(2), 137-144. doi:10.1007/s00775-016-1335-1
- Besse, F., & Ephrussi, A. (2008). Translational control of localized mRNAs: restricting protein synthesis in space and time. *Nat Rev Mol Cell Biol*, 9(12), 971-980. doi:10.1038/nrm2548
- Bibiloni, R. (2012). Rodent models to study the relationships between mammals and their bacterial inhabitants. *Gut Microbes*, 3(6), 536-543. doi:10.4161/gmic.21905
- Biswas, S., Van Dijck, P., & Datta, A. (2007). Environmental sensing and signal transduction pathways regulating morphopathogenic determinants of *Candida albicans*. *Microbiol Mol Biol Rev*, 71(2), 348-376. doi:10.1128/MMBR.00009-06
- Bocci, V. (1992). The neglected organ: bacterial flora has a crucial immunostimulatory role. *Perspect Biol Med*, 35(2), 251-260.

- Bohm, L., Muralidhara, P., & Perez, J. C. (2016). A *Candida albicans* regulator of disseminated infection operates primarily as a repressor and governs cell surface remodeling. *Mol Microbiol*, *100*(2), 328-344. doi:10.1111/mmi.13320
- Bohm, L., Torsin, S., Tint, S. H., Eckstein, M. T., Ludwig, T., & Perez, J. C. (2017). The yeast form of the fungus *Candida albicans* promotes persistence in the gut of gnotobiotic mice. *PLoS Pathog*, *13*(10), e1006699. doi:10.1371/journal.ppat.1006699
- Bolger, A. M., Lohse, M., & Usadel, B. (2014). Trimmomatic: a flexible trimmer for Illumina sequence data. *Bioinformatics*, *30*(15), 2114-2120. doi:10.1093/bioinformatics/btu170
- Bourgeois, C., Majer, O., Frohner, I. E., Tierney, L., & Kuchler, K. (2010). Fungal attacks on mammalian hosts: pathogen elimination requires sensing and tasting. *Curr Opin Microbiol*, *13*(4), 401-408. doi:10.1016/j.mib.2010.05.004
- Bowman, S. M., & Free, S. J. (2006). The structure and synthesis of the fungal cell wall. *Bioessays*, *28*(8), 799-808. doi:10.1002/bies.20441
- Braun, B. R., & Johnson, A. D. (1997). Control of filament formation in *Candida albicans* by the transcriptional repressor TUP1. *Science*, *277*(5322), 105-109.
- Braun, B. R., Kadosh, D., & Johnson, A. D. (2001). *NRG1*, a repressor of filamentous growth in *C. albicans*, is down-regulated during filament induction. *EMBO J*, *20*(17), 4753-4761. doi:10.1093/emboj/20.17.4753
- Braun, B. R., van Het Hoog, M., d'Enfert, C., Martchenko, M., Dungan, J., Kuo, A., . . . Nantel, A. (2005). A human-curated annotation of the *Candida albicans* genome. *PLoS Genet*, *1*(1), 36-57. doi:10.1371/journal.pgen.0010001
- Brawner, K. M., Morrow, C. D., & Smith, P. D. (2014). Gastric microbiome and gastric cancer. *Cancer J*, *20*(3), 211-216. doi:10.1097/PPO.0000000000000043
- Brown, A. J. (2002). Morphogenetic signaling pathways in *Candida albicans*. In C. RA (Ed.), *Candida and Candidiasis* (pp. 95-106). Washington, D.C.: ASM Press.
- Brown, A. J., Brown, G. D., Netea, M. G., & Gow, N. A. (2014). Metabolism impacts upon *Candida* immunogenicity and pathogenicity at multiple levels. *Trends Microbiol*, *22*(11), 614-622. doi:10.1016/j.tim.2014.07.001
- Brown, A. J., & Gow, N. A. (1999). Regulatory networks controlling *Candida albicans* morphogenesis. *Trends Microbiol*, *7*(8), 333-338.
- Brown, A. J., Haynes, K., & Quinn, J. (2009). Nitrosative and oxidative stress responses in fungal pathogenicity. *Curr Opin Microbiol*, *12*(4), 384-391. doi:10.1016/j.mib.2009.06.007
- Brown, G. D., & Gordon, S. (2001). Immune recognition. A new receptor for beta-glucans. *Nature*, *413*(6851), 36-37. doi:10.1038/35092620
- Bruno, V. M., Wang, Z., Marjani, S. L., Euskirchen, G. M., Martin, J., Sherlock, G., & Snyder, M. (2010). Comprehensive annotation of the transcriptome of the human fungal pathogen *Candida albicans* using RNA-seq. *Genome Res*, *20*(10), 1451-1458. doi:10.1101/gr.109553.110
- Bullock, S. L. (2007). Translocation of mRNAs by molecular motors: think complex? *Semin Cell Dev Biol*, *18*(2), 194-201. doi:10.1016/j.semcd.2007.01.004
- Bultman, S. J. (2014). Emerging roles of the microbiome in cancer. *Carcinogenesis*, *35*(2), 249-255. doi:10.1093/carcin/bgt392
- Butler, J. E., Lager, K. M., Splichal, I., Francis, D., Kacs Kovics, I., Sinkora, M., . . . Ramsoondar, J. (2009). The piglet as a model for B cell and immune system development. *Vet Immunol Immunopathol*, *128*(1-3), 147-170. doi:10.1016/j.vetimm.2008.10.321

- Buurman, E. T., Westwater, C., Hube, B., Brown, A. J., Odds, F. C., & Gow, N. A. (1998). Molecular analysis of CaMnt1p, a mannosyl transferase important for adhesion and virulence of *Candida albicans*. *Proc Natl Acad Sci U S A*, *95*(13), 7670-7675.
- Cabral, V., Znaidi, S., Walker, L. A., Martin-Yken, H., Dague, E., Legrand, M., . . . d'Enfert, C. (2014). Targeted changes of the cell wall proteome influence *Candida albicans* ability to form single- and multi-strain biofilms. *PLoS Pathog*, *10*(12), e1004542. doi:10.1371/journal.ppat.1004542
- Cain, C. W., Lohse, M. B., Homann, O. R., Sil, A., & Johnson, A. D. (2012). A conserved transcriptional regulator governs fungal morphology in widely diverged species. *Genetics*, *190*(2), 511-521. doi:10.1534/genetics.111.134080
- Calderone, R. (2002). Taxonomy and Biology of *Candida*. In *Candida and Candidiasis* (pp. 15-27). Washington D.C.: ASM Press.
- Calderone, R., & Clancy, C. J. (2012). *Candida and Candidiasis*. Washington DC, USA: ASM Press.
- Calderone, R. A. (1993). Recognition between *Candida albicans* and host cells. *Trends Microbiol*, *1*(2), 55-58.
- Carlisle, P. L., Banerjee, M., Lazzell, A., Monteagudo, C., Lopez-Ribot, J. L., & Kadosh, D. (2009). Expression levels of a filament-specific transcriptional regulator are sufficient to determine *Candida albicans* morphology and virulence. *Proc Natl Acad Sci U S A*, *106*(2), 599-604. doi:10.1073/pnas.0804061106
- Carter, P. B., & Foster, H. L. (2006). Gnotobiotics. In M. A. Suckow, S. H. Weisbroth, & C. L. Franklin (Eds.), *American College of Laboratory Animal Medicine, The Laboratory Rat* (Vol. 2, pp. 693-710): Academic Press.
- Cash, H. L., Whitham, C. V., Behrendt, C. L., & Hooper, L. V. (2006). Symbiotic bacteria direct expression of an intestinal bactericidal lectin. *Science*, *313*(5790), 1126-1130. doi:10.1126/science.1127119
- Cebra, J. J. (1999). Influences of microbiota on intestinal immune system development. *Am J Clin Nutr*, *69*(5), 1046S-1051S. doi:10.1093/ajcn/69.5.1046s
- Chaffin, W. L., Lopez-Ribot, J. L., Casanova, M., Gozalbo, D., & Martinez, J. P. (1998). Cell wall and secreted proteins of *Candida albicans*: identification, function, and expression. *Microbiol Mol Biol Rev*, *62*(1), 130-180.
- Cherbuy, C., Honvo-Houeto, E., Bruneau, A., Bridonneau, C., Mayeur, C., Duee, P. H., . . . Thomas, M. (2010). Microbiota matures colonic epithelium through a coordinated induction of cell cycle-related proteins in gnotobiotic rat. *Am J Physiol Gastrointest Liver Physiol*, *299*(2), G348-357. doi:10.1152/ajpgi.00384.2009
- Clancy, C. J., & Nguyen, H. M. (2012). Systemic candidiasis: candidemia and deep-organ infections. In C. R.A & C. C.J. (Eds.), *Candida and Candidiasis* (2nd Edition ed., pp. 429-441). Washington, DC: ASM Press.
- Clark, J. D. (1971). Influence of antibiotics or certain intestinal bacteria on orally administered *Candida albicans* in germ-free and conventional mice. *Infect Immun*, *4*(6), 731-737.
- Coelho, M. A., Bakkeren, G., Sun, S., Hood, M. E., & Giraud, T. (2017). Fungal Sex: The *Basidiomycota*. *Microbiol Spectr*, *5*(3). doi:10.1128/microbiolspec.FUNK-0046-2016
- Covitz, P. A., & Mitchell, A. P. (1993). Repression by the yeast meiotic inhibitor *RME1*. *Genes Dev*, *7*(8), 1598-1608.
- Csank, C., Schroppel, K., Leberer, E., Harcus, D., Mohamed, O., Meloche, S., . . . Whiteway, M. (1998). Roles of the *Candida albicans* mitogen-activated protein kinase homolog, Cek1p, in hyphal development and systemic candidiasis. *Infect Immun*, *66*(6), 2713-2721.

- Cutler, J. E. (1991). Putative virulence factors of *Candida albicans*. *Annu Rev Microbiol*, *45*, 187-218. doi:10.1146/annurev.mi.45.100191.001155
- Dalal, C. K., Zuleta, I. A., Mitchell, K. F., Andes, D. R., El-Samad, H., & Johnson, A. D. (2016). Transcriptional rewiring over evolutionary timescales changes quantitative and qualitative properties of gene expression. *Elife*, *5*. doi:10.7554/eLife.18981
- Dantas Ada, S., Day, A., Ikeh, M., Kos, I., Achan, B., & Quinn, J. (2015). Oxidative stress responses in the human fungal pathogen, *Candida albicans*. *Biomolecules*, *5*(1), 142-165. doi:10.3390/biom5010142
- Davis, D., Wilson, R. B., & Mitchell, A. P. (2000). *RIM101*-dependent and-independent pathways govern pH responses in *Candida albicans*. *Mol Cell Biol*, *20*(3), 971-978.
- Davis, D. A. (2009). How human pathogenic fungi sense and adapt to pH: the link to virulence. *Curr Opin Microbiol*, *12*(4), 365-370. doi:10.1016/j.mib.2009.05.006
- de Boer, A. D., de Groot, P. W., Weindl, G., Schaller, M., Riedel, D., Diez-Orejas, R., . . . Weig, M. (2010). The *Candida albicans* cell wall protein Rhd3/Pga29 is abundant in the yeast form and contributes to virulence. *Yeast*, *27*(8), 611-624. doi:10.1002/yea.1790
- Desai, J. V., Mitchell, A. P., & Andes, D. R. (2014). Fungal biofilms, drug resistance, and recurrent infection. *Cold Spring Harb Perspect Med*, *4*(10). doi:10.1101/cshperspect.a019729
- Ding, D., Parkhurst, S. M., Halsell, S. R., & Lipshitz, H. D. (1993). Dynamic Hsp83 RNA localization during *Drosophila* oogenesis and embryogenesis. *Mol Cell Biol*, *13*(6), 3773-3781.
- Dobin, A., Davis, C. A., Schlesinger, F., Drenkow, J., Zaleski, C., Jha, S., . . . Gingeras, T. R. (2013). STAR: ultrafast universal RNA-seq aligner. *Bioinformatics*, *29*(1), 15-21. doi:10.1093/bioinformatics/bts635
- Doedt, T., Krishnamurthy, S., Bockmuhl, D. P., Tebarth, B., Stempel, C., Russell, C. L., . . . Ernst, J. F. (2004). APSES proteins regulate morphogenesis and metabolism in *Candida albicans*. *Mol Biol Cell*, *15*(7), 3167-3180. doi:10.1091/mbc.e03-11-0782
- Domer, J. E. (1988). Intra-gastric colonization of infant mice with *Candida albicans* induces systemic immunity demonstrable upon challenge as adults. *J Infect Dis*, *157*(5), 950-958.
- Douglas, C. M., D'Ippolito, J. A., Shei, G. J., Meinz, M., Onishi, J., Marrinan, J. A., . . . Kurtz, M. B. (1997). Identification of the *FKS1* gene of *Candida albicans* as the essential target of 1,3-beta-D-glucan synthase inhibitors. *Antimicrob Agents Chemother*, *41*(11), 2471-2479.
- Douglas, L. J. (2003). *Candida* biofilms and their role in infection. *Trends Microbiol*, *11*(1), 30-36.
- Drell, T., Lillsaar, T., Tummeleht, L., Simm, J., Aaspollu, A., Vain, E., . . . Metsis, M. (2013). Characterization of the vaginal micro- and mycobiome in asymptomatic reproductive-age Estonian women. *PLoS One*, *8*(1), e54379. doi:10.1371/journal.pone.0054379
- Dunkler, A., Walther, A., Specht, C. A., & Wendland, J. (2005). *Candida albicans* *CHT3* encodes the functional homolog of the *Cts1* chitinase of *Saccharomyces cerevisiae*. *Fungal Genet Biol*, *42*(11), 935-947. doi:10.1016/j.fgb.2005.08.001
- Earle, K. A., Billings, G., Sigal, M., Lichtman, J. S., Hansson, G. C., Elias, J. E., . . . Sonnenburg, J. L. (2015). Quantitative Imaging of Gut Microbiota Spatial Organization. *Cell Host Microbe*, *18*(4), 478-488. doi:10.1016/j.chom.2015.09.002
- Edgar, R. C. (2004). MUSCLE: multiple sequence alignment with high accuracy and high throughput. *Nucleic Acids Res*, *32*(5), 1792-1797. doi:10.1093/nar/gkh340
- Edmond, M. B., Wallace, S. E., McClish, D. K., Pfaller, M. A., Jones, R. N., & Wenzel, R. P. (1999). Nosocomial bloodstream infections in United States hospitals: a three-year analysis. *Clin Infect Dis*, *29*(2), 239-244. doi:10.1086/520192

- Edwards, J. E. J. (2014). In J. E. Bennett, R. Dolin, & M. J. Blaser (Eds.), *Principles and Practice of Infectious Diseases* (8th Edition ed., pp. 2879–2894). Oxford: Elsevier LTD.
- Eklund, T., & Jarmund, T. (1983). Microculture model studies on the effect of various gas atmospheres on microbial growth at different temperatures. *J Appl Bacteriol*, *55*(1), 119-125.
- El Barkani, A., Kurzai, O., Fonzi, W. A., Ramon, A., Porta, A., Frosch, M., & Muhlschlegel, F. A. (2000). Dominant active alleles of *RIM101* (*PRR2*) bypass the pH restriction on filamentation of *Candida albicans*. *Mol Cell Biol*, *20*(13), 4635-4647.
- Elson, S. L., Noble, S. M., Solis, N. V., Filler, S. G., & Johnson, A. D. (2009). An RNA Transport System in *Candida albicans* Regulates Hyphal Morphology and Invasive Growth. *Plos Genetics*, *5*(9). doi:ARTN e100066410.1371/journal.pgen.1000664
- Fabry, W., Schmid, E. N., Schraps, M., & Ansorg, R. (2003). Isolation and purification of chlamydospores of *Candida albicans*. *Med Mycol*, *41*(1), 53-58.
- Falk, P. G., Hooper, L. V., Midtvedt, T., & Gordon, J. I. (1998). Creating and maintaining the gastrointestinal ecosystem: what we know and need to know from gnotobiology. *Microbiol Mol Biol Rev*, *62*(4), 1157-1170.
- Fan, D., Coughlin, L. A., Neubauer, M. M., Kim, J., Kim, M. S., Zhan, X., . . . Koh, A. Y. (2015). Activation of HIF-1alpha and LL-37 by commensal bacteria inhibits *Candida albicans* colonization. *Nat Med*, *21*(7), 808-814. doi:10.1038/nm.3871
- Fang, H. M., & Wang, Y. (2006). RA domain-mediated interaction of Cdc35 with Ras1 is essential for increasing cellular cAMP level for *Candida albicans* hyphal development. *Mol Microbiol*, *61*(2), 484-496. doi:10.1111/j.1365-2958.2006.05248.x
- Festa, R. A., & Thiele, D. J. (2012). Copper at the front line of the host-pathogen battle. *PLoS Pathog*, *8*(9), e1002887. doi:10.1371/journal.ppat.1002887
- Findley, K., Oh, J., Yang, J., Conlan, S., Deming, C., Meyer, J. A., . . . Segre, J. A. (2013). Topographic diversity of fungal and bacterial communities in human skin. *Nature*, *498*(7454), 367-370. doi:10.1038/nature12171
- Finkel, J. S., Xu, W., Huang, D., Hill, E. M., Desai, J. V., Woolford, C. A., . . . Mitchell, A. P. (2012). Portrait of *Candida albicans* adherence regulators. *PLoS Pathog*, *8*(2), e1002525. doi:10.1371/journal.ppat.1002525
- Fitzgerald, M. X., Rojas, J. R., Kim, J. M., Kohlhaw, G. B., & Marmorstein, R. (2006). Structure of a Leu3-DNA complex: recognition of everted CGG half-sites by a Zn₂Cys₆ binuclear cluster protein. *Structure*, *14*(4), 725-735. doi:10.1016/j.str.2005.11.025
- Fleming, A. (2001). On the antibacterial action of cultures of a penicillium, with special reference to their use in the isolation of *B. influenzae*. 1929. *Bull World Health Organ*, *79*(8), 780-790.
- Flint, A., Sun, Y. Q., Butcher, J., Stahl, M., Huang, H., & Stintzi, A. (2014). Phenotypic screening of a targeted mutant library reveals *Campylobacter jejuni* defenses against oxidative stress. *Infect Immun*, *82*(6), 2266-2275. doi:10.1128/IAI.01528-13
- Forrest, K. M., & Gavis, E. R. (2003). Live imaging of endogenous RNA reveals a diffusion and entrapment mechanism for nanos mRNA localization in *Drosophila*. *Curr Biol*, *13*(14), 1159-1168.
- Fradin, C., Poulain, D., & Jouault, T. (2000). beta-1,2-linked oligomannosides from *Candida albicans* bind to a 32-kilodalton macrophage membrane protein homologous to the mammalian lectin galectin-3. *Infect Immun*, *68*(8), 4391-4398.
- Francescone, R., Hou, V., & Grivennikov, S. I. (2014). Microbiome, inflammation, and cancer. *Cancer J*, *20*(3), 181-189. doi:10.1097/PPO.000000000000048

- Franzmann, T. M., Menhorn, P., Walter, S., & Buchner, J. (2008). Activation of the chaperone Hsp26 is controlled by the rearrangement of its thermosensor domain. *Mol Cell*, *29*(2), 207-216. doi:10.1016/j.molcel.2007.11.025
- Frohner, I. E., Bourgeois, C., Yatsyk, K., Majer, O., & Kuchler, K. (2009). *Candida albicans* cell surface superoxide dismutases degrade host-derived reactive oxygen species to escape innate immune surveillance. *Mol Microbiol*, *71*(1), 240-252. doi:10.1111/j.1365-2958.2008.06528.x
- Fu, Y., Ibrahim, A. S., Sheppard, D. C., Chen, Y. C., French, S. W., Cutler, J. E., . . . Edwards, J. E., Jr. (2002). *Candida albicans* Als1p: an adhesin that is a downstream effector of the *EFG1* filamentation pathway. *Mol Microbiol*, *44*(1), 61-72.
- Garcia-Sanchez, S., Aubert, S., Iraqui, I., Janbon, G., Ghigo, J. M., & d'Enfert, C. (2004). *Candida albicans* biofilms: a developmental state associated with specific and stable gene expression patterns. *Eukaryot Cell*, *3*(2), 536-545.
- Garcia-Santamarina, S., & Thiele, D. J. (2015). Copper at the Fungal Pathogen-Host Axis. *J Biol Chem*, *290*(31), 18945-18953. doi:10.1074/jbc.R115.649129
- Ghannoum, M. A., Jurevic, R. J., Mukherjee, P. K., Cui, F., Sikaroodi, M., Naqvi, A., & Gillevet, P. M. (2010). Characterization of the oral fungal microbiome (mycobiome) in healthy individuals. *PLoS Pathog*, *6*(1), e1000713. doi:10.1371/journal.ppat.1000713
- Gonsalvez, G. B., Urbinati, C. R., & Long, R. M. (2005). RNA localization in yeast: moving towards a mechanism. *Biol Cell*, *97*(1), 75-86. doi:10.1042/BC20040066
- Gonzalez-Rubio, G., Fernandez-Acero, T., Martin, H., & Molina, M. (2019). Mitogen-Activated Protein Kinase Phosphatases (MKPs) in Fungal Signaling: Conservation, Function, and Regulation. *Int J Mol Sci*, *20*(7). doi:10.3390/ijms20071709
- Gordon, H. A., & Pesti, L. (1971). The gnotobiotic animal as a tool in the study of host microbial relationships. *Bacteriol Rev*, *35*(4), 390-429.
- Gow, N. A., Brown, A. J., & Odds, F. C. (2002). Fungal morphogenesis and host invasion. *Curr Opin Microbiol*, *5*(4), 366-371.
- Gow, N. A., van de Veerdonk, F. L., Brown, A. J., & Netea, M. G. (2011). *Candida albicans* morphogenesis and host defence: discriminating invasion from colonization. *Nat Rev Microbiol*, *10*(2), 112-122. doi:10.1038/nrmicro2711
- Green, C. B., Cheng, G., Chandra, J., Mukherjee, P., Ghannoum, M. A., & Hoyer, L. L. (2004). RT-PCR detection of *Candida albicans* ALS gene expression in the reconstituted human epithelium (RHE) model of oral candidiasis and in model biofilms. *Microbiology*, *150*(Pt 2), 267-275. doi:10.1099/mic.0.26699-0
- Grover, M., & Kashyap, P. C. (2014). Germ-free mice as a model to study effect of gut microbiota on host physiology. *Neurogastroenterol Motil*, *26*(6), 745-748. doi:10.1111/nmo.12366
- Grumaz, C., Lorenz, S., Stevens, P., Lindemann, E., Schock, U., Retey, J., . . . Sohn, K. (2013). Species and condition specific adaptation of the transcriptional landscapes in *Candida albicans* and *Candida dubliniensis*. *BMC Genomics*, *14*, 212. doi:10.1186/1471-2164-14-212
- Gustafsson, B. E. (1948). *Germ-free rearing of rats: general technique*: Berlingska boktryckeriet.
- Hall, R. A. (2015). Dressed to impress: impact of environmental adaptation on the *Candida albicans* cell wall. *Mol Microbiol*, *97*(1), 7-17. doi:10.1111/mmi.13020
- Hall, R. A., Bates, S., Lenardon, M. D., Maccallum, D. M., Wagener, J., Lowman, D. W., . . . Gow, N. A. (2013a). The Mnn2 mannosyltransferase family modulates mannoprotein fibril length, immune recognition and virulence of *Candida albicans*. *PLoS Pathog*, *9*(4), e1003276. doi:10.1371/journal.ppat.1003276

- Hall, R. A., & Gow, N. A. (2013b). Mannosylation in *Candida albicans*: role in cell wall function and immune recognition. *Mol Microbiol*, *90*(6), 1147-1161. doi:10.1111/mmi.12426
- Hawksworth, D. L., & Lucking, R. (2017). Fungal Diversity Revisited: 2.2 to 3.8 Million Species. *Microbiol Spectr*, *5*(4). doi:10.1128/microbiolspec.FUNK-0052-2016
- Heilmann, C. J., Sorgo, A. G., & Klis, F. M. (2012). News from the fungal front: wall proteome dynamics and host-pathogen interplay. *PLoS Pathog*, *8*(12), e1003050. doi:10.1371/journal.ppat.1003050
- Hernday, A. D., Noble, S. M., Mitrovich, Q. M., & Johnson, A. D. (2010). Genetics and molecular biology in *Candida albicans*. *Methods Enzymol*, *470*, 737-758. doi:10.1016/S0076-6879(10)70031-8
- Hibbett, D. S., Binder, M., Bischoff, J. F., Blackwell, M., Cannon, P. F., Eriksson, O. E., . . . Zhang, N. (2007). A higher-level phylogenetic classification of the Fungi. *Mycol Res*, *111*(Pt 5), 509-547. doi:10.1016/j.mycres.2007.03.004
- Hodgkinson, V., & Petris, M. J. (2012). Copper homeostasis at the host-pathogen interface. *J Biol Chem*, *287*(17), 13549-13555. doi:10.1074/jbc.R111.316406
- Hoffmann, C., Dollive, S., Grunberg, S., Chen, J., Li, H., Wu, G. D., . . . Bushman, F. D. (2013). Archaea and fungi of the human gut microbiome: correlations with diet and bacterial residents. *PLoS One*, *8*(6), e66019. doi:10.1371/journal.pone.0066019
- Holt, C. E., & Bullock, S. L. (2009). Subcellular mRNA localization in animal cells and why it matters. *Science*, *326*(5957), 1212-1216. doi:10.1126/science.1176488
- Homann, O. R., Dea, J., Noble, S. M., & Johnson, A. D. (2009). A phenotypic profile of the *Candida albicans* regulatory network. *PLoS Genet*, *5*(12), e1000783. doi:10.1371/journal.pgen.1000783
- Homann, O. R., & Johnson, A. D. (2010). MochiView: versatile software for genome browsing and DNA motif analysis. *BMC Biol*, *8*, 49. doi:10.1186/1741-7007-8-49
- Hooper, L. V., Littman, D. R., & Macpherson, A. J. (2012). Interactions between the microbiota and the immune system. *Science*, *336*(6086), 1268-1273. doi:10.1126/science.1223490
- Hooper, L. V., Wong, M. H., Thelin, A., Hansson, L., Falk, P. G., & Gordon, J. I. (2001). Molecular analysis of commensal host-microbial relationships in the intestine. *Science*, *291*(5505), 881-884. doi:10.1126/science.291.5505.881
- Horne-Badovinac, S., & Bilder, D. (2008). Dynein regulates epithelial polarity and the apical localization of stardust A mRNA. *PLoS Genet*, *4*(1), e8. doi:10.1371/journal.pgen.0040008
- Hoyer, L. L. (2001). The ALS gene family of *Candida albicans*. *Trends Microbiol*, *9*(4), 176-180.
- Hubbard, M. J., Markie, D., & Poulter, R. T. (1986). Isolation and morphological characterization of a mycelial mutant of *Candida albicans*. *J Bacteriol*, *165*(1), 61-65. doi:10.1128/jb.165.1.61-65.1986
- Hull, C. M., Raisner, R. M., & Johnson, A. D. (2000). Evidence for mating of the "asexual" yeast *Candida albicans* in a mammalian host. *Science*, *289*(5477), 307-310.
- Inglis, D. O., & Johnson, A. D. (2002). Ash1 protein, an asymmetrically localized transcriptional regulator, controls filamentous growth and virulence of *Candida albicans*. *Mol Cell Biol*, *22*(24), 8669-8680.
- Jansen, R. P., Dowzer, C., Michaelis, C., Galova, M., & Nasmyth, K. (1996). Mother cell-specific *HO* expression in budding yeast depends on the unconventional myosin myo4p and other cytoplasmic proteins. *Cell*, *84*(5), 687-697.
- Jo, W. J., Loguinov, A., Chang, M., Wintz, H., Nislow, C., Arkin, A. P., . . . Vulpe, C. D. (2008). Identification of genes involved in the toxic response of *Saccharomyces cerevisiae* against

- iron and copper overload by parallel analysis of deletion mutants. *Toxicol Sci*, 101(1), 140-151. doi:10.1093/toxsci/kfm226
- Johansson, M. E., & Hansson, G. C. (2012). Preservation of mucus in histological sections, immunostaining of mucins in fixed tissue, and localization of bacteria with FISH. *Methods Mol Biol*, 842, 229-235. doi:10.1007/978-1-61779-513-8_13
- Johansson, M. E., Jakobsson, H. E., Holmen-Larsson, J., Schutte, A., Ermund, A., Rodriguez-Pineiro, A. M., . . . Hansson, G. C. (2015). Normalization of Host Intestinal Mucus Layers Requires Long-Term Microbial Colonization. *Cell Host Microbe*, 18(5), 582-592. doi:10.1016/j.chom.2015.10.007
- Johansson, M. E., Phillipson, M., Petersson, J., Velcich, A., Holm, L., & Hansson, G. C. (2008). The inner of the two Muc2 mucin-dependent mucus layers in colon is devoid of bacteria. *Proc Natl Acad Sci U S A*, 105(39), 15064-15069. doi:10.1073/pnas.0803124105
- Kadosh, D. (2017). *Candida albicans: Cellular and Molecular Biology*. In R. Prasad (Ed.), *Morphogenesis in C. albicans* (pp. 41-62). Cham, Switzerland: Springer International Publishing.
- Kadosh, D., & Johnson, A. D. (2001). Rfg1, a protein related to the *Saccharomyces cerevisiae* hypoxic regulator Rox1, controls filamentous growth and virulence in *Candida albicans*. *Mol Cell Biol*, 21(7), 2496-2505. doi:10.1128/MCB.21.7.2496-2505.2001
- Kamada, Y., Qadota, H., Python, C. P., Anraku, Y., Ohya, Y., & Levin, D. E. (1996). Activation of yeast protein kinase C by Rho1 GTPase. *J Biol Chem*, 271(16), 9193-9196.
- Kankainen, M., Paulin, L., Tynkkynen, S., von Ossowski, I., Reunanen, J., Partanen, P., . . . de Vos, W. M. (2009). Comparative genomic analysis of *Lactobacillus rhamnosus* GG reveals pili containing a human- mucus binding protein. *Proc Natl Acad Sci U S A*, 106(40), 17193-17198. doi:10.1073/pnas.0908876106
- Karlsson, F., Tremaroli, V., Nielsen, J., & Backhed, F. (2013). Assessing the human gut microbiota in metabolic diseases. *Diabetes*, 62(10), 3341-3349. doi:10.2337/db13-0844
- Kastora, S. L., Herrero-de-Dios, C., Avelar, G. M., Munro, C. A., & Brown, A. J. P. (2017). Sfp1 and Rtg3 reciprocally modulate carbon source-conditional stress adaptation in the pathogenic yeast *Candida albicans*. *Mol Microbiol*, 105(4), 620-636. doi:10.1111/mmi.13722
- Kennedy, M. J. (1988). Adhesion and Association Mechanisms of *Candida albicans*. In M. R. McGinnis (Ed.), *Current Topics in Medical Mycology*. (Vol. 2). New York: Springer.
- Kennedy, M. J., & Volz, P. A. (1985). Ecology of *Candida albicans* gut colonization: inhibition of *Candida* adhesion, colonization, and dissemination from the gastrointestinal tract by bacterial antagonism. *Infect Immun*, 49(3), 654-663.
- King, M. L., Messitt, T. J., & Mowry, K. L. (2005). Putting RNAs in the right place at the right time: RNA localization in the frog oocyte. *Biol Cell*, 97(1), 19-33. doi:10.1042/BC20040067
- Klengel, T., Liang, W. J., Chaloupka, J., Ruoff, C., Schroppel, K., Naglik, J. R., . . . Muhlschlegel, F. A. (2005). Fungal adenylyl cyclase integrates CO₂ sensing with cAMP signaling and virulence. *Curr Biol*, 15(22), 2021-2026. doi:10.1016/j.cub.2005.10.040
- Kloc, M., Zearfoss, N. R., & Etkin, L. D. (2002). Mechanisms of subcellular mRNA localization. *Cell*, 108(4), 533-544.
- Koh, A. Y., Kohler, J. R., Coggshall, K. T., Van Rooijen, N., & Pier, G. B. (2008). Mucosal damage and neutropenia are required for *Candida albicans* dissemination. *PLoS Pathog*, 4(2), e35. doi:10.1371/journal.ppat.0040035
- Korting, H. C., Hube, B., Oberbauer, S., Januschke, E., Hamm, G., Albrecht, A., . . . Schaller, M. (2003). Reduced expression of the hyphal-independent *Candida albicans* proteinase genes *SAP1*

- and *SAP3* in the *efg1* mutant is associated with attenuated virulence during infection of oral epithelium. *J Med Microbiol*, 52(Pt 8), 623-632. doi:10.1099/jmm.0.05125-0
- Kubelkova, K., Benuchova, M., Kozakova, H., Sinkora, M., Krocova, Z., Pejchal, J., & Macela, A. (2016). Gnotobiotic mouse model's contribution to understanding host-pathogen interactions. *Cell Mol Life Sci*, 73(20), 3961-3969. doi:10.1007/s00018-016-2341-8
- Kumamoto, C. A., & Vines, M. D. (2005). Contributions of hyphae and hypha-co-regulated genes to *Candida albicans* virulence. *Cell Microbiol*, 7(11), 1546-1554. doi:10.1111/j.1462-5822.2005.00616.x
- Kuranda, K., Leberre, V., Sokol, S., Palamarczyk, G., & Francois, J. (2006). Investigating the caffeine effects in the yeast *Saccharomyces cerevisiae* brings new insights into the connection between *TOR*, *PKC* and *Ras/cAMP* signalling pathways. *Mol Microbiol*, 61(5), 1147-1166. doi:10.1111/j.1365-2958.2006.05300.x
- Kvaal, C., Lachke, S. A., Srikantha, T., Daniels, K., McCoy, J., & Soll, D. R. (1999). Misexpression of the opaque-phase-specific gene *PEP1* (*SAP1*) in the white phase of *Candida albicans* confers increased virulence in a mouse model of cutaneous infection. *Infect Immun*, 67(12), 6652-6662.
- Laforet, L., Moreno, I., Sanchez-Fresneda, R., Martinez-Esparza, M., Martinez, J. P., Arguelles, J. C., . . . Valentin-Gomez, E. (2011). Pga26 mediates filamentation and biofilm formation and is required for virulence in *Candida albicans*. *FEMS Yeast Res*, 11(5), 389-397. doi:10.1111/j.1567-1364.2011.00727.x
- Lane, S., Birse, C., Zhou, S., Matson, R., & Liu, H. (2001a). DNA array studies demonstrate convergent regulation of virulence factors by Cph1, Cph2, and Efg1 in *Candida albicans*. *J Biol Chem*, 276(52), 48988-48996. doi:10.1074/jbc.M104484200
- Lane, S., Zhou, S., Pan, T., Dai, Q., & Liu, H. (2001b). The basic helix-loop-helix transcription factor Cph2 regulates hyphal development in *Candida albicans* partly via TEC1. *Mol Cell Biol*, 21(19), 6418-6428.
- Leberer, E., Harcus, D., Broadbent, I. D., Clark, K. L., Dignard, D., Ziegelbauer, K., . . . Thomas, D. Y. (1996). Signal transduction through homologs of the Ste20p and Ste7p protein kinases can trigger hyphal formation in the pathogenic fungus *Candida albicans*. *Proc Natl Acad Sci U S A*, 93(23), 13217-13222.
- Leberer, E., Ziegelbauer, K., Schmidt, A., Harcus, D., Dignard, D., Ash, J., . . . Thomas, D. Y. (1997). Virulence and hyphal formation of *Candida albicans* require the Ste20p-like protein kinase CaCla4p. *Curr Biol*, 7(8), 539-546.
- Lederberg, J. (2000). Infectious history. *Science*, 288(5464), 287-293. doi:10.1126/science.288.5464.287
- Levin, D. E. (2005). Cell wall integrity signaling in *Saccharomyces cerevisiae*. *Microbiol Mol Biol Rev*, 69(2), 262-291. doi:10.1128/MMBR.69.2.262-291.2005
- Li, H., & Durbin, R. (2009). Fast and accurate short read alignment with Burrows-Wheeler transform. *Bioinformatics*, 25(14), 1754-1760. doi:10.1093/bioinformatics/btp324
- Liu, H., Kohler, J., & Fink, G. R. (1994). Suppression of hyphal formation in *Candida albicans* by mutation of a *STE12* homolog. *Science*, 266(5191), 1723-1726.
- Lo, H. J., Kohler, J. R., DiDomenico, B., Loebenberg, D., Cacciapuoti, A., & Fink, G. R. (1997). Nonfilamentous *C. albicans* mutants are avirulent. *Cell*, 90(5), 939-949.
- Lohse, M. B., & Johnson, A. D. (2008). Differential phagocytosis of white versus opaque *Candida albicans* by *Drosophila* and mouse phagocytes. *PLoS One*, 3(1), e1473. doi:10.1371/journal.pone.0001473

- Lorenz, M. C. (2013). Carbon catabolite control in *Candida albicans*: new wrinkles in metabolism. *MBio*, 4(1), e00034-00013. doi:10.1128/mBio.00034-13
- Lorenz, M. C., Bender, J. A., & Fink, G. R. (2004). Transcriptional response of *Candida albicans* upon internalization by macrophages. *Eukaryot Cell*, 3(5), 1076-1087. doi:10.1128/EC.3.5.1076-1087.2004
- Love, M. I., Huber, W., & Anders, S. (2014). Moderated estimation of fold change and dispersion for RNA-seq data with DESeq2. *Genome Biol*, 15(12), 550. doi:10.1186/s13059-014-0550-8
- Lu, Y., Su, C., & Liu, H. (2014). *Candida albicans* hyphal initiation and elongation. *Trends Microbiol*, 22(12), 707-714. doi:10.1016/j.tim.2014.09.001
- Luckey, T. D. (1963). *Germfree Life and Gnotobiology*: Academic Press.
- Luckey, T. D. (1965). Effects of microbes on germfree animals. *Adv Appl Microbiol*, 7, 169-223.
- Luo, L., Tong, X., & Farley, P. C. (2007). The *Candida albicans* gene *HGT12* (*orf19.7094*) encodes a hexose transporter. *FEMS Immunol Med Microbiol*, 51(1), 14-17. doi:10.1111/j.1574-695X.2007.00274.x
- Luongo, M., Porta, A., & Maresca, B. (2005). Homology, disruption and phenotypic analysis of *CaGS* *Candida albicans* gene induced during macrophage infection. *FEMS Immunol Med Microbiol*, 45(3), 471-478. doi:10.1016/j.femsim.2005.06.007
- Lynch, S. V., & Pedersen, O. (2016). The Human Intestinal Microbiome in Health and Disease. *N Engl J Med*, 375(24), 2369-2379. doi:10.1056/NEJMra1600266
- MacPherson, S., Akache, B., Weber, S., De Deken, X., Raymond, M., & Turcotte, B. (2005). *Candida albicans* zinc cluster protein Upc2p confers resistance to antifungal drugs and is an activator of ergosterol biosynthetic genes. *Antimicrob Agents Chemother*, 49(5), 1745-1752. doi:10.1128/AAC.49.5.1745-1752.2005
- MacPherson, S., Larochelle, M., & Turcotte, B. (2006). A fungal family of transcriptional regulators: the zinc cluster proteins. *Microbiol Mol Biol Rev*, 70(3), 583-604. doi:10.1128/MMBR.00015-06
- Maguire, S. L., OhEigeartaigh, S. S., Byrne, K. P., Schroder, M. S., O'Gaora, P., Wolfe, K. H., & Butler, G. (2013). Comparative genome analysis and gene finding in *Candida* species using CGOB. *Mol Biol Evol*, 30(6), 1281-1291. doi:10.1093/molbev/mst042
- Makhnevych, T., & Houry, W. A. (2012). The role of Hsp90 in protein complex assembly. *Biochim Biophys Acta*, 1823(3), 674-682. doi:10.1016/j.bbamcr.2011.09.001
- Martin, K. C., & Ephrussi, A. (2009). mRNA localization: gene expression in the spatial dimension. *Cell*, 136(4), 719-730. doi:10.1016/j.cell.2009.01.044
- Martin, R., Bermudez-Humaran, L. G., & Langella, P. (2016). Gnotobiotic Rodents: An *In Vivo* Model for the Study of Microbe-Microbe Interactions. *Front Microbiol*, 7, 409. doi:10.3389/fmicb.2016.00409
- Martin, S. W., Douglas, L. M., & Konopka, J. B. (2005). Cell cycle dynamics and quorum sensing in *Candida albicans* chlamydospores are distinct from budding and hyphal growth. *Eukaryot Cell*, 4(7), 1191-1202. doi:10.1128/EC.4.7.1191-1202.2005
- Martinez, J. P., Gil, M. L., Lopez-Ribot, J. L., & Chaffin, W. L. (1998). Serologic response to cell wall mannoproteins and proteins of *Candida albicans*. *Clin Microbiol Rev*, 11(1), 121-141.
- Martins, M., Aymeric, L., du Merle, L., Danne, C., Robbe-Masselot, C., Trieu-Cuot, P., . . . Dramsi, S. (2015). *Streptococcus gallolyticus* Pil3 Pilus Is Required for Adhesion to Colonic Mucus and for Colonization of Mouse Distal Colon. *J Infect Dis*, 212(10), 1646-1655. doi:10.1093/infdis/jiv307

- Marvin, M. E., Mason, R. P., & Cashmore, A. M. (2004). The *CaCTR1* gene is required for high-affinity iron uptake and is transcriptionally controlled by a copper-sensing transactivator encoded by *CaMAC1*. *Microbiology*, *150*(Pt 7), 2197-2208. doi:10.1099/mic.0.27004-0
- Mayer, F. L., Wilson, D., Jacobsen, I. D., Miramon, P., Slesiona, S., Bohovych, I. M., . . . Hube, B. (2012). Small but crucial: the novel small heat shock protein Hsp21 mediates stress adaptation and virulence in *Candida albicans*. *PLoS One*, *7*(6), e38584. doi:10.1371/journal.pone.0038584
- McBride, A. E. (2017). Messenger RNA transport in the opportunistic fungal pathogen *Candida albicans*. *Curr Genet*, *63*(6), 989-995. doi:10.1007/s00294-017-0707-6
- McGreal, E. P., Rosas, M., Brown, G. D., Zamze, S., Wong, S. Y., Gordon, S., . . . Taylor, P. R. (2006). The carbohydrate-recognition domain of Dectin-2 is a C-type lectin with specificity for high mannose. *Glycobiology*, *16*(5), 422-430. doi:10.1093/glycob/cwj077
- Meignin, C., & Davis, I. (2010). Transmitting the message: intracellular mRNA localization. *Curr Opin Cell Biol*, *22*(1), 112-119. doi:10.1016/j.ceb.2009.11.011
- Merenstein, D., Hu, H., Wang, C., Hamilton, P., Blackmon, M., Chen, H., . . . Li, D. (2013). Colonization by *Candida* species of the oral and vaginal mucosa in HIV-infected and noninfected women. *AIDS Res Hum Retroviruses*, *29*(1), 30-34. doi:10.1089/AID.2012.0269
- Mitchell, A. P. (1998). Dimorphism and virulence in *Candida albicans*. *Curr Opin Microbiol*, *1*(6), 687-692.
- Mora-Montes, H. M., Bates, S., Netea, M. G., Castillo, L., Brand, A., Buurman, E. T., . . . Gow, N. A. (2010). A multifunctional mannosyltransferase family in *Candida albicans* determines cell wall mannan structure and host-fungus interactions. *J Biol Chem*, *285*(16), 12087-12095. doi:10.1074/jbc.M109.081513
- Munchow, S., Sauter, C., & Jansen, R. P. (1999). Association of the class V myosin Myo4p with a localised messenger RNA in budding yeast depends on She proteins. *J Cell Sci*, *112* (Pt 10), 1511-1518.
- Murad, A. M., d'Enfert, C., Gaillardin, C., Tournu, H., Tekaia, F., Talibi, D., . . . Brown, A. J. (2001a). Transcript profiling in *Candida albicans* reveals new cellular functions for the transcriptional repressors *CaTup1*, *CaMig1* and *CaNrg1*. *Mol Microbiol*, *42*(4), 981-993.
- Murad, A. M., Leng, P., Straffon, M., Wishart, J., Macaskill, S., MacCallum, D., . . . Brown, A. J. (2001b). *NRG1* represses yeast-hypha morphogenesis and hypha-specific gene expression in *Candida albicans*. *EMBO J*, *20*(17), 4742-4752. doi:10.1093/emboj/20.17.4742
- Muralidhara, P. (2015). *Virulence control by the Candida albicans regulator ZCF21*. University of Wuerzburg,
- Naglik, J. R., Challacombe, S. J., & Hube, B. (2003). *Candida albicans* secreted aspartyl proteinases in virulence and pathogenesis. *Microbiol Mol Biol Rev*, *67*(3), 400-428, table of contents. doi:10.1128/mubr.67.3.400-428.2003
- Navarro-Garcia, F., Alonso-Monge, R., Rico, H., Pla, J., Sentandreu, R., & Nombela, C. (1998). A role for the MAP kinase gene *MKC1* in cell wall construction and morphological transitions in *Candida albicans*. *Microbiology*, *144* (Pt 2), 411-424. doi:10.1099/00221287-144-2-411
- Netea, M. G., Gow, N. A., Munro, C. A., Bates, S., Collins, C., Ferwerda, G., . . . Kullberg, B. J. (2006). Immune sensing of *Candida albicans* requires cooperative recognition of mannans and glucans by lectin and Toll-like receptors. *J Clin Invest*, *116*(6), 1642-1650. doi:10.1172/JCI27114
- Nobile, C. J., Andes, D. R., Nett, J. E., Smith, F. J., Yue, F., Phan, Q. T., . . . Mitchell, A. P. (2006a). Critical role of Bcr1-dependent adhesins in *C. albicans* biofilm formation *in vitro* and *in vivo*. *PLoS Pathog*, *2*(7), e63. doi:10.1371/journal.ppat.0020063

- Nobile, C. J., Fox, E. P., Nett, J. E., Sorrells, T. R., Mitrovich, Q. M., Hernday, A. D., . . . Johnson, A. D. (2012). A recently evolved transcriptional network controls biofilm development in *Candida albicans*. *Cell*, *148*(1-2), 126-138. doi:10.1016/j.cell.2011.10.048
- Nobile, C. J., & Mitchell, A. P. (2005). Regulation of cell-surface genes and biofilm formation by the *C. albicans* transcription factor Bcr1p. *Curr Biol*, *15*(12), 1150-1155. doi:10.1016/j.cub.2005.05.047
- Nobile, C. J., Nett, J. E., Andes, D. R., & Mitchell, A. P. (2006b). Function of *Candida albicans* adhesin Hwp1 in biofilm formation. *Eukaryot Cell*, *5*(10), 1604-1610. doi:10.1128/EC.00194-06
- Nobile, C. J., Solis, N., Myers, C. L., Fay, A. J., Deneault, J. S., Nantel, A., . . . Filler, S. G. (2008). *Candida albicans* transcription factor Rim101 mediates pathogenic interactions through cell wall functions. *Cell Microbiol*, *10*(11), 2180-2196. doi:10.1111/j.1462-5822.2008.01198.x
- Noble, S. M., French, S., Kohn, L. A., Chen, V., & Johnson, A. D. (2010). Systematic screens of a *Candida albicans* homozygous deletion library decouple morphogenetic switching and pathogenicity. *Nat Genet*, *42*(7), 590-598. doi:10.1038/ng.605
- Noble, S. M., Gianetti, B. A., & Witchley, J. N. (2017). *Candida albicans* cell-type switching and functional plasticity in the mammalian host. *Nat Rev Microbiol*, *15*(2), 96-108. doi:10.1038/nrmicro.2016.157
- O'Meara, T. R., Robbins, N., & Cowen, L. E. (2017). The Hsp90 Chaperone Network Modulates *Candida* Virulence Traits. *Trends Microbiol*, *25*(10), 809-819. doi:10.1016/j.tim.2017.05.003
- Odds, F. C. (1985). Morphogenesis in *Candida albicans*. *Crit Rev Microbiol*, *12*(1), 45-93. doi:10.3109/10408418509104425
- Odds, F. C. (1987). *Candida* infections: an overview. *Crit Rev Microbiol*, *15*(1), 1-5. doi:10.3109/10408418709104444
- Odds, F. C. (1988). *Candida and Candidosis: a Review and Bibliography* (W. B. Saunders Ed. 2nd Edition ed.). London.
- Oehl, F., Sieverding, E., Palenzuela, J., Ineichen, K., & Alves da Silva, G. (2011). Advances in *Glomeromycota* taxonomy and classification. *IMA Fungus*, *2*(2), 191-199. doi:10.5598/imafungus.2011.02.02.10
- Ollert, M. W., Sohnchen, R., Korting, H. C., Ollert, U., Brautigam, S., & Brautigam, W. (1993). Mechanisms of adherence of *Candida albicans* to cultured human epidermal keratinocytes. *Infect Immun*, *61*(11), 4560-4568.
- Oyeka, C. A., & Ugwu, L. O. (2002). Fungal flora of human toe webs. *Mycoses*, *45*(11-12), 488-491.
- Pande, K., Chen, C., & Noble, S. M. (2013). Passage through the mammalian gut triggers a phenotypic switch that promotes *Candida albicans* commensalism. *Nat Genet*, *45*(9), 1088-1091. doi:10.1038/ng.2710
- Perez, A., Pedros, B., Murgui, A., Casanova, M., Lopez-Ribot, J. L., & Martinez, J. P. (2006). Biofilm formation by *Candida albicans* mutants for genes coding fungal proteins exhibiting the eight-cysteine-containing CFEM domain. *FEMS Yeast Res*, *6*(7), 1074-1084. doi:10.1111/j.1567-1364.2006.00131.x
- Perez, J. C., Fordyce, P. M., Lohse, M. B., Hanson-Smith, V., DeRisi, J. L., & Johnson, A. D. (2014). How duplicated transcription regulators can diversify to govern the expression of nonoverlapping sets of genes. *Genes Dev*, *28*(12), 1272-1277. doi:10.1101/gad.242271.114
- Perez, J. C., & Johnson, A. D. (2013a). Regulatory circuits that enable proliferation of the fungus *Candida albicans* in a mammalian host. *PLoS Pathog*, *9*(12), e1003780. doi:10.1371/journal.ppat.1003780

- Perez, J. C., Kumamoto, C. A., & Johnson, A. D. (2013b). *Candida albicans* commensalism and pathogenicity are intertwined traits directed by a tightly knit transcriptional regulatory circuit. *PLoS Biol*, *11*(3), e1001510. doi:10.1371/journal.pbio.1001510
- Perfect, J. R., & Casadevall, A. (2006). Fungal Molecular Pathogenesis: What Can It Do and Why Do We Need it? In J. Heitman, S. G. Filler, J. E. Edwards, & A. Mitchell (Eds.), *Molecular principles of fungal pathogenesis* (pp. 3-11). Washington D.C.: ASM Press.
- Perlroth, J., Choi, B., & Spellberg, B. (2007). Nosocomial fungal infections: epidemiology, diagnosis, and treatment. *Med Mycol*, *45*(4), 321-346. doi:10.1080/13693780701218689
- Pfaller, M. A., & Diekema, D. J. (2007). Epidemiology of invasive candidiasis: a persistent public health problem. *Clin Microbiol Rev*, *20*(1), 133-163. doi:10.1128/CMR.00029-06
- Phan, Q. T., Myers, C. L., Fu, Y., Sheppard, D. C., Yeaman, M. R., Welch, W. H., . . . Filler, S. G. (2007). Als3 is a *Candida albicans* invasin that binds to cadherins and induces endocytosis by host cells. *PLoS Biol*, *5*(3), e64. doi:10.1371/journal.pbio.0050064
- Phillips, A. W., & Balish, E. (1966). Growth and invasiveness of *Candida albicans* in the germ-free and conventional mouse after oral challenge. *Appl Microbiol*, *14*(5), 737-741.
- Piekarska, K., Mol, E., van den Berg, M., Hardy, G., van den Burg, J., van Roermund, C., . . . Distel, B. (2006). Peroxisomal fatty acid beta-oxidation is not essential for virulence of *Candida albicans*. *Eukaryot Cell*, *5*(11), 1847-1856. doi:10.1128/EC.00093-06
- Pope, L. M., Cole, G. T., Guentzel, M. N., & Berry, L. J. (1979). Systemic and gastrointestinal candidiasis of infant mice after intragastric challenge. *Infect Immun*, *25*(2), 702-707.
- Rajilic-Stojanovic, M., & de Vos, W. M. (2014). The first 1000 cultured species of the human gastrointestinal microbiota. *FEMS Microbiol Rev*, *38*(5), 996-1047. doi:10.1111/1574-6976.12075
- Ram, A. F., & Klis, F. M. (2006). Identification of fungal cell wall mutants using susceptibility assays based on Calcofluor white and Congo red. *Nat Protoc*, *1*(5), 2253-2256. doi:10.1038/nprot.2006.397
- Redondo, R. L., & Morris, R. G. (2011). Making memories last: the synaptic tagging and capture hypothesis. *Nat Rev Neurosci*, *12*(1), 17-30. doi:10.1038/nrn2963
- Reinke, A., Chen, J. C., Aronova, S., & Powers, T. (2006). Caffeine targets TOR complex I and provides evidence for a regulatory link between the FRB and kinase domains of Tor1p. *J Biol Chem*, *281*(42), 31616-31626. doi:10.1074/jbc.M603107200
- Reuss, O., Vik, A., Kolter, R., & Morschhauser, J. (2004). The SAT1 flipper, an optimized tool for gene disruption in *Candida albicans*. *Gene*, *341*, 119-127. doi:10.1016/j.gene.2004.06.021
- Riggle, P. J., & Kumamoto, C. A. (2000). Role of a *Candida albicans* P1-type ATPase in resistance to copper and silver ion toxicity. *J Bacteriol*, *182*(17), 4899-4905. doi:10.1128/jb.182.17.4899-4905.2000
- Roman, E., Arana, D. M., Nombela, C., Alonso-Monge, R., & Pla, J. (2007). MAP kinase pathways as regulators of fungal virulence. *Trends Microbiol*, *15*(4), 181-190. doi:10.1016/j.tim.2007.02.001
- Roman, E., Correia, I., Prieto, D., Alonso, R., & Pla, J. (2019). The HOG MAPK pathway in *Candida albicans*: more than an osmosensing pathway. *Int Microbiol*. doi:10.1007/s10123-019-00069-1
- Romani, L., Mocci, S., Bietta, C., Lanfaloni, L., Puccetti, P., & Bistoni, F. (1991). Th1 and Th2 cytokine secretion patterns in murine candidiasis: association of Th1 responses with acquired resistance. *Infect Immun*, *59*(12), 4647-4654.

- Rosenbach, A., Dignard, D., Pierce, J. V., Whiteway, M., & Kumamoto, C. A. (2010). Adaptations of *Candida albicans* for growth in the mammalian intestinal tract. *Eukaryot Cell*, 9(7), 1075-1086. doi:10.1128/EC.00034-10
- Rouabhia, M., Schaller, M., Corbucci, C., Vecchiarelli, A., Prill, S. K., Giasson, L., & Ernst, J. F. (2005). Virulence of the fungal pathogen *Candida albicans* requires the five isoforms of protein mannosyltransferases. *Infect Immun*, 73(8), 4571-4580. doi:10.1128/IAI.73.8.4571-4580.2005
- Ruchel, R., Zimmermann, F., Boning-Stutzer, B., & Helmchen, U. (1991). Candidiasis visualised by proteinase-directed immunofluorescence. *Virchows Arch A Pathol Anat Histopathol*, 419(3), 199-202.
- Samonis, G., Anaissie, E. J., Rosenbaum, B., & Bodey, G. P. (1990). A model of sustained gastrointestinal colonization by *Candida albicans* in healthy adult mice. *Infect Immun*, 58(6), 1514-1517.
- Sanglard, D., Hube, B., Monod, M., Odds, F. C., & Gow, N. A. (1997). A triple deletion of the secreted aspartyl proteinase genes *SAP4*, *SAP5*, and *SAP6* of *Candida albicans* causes attenuated virulence. *Infect Immun*, 65(9), 3539-3546.
- Saville, S. P., Lazzell, A. L., Monteagudo, C., & Lopez-Ribot, J. L. (2003). Engineered control of cell morphology *in vivo* reveals distinct roles for yeast and filamentous forms of *Candida albicans* during infection. *Eukaryot Cell*, 2(5), 1053-1060.
- Schoch, C. L., Sung, G. H., Lopez-Giraldez, F., Townsend, J. P., Miadlikowska, J., Hofstetter, V., . . . Spatafora, J. W. (2009). The *Ascomycota* tree of life: a phylum-wide phylogeny clarifies the origin and evolution of fundamental reproductive and ecological traits. *Syst Biol*, 58(2), 224-239. doi:10.1093/sysbio/syp020
- Schwabe, R. F., & Jobin, C. (2013). The microbiome and cancer. *Nat Rev Cancer*, 13(11), 800-812. doi:10.1038/nrc3610
- Schweizer, A., Rupp, S., Taylor, B. N., Rollinghoff, M., & Schroppel, K. (2000). The *TEA/ATTS* transcription factor CaTec1p regulates hyphal development and virulence in *Candida albicans*. *Mol Microbiol*, 38(3), 435-445.
- Selman, M., & Corradi, N. (2011). *Microsporidia*: Horizontal gene transfers in vicious parasites. *Mob Genet Elements*, 1(4), 251-255. doi:10.4161/mge.18611
- Semotok, J. L., Luo, H., Cooperstock, R. L., Karaiskakis, A., Vari, H. K., Smibert, C. A., & Lipshitz, H. D. (2008). *Drosophila* maternal Hsp83 mRNA destabilization is directed by multiple SMAUG recognition elements in the open reading frame. *Mol Cell Biol*, 28(22), 6757-6772. doi:10.1128/MCB.00037-08
- Shannon, P., Markiel, A., Ozier, O., Baliga, N. S., Wang, J. T., Ramage, D., . . . Ideker, T. (2003). Cytoscape: a software environment for integrated models of biomolecular interaction networks. *Genome Res*, 13(11), 2498-2504. doi:10.1101/gr.1239303
- Shapiro, R. S., Uppuluri, P., Zaas, A. K., Collins, C., Senn, H., Perfect, J. R., . . . Cowen, L. E. (2009). Hsp90 orchestrates temperature-dependent *Candida albicans* morphogenesis via Ras1-PKA signaling. *Curr Biol*, 19(8), 621-629. doi:10.1016/j.cub.2009.03.017
- Sherrington, S. L., Sorsby, E., Mahtey, N., Kumwenda, P., Lenardon, M. D., Brown, I., . . . Hall, R. A. (2017). Adaptation of *Candida albicans* to environmental pH induces cell wall remodelling and enhances innate immune recognition. *PLoS Pathog*, 13(5), e1006403. doi:10.1371/journal.ppat.1006403
- Sil, A., & Herskowitz, I. (1996). Identification of asymmetrically localized determinant, Ash1p, required for lineage-specific transcription of the yeast *HO* gene. *Cell*, 84(5), 711-722.
- Sohn, K., Urban, C., Brunner, H., & Rupp, S. (2003). *EFG1* is a major regulator of cell wall dynamics in *Candida albicans* as revealed by DNA microarrays. *Mol Microbiol*, 47(1), 89-102.

- Soll, D. R. (1992). High-frequency switching in *Candida albicans*. *Clin Microbiol Rev*, 5(2), 183-203. doi:10.1128/cmr.5.2.183
- Soll, D. R. (2004). Mating-type locus homozygosity, phenotypic switching and mating: a unique sequence of dependencies in *Candida albicans*. *Bioessays*, 26(1), 10-20. doi:10.1002/bies.10379
- Sonneborn, A., Bockmuhl, D. P., Gerads, M., Kurpanek, K., Sanglard, D., & Ernst, J. F. (2000). Protein kinase A encoded by *TPK2* regulates dimorphism of *Candida albicans*. *Mol Microbiol*, 35(2), 386-396.
- Sorrells, T. R., & Johnson, A. D. (2015). Making sense of transcription networks. *Cell*, 161(4), 714-723. doi:10.1016/j.cell.2015.04.014
- Sparrow, F. K. (1960). *Aquatic phycomycetes* (Vol. 2nd). Ann Arbor, Michigan: University of Michigan Press.
- St Johnston, D. (2005). Moving messages: the intracellular localization of mRNAs. *Nat Rev Mol Cell Biol*, 6(5), 363-375. doi:10.1038/nrm1643
- Stamatakis, A. (2006). RAxML-VI-HPC: maximum likelihood-based phylogenetic analyses with thousands of taxa and mixed models. *Bioinformatics*, 22(21), 2688-2690. doi:10.1093/bioinformatics/btl446
- Stoldt, V. R., Sonneborn, A., Leuker, C. E., & Ernst, J. F. (1997). Efg1p, an essential regulator of morphogenesis of the human pathogen *Candida albicans*, is a member of a conserved class of bHLH proteins regulating morphogenetic processes in fungi. *EMBO J*, 16(8), 1982-1991. doi:10.1093/emboj/16.8.1982
- Strimmer, K. (2008). fdrtool: a versatile R package for estimating local and tail area-based false discovery rates. *Bioinformatics*, 24(12), 1461-1462. doi:10.1093/bioinformatics/btn209
- Sudbery, P., Gow, N., & Berman, J. (2004). The distinct morphogenic states of *Candida albicans*. *Trends Microbiol*, 12(7), 317-324. doi:10.1016/j.tim.2004.05.008
- Sudbery, P. E. (2011). Growth of *Candida albicans* hyphae. *Nat Rev Microbiol*, 9(10), 737-748. doi:10.1038/nrmicro2636
- Tada, H., Nemoto, E., Shimauchi, H., Watanabe, T., Mikami, T., Matsumoto, T., . . . Takada, H. (2002). *Saccharomyces cerevisiae*- and *Candida albicans*-derived mannan induced production of tumor necrosis factor alpha by human monocytes in a CD14- and Toll-like receptor 4-dependent manner. *Microbiol Immunol*, 46(7), 503-512.
- Taipale, M., Jarosz, D. F., & Lindquist, S. (2010). *HSP90* at the hub of protein homeostasis: emerging mechanistic insights. *Nat Rev Mol Cell Biol*, 11(7), 515-528. doi:10.1038/nrm2918
- Taipale, M., Tucker, G., Peng, J., Krykbaeva, I., Lin, Z. Y., Larsen, B., . . . Lindquist, S. (2014). A quantitative chaperone interaction network reveals the architecture of cellular protein homeostasis pathways. *Cell*, 158(2), 434-448. doi:10.1016/j.cell.2014.05.039
- Tamura, K., Stecher, G., Peterson, D., Filipowski, A., & Kumar, S. (2013). MEGA6: Molecular Evolutionary Genetics Analysis version 6.0. *Mol Biol Evol*, 30(12), 2725-2729. doi:10.1093/molbev/mst197
- Tao, L., Du, H., Guan, G., Dai, Y., Nobile, C. J., Liang, W., . . . Huang, G. (2014). Discovery of a "white-gray-opaque" tristable phenotypic switching system in *Candida albicans*: roles of non-genetic diversity in host adaptation. *PLoS Biol*, 12(4), e1001830. doi:10.1371/journal.pbio.1001830
- Taylor, P. R., Brown, G. D., Herre, J., Williams, D. L., Willment, J. A., & Gordon, S. (2004). The role of SIGNR1 and the beta-glucan receptor (dectin-1) in the nonopsonic recognition of yeast by specific macrophages. *J Immunol*, 172(2), 1157-1162.

- Thompson, G. R., & Trexler, P. C. (1971). Gastrointestinal structure and function in germ-free or gnotobiotic animals. *Gut*, *12*(3), 230-235.
- Thornton, B. P., Vetvicka, V., Pitman, M., Goldman, R. C., & Ross, G. D. (1996). Analysis of the sugar specificity and molecular location of the beta-glucan-binding lectin site of complement receptor type 3 (CD11b/CD18). *J Immunol*, *156*(3), 1235-1246.
- Tilg, H., & Kaser, A. (2011). Gut microbiome, obesity, and metabolic dysfunction. *J Clin Invest*, *121*(6), 2126-2132. doi:10.1172/JCI158109
- Tlaskalova-Hogenova, H., Vannucci, L., Klimesova, K., Stepankova, R., Krizan, J., & Kverka, M. (2014). Microbiome and colorectal carcinoma: insights from germ-free and conventional animal models. *Cancer J*, *20*(3), 217-224. doi:10.1097/PPO.0000000000000052
- Trapnell, C., Hendrickson, D. G., Sauvageau, M., Goff, L., Rinn, J. L., & Pachter, L. (2013). Differential analysis of gene regulation at transcript resolution with RNA-seq. *Nat Biotechnol*, *31*(1), 46-53. doi:10.1038/nbt.2450
- Tso, G. H. W., Reales-Calderon, J. A., Tan, A. S. M., Sem, X., Le, G. T. T., Tan, T. G., . . . Pavelka, N. (2018). Experimental evolution of a fungal pathogen into a gut symbiont. *Science*, *362*(6414), 589-595. doi:10.1126/science.aat0537
- Tuch, B. B., Mitrovich, Q. M., Homann, O. R., Hernday, A. D., Monighetti, C. K., De La Vega, F. M., & Johnson, A. D. (2010). The transcriptomes of two heritable cell types illuminate the circuit governing their differentiation. *PLoS Genet*, *6*(8), e1001070. doi:10.1371/journal.pgen.1001070
- Uhl, M. A., Biery, M., Craig, N., & Johnson, A. D. (2003). Haploinsufficiency-based large-scale forward genetic analysis of filamentous growth in the diploid human fungal pathogen *C. albicans*. *EMBO J*, *22*(11), 2668-2678. doi:10.1093/emboj/cdg256
- Umesaki, Y. (2014). Use of gnotobiotic mice to identify and characterize key microbes responsible for the development of the intestinal immune system. *Proc Jpn Acad Ser B Phys Biol Sci*, *90*(9), 313-332.
- Umesaki, Y., & Setoyama, H. (2000). Structure of the intestinal flora responsible for development of the gut immune system in a rodent model. *Microbes Infect*, *2*(11), 1343-1351.
- Underhill, D. M., & Iliev, I. D. (2014). The mycobiota: interactions between commensal fungi and the host immune system. *Nat Rev Immunol*, *14*(6), 405-416. doi:10.1038/nri3684
- Underhill, D. M., & Pearlman, E. (2015). Immune Interactions with Pathogenic and Commensal Fungi: A Two-Way Street. *Immunity*, *43*(5), 845-858. doi:10.1016/j.immuni.2015.10.023
- Vaishnava, S., Yamamoto, M., Severson, K. M., Ruhn, K. A., Yu, X., Koren, O., . . . Hooper, L. V. (2011). The antibacterial lectin RegIIIgamma promotes the spatial segregation of microbiota and host in the intestine. *Science*, *334*(6053), 255-258. doi:10.1126/science.1209791
- Van den Abbeele, P., Grootaert, C., Possemiers, S., Verstraete, W., Verbeken, K., & Van de Wiele, T. (2009). *In vitro* model to study the modulation of the mucin-adhered bacterial community. *Appl Microbiol Biotechnol*, *83*(2), 349-359. doi:10.1007/s00253-009-1947-2
- Vandeputte, P., Ischer, F., Sanglard, D., & Coste, A. T. (2011). In vivo systematic analysis of *Candida albicans* Zn₂-Cys₆ transcription factors mutants for mice organ colonization. *PLoS One*, *6*(10), e26962. doi:10.1371/journal.pone.0026962
- Vieira, N., Casal, M., Johansson, B., MacCallum, D. M., Brown, A. J., & Paiva, S. (2010). Functional specialization and differential regulation of short-chain carboxylic acid transporters in the pathogen *Candida albicans*. *Mol Microbiol*, *75*(6), 1337-1354. doi:10.1111/j.1365-2958.2009.07003.x
- Wagener, J., Malireddi, R. K., Lenardon, M. D., Koberle, M., Vautier, S., MacCallum, D. M., . . . Gow, N. A. (2014). Fungal chitin dampens inflammation through IL-10 induction mediated by

- NOD2* and *TLR9* activation. *PLoS Pathog*, 10(4), e1004050. doi:10.1371/journal.ppat.1004050
- Wallen, R. M., & Perlin, M. H. (2018). An Overview of the Function and Maintenance of Sexual Reproduction in Dikaryotic Fungi. *Front Microbiol*, 9, 503. doi:10.3389/fmicb.2018.00503
- Wang, X., Liu, X., & Groenewald, J. Z. (2017). Phylogeny of anaerobic fungi (phylum *Neocallimastigomycota*), with contributions from yak in China. *Antonie Van Leeuwenhoek*, 110(1), 87-103. doi:10.1007/s10482-016-0779-1
- Wang, Y., Hoenig, J. D., Malin, K. J., Qamar, S., Petrof, E. O., Sun, J., . . . Claud, E. C. (2009). 16S rRNA gene-based analysis of fecal microbiota from preterm infants with and without necrotizing enterocolitis. *ISME J*, 3(8), 944-954. doi:10.1038/ismej.2009.37
- Wanke, V., Cameroni, E., Uotila, A., Piccolis, M., Urban, J., Loewith, R., & De Virgilio, C. (2008). Caffeine extends yeast lifespan by targeting *TORC1*. *Mol Microbiol*, 69(1), 277-285. doi:10.1111/j.1365-2958.2008.06292.x
- Wapinski, I., Pfeffer, A., Friedman, N., & Regev, A. (2007). Natural history and evolutionary principles of gene duplication in fungi. *Nature*, 449(7158), 54-61. doi:10.1038/nature06107
- Webster, C. E., & Odds, F. C. (1987). Growth of pathogenic *Candida* isolates anaerobically and under elevated concentrations of CO₂ in air. *J Med Vet Mycol*, 25(1), 47-53.
- Weissman, Z., Berdicevsky, I., Cavari, B. Z., & Kornitzer, D. (2000). The high copper tolerance of *Candida albicans* is mediated by a P-type ATPase. *Proc Natl Acad Sci U S A*, 97(7), 3520-3525. doi:10.1073/pnas.97.7.3520
- White, S. J., Rosenbach, A., Lephart, P., Nguyen, D., Benjamin, A., Tzipori, S., . . . Kumamoto, C. A. (2007). Self-regulation of *Candida albicans* population size during GI colonization. *PLoS Pathog*, 3(12), e184. doi:10.1371/journal.ppat.0030184
- Whiteway, M., & Bachewich, C. (2007). Morphogenesis in *Candida albicans*. *Annu Rev Microbiol*, 61, 529-553. doi:10.1146/annurev.micro.61.080706.093341
- Williams, D. W., Jordan, R. P., Wei, X. Q., Alves, C. T., Wise, M. P., Wilson, M. J., & Lewis, M. A. (2013). Interactions of *Candida albicans* with host epithelial surfaces. *J Oral Microbiol*, 5. doi:10.3402/jom.v5i0.22434
- Witchley, J. N., Penumetcha, P., Abon, N. V., Woolford, C. A., Mitchell, A. P., & Noble, S. M. (2019). *Candida albicans* Morphogenesis Programs Control the Balance between Gut Commensalism and Invasive Infection. *Cell Host Microbe*, 25(3), 432-443 e436. doi:10.1016/j.chom.2019.02.008
- Wysocki, R., & Tamas, M. J. (2010). How *Saccharomyces cerevisiae* copes with toxic metals and metalloids. *FEMS Microbiol Rev*, 34(6), 925-951. doi:10.1111/j.1574-6976.2010.00217.x
- Xie, J., Tao, L., Nobile, C. J., Tong, Y., Guan, G., Sun, Y., . . . Huang, G. (2013). White-opaque switching in natural MTL α /alpha isolates of *Candida albicans*: evolutionary implications for roles in host adaptation, pathogenesis, and sex. *PLoS Biol*, 11(3), e1001525. doi:10.1371/journal.pbio.1001525
- Xie, J. L., Grahl, N., Sless, T., Leach, M. D., Kim, S. H., Hogan, D. A., . . . Cowen, L. E. (2016). Signaling through Lrg1, Rho1 and Pkc1 Governs *Candida albicans* Morphogenesis in Response to Diverse Cues. *PLoS Genet*, 12(10), e1006405. doi:10.1371/journal.pgen.1006405
- Xu, W., Solis, N. V., Ehrlich, R. L., Woolford, C. A., Filler, S. G., & Mitchell, A. P. (2015). Activation and alliance of regulatory pathways in *C. albicans* during mammalian infection. *PLoS Biol*, 13(2), e1002076. doi:10.1371/journal.pbio.1002076

- Xu, X. L., Lee, R. T., Fang, H. M., Wang, Y. M., Li, R., Zou, H., . . . Wang, Y. (2008). Bacterial peptidoglycan triggers *Candida albicans* hyphal growth by directly activating the adenylyl cyclase Cyr1p. *Cell Host Microbe*, 4(1), 28-39. doi:10.1016/j.chom.2008.05.014
- Yamaguchi, N., Sonoyama, K., Kikuchi, H., Nagura, T., Aritsuka, T., & Kawabata, J. (2005). Gastric colonization of *Candida albicans* differs in mice fed commercial and purified diets. *J Nutr*, 135(1), 109-115. doi:10.1093/jn/135.1.109
- Zenklusen, D., & Singer, R. H. (2010). Analyzing mRNA expression using single mRNA resolution fluorescent *in situ* hybridization. *Methods Enzymol*, 470, 641-659. doi:10.1016/S0076-6879(10)70026-4
- Zhao, X., Daniels, K. J., Oh, S. H., Green, C. B., Yeater, K. M., Soll, D. R., & Hoyer, L. L. (2006). *Candida albicans* Als3p is required for wild-type biofilm formation on silicone elastomer surfaces. *Microbiology*, 152(Pt 8), 2287-2299. doi:10.1099/mic.0.28959-0
- Zink, S., Nass, T., Rosen, P., & Ernst, J. F. (1996). Migration of the fungal pathogen *Candida albicans* across endothelial monolayers. *Infect Immun*, 64(12), 5085-5091.
- Zuiderweg, E. R., Hightower, L. E., & Gestwicki, J. E. (2017). The remarkable multivalency of the Hsp70 chaperones. *Cell Stress Chaperones*, 22(2), 173-189. doi:10.1007/s12192-017-0776-y

8) List of Publications

Publications included in this thesis

Bohm, L., Torsin, S., Tint, S. H., Eckstein, M. T., Ludwig, T., & Perez, J. C. (2017). The yeast form of the fungus *Candida albicans* promotes persistence in the gut of gnotobiotic mice. *PLoS Pathog*, 13(10), e1006699. doi:10.1371/journal.ppat.1006699

Bohm, L., Muralidhara, P., & Perez, J. C. (2016). A *Candida albicans* regulator of disseminated infection operates primarily as a repressor and governs cell surface remodeling. *Mol Microbiol*, 100(2), 328-344. doi:10.1111/mmi.13320

Other Publications

Atsem, S., Reichenbach, J., Potabattula, R., Dittrich, M., Nava, C., Depienne, C., Böhm, L., Rost, S., Hahn, T., Schorsch, M., Haaf, T., El Hajj, N. (2016). Paternal age effects on sperm FOXX1 and KCNA7 methylation and transmission into the next generation. *Hum Mol Genet*, 25(22), 4996-5005. doi:10.1093/hmg/ddw328

Kuhtz, J., Schneider, E., El Hajj, N., Zimmermann, L., Fust, O., Linek, B., Seufert, R., Hahn, T., Schorsch, M., Haaf, T. (2014). Epigenetic heterogeneity of developmentally important genes in human sperm: implications for assisted reproduction outcome. *Epigenetics*, 9(12), 1648-1658. doi:10.4161/15592294.2014.988063

9) CV

Personal data

Name: Lena Böhm

Address:

Birthdate:

Nationality:

Family status:

Education

04.2012 – 03.2014	University of Würzburg, Course of studies: Biology Degree: Master of Science Master's thesis: „Male age effects on the sperm and offspring epigenome.“
10.2007 – 10.2010	University of Würzburg, Course of studies: Biology Degree: Bachelor of Science Bachelor's thesis: „Untersuchungen zum Einfluss uteriner Faktoren auf humane Spermatozoen“
09.1998 - 06.2007	Siebold-Gymnasium Würzburg
09.1994 - 07.1998	Basic primary school Bergtheim

Internships

08.2012 – 09.2012	Internship at the institute of human genetics, topic: „Untersuchungen von Methylierungsmustern bestimmter Gene bei Einzelspermien“
08.2009 – 09.2009	Internship at the center of reproductive medicine, genetics and prenatal diagnostics Würzburg

Experience

01.2015 – 12.2018	PhD student in the group of Dr. J. Christian Pérez at the institute of molecular infectious biology, Würzburg
06.2014 – 11.2014	Biologist at an IVF center in Offenbach/Main
10.2010 – 02.2012	Scientific assistant in the IVF center at Universitäts-Frauenklinik Würzburg

Publication list

Bohm, L., Torsin, S., Tint, S. H., Eckstein, M. T., Ludwig, T., & Perez, J. C. (2017). The yeast form of the fungus *Candida albicans* promotes persistence in the gut of gnotobiotic mice. *PLoS Pathog*, 13(10), e1006699. doi:10.1371/journal.ppat.1006699

Bohm, L., Muralidhara, P., & Perez, J. C. (2016). A *Candida albicans* regulator of disseminated infection operates primarily as a repressor and governs cell surface remodeling. *Mol Microbiol*, 100(2), 328-344. doi:10.1111/mmi.13320

Atsem, S., Reichenbach, J., Potabattula, R., Dittrich, M., Nava, C., Depienne, C., Böhm, L., Rost, S., Hahn, T., Schorsch, M., Haaf, T., El Hajj, N. (2016). Paternal age effects on sperm FOXP1 and KCNA7 methylation and transmission into the next generation. *Hum Mol Genet*, 25(22), 4996-5005. doi:10.1093/hmg/ddw328

Kuhtz, J., Schneider, E., El Hajj, N., Zimmermann, L., Fust, O., Linek, B., Seufert, R., Hahn, T., Schorsch, M., Haaf, T. (2014). Epigenetic heterogeneity of developmentally important genes in human sperm: implications for assisted reproduction outcome. *Epigenetics*, 9(12), 1648-1658. doi:10.4161/15592294.2014.988063

Skills

Languages: German (native)
 English (fluent)
 French (basic)

IT-Knowledges: Microsoft Office (Word, Excel, Power Point)
 Image processing with Illustrator and Fiji
 Statistical analysis with SPSS
 Genome data analysis with Mochi View

 Place, Date

 Signature

10) Affidavit

Affidavit

I hereby confirm that my thesis entitled „Dissecting mechanisms of host colonization by *C. albicans*“ is the result of my own work. I did not receive any help or support from commercial consultants. All sources and / or materials applied are listed and specified in the thesis.

Furthermore, I confirm that this thesis has not yet been submitted as part of another examination process neither in identical nor in similar form.

Place, Date

Signature

Eidesstattliche Erklärung

Hiermit erkläre ich an Eides statt, die Dissertation „Dissecting mechanisms of host colonization by *C. albicans*“ eigenständig, d.h. insbesondere selbständig und ohne Hilfe eines kommerziellen Promotionsberaters, angefertigt und keine anderen als die von mir angegebenen Quellen und Hilfsmittel verwendet zu haben.

Ich erkläre außerdem, dass die Dissertation weder in gleicher noch in ähnlicher Form bereits in einem anderen Prüfungsverfahren vorgelegen hat.

Ort, Datum

Unterschrift